Phy Sci
& Engr
QE
89
A1
C32
no.114

UNIVERSITY OF CALIFORNIA DAVIS
3 1175 01715 6616

Special Publication 114

FIELD GUIDE to the GEOLOGY and TAMORPHISM of the FRANCISCAN COMPLEX and WESTERN METAMORPHIC BELT of NORTHERN CALIFORNIA

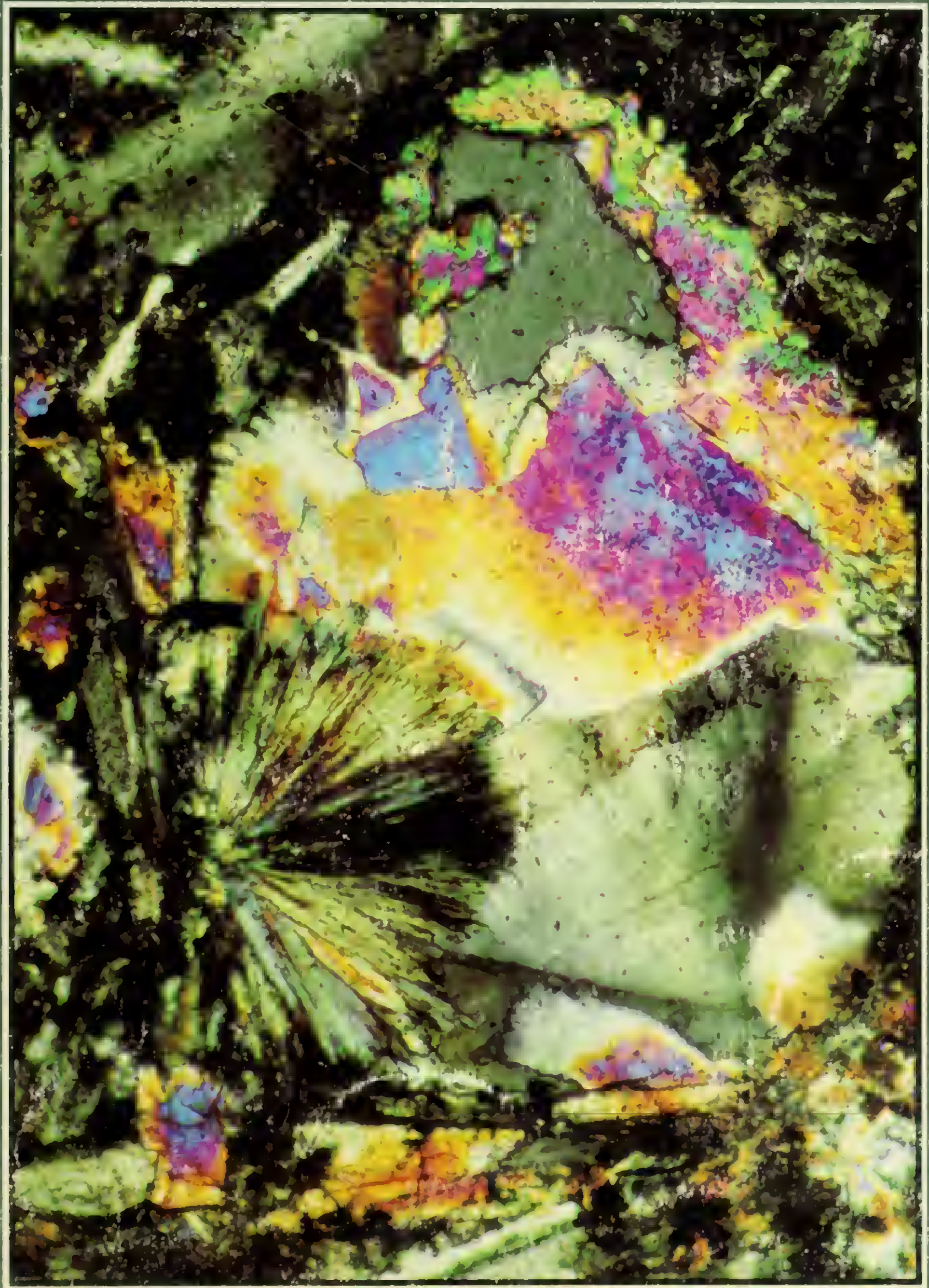

PETE WILSON, *Governor*
STATE OF CALIFORNIA

DOUGLAS P. WHEELER, *Secretary*
THE RESOURCES AGENCY

EDWARD G. HEIDIG, *Director*
DEPARTMENT OF CONSERVATION

THE GREAT SEAL OF THE STATE OF CALIFORNIA

EUREKA

JAMES F. DAVIS
State Geologist

Field Trip Guidebook for the International Symposium "The Transition from Basalt to Metabasalt: Environments, Processes, and Petrogenesis," University of California, Davis, September 9-15, 1992. This guidebook is available for purchase from the Division of Mines and Geology.

COVER PHOTO: Photomicrograph of low-grade metamorphic mineral assemblage in an amygdaloidal basalt from the Jurassic Smartville Complex, northern Sierra Nevada, California; crosspolarized light, field of view is 0.9 mm by 0.6 mm.

The amygdule (gas cavity or vesicle filled with secondary minerals) is filled with radial pumpellyite (lower left), prehnite (gray, white, yellow, red and blue in center), epidote (yellow, green and pink in upper right), quartz (gray between prehnite and epidote) and chlorite (very dark colored mineral, rimming epidote in upper right).

This assemblage is representative of the prehnite-pumpellyite metamorphic zone of the Smartville Complex and is thought to reflect metamorphic recrystallization at a temperature of 250-350°C and a pressure of 2-3 kbar. *Photo by R.E. Beiersdorfer.*

Special Publication 114

FIELD GUIDE to the GEOLOGY and METAMORPHISM of the FRANCISCAN COMPLEX and WESTERN METAMORPHIC BELT of NORTHERN CALIFORNIA

1992

Editors

PETER SCHIFFMAN
University of California, Davis

and

DAVID L. WAGNER
Division of Mines and Geology

California Department of Conservation
DIVISION OF MINES AND GEOLOGY
801 K street
Sacramento, CA 95814

UNIVERSITY OF CALIFORNIA
DAVIS
OCT 05 1992
CALIF. DEPOS.
GOV'T. DOCS. - LIBRARY

Editors: Peter Schiffman and David Wagner
Graphic Design and layout: Peggy Walker
Printing: University of California Printing Services, Berkeley

CONTENTS

Preface v

Introduction vii
Peter Schiffman

METAMORPHISM AND TECTONIC ORIGIN OF FRANCISCAN METABASITES AND A FIELD TRIP GUIDE TO THREE LOCALITIES IN THE SAN FRANCISCO BAY AREA 1
John Wakabayashi

TECTONIC SETTING AND METAMORPHISM OF THE SIERRA NEVADA, CALIFORNIA 12
Howard W. Day

METAMORPHIC FEATURES OF THE SMARTVILLE COMPLEX NORTHERN SIERRA NEVADA, CALIFORNIA 29
Raymond E. Beiersdofer and Howard W. Day

A GLIMPSE OF THE CENTRAL AND FEATHER RIVER BELTS, NORTHERN SIERRA NEVADA 48
Howard W. Day

GEOLOGY OF THE EASTERN BELT OF THE NORTHERN SIERRA NEVADA 54
Elwood R. Brooks

Digitized by the Internet Archive
in 2012 with funding from
University of California, Davis Libraries

http://archive.org/details/fieldguidetogeol114schi

PREFACE

Special Publication 114 contains five chapters that discuss metamorphism and tectonics affecting Mesozoic rocks in the Coast Ranges and Sierra Nevada provinces of northern California. The publication was prepared for an international symposium, The Transition from Basalt to Metabasalt: Environments, Processes, and Petrogenesis, held at University of California, Davis, September 9-15, 1992.

Four of the chapters are guides for field trips conducted before and after the symposium. Chapter 1 is a guide for a trip in the San Francisco Bay area where metabasalts of the Franciscan Complex are exposed. Chapter 2 is an overview of the western Metamorphic Belt of the Sierra Nevada. Chapters 3, 4, and 5 are guides for field trips in the northern part of the Western Metamorphic Belt. These trips are in an area that is covered by the new 1:250,000 scale Geologic Map of the Chico Quadrangle, California. This map is the latest of the Division of Mines and Geology Regional Geologic Map Series (RGM 007A).

The editors would like to thank the many individuals who helped make this publication possible. We gratefully acknowledge the people who provided peer reviews of the manuscripts: Diane Moore, J.G. Liou, James Beard, Doug Robinson, Richard Bevins, Robert Springer, Judith Hannah, and David Harwood. We extend our thanks to Charlie Scribner and the folks at the University of California Printing Services.

Thanks also go to Jim Davis, Bill Guerard, Jeff Tambert, and Jim Williams of DMG for their support. Special gratitude goes to Peggy Walker of the DMG Publications unit for the design and layout of the report.

Peter Schiffman and
David Wagner, Editors

INTRODUCTION

PETER SCHIFFMAN

Paleozoic and Mesozoic rocks of northern California record a complex history of deformation and metamorphism. Mostly low-grade metamorphic rocks are well exposed in portions of the Franciscan Complex of the California Coast Ranges and in the Western Metamorphic Belt of the northern Sierra Nevada. This guide presents reviews of the geology and metamorphism of each region as well as descriptions of selected localities where these rocks can be examined.

The Franciscan Complex formed as a subduction complex along the western margin of the North American plate from the Late Jurassic through the Early Tertiary. In Chapter 1, J. Wakabayashi describes the blueschist and transitional greenschist facies metamorphism of basaltic rocks from the Franciscan in the San Francisco Bay area. These metabasalts occur both in coherent thrust sheets as well as in tectonic blocks within melange. Mineral assemblages within these rocks, particularly the blocks, record a complex, polymetamorphic history of subduction and accretion. The chapter concludes with a field excursion to three Bay Area locations to examine coherent blueschists (in the El Cerrito hills) and tectonic blocks (in the Tiburon Peninsula) as well as zeolite grade pillow basalts (in the Marin headlands).

The Western Metamorphic Belt of the northern Sierra Nevada is comprised of four major lithotectonic belts containing rocks of contrasting origin and metamorphism. In Chapter 2, H. W. Day presents an overview of the diverse tectonic settings and metamorphic histories of each of these four major belts. Subsequent chapters (3-5) address the geology of these belts in more detail. The boundary faults which separate these belts are generally discontinuities in metamorphic grade as well as lithology. Since many of these faults are cut by late Jurassic, "Nevadan" plutons, it appears that much of the metamorphism of rocks within these four belts must predate their assembly.

The Smartville Complex, which is the western-most of the four belts, is a middle- to late-Jurassic, rifted volcanic arc. In Chapter 3, R.E. Beiersdorfer and H.W. Day document the complex metamorphic features of this arc. This metamorphism encompasses several distinct styles including burial, contact, hydrothermal, and dynamothermal recrystallization. The former three are types of metamorphism which occured during the construction of the submarine volcanic arc. Only the dynamothermal metamorphism appears to be related to the deformation that culminated the Jurassic accretionary events in western North America. The field excursion visits localities where the products of these metamorphic styles are preserved in outcrop.

The Central and Feather River belts occupy the middle portions of the Western Metamorphic Belt. In Chapter 4, H.W. Day presents a brief introduction to, and field excursion through, these two belts. The Central Belt is structurally complex and comprises dominantly Mesozoic volcanic arc rocks and oceanic sediments. The Feather River Belt is composed mainly of peridotite with structurally intercalated metabasites and metasediments. The metamorphism of both these belts is not well understood. The Central Belt contains both greenschist and sub-greenschist facies rocks. Both blueschist and amphibolite rocks have been identified in the Feather River Belt.

The Eastern Belt includes three distinct volcanic arc sequences which stratigraphically overlie an early Paleozoic, (probable) continental margin sequence, the Shoo Fly Complex. The Shoo Fly Complex is a pre-Devonian, largely sedimentary assemblage whose depositional, structural, and metamorphic histories are imperfectly understood. In Chapter 5, E.R. Brooks presents a brief introduction and field excursion to the Shoo Fly Complex. Arc sequences are of late Devonian-early Mississippian, Permian, and Jurassic ages overlie the Shoo Fly complex. Also in Chapter 5, Brooks presents a detailed investigation of the oldest arc rocks, the Taylorsville sequence. Volcanogenic rocks of the Taylorsville sequence appear to have experienced pre-Nevadan, sub-greenschist metamorphism. Sedimentary rocks of the Shoo Fly Complex have undergone earlier, pre-late-Devonian deformation and metamorphism.

A synthesis of the studies reported in this volume reveals that Paleozoic and Mesozoic rocks of northern California have undergone a considerably more complex structural and metamorphic evolution than that predicted by the first generation plate tectonic models of the 1970's. Specifically (as H.W. Day notes in Chapter 2) these studies do not support the notion that the Franciscan Complex and Western Metamorphic Belt respectively comprise the high and low P/T portions of a paired metamorphic belt formed through underthrusting of oceanic crust beneath western North America during the Cretaceous. Rather, rocks of the Western Metamorphic Belt are of ubiquitously low metamorphic grade, much of which is pre-Cretaceous in age. Similarly, much of the metamorphism within each of the four lithotectonic belts of the Western Metamorphic Belt is internal to, and predates the accretion of, these belts.

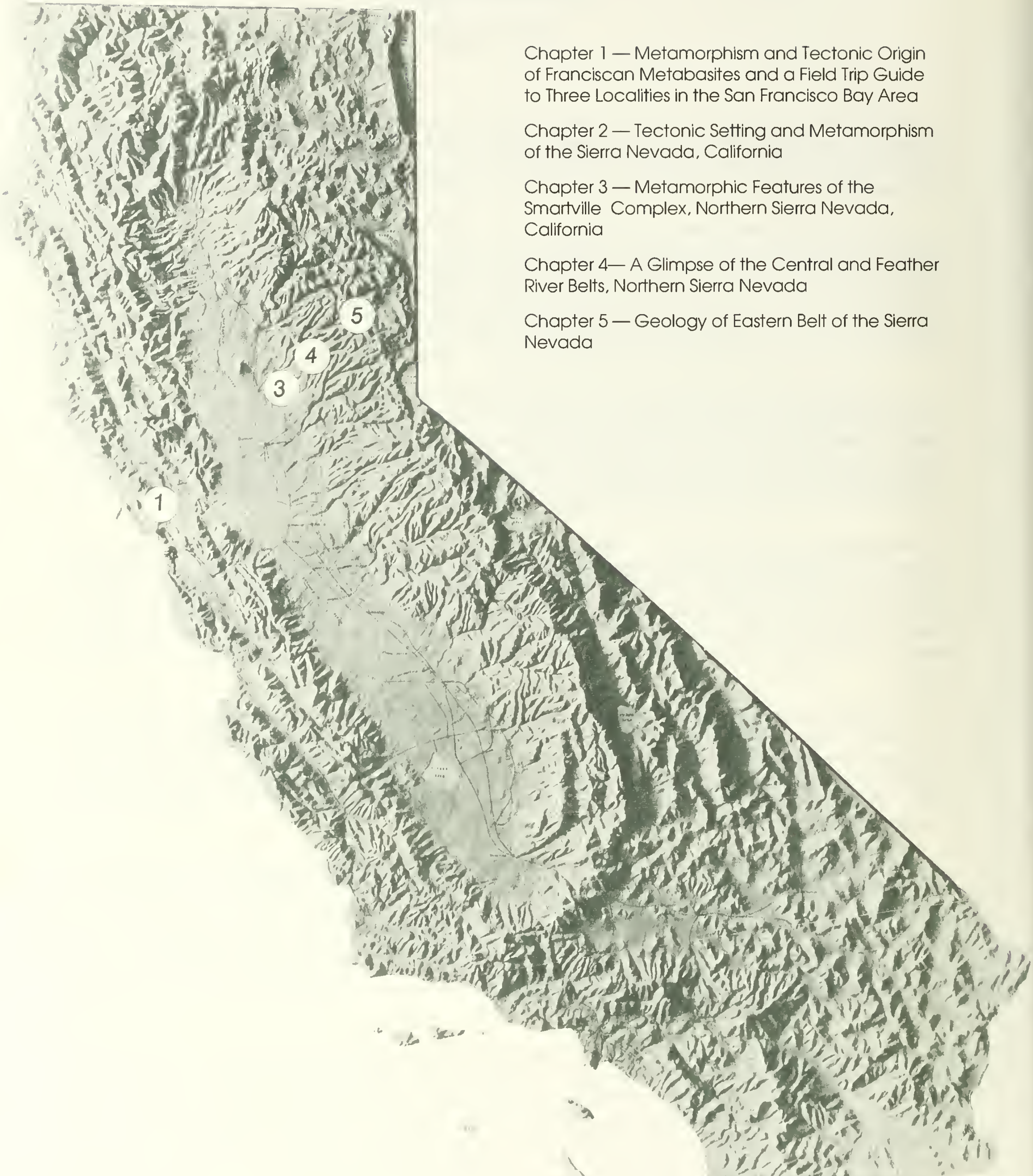

Chapter 1 — Metamorphism and Tectonic Origin of Franciscan Metabasites and a Field Trip Guide to Three Localities in the San Francisco Bay Area

Chapter 2 — Tectonic Setting and Metamorphism of the Sierra Nevada, California

Chapter 3 — Metamorphic Features of the Smartville Complex, Northern Sierra Nevada, California

Chapter 4— A Glimpse of the Central and Feather River Belts, Northern Sierra Nevada

Chapter 5 — Geology of Eastern Belt of the Sierra Nevada

METAMORPHISM AND TECTONIC ORIGIN OF FRANCISCAN METABASITES AND A FIELD TRIP GUIDE TO THREE LOCALITIES IN THE SAN FRANCISCO BAY AREA

JOHN WAKABAYASHI
Earth Sciences Associates
701 Welch Road
Palo Alto, CA 94304

INTRODUCTION

The Franciscan Complex of the California Coast Ranges formed as a subduction complex associated with east-dipping subduction along the western North American plate margin from the Late Jurassic through the Early Tertiary, a period of over 140 million years (Wakabayashi, 1992). Franciscan rocks are exposed in a nearly continuous belt of rocks over 800 km long and up to 120 km across (Fig.1). Franciscan lithologies are predominantly detrital sedimentary rocks with subordinate basaltic rocks and chert, and minor limestone. The detrital rocks may represent offscraped and underplated trench-fill sediments (Dickinson, 1970). The pelagic and volcanic rocks may represent fragments of seamounts and parts of the subducted oceanic crust (Hamilton, 1969; MacPherson, 1983; Tarduno, et al. 1985; Maruyama, et al. 1989), possibly with a component of olistostromal blocks from the upper plate (MacPherson, et al. 1990). The Franciscan is composed of both coherent thrust sheets and melanges. In regions that are not significantly overprinted by post-subduction Cenozoic deformation, Franciscan rock units, including melanges, comprise a stack of nappes (Seiders, 1991; Wakabayashi, 1992). Apparent accretion ages of nappes young structurally downward suggesting emplacement as a result of sequential underplating or offscraping at the trench (Seiders, 1991; Wakabayashi, 1992). See Blake, et al. (1988) for a somewhat different view point. This nappe structure is particularly well-displayed in the San Francisco Bay area, the site of this field trip (Fig. 2,3).

The Franciscan is well-known for the occurrence of high P/T rocks (Ernst, et al. 1970; Ernst, 1970; 1971), but some metamorphism took place at higher thermal gradients (Wakabayashi, 1990). Franciscan metamorphic rocks consist of both intact thrust sheets, herein termed coherent metamorphic rocks, and tectonic blocks in melanges. The most striking tectonic blocks are the coarse-grained (grain size up to 1 cm or more) amphibolites, eclogites and blueschists, referred to as 'high-grade blocks' or 'knockers' in Franciscan literature (Coleman and Lanphere, 1971). An overwhelming majority of high-grade blocks are metabasites although blocks metaironstones, metacherts and metatuffs also occur. These blocks have only one 'coherent' equivalent in the Franciscan, the Goat Mtn. schists, (Ernst, et al. 1970, Suppe and Foland; 1978), an exposure of several thrust slices up to 3 km long. Although high-grade blocks make up much less than 1% of the Franciscan (Bailey, et al. 1964), they are undoubtedly the most famous metamorphic rocks in the terrane. Other tectonic blocks are

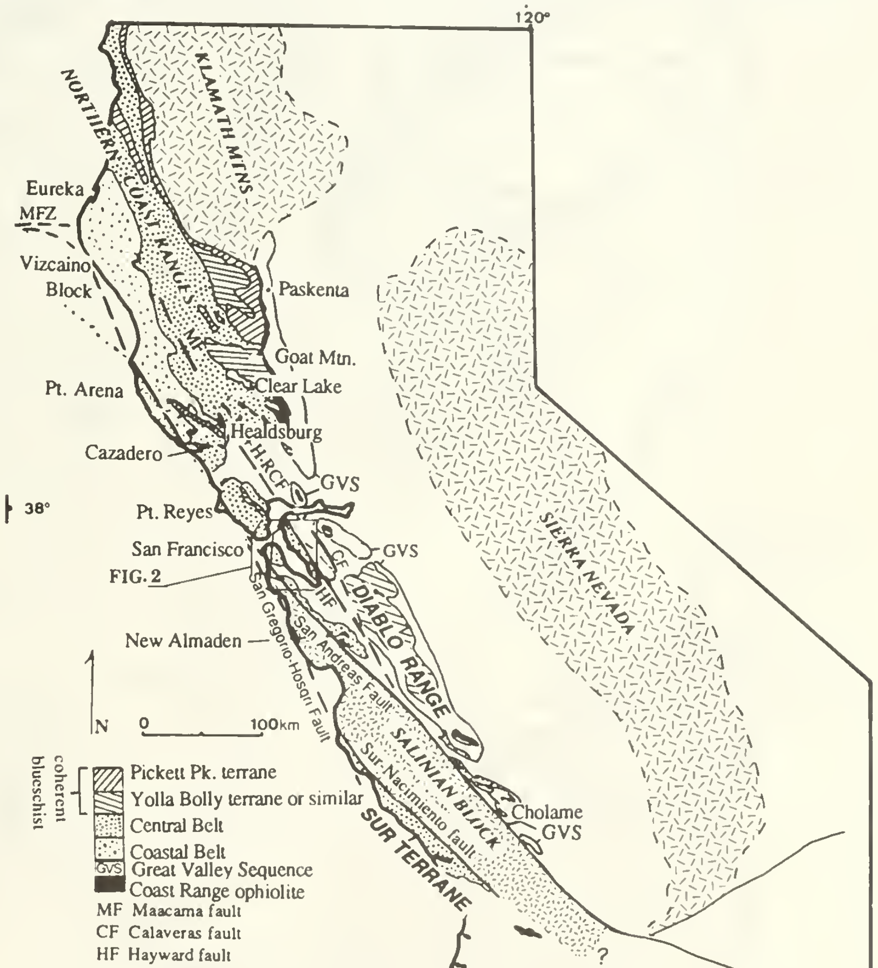

Figure 1. Generalized geologic map of Franciscan rocks in California. Adapted from Wakabayashi (1992).

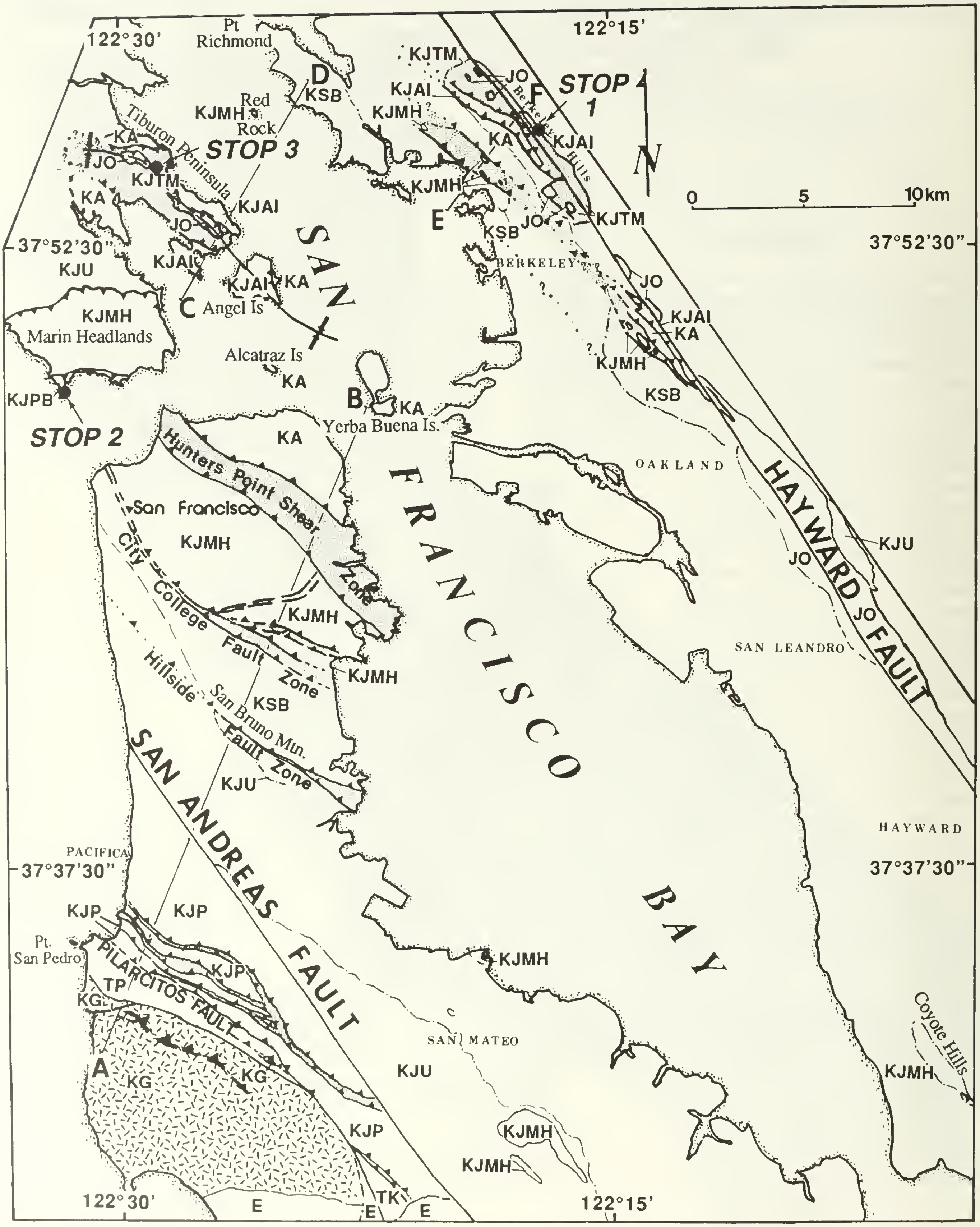

Figure 2. Map of Franciscan nappes in the San Francisco Bay area. Field trip stop locations are numbered. Adapted from Wakabayashi (1992).

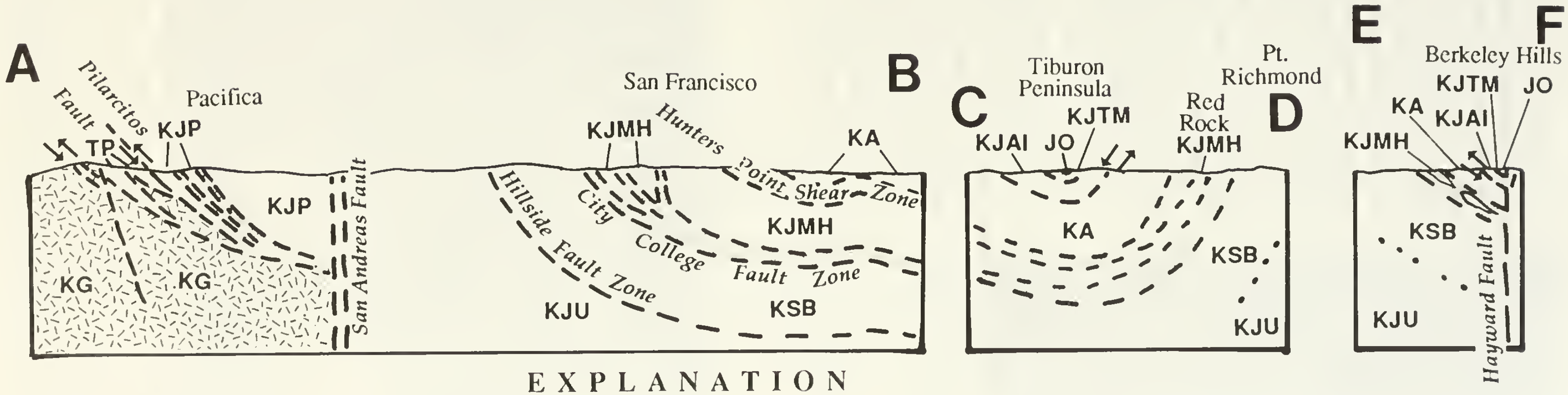

EXPLANATION

Franciscan Units:

KJTM: Tiburon Melange: shale and serpentinite matrix melange with numerous 'high-grade' blocks.

KJAI: Angel Island nappe: metavolanic and metaclastic rocks; blueschist grade; incipiently foliated to schistose.

KA: Alcatraz terrane: quartzofeldspathic sandstone and shale; prehnite pumpellyite grade; Valanginian age

KJPB: Rocks of Point Bonita: similar to Marin Headlands terrane but basalts differ chemically and contain interpillow limestone; prehnite pumpellyite grade

KJMH: Marin Headlands terrane: basalt, chert, sandstone and shale; prehnite pumpellyite grade; detrital rocks of Albian to Cenomanian age.

KSB: San Bruno Mtn. nappe (San Bruno Mtn. and Novato Quarry terranes): K-feldspar-bearing quartzofeldspathic sandstone and shale; prehnite pumpellyite grade; Campanian age for Novato Quarry terrane, no fossils from San Bruno Mtn. terrane

KJP: Permanente terrane: basalt, sandstone, shale, limestone and chert; prehnite pumpellyite to blueschist grade

Hunters Point Shear Zone, City College Fault Zone, Hillside Fault Zone: major terrane-bounding melanges; shale and/or serpentinite matrix with relatively rare 'high-grade' blocks; shown in stipple

KJU: undifferentiated Franciscan

Non-Franciscan rock units:

JO: Coast Range ophiolite and correlative rocks

KG: plutonic rocks of the Salinian block

TK: Upper Cretaceous and (?) Paleocene (?) sandstone and shale of the Salinian block; locally melange.

TP: Paleocene sandstone and shale of the Salinian block.

E: Eocene and younger clastic rocks of the San Francisco peninsula.

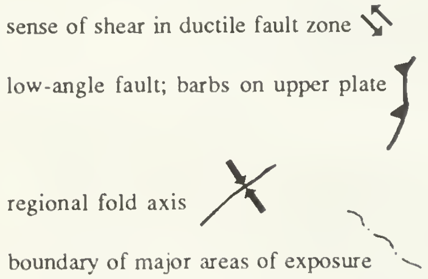
sense of shear in ductile fault zone
low-angle fault; barbs on upper plate
regional fold axis
boundary of major areas of exposure

Figure 3. Schematic cross section of corresponding to cross section line in Figure 2. No vertical exaggeration. Adapted from Wakabayashi (1992).

finer grained (grain sizes generally much less than 1mm) and lower grade, ranging from zeolite to blueschist-greenschist transition grade and are equivalent to coherent metamorphic rocks found in the Franciscan.

By far the greatest amount of research on Franciscan metabasites has focused on the high-grade blocks (Coleman and Lanphere, 1971; Moore, 1984; Moore and Blake, 1989; Wakabayashi, 1990), with a lesser amount of research on the coherent blueschist to blueschist-greenschist grade rocks (Maruyama and Liou, 1988; Brown and Ghent, 1983), and little research on sub-greenschist facies rocks (Swanson and Schiffman, 1979). Consequently, most of this review will focus on the high-grade blocks and coherent blueschist or blueschist-greenschist transition rocks.

METABASITE ASSEMBLAGES

High-Grade Blocks

The high-grade blocks commonly have assemblages that suggest early metamorphism at higher temperatures (epidote amphibolite, garnet amphibolite and rarely, amphibolite-granulite facies), with retrograde assemblages that reflect a decrease in temperature and increase in P/T ratio (eclogite, blueschist facies)(Wakabayashi, 1990). Even in rocks composed nearly entirely of high P/T-type assemblages, some evidence of earlier higher thermal gradients exists, either as inclusions or as relict core regions of minerals with different compositions (not always petrographically obvious). An actinolite and chlorite-rich rind encloses many of the blocks and appears to have formed after the earliest part of the blueschist metamorphic stage (Moore, 1984), probably from a reaction between the blocks and enclosing ultramafic rocks (Coleman and Lanphere, 1971). Some typical assemblages are described below (for details see Coleman and Lanphere, 1971, Moore and Blake, 1989, Oh and Liou, 1990, Wakabayashi, 1990).

1. A high temperature assemblage includes: pargasite+probable plagioclase+garnet-quartz+rutile+FeTi oxides. In retrograde assemblages, pargasite is replaced progressively by magnesio-taramite/subcalcic pargasitic hornblende to barroisite to glaucophane; lawsonite, jadeitic pyroxene+quartz-albite replaces probable plagioclase; sphene replaces rutile.

2. A rare but spectacular high temperature assemblage that includes: pargasite+diopside+garnet+probable plagioclase+rutile+FeTi oxides. In retrograde assemblages, pargasite is replaced by hornblende and then crossite; probable plagioclase replaced by lawsonite or pumpellyite; sphene replaces rutile.

3. A high temperature assemblage that includes: pargasite or pargasitic hornblende_actinolite+probable plagioclase or albite+epidote-quartz+sphene+FeTi oxides. This assemblage commonly shows very little evidence of any high P/T overprint. In the more retrograded samples, glaucophane-crossite replaces the amphibole, lawsonite forms at the expense of probable plagioclase.

4. A high temperature assemblage that includes: magnesio-taramite+garnet+epidote+white mica-albite-quartz-clinopyroxene (generally less than 30% jadeite)+rutile+FeTi oxides. Severe overprinting by high P/T assemblages is common. Many so-called 'high-grade blueschists' (generally garnet-bearing blueschists) are probably retrograded equivalents of this assemblage. Compositional zoning of garnets in these 'blueschists' reflects an earlier higher temperature phase of metamorphism. Commonly at least one generation of white mica and epidote cores are relics of earlier higher T or intermediate assemblages. In rocks that preserve many of the intermediate steps of retrograde metamorphism, initial clinopyroxene is rimmed by more jadeite rich clinopyroxene (35-50 % jadeite), and amphibole is replaced first by barroisite and then by glaucophane, and sphene replaces rutile. In both thin section and outcrop the progression of metamorphism from garnet amphibolite to eclogite to blueschist is commonly observed (see stop 3 description).

In high-grade blocks, the retrograde phases commonly rim earlier-formed minerals of the same species (amphiboles, clinopyroxenes, epidote, garnet and rarely white mica), forming concentric zoning. Cross-cutting relationships involving three different generations of white mica or amphibole are not uncommon. Vein assemblages of lawsonite, pumpellyite, blue amphibole and garnet are present in some rocks in addition to more common vein minerals such as albite and quartz. All stages of mineral growth, except veins, are associated with a strong foliation or schistosity.

Coherent Metabasites—Blueschist and blueschist-green schist transition rocks

Probably the most extensively studied Franciscan coherent metabasites occur in the Ward Creek area near Cazadero (located on Fig. 1) (Coleman and Lee, 1963, Maruyama and Liou, 1988). These rocks range from in grade from incipiently recrystallized Na-amphibole-bearing metabasites to strongly foliated epidote blueschists. Metamorphic grain sizes range up to 1 mm, the coarsest of any coherent metamorphic rocks in the Franciscan. These rocks encompass nearly the entire range of mineral assemblages found in other Franciscan blueschist or blueschist-greenschist grade coherent rocks. Similar but somewhat finer-grained rocks of about the same metamorphic age are found in the Pickett Peak terrane of the northern Coast Ranges (Brown and Ghent, 1983; Blake, et al. 1988) (Fig. 1) and may be correlative (Blake, et al. 1984; Wakabayashi, 1992). In addition to the difference in grain size, only higher grade Ward Creek metabasites are completely recrystallized and foliated, whereas nearly all lithologies and metamorphic grades of the Pickett Peak terrane are strongly foliated and recrystallized. At Ward Creek, the lower grade metabasites commonly preserve relict igneous textures. Maruyama and Liou (1988) documented a series of assemblages at Ward Creek, some with multiple overprinting generations of mineral growth present in the same rock, that suggest a prograde metamorphic evolution in the metabasites. Starting with metabasites with well-preserved igneous textures, riebeckite-crossite appears (± quartz, albite) with lawsonite and clinopyroxene. As grade increases, pumpellyite replaces lawsonite, clinopyroxene becomes more jadeite-rich, sodic am-

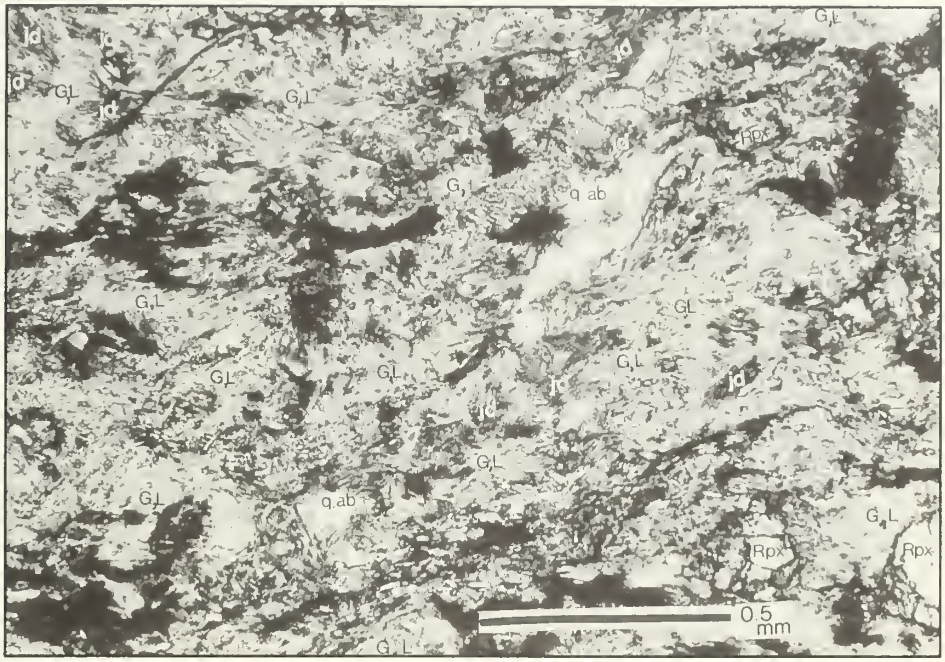

Figure 4. Photomicrograph of coherent blueschist facies metabasite from the North Berkeley Hills, Stop 1. G,L= fine grained sodic amphibole and lawsonite; q,ab=quartz and albite; jd=jadeitic clinopyroxene; Rpx=relict igneous clinopyroxene.

phibole becomes more aluminum-rich. At still higher grades, along with complete textural reconstitution, sodic amphibole coexists with actinolite, epidote becomes the dominant CaAl silicate, and clinopyroxene becomes somewhat poorer in jadeite. In places, an eclogitic assemblage of clinopyroxene+ garnet+sodic amphibole+epidote occurs (Oh, et al., 1991). At the very highest grade, winchite replaces the coexisting amphiboles. The intensity of tectonite fabric also increases with increasing grade. The Ward Creek and Pickett Peak terrane metabasites are the only coherent Franciscan metamorphic rocks that record blueschist-greenschist transition metamorphism. Most of the other Franciscan high P/T metabasites have mineral assemblages similar to the lower grade part of the metamorphic evolution at Ward Creek and have weak or absent tectonite fabric. Blueschist facies metabasites exposed in the North Berkeley Hills (Stop 1) show almost complete textural reconstitution and contain lawsonite, jadeitic pyroxene, albite, quartz, and glaucophane that is more Al-rich than amphi bole in lawsonite-zone metabasites at Ward Creek. So mewhat lower grade and less recrystallized rocks are present on Angel Island (Fig. 2). San Francisco Bay area coherent metabasites may be intermediate in grade between the Ward Creek Pickett Peak terrane rocks and coherent high P/T metabasites found elsewhere in the Franciscan.

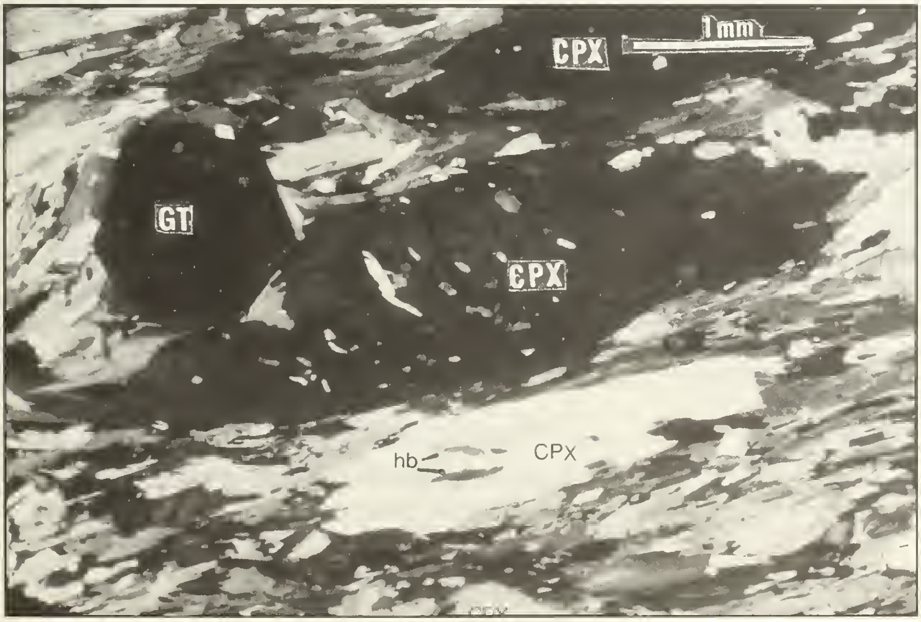

Figure 5. Photomicrograph of representative high-grade block from Tiburon Peninsula showing typical evidence of polymetamorphism. Finer grained minerals are mostly glaucophane, epidote and white mica. These minerals define a foliation that wraps around older garnet (GT) and omphacite (cpx). Inclusions in omphacite include quartz, albite, epidote, magnesio-taramite (hb) and clinopyroxene (cannot be seen in this view) that are poorer in jadeite component than the host. Inclusions in garnet (difficult to see in this view) include jadeite-poor clinopyroxene, epidote, quartz and albite.

Coherent metabasites-sub greenschist grade

Sub-greenschist facies metabasites have received the least attention of all Franciscan metamorphic rocks. These rocks commonly have well-preserved pillow structures and ophitic textures. Primary igneous minerals such as plagioclase, olivine and augite are locally well-preserved. Pillow rims have a metamorphic assemblages of pumpellyite, chlorite, quartz, prehnite and sphene. Vein minerals include pumpellyite, harmotome, quartz and laumontite. Amygdules may contain pumpellyite+chlorite, analcime+chlorite and calcite+chlorite assemblages (Swanson and Schiffman, 1979; Blake, et al., 1988). These rocks lack tectonite fabric, with the exception of incipient cleavage development in basaltic metatuffs in the Permanente terrane of the San Francisco Bay area (Wakabayashi, 1992). However, the Permanente terrane rocks also display local incipient blueschist metamorphism (Larue, et al., 1990).

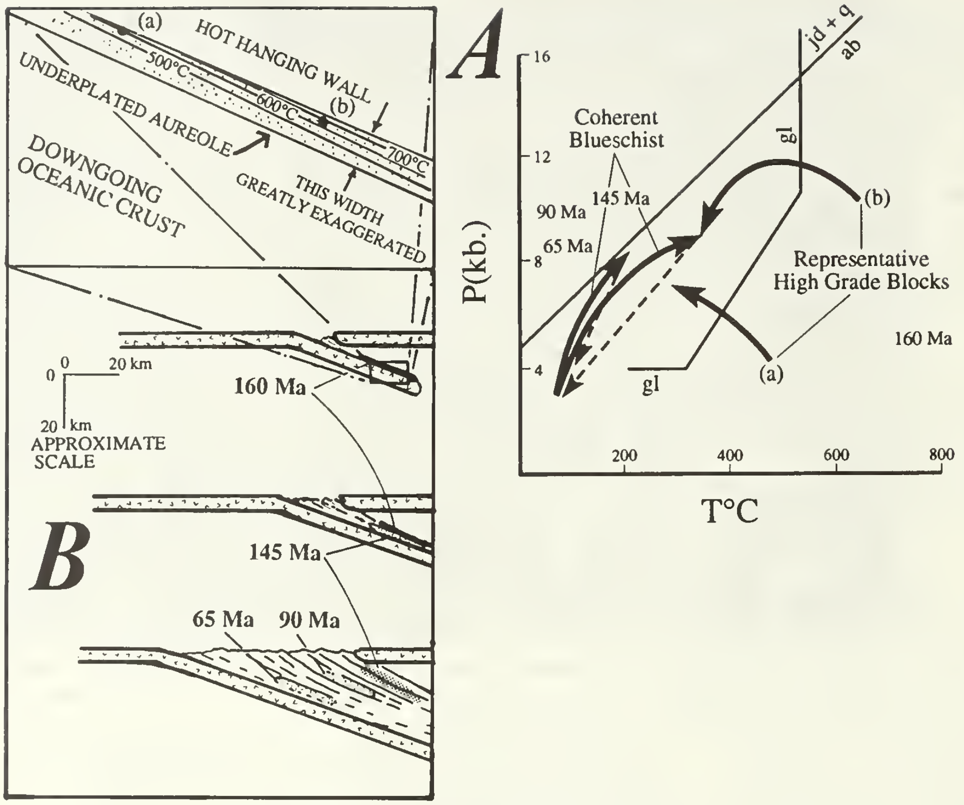

Figure 6. Adapted from Wakabayashi (1992)

A: Evolution of Franciscan metamorphism: P-T paths shown are for material subducted at about: (1) 160 Ma (two representative P-T paths for high-grade blocks shown), (2) 145 Ma (Ward Creek coherent blueschist), (3) 90Ma (Diablo Range) and 65 Ma (Permanente terrane). Note the drop in peak metamorphic temperatures with time, with most of the decrease within the first 15 Ma. A steady state subduction geotherm may have developed at or before 100 Ma. The cooling of the subduction complex is attributed to the dissipation of heat from the hanging wall of the subduction zone. gl: stability field of glaucophane from Maresch (1977); ab=jd+q: albite=jadeite + quartz from Newton and Smith (1967). Sources: (1) Wakabayashi (1990), (2) Maruyama and Liou (1988), (3) Maruyama et al. (1985), Larue et al. (1989).

B: Cartoons illustrating Franciscan metamorphic evolution. The cartoons depict the relative structural position of units subducted, underplated and metamorphosed at 160, 145, 90 and 65 Ma. Inset at top of figure is a schematic enlargement of the dynamothermal aureole formed during subduction initiation. The thickness of the aureole is greatly exaggerated. This inset illustrates the origin of the wide variation in peak metamorphic temperatures and pressures in Franciscan high grade blocks (Wakabayashi 1990). Temperature variation is influenced by rather small differences in distance from the hanging wall and pressure is influenced by depth of underplating in the subduction zone. Points (a) and (b) in the inset correspond to the two representative P-T paths for high-grade blocks shown in 'A'.

P-T CONDITIONS OF METAMORPHISM

High-grade blocks

Because of the presence of mineral assemblages that can be analyzed with well-known geothermometers or geobarometers, P-T estimates are easier in high-grade blocks than in other Franciscan metamorphic rocks though still quite difficult. Metamorphic temperatures are generally estimated with garnet-hornblende or garnet-clinopyroxene thermometry. Pressures are estimated by albite=jadeite+quartz sliding equilibria. P-T estimates have been difficult because of polymetamorphism and the comparative rarity of appropriate mineral assemblages. In many rocks it is possible to determine metamorphic temperatures for one stage of metamorphism, but it is rarely possible to determine pressure conditions in the same rock. Rarer still are samples in which P-T determinations are possible for multiple stages of metamorphism because quartz is often absent, and albite and clinopyroxene seldom coexist. Inspection of hundreds of samples is generally necessary to obtain rocks with appropriate assemblages and textural relationships. Careful analysis of crosscutting textural relationships, mineral zoning, and mineral inclusions have helped unravel the puzzle of these polymetamorphic high-grade rocks (Moore, 1984; Moore and Blake, 1989; Oh and Liou, 1990; Wakabayashi, 1990), although many details await further study. Polymetamorphism in Franciscan high-grade blocks records progressive metamorphism under conditions of decreasing geothermal gradient or a 'counterclockwise' P-T path (Wakabayashi, 1990) (see Fig. 6). Temperature estimates for the amphibolite phase of metamorphism range from 500°C to 700+°C (Wakabayashi, 1990; Moore and Blake, 1989) and pressures generally less than 10 kb (Wakabayashi, 1990). Eclogite overprints range from 450 to 550°C (Wakabayashi, 1990; Oh and Liou 1990) at 10-12 kb and higher (Wakabayashi, 1990; Oh and Liou, 1990). Blueschist overprints are under 400°C at 5-9 kb (Moore, 1984; Wakabayashi, 1990). Blueschist P-T conditions were not estimated directly but rather were estimated on the basis of comparison to similar Franciscan rocks and constrained by limiting reactions. One sample, from Mill Valley in Marin County, contains a diopside+ garnet+ pargasite assemblage that yielded garnet-clinopyroxene (Ellis and Green, 1979 calibration) and garnet-hornblende (Graham and Powell, 1984 calibration) temperatures of 790-900°C (Wakabayashi, 1987).

Coherent blueschists, blueschist greenschist transition rocks

In these rocks most of the geothermometry has been oxygen isotope thermometry conducted on samples from Ward Creek and the Pickett Peak terrane (J. Drotleff, oral comm. cited in

Blake, et al., 1988), and vitrinite reflectance (Blake, et al., 1988; Underwood, et al., 1988). Other temperature estimates have been based on comparison to similar assemblages with directly calculated temperatures. Once temperature has been estimated, pressure is generally estimated by using the albite=jadeite+quartz sliding equilibria, commonly with the constraint of the presence of aragonite. In addition, the Al content of sodic amphibole in blueschist-greenschist transition rocks has been used to determine pressure at Ward Creek (Maruyama, et al., 1986). At the well-studied Ward Creek locality, prograde metamorphism appears to define metamorphism under low geothermal gradients (lawsonite and lower pumpellyite zones of Maruyama and Liou, 1988) to approximately 180-220°C and 5-8 kb. These metamorphic conditions then evolved to somewhat higher geothermal gradients in the blueschist-greenschist transition rocks at 300-400°C and pressures of 8 kb or slightly higher (a 'clockwise' P-T path) (Maruyama and Liou, 1988). Similar relationships are found in the rocks of the Pickett Peak terrane (Blake, et al., 1988; Brown and Ghent, 1983). High P/T coherent metabasites in the Diablo Range and elsewhere are similar to lawsonite-zone Ward Creek rocks and appear to yield similar P-T estimates (P-T estimates given in published work for Diablo Range rocks are for related metagreywackes: e.g. Maruyama et al. 1985). Larue et al. (1989) have obtained similar P-T estimates for metabasalt with incipient blueschist metamorphism in the Permanente terrane of the San Francisco Bay area.

Coherent sub-greenschist facies rocks

Because of the lack of calibrated geothermometers and geobarometers for rocks of this grade, most P-T estimates have involved large uncertainties. However, these metabasites contain the index zeolite facies assemblage of laumontite + Fe-rich pumpellyite + prehnite. Metamorphism of these rocks is generally suggested to have taken place at 3 kb or less (Blake, et al., 1988; Liou, et al., 1986) and temperatures of less than 250°C (Blake, et al., 1988).

METAMORPHISM AND TECTONICS

As noted previously, the metamorphism of the high-grade blocks follows a counterclockwise P-T path. Wakabayashi (1990) suggested that the P-T path was the product of an evolving metamorphic event rather than an artifact of superimposed, unrelated tectonometamorphic episodes. This is based, in part, on the observations that:

(1) Metamorphism evolved from amphibolite through P-T conditions intermediate between initial amphibolite and final blueschist conditions;

(2) Geochronologic data suggests that amphibolite to blueschist evolution may have taken place in less than 5 Ma.

High-grade block isotopic ages can be summarized as follows:

(1) Amphibolite stage of metamorphism: 158-163 Ma (Ar-Ar incremental heating, hornblende, Ross and Sharp, 1988);

(2) Earliest blueschist metamorphism: 157-162 Ma (Ar-Ar incremental heating, sodic amphibole: Ross and Sharp (1986); and U-Pb isochron from blueschist: Mattinson (1986); K-Ar, actinolite from rind enclosing block: Coleman and Lanphere (1971); K-Ar, white mica: McDowell et al. (1984). Note that the rind has been observed to be coincident in time of crystallization with the last stage or stages of blueschist metamorphism in the blocks (Moore, 1984).

(3) Extended residence time under blueschist facies conditions: 159-138 Ma (K-Ar, white mica, Coleman and Lanphere, 1971; Suppe and Armstrong, 1972; McDowell, et al., 1984; and Ar-Ar incremental heating, white mica, Wakabayashi and Deino, 1989).

The P-T conditions and the age of metamorphism of late stage blueschist overprints in the high-grade blocks overlap the P-T conditions of metamorphism of the coherent blueschist. Ages of the highest grade coherent metamorphic rocks range from 110-146 Ma (K/Ar whole rock: Suppe and Armstrong, 1972 and Ar/Ar whole rock total fusion Lanphere, et al., 1978) with an age of 143 Ma from the Ward Creek unit (Ar-Ar incremental heating on white mica: Wakabayashi and Deino, 1989). Lower grade blueschist metamorphism continued until at least 80 Ma and possibly to 65 Ma (Wakabayashi, 1992).

Continuity in age and metamorphic conditions between high-grade suggests that both types of rocks formed during Franciscan subduction (Wakabayashi, 1992; Cloos, 1985; Suppe and Foland, 1978), rather than as a product of separate metamorphic and tectonic events (Coleman and Lanphere, 1971; Blake, et al., 1984). Among coherent metamorphic rocks, metamorphic ages and, generally, metamorphic grade decrease structurally downward.

A model for Franciscan metamorphic evolution

High-grade block precursors formed as amphibolites under the hot hanging wall of the just-initiated Franciscan subduction zone and were subsequently underplated to the upper plate (Platt, 1975; Suppe and Foland, 1978; Cloos, 1985). The large variation in P-T conditions of early amphibolite metamorphism can be explained by the extremely steep thermal gradient formed beneath the hot hanging wall and by differential depths of metamorphism down the subduction zone (Wakabayashi, 1990) (Fig. 6). The initial depth of amphibolite metamorphism strongly influenced the type of retrograde metamorphism (Wakabayashi, 1990). For example, eclogitic assemblages overprint only higher pressure amphibolites. Low pressure amphibolites do not have eclogitic overprints. With continued subduction, the hanging wall cooled rapidly and the amphibolites were overprinted with assemblages of higher P/T ratio. The pressure increase noted during retrograde metamorphism (Fig. 6) may result from: (1) Imbrication of the upper plate after underplating, including shortening at upper crustal levels as well as imbrication of the underplating unit itself; and/or (2) Plucking of pieces of the underplated material by flow melange (e.g. Cloos 1984) that circulates rocks to deeper levels under cooler conditions than at the initiation of underplating. The upper mantle wedge present above the zone of amphibolite formation in the subduction zone may have been the source for the serpentinite that is commonly found in close association with the blocks. The metamorphic ages of the block rinds are within the same range as amphibolite metamorphism in the blocks. In addition, at one locality, rind material is tightly folded into the margin of a block and includes the relatively high temperature metaultramafic assemblage of tremolite+talc+chlorite (Liou, 1990). These relationships suggest that the blocks were in contact with ultramafic material while still at elevated temperatures. Although they have been emplaced into melange zones at different structural levels in other Franciscan regions, over 99% of the high-grade blocks in the San Francisco Bay area section (Fig. 2) occur in the structurally highest Franciscan horizon above coherent blueschists (Wakabayashi 1992). The structural level of the high-grade blocks in the San Francisco Bay area may reflect the original horizon of high-grade block accretion (Wakabayashi 1992). Explanations for high-grade block emplacement at lower structural levels are complex and are discussed in detail in Wakabayashi (1992) and references therein.

Based on structural, petrologic and geochronologic data, Franciscan coherent blueschists may be interpreted to represent a unit subducted after and underplated structurally below the accretionary horizon of the high-grade blocks. The structurally highest and highest grade Pickett Peak terrane and the correlative Ward Creek/Skaggs Springs blueschists were accreted and metamorphosed first, followed by the Yolla Bolly terrane/Diablo Range. The trend of decreasing peak metamorphic temperatures and decreasing apparent geothermal gradient with decreasing age (Fig. 6) may be attributed to the continued dissipation of heat from the hot hanging wall of the subduction zone. Most of the temperature decrease occured within the first 15 Ma or less after subduction initiation, as predicted by thermal models (Cloos, 1985; Peacock, 1988). Sub-blueschist grade blocks represent rocks that were not subducted to great enough depths for blueschist facies metamorphism. In the lowest grade metabasites it is difficult to determine whether the metamorphism is the product of burial or sea floor metamorphism (Swanson and Schiffman, 1979).

Franciscan high P/T rocks do not have greenschist or amphibolite overprints typical of many other high P/T terranes (Ernst 1988) suggesting that: (1) subduction was uninterrupted during the time span of high P/T metamorphism; and (2) high P/T rocks were uplifted to shallow crustal levels before the cessation of subduction (note that subduction apparently continued for at least 40 Ma after the metamorphism of the youngest exposed high P/T rocks). Given no interruption in subduction, one curiosity is why the P-T path of the highest-grade coherent metamorphic rocks is somewhat clockwise (Maruyama and Liou 1988). One explanation is that although the subduction zone had cooled significantly by the time of peak metamorphism in these rocks, the apparent geothermal gradient produced during transit on the downgoing plate will always be lower than the ambient one (except, possibly, under conditions such as the subduction of very young ocean crust or a hot spot in an old subduction zone). The 'inflection point' in the P-T path, whereby metamorphism apparently started to evolve to higher thermal gradient, probably corresponds to the underplating of the unit as it was physically transferred to the upper plate (Maruyama and Liou, 1988). If the slower apparent increase in pressure through the inflection point is real, it may reflect the continued imbrication (duplexing etc.), and resulting deeper burial, taking place after the unit was transferred to the upper plate.

Peak conditions of metamorphism for the younger, lower grade coherent blueschists were so low that there is little evidence of any 'inflection' point in the P-T path. This is probably because: (a) At the low temperatures that prevailed during the subduction path, P-T conditions of are poorly constrained and/or (b) Temperatures on the subduction path were so low and transit time was so short that little metamorphic mineral growth of any kind took place until underplating of the unit.

ROAD LOG

Directions to Stop 1

From San Francisco, take Interstate highway 80 east. From Sacramento or Davis, take Interstate highway 80 west. From Interstate highway 80 take the Potrero Avenue exit and head east to San Pablo Avenue, then turn right (south). Proceed south on San Pablo Avenue to Moeser Avenue, then turn left (east). Proceed east on Moeser Avenue until the road steepens and there is an open field to the left. This is part of a large landslide complex (such old landslides are numerous in this area and many of the homes visible in the area are built on such deposits) that includes many high-grade blocks that can be observed as isolated outcrops sticking out of the grass. Continue on Moeser Avenue until Arlington Blvd, then turn left (north). Proceed north on Arlington past a small park and turn right (east) onto Thors Bay road, a short steep road. The trace of the active Hayward fault crosses the road where it steepens after leaving Arlington Blvd.. After two short, steep blocks the road curves left (north), and the outcrop is on to the right (east).

Stop 1

Coherent blueschist facies metabasites
at Thors Bay Rd., El Cerrito hills

Most of the Franciscan exposures in this part of eastern San Francisco Bay area comprise a set of east-dipping nappes (Wakabayashi 1992)(see Fig.2,3), but this particular locality is in a narrow, kilometer-wide belt that has been disrupted by Neogene strike-slip faulting associated with the Hayward fault. The outcrop is part of a fault-bounded slice of coherent blueschist-grade metavolcanic rock. The rock exhibits a pronounced tectonite fabric. Igneous textures have been almost completely obliterated by metamorphic mineral growth, and the fine-grained metamorphic assemblage (minerals generally less than 0.3 mm in size) includes sodic amphibole (9-10.5% Al_2O_3)+ lawsonite+ jadeitic pyroxene (about jadeite 80)+ quartz + albite , with some relict igneous clinopyroxene (see photomicrograph Fig. 4). Locally, 'intermediate' acmitic clinopyroxene mantles the relict clinopyroxene and is in turn rimmed by fibrous jadeitic pyroxene.

Directions to Stop 2

From stop 1 reverse directions back toward San Pablo Ave.. After descending Moeser Lane to San Pablo, turn left (south) on San Pablo, then immediatly right (west) on Plumas, a short street that leads to Carlson Blvd. At Carlson Blvd. turn right (northwest) and follow Carlson, passing underneath Interstate 80 and, shortly thereafter, turn left on Bayview, and then right onto Interstate Highway 580 (bound for the Richmond-San Rafael Bridge). After crossing the Richmond-San Rafael bridge, exit on

Sir Francis Drake Blvd. and drive west. As you approach U.S. Highway 101, get into the left lane and, after passing under Highway 101, turn left onto a ramp to head south on Highway 101. After passing through a tunnel, and just before reaching the Golden Gate Bridge, exit right. Immediately after exiting, turn left (south) at the stop sign. Shortly after making this turn, turn right (west) and start up a hill with spectacular views of the Golden Gate Bridge and San Francisco to the left (south). The rocks in the roadcuts along this road are the cherts, basalts and grey-wackes of the Marin Headlands terrane, a coherent Franciscan unit that is metamorphosed in the zeolite to prehnite-pumpellyite facies (Swanson and Schiffman 1979). The Marin Headlands terrane is a unit that displays good evidence of internal imbrication that may have taken place during the underplating or off-scraping process. The depositional sequence of basalt-chert-greywacke is repeated by multiple thrust faults and the resultant thrust sheets dip to the south. (Wahrhaftig 1984a) At a fork in the road at a saddle, turn right (north) and head downhill. At the bottom of this grade turn left (west) and continue until just short of a lagoon, then take a left fork and follow signs to the Point Bonita lighthouse hiking trail parking lot.

From this parking lot take a paved hiking trail toward the Point Bonita lighthouse. This short hike is one of the most picturesque in the entire San Francisco Bay region, with unsurpassed views of the Golden Gate area, San Francisco and the rugged Marin Headlands coast (Note that the lighthouse and the most scenic part of the trail are only open on weekends from 12:30-3:30 p.m.). Just before reaching our pillow basalt outcrop, pass a saddle in the ridge where a melange zone crosses it. This melange may represent part of the tectonic contact between the Marin Headlands terrane to the north and different rocks to the south (and structurally higher). The rocks to the south differ from those of the Marin Headlands terrane (although they are similar in degree of metamorphism) in that the basalts are of different chemical composition (alkali basalt versus MORB) and locally contain interpillow limestone (Shervais 1989). These rocks have been called the Point Bonita slice by Wakabayashi (1992) and tentatively correlated to the Nicasio Reservoir terrane, a terrane containing similar basalts. Several kilometers to the north, the Nicasio Reservoir terrane occupies an analogous structural horizon above Marin Headlands type rocks.

Stop 2

Franciscan pillow basalts at Point Bonita

After passing the above-mentioned saddle, several hundred meters from the parking lot, a cliff on the uphill side of the trail exposes pillow basalts. A much better pillow basalt locality displaying excellent three-dimensonal pillow forms is found nearby at Bonita Cove, a locality that requires somewhat more walking and is described in detail in Wahrhaftig (1984b). These basalts exhibit nearly complete preservation of igneous textures and variable preservation of igneous mineralogy. Metamorphic minerals include pumpellyite, prehnite, chlorite, laumontite, analcime and albite (Swanson and Schiffman 1979).

Directions to Stop 3

Leaving the Point Bonita parking lot, reverse direction back toward Highway 101. Just before reaching Highway 101, turn left (north) and, after crossing beneath Highway 101, make a right turn onto a ramp that loops onto north-bound Highway 101. Travel north on Highway 101 to the Tiburon Blvd. exit, then exit east-bound. Take Tiburon Blvd. to Trestle Glen Blvd., then turn left (east) and continue on Trestle Glen Blvd. to the crest of the hill. At the crest, turn left (north) onto a church driveway to a parking lot. From the parking lot, take a hiking trail to the northwest.

Stop 3

High-grade blocks of Tiburon Peninsula.

After walking a few hundred meters, the first of many high-grade blocks comes into view just to the right (north) of the trail (this block appears very dark-colored from a distance). Of many localities with Franciscan high-grade blocks, Tiburon Peninsula is probably the best because of the amazing variety of assemblages seen in the blocks there. Amphibolites, eclogites, and blueschists occur, and, in many blocks, the metamorphic evolution of amphibolite to eclogite to blueschist can be seen. A map showing the locations of the largest tectonic blocks is presented in Liou (1990). Please note this locality is part of a park in which collecting samples of the rocks is prohibited without a special permit from the Nature Conservancy. High-grade blocks are exposed in a melange at Tiburon that represents the highest structural level in the Franciscan (Wakabayashi, 1992) (Fig. 3). The tectonic blocks are enclosed by either a serpentinite or shale matrix, although the matrix is rarely exposed. During construction of a housing development near the crest of the ridge, good exposures of serpentinite matrix were seen. Most of the serpentinite is chrysotile and/or lizardite, but locally antigorite is preserved (Wakabayashi 1992).

The first block seen along the trail is an excellent example of one which records the sequential evolution from amphibolite to eclogite to blueschist. On one side of the block the garnet epidote amphibolite has suffered little retrograde metamorphism. Walking around the block from this side you can see vein-like areas and pockets of eclogitic retrograde metamorphism. In one area of the block, the rock is essentially an eclogite, assemblage that is overprinted by blueschist assemblages in another area. The mineral chemistry and petrography of the block is described in Wakabayashi (1990) (sample TIBB in that paper). A representative photomicrograph of a different block is shown in Fig. 5.

Returning to the trail, continue to walk in a northwesterly direction and, after passing a large block in the shade of a tree on the left, angle left off the trail and walk about 400 meters across the rolling, grass-covered slope to a very large block (over 20 m in size). The hummocky terrain observed on these slopes is typical of areas underlain by Franciscan melange. The landform is influenced by the extreme contrast in weathering resistance between the blocks and matrix and by numerous landslides. This block is described in Liou (1990) and is a particularly good example of textural relationships between a high-grade block and its rind. The rind appears to be tightly folded along with one of the later stages of folding in the block. The infolded rind material contains the relatively high temperature assemblage tremolite+talc+chlorite (Trommsdorff and Evans, 1974). These relationships suggest that the block was in contact with ultramafic material at rexlatively high temperatures, probably in the hanging wall of the subduction zone.

ACKNOWLEDGEMENTS

Janice Fong, illustrator for the Department of Geology at U.C. Davis, assisted with the drafting of the figures. D. E. Moore and J. G. Liou provided helpful, constructive reviews.

REFERENCES

Bailey, E. H., Irwin, W. P., and Jones, D. L., 1964, The Franciscan and related rocks and their significance in the geology of western California: California Division of Mines and Geology Bulletin 183, 177p.

Blake, M. C., Jr.; Howell, D. G., and Jayko, A. S., 1984, Tectonostratigraphic terranes of the San Francisco Bay Region, in Blake, M. C., Jr., ed., Franciscan geology of northern California: Pacific Section of the Society of Economic Paleontologists and Mineralogists, v. 43, p. 5-22.

Blake M. C., Jr.,; Jayko, A. S.; McLaughlin, R. J.; and Underwood, M. B., 1988, Metamorphic and tectonic evolution of the Franciscan Complex, northern California: in Ernst, W. G., ed., Metamorphism and crustal evolution of the western United States: Rubey Volume VII, p. 1035-1060.

Brown, E. H., and Ghent, E. D., 1983, Mineralogy and phase relations in the blueschist facies of the Black Butte and Ball Rock areas, northern California Coast Ranges: American Mineralogist, v. 68, p. 365-372.

Cloos, M., 1984, Flow melanges and the structural evolution of accretionary wedges: Geologic Society of America Special Paper 198, p. 71-80.

Cloos, M., 1985, Thermal evolution of convergent plate-margins: thermal modelling and re-evaluation of isotopic Ar-ages for blueschists in the Franciscan Complex of California: Tectonics, v. 4, p. 421-433.

Coleman, R. G., and Lanphere, M. A., 1971, Distribution and age of high-grade blueschists, associated eclogites, and amphibolites from Oregon and California: Geological Society of America Bulletin, v. 82, p. 2397-2412.

Coleman, R. G., and Lee, D. E., 1963, Glaucophane-bearing metamorphic rock types of the Cazadero area, California: Journal of Petrology, v. 4, p. 260-301.

Dickinson, W. R., 1970, Relations of andesites, granites and derivative sandstones to arc-trench tectonics: Reviews in Geophysics and Space Physics, v. 8, p. 813-860.

Ellis, D. J., and Green, D. H., 1979, An experimental study of the effect of Ca upon garnet-clinopyroxene Fe-Mg exchange equilibria: Contributions to Mineralogy and Petrology. v. 71, p. 13-22.

Ernst, W. G., 1965, Mineral parageneses of Franciscan metamorphic rocks, Panoche Pass, California: Geological Society of America Bulletin, v. 76, p. 879-914.

Ernst, W. G., 1970, Tectonic contact between the Franciscan melange and the Great Valley Sequence, crustal expression of a Late Mesozoic Benioff Zone: Journal of Geophysical Research, v. 75, p. 886-902

Ernst, W. G., 1971, Do mineral parageneses reflect unusually high pressure conditions of Franciscan metamorphism?: American Journal of Science, v. 271,p. 81-108.

Ernst, W. G., 1988, Tectonic history of subduction zones inferred from retrograde blueschist P-T paths: Geology, v. 16, p. 1081-1084.

Ernst, W. G., Seki, Y.; Onuki, H.; and Gilbert M. C., 1970, Comparative study of low-grade metamorphism in the California Coast Ranges and the outer metamorphic belt of Japan: Geological Society of America Memoir 124, 276 p.

Graham, C. M., and Powell, R., 1984, A garnet-hornblende geothermometer: calibration, testing, and application to the Pelona schist, southern California: Journal of Metamorphic Geology, v. 2, p. 13-31.

Hamilton, W. B., 1969, Mesozoic California and underflow of the Pacific mantle: Geol. Soc. America Bull., v. 80, p. 2409-2430.

Lanphere, M. A., Blake, M. C., Jr., and Irwin, W. P., 1978, Early Cretaceous metamorphic age of the South Fork Mountain Schist in the northern Coast Ranges of California: American Journal Science, v. 278, p. 798-815.

Larue, D. K., Barnes, I., and Sedlock, R. L., 1989, Subduction and accretion of the Permanente terrane near San Francisco, California: Tectonics, v. 8, p. 221-235.

Liou, J. G., 1990, High grade blueschists and eclogites in Franciscan serpentinite melange at Ring Mountain, Tiburon: in Wahrhaftig, C., and Sloan, D., eds., Geology of San Francisco and Vicinity, 28th International Geological Congress Field Trip Guidebook T105, p. 44-45.

Liou, J. G., Maruyama, S., Coleman, R. G., and Gilbert, M. C., 1986, Field trip guidebook to Franciscan blueschists and eclogites in northern California: 14th General Meeting International Mineralogical Association.

MacPherson, G. J., 1983, The Snow Mountain complex: an on-land seamount in the Franciscan terrain, California: Journal of Geology, v. 91, p. 73-92.

MacPherson, G. J., Phipps, S. P., and Grossman, J. N., 1990, Diverse sources for igneous blocks in Franciscan melanges, California Coast Ranges: Journal of Geology, v. 98, p. 845-862.

Maresch, W. V., 1977, Experimental studies on glaucophane: An analysis of present knowledge: Tectonphysics, v. 43, p. 109-125.

Maruyama, S. and Liou, J. G., 1988, Petrology of Franciscan metabasites along the jadeite-glaucophane type facies series, Cazadero, California: Journal of Petrology, v. 29, p. 1-37.

Maruyama, S., Liou, J. G. and Sasakura, Y., 1985, Low-temperature recrystallization of Franciscan graywackes from Pacheco Pass, California: Mineralogical Magazine, v. 49, p. 345-355.

Maruyama, S., Liou, J. G., and Seno, , 1989, Possible depth limit of underplating by a seamount: Tectonophysics, v. 160, p. 327-339.

Maruyama, S; Cho, M.; and Liou, J. G., 1986, Pressure dependence of Al2O3 contents in sodic amphibole-a new geobarometer: Geological Society of America Memoir 164, p. 1-16.

Mattinson, J. M., 1986, Geochronology of high-pressure-low-temperature Franciscan metabasites: A new approach using the U-Pb system: Geological Society of America Memoir 164, p. 95-105.

McDowell, F., Lehman, D. H.,Gucwa, P. R., Fritz, D., and Maxwell, J. C., 1984, Glaucophane schists and ophiolites of the northern California Coast Ranges: isotopic ages and their tectonic implications: Geological Society of America Bulletin v. 95, p. 1373-1382.

Moore, D. E., 1984, Metamorphic history of a high-grade blueschist exotic block from the Franciscan Complex, California: Petrology, v. 25, p. 126-150.

Moore, D. D., and Blake, M. C., Jr., 1989, New evidence for polyphase metamorphism of glaucophane schist and eclogite exotic blocks in the Franciscan Complex, California and Oregon: Journal of Metamorphic Geology, v. 7, p. 211-228.

Newton, R. C., and Smith, J. V., 1967, Investigations concerning the breakdown of albite at depth in the earth: Journal Geology, v. 75, p. 268-286.

Oh, C. W., and Liou, J. G., 1990, Metamorphic evolution of two different eclogites in the Franciscan Complex, California, USA: Lithos, v. 25, p. 41-54.

Oh, C. W., Liou, J. G., and Maruyama, S., 1991, Low-temperature eclogites and eclogitic schists in Mn-rich metabasites in Ward Creek, California; Mn and Fe effects on the transition between blueschist and eclogite: Journal Petrology, v. 32, p. 275-301.

Peacock, S. M., 1988, Inverted metamorphic gradients in the westernmost Cordillera: in Ernst, W. G., ed., Metamorphism and crustal evolution, western United States, Rubey Volume VII, Prentice-Hall, New Jersey, p. 954-975.

Platt, J. P., 1975, Metamorphic and deformational processes in the Franciscan Complex, California: Some insights from the Catalina Schist terrane: Geological Society of America Bulletin, v. 86, p. 1337-1347.

Ross, J. A., and Sharp, W. D., 1986, 40Ar/39Ar and Sm/Nd dating of garnet amphibolite in the Coast Ranges, California: EOS, v. 67, p. 1249

Ross, J. A., and Sharp, W. D., 1988, The effects of sub-blocking temperature metamorphism on the K/Ar systematics of hornblendes: 40Ar/39Ar dating of polymetamorphic garnet amphibolite from the Franciscan Complex, California: Contributions to Mineralogy and Petrology, v. 100, p. 213-221.

Seiders, V. M., 1991, Conglomerate stratigraphy and tectonics in the Franciscan assemblage of northern California and implications for Cordilleran tectonics: U. S. Geological Survey Open File Report, OFR 91-50, 21p.

Shervais, J. W., 1989, Geochemistry of igneous rocks from Marin Headlands: in Wahrhaftig, C., and Sloan, D., eds., Geology of San Francisco and Vicinity, International Geological Congress Field Trip Guidebook T105, p. 40-41.

Suppe, J., and Armstrong, R. L., 1972, Potassium-argon dating of Franciscan metamorphic rocks: American Journal of Science, v. 272, p. 217-233.

Suppe, J., and Foland, K. A., 1978, The Goat Mountain Schists and Pacific Ridge Complex: A redeformed, but still intact, late Mesozoic schuppen complex; in Howell, D. G., and McDougall, K. A., eds., Mesozoic paleogeography of the western United States, Pacific Section, Society of Economic Paleontologists and Mineralogists, Pacific Coast Paleogeography Symposium 2, p. 431-451.

Swanson, S. E., and Schiffman, P., 1979, Textural evolution and metamorphism of pillow basalts from the Franciscan Complex, western Marin County, California: Contributions to Mineralogy and Petrology, v. 69, p. 291-299.

Tarduno, J. A., McWilliams, M. O., Debiche, M. G., Sliter, W.V., and Blake, M. C., Jr., 1985, Franciscan Complex Calera limestones: accreted remnants of Farallon Plate oceanic plateaus: Nature, v. 317, p. 345-347.

Trommsdorff, V., and Evans, B. W., 1974, Alpine metamorphism of peridotitic rocks: Schweiz. Mineral. Petrogr. Mitteil., v. 54, p. 333-352.

Underwood, M. B., O'Leary, J. D., and Strong, R. H., 1988, Contrasts in thermal maturity within terranes and across terrane boundaries of the Franciscan Complex, northern California: Journal of Geology, v.96, p. 809-817.

Wahrhaftig, C., 1984a, Structure of the Marin Headlands block, California: A progress report: in Blake, M. C., ed., Franciscan Geology of Northern California, Pacific Section, Society of Economic Paleontologists and Mineralogists, v. 43, p. 31-50.

Wahrhaftig, C., 1984b, A Streetcar to subduction and other plate tectonic trips by public transportation in San Francisco: American Geophysical Union, 72 p.

Wakabayashi, J., 1987, Amphibolite grade metamorphism of Franciscan rocks from the San Francisco Bay area, California: Geological Society of America Abstracts with Programs, v. 19, p. 460.

Wakabayashi, J., 1990, Counterclockwise P-T-t paths from amphibolites, Franciscan Complex, California: relics from the early stages of subduction zone metamorphism: Journal of Geology, v. 98, p. 657-680.

Wakabayashi, J., 1992, Nappes, tectonics of oblique plate convergence and metamorphic evolution related to 140 million years of continuous subduction, Franciscan Complex, California: Jour. Geology, v. 100, p. 19-40.

Wakabayashi, J., and Deino, A., 1989, Laser-probe 40Ar/39Ar ages from high grade blocks and coherent blueschists. Franciscan Complex, California: Preliminary results and implications for Franciscan tectonics: Geological Society of America Abstracts with Programs, v. 19, p. A267.

TECTONIC SETTING AND METAMORPHISM OF THE SIERRA NEVADA, CALIFORNIA

HOWARD W. DAY
Department of Geology
University of California
Davis, California 95616

INTRODUCTION

It is an article of faith among petrologists that the tectonic setting of metamorphic rocks is an indicator of the process or controls on metamorphism, but the link between tectonic setting and the details of thermal history is poorly defined. Most Phanerozoic metamorphic belts are exposed in orogenic belts that were originally at continental margins. Continental collision zones and ocean-continent subduction zones, such as the Alps and the California Coast Ranges, are perhaps the most familiar examples. The nature of metamorphism and the thermal history in arc-continent collision zones, intra-oceanic subduction zones, and transform margins has been little studied, however, and even the basic characteristics have not been examined systematically. The Sierra Nevada of California (Fig. 1) have been the site of active continental margin tectonic processes since the early Paleozoic and offer an opportunity to study the relationship among tectonic setting, metamorphism and thermal processes at a long-lived continental margin.

The broad outline of the history of the continental margin in California is reasonably well-established (Burchfiel and Davis, 1972; Dickinson, 1981) (Fig. 1). Precambrian igneous and metamorphic rocks are exposed in southeastern California and the limits of Precambrian basement have been inferred from the western and northern limits of Mesozoic igneous rocks having initial 87Sr/86Sr ratios of 0.706 or greater (Fig. 1) (Kistler and Peterman, 1973). A continental margin was probably first established during the late Precambrian when miogeoclinal sedimentary rocks were deposited unconformably across the trends of all major Precambrian age belts (Dickinson, 1981). In southeastern California, a miogeoclinal sequence of Lower Paleozoic sedimentary rocks was deposited, but in the northern Sierra Nevada, pre-Upper Devonian metasedimentary rocks were deposited in continental rise or slope-rise environments (Bond and DeVay, 1980). The pre-Upper Devonian metasedimentary rocks are overlain by three younger volcanic-plutonic complexes that were formed in continental or near-continental marine settings during the Devonian, Permo-Triassic, and Middle Jurassic periods (Hannah and Moores, 1986). Triassic truncation of the continental margin has been inferred from the abrupt termination of Precambrian - Paleozoic structural, sedimentary, and geochronological trends by Mesozoic lithotectonic belts, but the nature of that truncation remains controversial (Burchfiel and Davis, 1972; Saleeby, 1981). During the Jurassic, marine sedimentary and volcanic rocks, and arc-ophiolite suites were added to the continental margin and occupy the inferred zone of Triassic truncation. Whether these rocks formed near the continental margin or are far-traveled terranes remains an open question (Burchfiel and Davis, 1981; Moores and Day, 1984; Schweickert and Cowan, 1975). Jurassic and Cretaceous glaucophane schists in the coastal Franciscan Complex mark the onset of oceanic subduction and continental accretion that persisted into the Tertiary Era. The Sierra Nevada batholith was emplaced mostly during that time and is commonly regarded as a magmatic arc overlying the Franciscan subduction zone (Miyashiro, 1973). However, granitoid intrusions are also important elements of the Paleozoic, Triassic and Jurassic history of the continental margin. Eocene auriferous gravels and Miocene and Pliocene volcanic rocks mantle much of the Sierra Nevada. Tertiary sedimentary

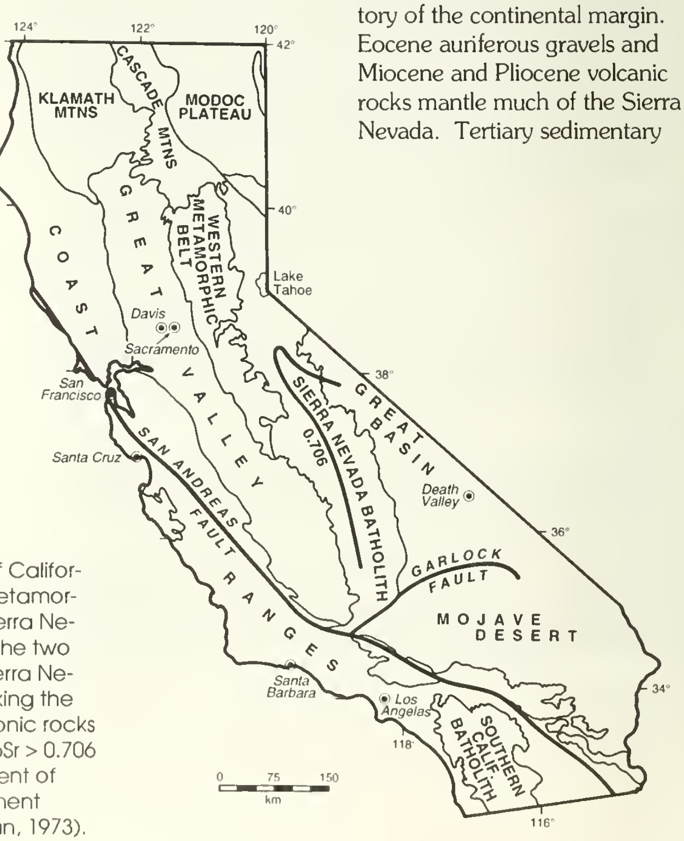

Fig. 1. Index Map of California. The Western Metamorphic Belt and the Sierra Nevada Batholith are the two main parts of the Sierra Nevada. The line marking the western limit of plutonic rocks having initial 87Sr/86Sr > 0.706 may indicat the extent of Precambrian basement (Kistler and Peterman, 1973).

and volcanic rocks in coastal California record the transition from subduction to transform tectonics at the continental margin.

Much of the history of the active continental margin is recorded in the Western Sierra Nevada Metamorphic Belt (Fig. 1), which contains all metamorphosed and deformed rocks west of the Sierra Nevada batholith and east of the sedimentary rocks in the Great Valley (Clark, 1964). At least three orogenic events are recorded in the deformation of the Western Metamorphic Belt, which correspond to the Devonian "Antler", Permo-Triassic "Sonoman", and Jurassic "Nevadan" Orogenies (Dickinson, 1981). Each is marked by a profound angular unconformity. In the Eastern Belt of the Sierra (Fig. 2), pre-late Devonian and pre-late Triassic unconformities are well-documented (Hannah and Moores, 1986; Harwood, 1983; Harwood, 1988; Varga and Moores, 1981) . In the Western Belt, at the eastern edge of the Great Valley, (Fig. 2), undeformed, Upper Cretaceous and Tertiary sedimentary rocks unconformably overlie penetratively deformed, Upper Jurassic and older metamorphic rocks (Whitney, 1865). The major regional faults that control the present distribution of rocks in the Western Metamorphic Belt (Fig. 2) are known collectively as the Foothills Fault System (Clark, 1960) and are largely artifacts of the Jurassic Nevadan deformation.

The purpose of this contribution is to introduce the tectonic setting, age and conditions of metamorphism in the Western Metamorphic Belt north of latitude 39° N, where the pre-batholithic rocks are exposed over a wide expanse. Although the tectonic history remains controversial and the metamorphic history of the Sierra is poorly known, several major points emerge from the available data: (1) Major regional faults tectonically juxtapose rocks of significantly different age and metamorphic grade; (2) The Western, Central and parts of the Feather River Belts (Fig. 2) contain late Paleozoic and Mesozoic volcanic arc, ophiolitic and marine sedimentary assemblages that were amalgamated with the Eastern Belt during the Jurassic Nevadan deformation; (3) There have been several episodes of Paleozoic and Mesozoic low grade metamorphism; (4) Much of the low grade metamorphic character of Sierran rocks may have been acquired in volcanic arc or other oceanic settings prior to, and modified during, the latest phases of Nevadan deformation; (5) There is little unambiguous regional metamorphism associated with the Cretaceous intrusion of the Sierra Nevada batholith.

GEOLOGIC SETTING

The Western Metamorphic Belt (Fig. 3) is bounded on the east by Tertiary rocks and Mesozoic granitoid batholiths, on the north by Tertiary and Quaternary volcanic rocks and is overlain unconform- ably on the west by unmetamorphosed, Upper Cretaceous and Tertiary sedimentary rocks in the Great Valley. Steep faults of the Foothills Fault System define at least four lithotectonic belts that extend along strike for about four hundred kilometers in the Sierra and may have counterparts in the Klamath Mts. of northern California and Oregon. The faults deform Upper Jurassic rocks, but their history, sense of movement, and tectonic significance are poorly known and controversial (Burchfiel and Davis, 1981; Clark, 1960; Day, et al., 1985; Edelman, et al., 1989; Moores and Day, 1984; Saleeby, 1981; Schweickert and Cowan, 1975; Tobisch, et al., 1989).

The Eastern Belt (Fig. 3) comprises early Paleozoic siliciclastic sedimentary rocks on which Devonian-Mississipian, Permo-Triassic, and early - middle Jurassic volcanic rocks were deposited (D'Allura, et al., 1977; Hannah and Moores, 1986; Harwood, 1988). Although the sedimentary basement rocks are exposed throughout the length of the belt, the volcanic sequences are restricted to regions north of latitude 39°N. The early Paleozoic sedimentary rocks were probably deposited in a continental slope or rise environment (Bond and DeVay, 1980) and the Paleozoic-Mesozoic section may have been at or near the continental margin throughout its history. In the northern Sierra, the continental margin assemblage in the Eastern Belt is separated from primarily Mesozoic oceanic rocks to the west by the fault-bounded Feather River Belt (Day, et al., 1985), which contains Paleozoic metaperidotite, serpentinite, and associated mafic rocks as well as Mesozoic blueschist . The Feather River Belt apparently passes southward into the so-called Calaveras-Shoo-Fly thrust (Schweickert, 1981).

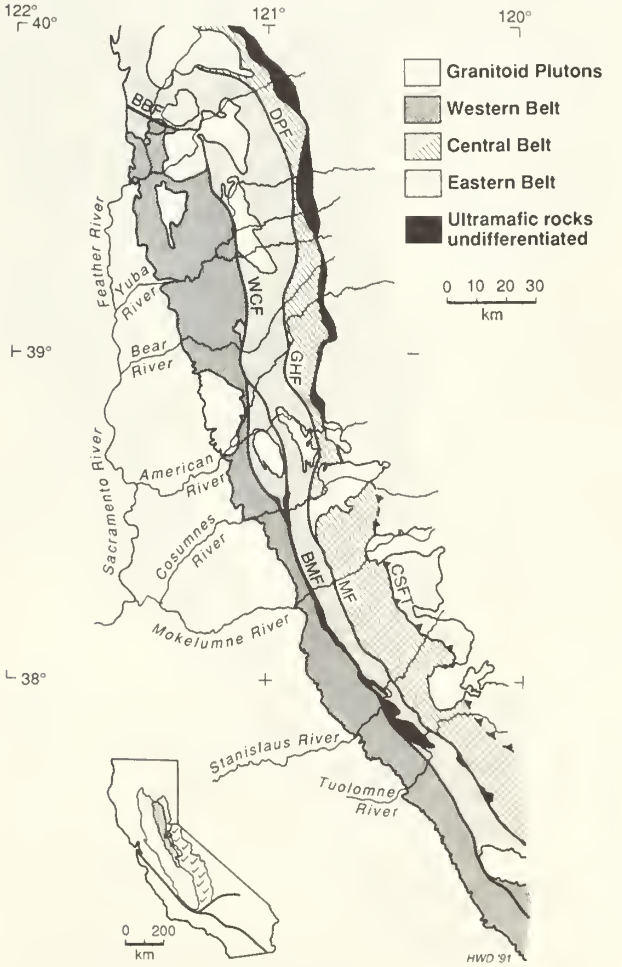

Fig. 2. Lithotectonic Belts of the Western Metamorphic Belt, Sierra Nevada. Abbreviations for faults: BBF - Big Bend Fault; BMF - Bear Mountains Fault; CSFT - Calaveras Shoo Fly Thrust; DPF - Dogwood Peak Fault; GHF - Gillis Hill Fault - MF - Melones Fault; WCF - Wolf Creek Fault.

The Western and Central Belts (Fig. 2) contain primarily Jurassic assemblages of ophiolites and marine volcanic and sedimentary rocks that were added to the continental margin during Jurassic time. The Western Belt is dominated by Middle and Upper Jurassic volcanic and volcan- iclastic rocks with associated intrusive complexes. These rocks are interbedded with and overlain by Upper Jurassic, fine grained, siliciclastic sedimentary rocks with subordinate volcanogenic detritus. The Western and Central Belts are separated by a poorly understood, steep fault zone known as the Big Bend-Wolf Creek fault in the north and the Bear Mts. fault zone in the south.

The Central Belt (Fig. 2) is a structurally complex association of primarily Mesozoic ophiolite, volcanic arc assem- blages,and marine sedimentary rocks that is split into eastern and western halves by the Dogwood Peak - Gillis Hill - Melones fault zone ((Clark, 1960; Hietanen, 1976; Hietanen, 1981). The western half of the Central Belt is characterized by abundant early Jurassic ophiolite and volcanic arc assemblages and early Jurassic(?), fine-grained volcaniclastic sedimentary rocks and chert-argillite. In the south (Fig. 2), Middle and Upper Jurassic rocks similar to those in the Western Belt are exposed in the so-called Mother Lode Belt. The eastern half of the Central Belt contains the late Paleozoic - early Mesozoic Calaveras Complex in which a tripartite sequence of metavolcanic rocks, silici- clastic sedimentary rocks, and chert - argillite has been recognized at least since the early work of Turner (Turner, 1897). Some workers prefer to assign the volcanic rocks to a separate, fault - bounded terrane (Schweickert, et al., 1988), but there is no consensus on the matter (Paterson et al, 1991).

The Western, Central, and Eastern Belts can be recognized throughout the length of the Western Metamorphic Belt and have played a major role in applying concepts of terrane tectonics to the Sierra Nevada (Edelman, et al., 1989; Edelman and Sharp, 1989; Schweickert, et al., 1988). The belts are widest in the north and quite attenuated in the south, which may have contributed to significant differences among tectonic interpretations of workers who have concentrated their efforts in the south or in the north. This contribution emphasizes studies that have been completed in the area north of latitude 39o N, with which I am most familiar, and where preservation of some of the lithotectonic elements may be more complete (Fig. 3).

Western Belt

The Western Belt in the northern Sierra (Fig. 3) is occupied by the Jurassic Smartville Complex, including a rifted volcanic and plutonic arc, fragments of its sedimentary cover, and, perhaps, its basement (Beard and Day, 1987; Beiersdorfer, et al., 1991; Day, et al., 1985). It is bounded on the west by undeformed Upper Cretaceous and Tertiary sedimentary rocks and, on the north and east, by the Big Bend and Wolf Creek faults (Day, et al., 1985; Hietanen, 1977). Abundant isotopic and sparse fossil data suggest that the volcanic and intrusive rocks as well as their sedimentary cover were formed during a short interval near the Bathonian - Callovian or Kimmeridgian - Oxfordian boundaries (Harland, et al., 1990) . The former estimate is based numerous isotopic ages of about 161±2 Ma (Bickford and Day, 1988; Edelman, et al., 1989; Saleeby, et al., 1989) and the most recent time scale of Harland et al. (1990), whereas the latter is based on the fossils (Creely, 1965; Marlette, et al., 1979; Xenophontos, 1984).

The main part of the Smartville Complex is composed of basaltic to andesitic volcanic and volcaniclastic rocks (Jv, Fig. 4) intruded by hypabyssal and plutonic rocks (Beard and Day, 1987; Beard and Day, 1988). The volcanic units include a lower unit of pillowed and massive flows and a widespread upper unit of distinctive clinopyroxene - phyric pyroclastic and epiclastic breccias (Xenophontos, 1984). The hypabyssal rocks include exposures of 100% diabase dikes, which may be "sheeted" or "unsheeted", and areas in which the diabase appears to be massive and no dike structures can be detected (Jd, Fig. 4). Two unrelated suites of plutonic rocks appear to be coeval with the intrusion of the sheeted and unsheeted dikes. Elongate plutons of hornblende - biotite tonalite, granophyric tonalite and granodiorite (Jt, Fig. 4) are parallel to the strike of diabase dikes. Gabbro-diorite plutons (Jgb, Fig. 4) range greatly in size and also tend to be parallel to the strike of diabase dikes. The largest gabbro - diorite plutons are zoned continuously from olivine gabbro cores to quartz diorite rims (Beard and Day, 1988).

The basement on which the Jurassic volcanic arc was constructed has not been documented unambiguously anywhere in the Western Belt (Fig. 3). However, the oldest intrusive rocks in the Smartville Complex are massive metadiabase and metadiabase dikes associated with metagabbro screens and intrusions exposed in and north of a half-window on the southeastern margin and in the central parts of the Complex (not distinguished from Jd in Fig. 4) (Beard and Day, 1987). These units are cut by all other major intrusive bodies and they may be part of the basement on which the volcanic arc was constructed (Beiersdorfer, et al., 1991), but their relationship to the volcanic rocks is not exposed. In the easternmost Smartville Complex, 161 ± 2 Ma tonalite dikes and a related tonalite pluton, also dated at 161 ± 2 Ma, intrude 198 ± 2 Ma tonalite (the easternmost body of Jt, Fig. 4) (Bickford and Day, 1988; Edelman, et al., 1989; Souter and Day, 1991) suggesting that the basement of the volcanic arc included fragments of earlier volcano-plutonic complexes similar to those in the Central Belt. Edelman et al. (1989) suggested that the basement of the 160 Ma volcanic arc might include sedimentary rocks of the Central Belt similar to those exposed along its margin (EJs, Fig. 4), similar to earlier suggestions of Saleeby (1981) and Schweickert (1981).

Jurassic sedimentary cover (Js, Fig. 4) of the volcanoplutonic complex is exposed only in the northwestern part of the area (Day, et al., 1985) where it is known as the Monte de Oro Formation (Creely, 1965). The rocks are lithic quartz sandstones containing fragments of monocrystalline quartz, chert, slate, and volcanic detritus. In most places, the contacts with underlying rocks of the upper volcanic unit are faults, but an overturned depositional contact was reported in the northernmost Smartville Complex between rocks equivalent to the Monte de Oro and the upper volcanic unit (Vaitl, 1980). This sedimentary cover appears similar in age, lithology, and stratigraphic position to Upper Jurassic sedimentary rocks in the southern part of the Western Belt (Fig. 2).

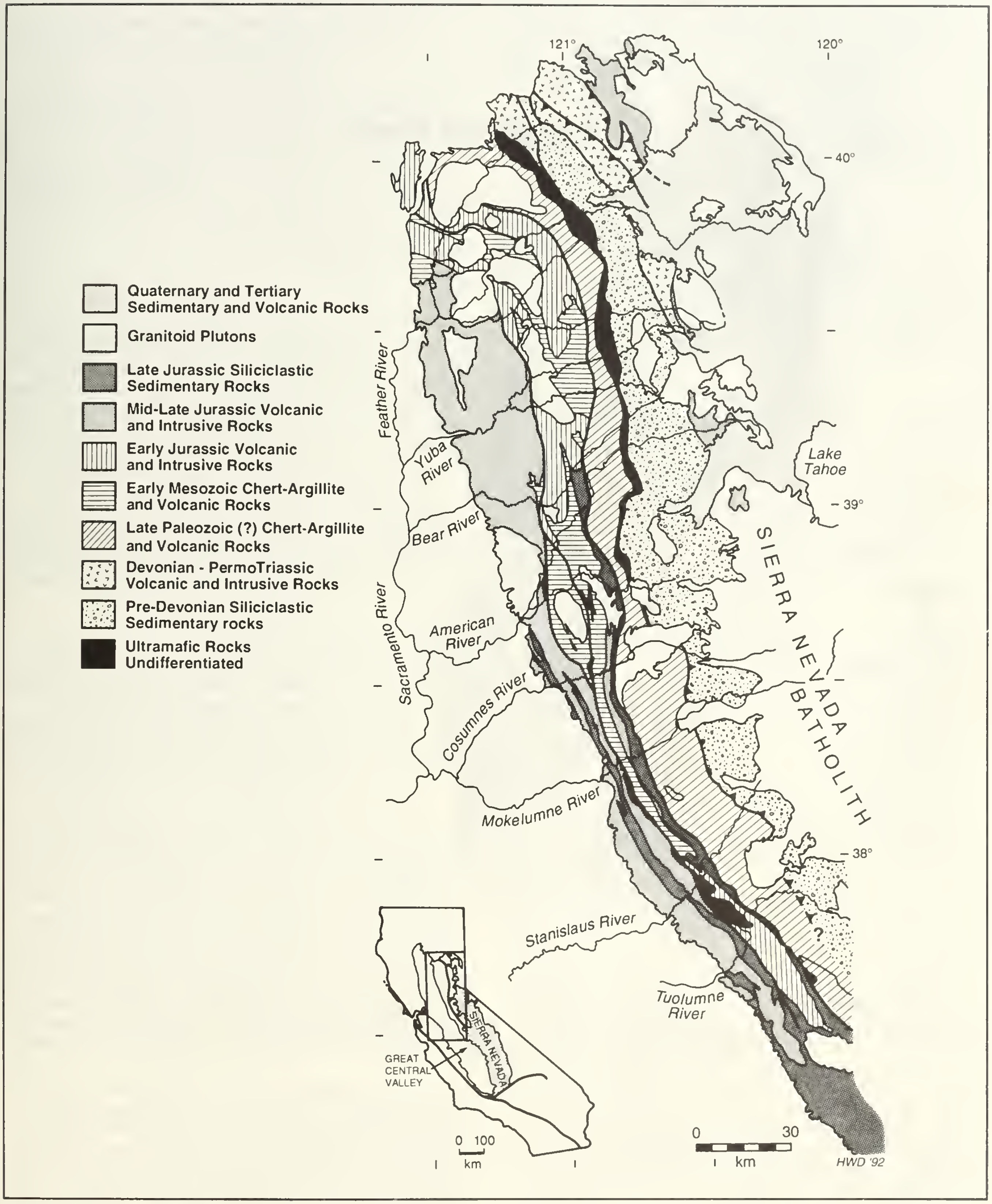
Quaternary and Tertiary Sedimentary and Volcanic Rocks
Granitoid Plutons
Late Jurassic Siliciclastic Sedimentary Rocks
Mid-Late Jurassic Volcanic and Intrusive Rocks
Early Jurassic Volcanic and Intrusive Rocks
Early Mesozoic Chert-Argillite and Volcanic Rocks
Late Paleozoic (?) Chert-Argillite and Volcanic Rocks
Devonian - PermoTriassic Volcanic and Intrusive Rocks
Pre-Devonian Siliciclastic Sedimentary rocks
Ultramafic Rocks Undifferentiated
121°
120°
40°
39°
38°
Feather River
Yuba River
Bear River
American River
Sacramento River
Cosumnes River
Mokelumne River
Stanislaus River
Tuolumne River
Lake Tahoe
SIERRA NEVADA BATHOLITH
?
GREAT CENTRAL VALLEY
SIERRA NEVADA
0 100 km
0 30 km
HWD '92

Fig. 3. Geological Sketch Map of the Western Metamorphic Belt, Sierra Nevada.

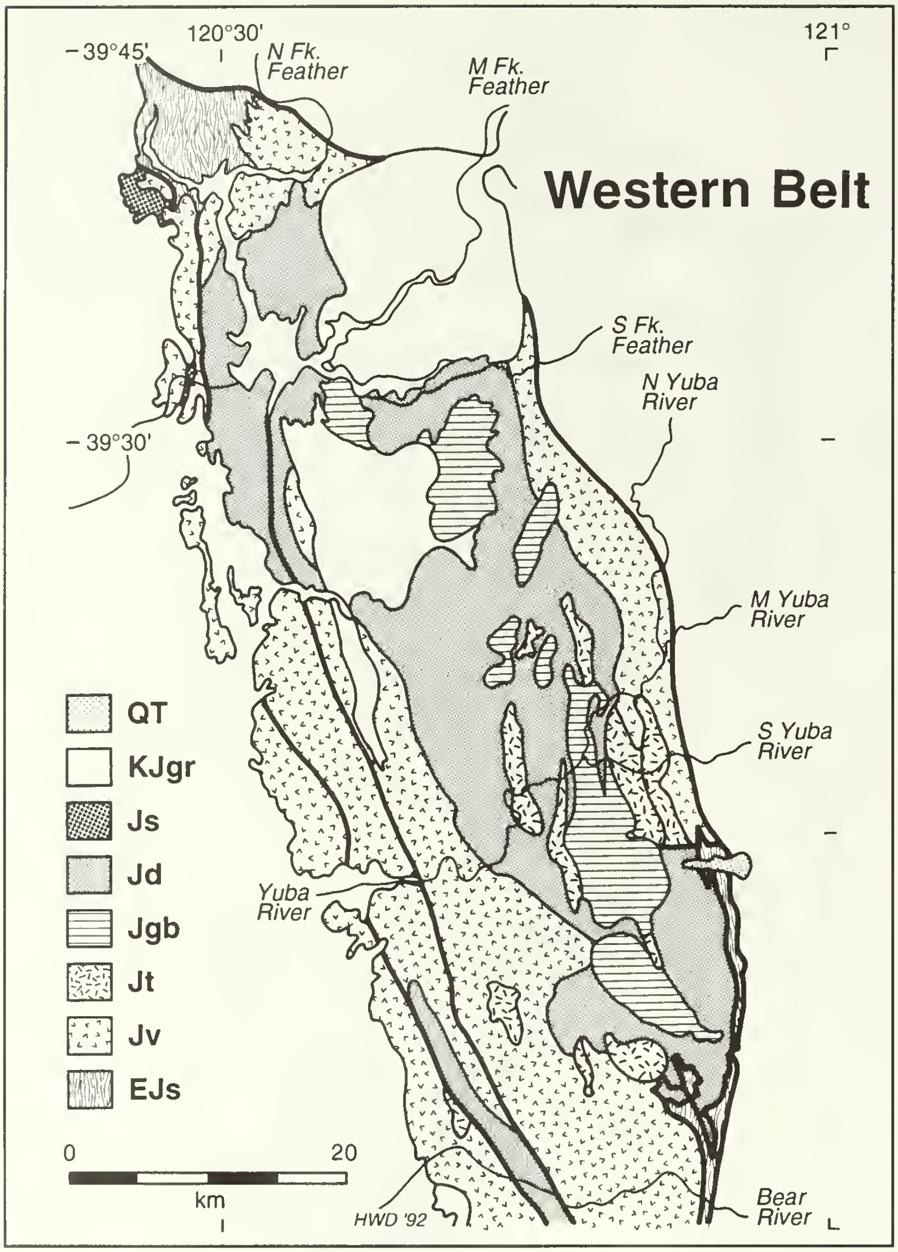

Fig. 4. Geological Sketch Map of the Smartville Complex, Western Belt. Abbreviations: QT - Quaternary and Tertiary sedimentary cover; KJgr - Cretaceous or Jurassic granitoid intrusives. Smartville Complex: Js - Late Jurassic sedimentary rocks; Jd - Jurassic diabase and dike complex; Jgb - Jurassic gabbro-diorite; Jt - Jurassic tonalite and granodiorite; Jv - Jurassic volcanic and volcaniclastic rocks. EJs - Early Jurassic or older chert - argillite melange and broken formation in the Central Belt.

Central Belt

The Central Belt is bounded on the west by the Big Bend - Wolf Creek Fault and on the east by the Feather River Belt (Figure 2) (Day, et al., 1985). The Belt is divided into eastern and western halves by the Dogwood Peak - Gillis Hill Fault. Although it is structurally and lithologically complex and has been termed "melange" (Schweickert and Cowan, 1975), recent mapping has revealed large, relatively intact volcanic arc - ophiolite complexes (Edelman, 1986; Tuminas, 1983; Zigan, 1981) that may be keys to unraveling the Mesozoic tectonic history of the Sierra Nevada.

Western Half of the Central Belt: The western half of the Central Belt contains two Jurassic volcanic arc - ophiolite complexes that appear to overlie tectonically a complex sedimentary and ophiolitic basement of similar or slightly older Mesozoic age. The Slate Creek and Lake Combie Complexes are Jurassic volcanic arc - ophiolites (SCC, LCC; Fig 5). Tectonically underlying these units are fine grained sedimentary and volcanic rocks (chert-argillite) with locally abundant sepentinite bodies (EJs, Fig. 5). In the northwestern part of the area, disrupted ophiolite, ophiolitic melange, are summarized as Older Ophiolite (OO, Fig. 5) and may be overlain by and structurally interleaved with the chert-argillite unit.

The Slate Creek Complex (SCC, Fig. 5) (Day, et al., 1985; Edelman, et al., 1989) is a pseudostratigraphic sequence of serpentinized ultramafic rocks (um, Fig. 5), overlain and apparently intruded by tonalite bodies (Jp, Fig. 5) that, in turn, intrude upward into overlying volcanic and volcaniclastic rocks (Jv, Fig. 5). The ultramafic unit may also include some cumulate rocks related to the overlying plutonic unit. Hypabyssal intrusives and dikes are a minor part of the sequence that occur near the contact between the plutonic and volcanic rocks. The ultramafic unit overlies deformed metasedimentary rocks along a fault that dips steeply east. The sequence is interpreted, therefore, as a volcanic arc and its ultramafic basement that were thrust over underlying metasedimentary rocks and deformed by later steep faults and folds (Edelman, et al., 1989).

The age of the plutonic unit in the Slate Creek Complex is early Jurassic (205 ± 3 Ma; U-Pb, zircon) (Bickford and Day, 1988; Edelman, et al., 1989; Saleeby, et al., 1989). The fault contact between the volcanic unit and the underlying sedimentary rocks of the chert-argillite unit (EJs, Fig. 5) is intruded by younger plutons dated by U-Pb (zircon) as 165 ± 3 Ma and 152 ± 2 Ma (Bickford and Day, 1988; Edelman, et al., 1989). Saleeby et al. (1989) reported an age of 193 +4/-7 Ma from a keratophyre on strike with the volcanic unit of the Slate Creek

Complex, north of the S. Fork Feather River (Fig. 5). Thus, the age of the Slate Creek Complex is early Jurassic and it was thrust into place no later than about 165 Ma.

The Slate Creek Complex is well-defined southward from the S. Fork Feather River (Fig. 5), but there is no consensus about which rocks to the north, if any, should properly be included in the Complex (Bickford and Day, 1988; Dilek, et al., 1990; Edelman, et al., 1989; Hacker and Goodge, 1990; Saleeby, et al., 1989)because the area is structurally complex and has not been mapped since the early work of Heitanen (Hietanen, 1973; Hietanen, 1976; Hietanen, 1981). For the purposes of this overview, rocks mapped by Heitanen as Franklin Canyon Formation have been included in the Slate Creek Complex (Fig. 5).

The Lake Combie Complex (LCC, Fig. 5) (Day, et al., 1985; Tuminas, 1983) is a relatively intact volcanic arc complex, similar in many respects to the Smartville Complex to the west and the Slate Creek Complex to the north (Fig. 4). It is bounded by the Wolf Creek fault zone on the west and the Gillis Hill fault on the east. It is intruded by the Yuba Rivers pluton on the north, but its southern termination has not been mapped. It consists of a pseudostratigraphic sequence of gabbroic and tonalitic plutons (Jp, Fig. 5), massive diabase with subordinate dikes (Jd, Fig. 5), minor pillow lavas and a thick sequence of volcaniclastic and epiclastic tuffs and breccias (Jv, Fig. 5) (Tuminas, 1983). It differs from the Smartville Complex by the comparative lack of dikes and pillow lavas and from the Slate Creek Complex by the lack of a regionally extensive ultramafic unit.

The Complex is cut by several generations of steep fault zones that expose chert-argillite (EJs, Fig. 5)(Day, et al., 1985; Tuminas, 1983). In two localities , massive diabase overlies the chert - argillite unit in low angle, tectonic contact with no evidence of contact metamorphism (Tuminas, 1983). The contact between the Lake Combie Complex and the chert-argillite unit has been interpreted as a thrust fault modified by later steep faulting and folding (Day, et al., 1985; Tuminas, 1983).

The age of the Lake Combie Complex is shown in Figure 3 as early Jurassic. However, no fossils have been recovered from units of the Lake Combie Complex and no modern isotopic data constrain its age. Lithologic similarity and proximity to the Smartville Complex suggest a similar age (~160 Ma) (Day, et al., 1985), but diabase in the Lake Combie Complex is similar to that in the adjacent Smartville, which may be an older, 200 Ma basement (Beiersdorfer, et al., 1991; Bickford and Day, 1988; Edelman, et al., 1989). Furthermore, the settings of the Lake Combie and 200 Ma Slate Creek Complexes are similar, so that it is reasonable and useful to speculate that the Lake Combie Complex could be as old as early Jurassic.

The northwestern part of the Central Belt is underlain by a melange of ultramafic, metavolcanic, metaplutonic, and metasedimentary rocks. The area containing abundant fragments of disrupted ophiolite is summarized as Older Ophiolite (OO, Fig. 5). The unit contains numerous bodies of serpentinite and metavolcanic rocks, fragments of serpentinite-matrix, ophiolitic melange up to 10 km long , detrital serpentinites, heterolithic mafic breccias, and deformed gabbro-diorite bodies with a distinctive flaser texture (Day, et al., 1985; Edelman, et al., 1989). The unit also contains phyllite, chert and other metasedimentary rocks similar to the chert argillite unit (EJs, Fig. 5). Portions of the unit have been interpreted as a fossil transform fault system (Dilek and Moores, 1986).

The "Older Ophiolite" has not been studied in sufficient detail to be sure that all parts of the unit are genetically related or to ascertain its relationship to the nearby Slate Creek Complex. A pluton of flaser diorite and a quartz diorite dike, which intrude serpentinite and mafic rocks in the drainage of the N. Fk. Feather River, yield U-Pb (zircon) ages of 204 ± 2 Ma and 196 ± 15 Ma, respectively (Saleeby, et al., 1989). These are similar to ages found in the Slate Creek Complex to the east and suggest that much of the volcanic and ultramafic rocks in the Older Ophiolite unit are older than the Slate Creek Complex. Near the drainage of the N. Yuba River, ophiolitic melange appears to be overlain depositionally by the chert argillite unit (EJs, Fig. 5) (Edelman, et al., 1989).

The chert-argillite unit (EJs Fig. 5) is dominated by exposures of black, siliceous argillite and ribbon chert. Volcaniclastic sandstone, sedimentary breccia, diamictite, and marble lenses, are subordinate. Some of the siliceous argillite contains plagioclase and hornblende phenocrysts and is interpreted as silicified tuff. Ribbon chert from two localities in the eastern part of this belt contains middle Triassic - early Jurassic radiolaria (Hietanen, 1981) and chert from the western part of the belt contains radiolaria that could be identified only as Mesozoic (Edelman and Sharp, 1989).

Eastern Half of the Central Belt: The eastern half of the Central Belt contains rocks assigned to the late Paleozoic - early Mesozoic Calaveras Complex (Edelman and Sharp, 1989; Hietanen, 1981; Schweickert and Snyder, 1981). The complex contains volcanic, phyllite, and chert units with uncertain stratigraphic relationships. The phyllite and chert units dominate the Complex north of latitude 39·°N and are not differentiated in Figure 5. The black phyllite is interlayered with a small amount of chert and contains a penetrative foliation that is commonly overprinted by a crenulation cleavage. The chert is typically tan to light gray with interbeds of lithic sandstones. South of latitude 39°N, siltstone and sandstone are a more prominent part of the sedimentary assemblage and the unit has been interpreted as an accretionary prism (Sharp, 1988). Pennsylvanian or Permian and early Permian fossils have been found in marble enclosed within the chert unit (Hietanen, 1981; Standlee and Nestell, 1985) but the chert itself has yielded late Triassic radiolaria (Irwin, et al., 1978). Near the south end of this belt, Figure 2, early Triassic conodonts have been recovered from marble lenses in the phyllite unit (Bateman, et al., 1985).

Feather River Belt

In the northern Sierra, the Central and Eastern Belts are separated by the narrow, fault - bounded Feather River Belt (Figs. 2, 5). A large body of Paleozoic serpentinized metaperidotite and related mafic rocks occupy the north end of the Feather River Belt (um, Fig. 5). The metaperidotite has been studied in detail only near the N. Fk. Feather River (Ehrenberg, 1975; Gefell, 1989; Weisenberg, 1979) and has been interpreted as the lower part of an ophiolite based on the presence of peridotite tectonite, cumulate ultramafic rocks, and both layered and massive gabbro (Moores, 1972; Standlee, 1978). South of the S. Fk. Feather River, the belt comprises early Mesozoic (?) metasedimentary and volcanic rocks(EJbs, Fig. 5), and Paleozoic amphibolites (Pa, Fig. 5), in addition to serpentinized ultramafic rocks. All contacts among the three units are faults. The early Mesozoic metasedimentary and volcanic rocks are especially notable because they contain the only known occurrences of lawsonite and glaucophane-crossite in the Sierra Nevada (Ferguson and Gannett, 1932; Hietanen, 1981; Schweickert, et al., 1980). Amphibolite and mafic rocks between the S. Fk. Feather and North Yuba rivers are interpreted as a fragment of the Paleozoic Devils Gate ophiolite based on the discovery of sheeted dikes and pillow structures (Edelman, et al., 1989).

Isotopic data reflect a poorly understood Paleozoic igneous and metamorphic history. Igneous rocks intruding the metaperidotite appear to be middle Paleozoic or older. Standlee (1978) reported an 40Ar/39Ar hornblende age of 387±7 Ma from a dike that intrudes mafic rocks associated with the metaperidotite. Saleeby et al. (1978) determined an U-Pb zircon, upper intercept age of 388±17 Ma on a granite that intrudes amphibolite. late Paleozoic igneous and metamorphic events are also reflected in the data. Saleeby et al. reported an U-Pb age (upper intercept) of 314±10 Ma for zircon from plagiogranite in a mafic dike complex(Saleeby and Moores,

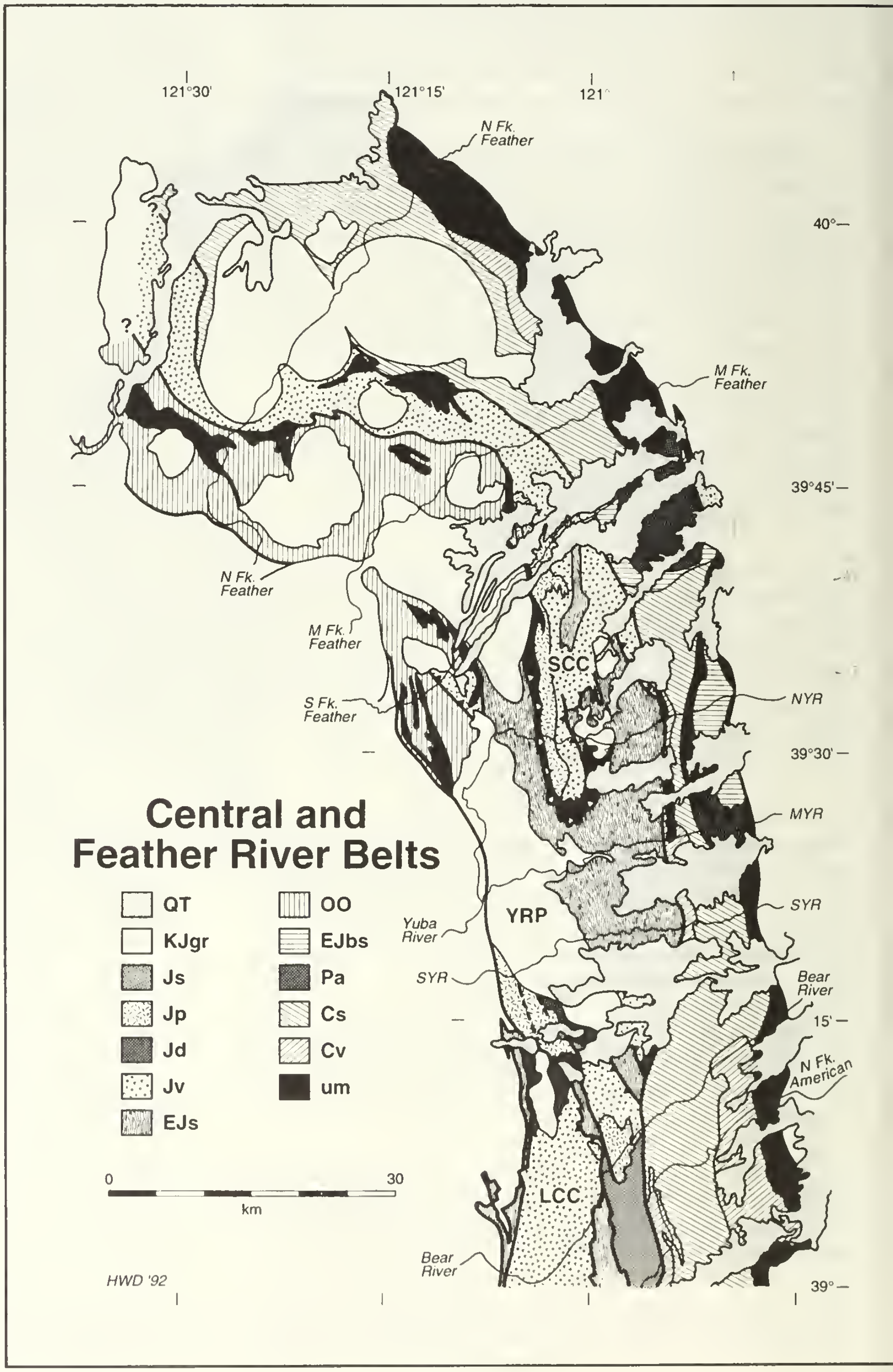

Fig. 5. Geological Sketch Map of the Central and Feather River Belts. Abbreviations: QT - Quaternary and Tertiary sedimentary and volcanic cover; KJgr - Late Jurassic and Cretaceous granitoid intrusives; Js - Late Jurassic siliciclastic sedimentary rocks; Jp - Early Jurassic and younger (?) plutonic rocks in the Slate Creek (SCC) and Lake Combie Complexes (LCC); Jd - Jurassic diabase and dikes in the Lake Combie Complex; Jv - Jurassic volcanic and volcaniclastic rocks in the Slate Creek, Lake Combie and related complexes; EJs - Early Jurassic (?) or older (?) chert - argillite and tuffaceous rocks (called Fiddle Creek Complex by Edelman et al., 1989); OO - Older Ophiolite comprising highly disrupted volcanic, plutonic, sedimentary and ultramafic rocks and including undifferentiated chert-argillite; EJbs - Early Jurassic or older metasedimentary and volcanic rocks with blueschist assemblages; Pa - Paleozoic amphibolite in the Feather River Belt, including both Permian (?) rocks to the north, and Devonian(?) rocks to the south of the N. Yuba River; Cs - chert and phyllite of the Carboniferous or younger Calaveras Complex; Cv - volcanic rocks associated with the Carboniferous or younger sedimentary rocks of the Calaveras Complex; um - undifferentiated ultramafic rocks. LCC - Lake Combie Complex; SCC - Slate Creek Complex; YRP - Yuba Rivers Pluton.

1979), but K-Ar ages of amphibole from mafic rocks range from 236 - 345 Ma and suggest late Paleozoic metamorphism (Bohlke and McKee, 1984; Hietanen, 1981; Standlee, 1978; Weisenberg and Ave Lallemant, 1977).

The metasedimentary and metavolcanic blueschists are early Jurassic or older, based on K-Ar ages of 174 Ma in white mica (Schweickert, et al., 1980). These rocks may be the southernmost exposure of blueschists better exposed in the Klamath Mountains of northern California (Hacker and Goodge, 1990)

Eastern Belt

The Eastern Belt (Fig. 6) is bounded on the west by a complex fault zone and the Feather River Belt, on the north by Tertiary and Quaternary volcanic rocks, and on the east by Mesozoic granitoid intrusive rocks and Tertiary volcanic and sedimentary rocks. It marks the continental margin during Mesozoic time and comprises the early Paleozoic Shoo Fly Complex, and three younger volcanic sequences that mark periods of significant volcanism during Devonian-Mississippian, Permian, and Jurassic periods (D'Allura, et al., 1977; Hannah and Moores, 1986; Harwood, 1988). Each of these sequences is separated by a marked erosional interval or unconformity.

Sedimentary rocks of Shoo Fly Complex(ODsf, Fig. 6) are exposed along the entire length of the Eastern Belt and form the basement on which three distinct volcanic sequences were deposited. The metasedimentary rocks are include quartz sandstone, shale, chert and melange that have been mapped as three or four, controversial, lithotectonic units. In the south, four units have been mapped as thrust - bounded allochthons (Schweickert, et al., 1984), whereas only three units were recognized in the north and were interpreted to define regional scale folds (Hannah and Moores, 1986). The lowest unit recognized in the south is the Lang sequence, which is composed of quartz sandstone and shale turbidites that formed in a near continental setting (Bond and DeVay, 1980). The Duncan Peak and Culbertson Lake allochthons contain abundant chert and argillite where they were defined in the southern half of the belt (Schweickert, et al., 1984). The structurally highest unit is the Sierra City melange, which consists of blocks of serpentinite, gabbro, basalt and sedimentary rocks in a matrix of slate and sandstone.

The age of the Shoo Fly Complex is not well known but must be early Paleozoic. The faults that bound the allochthons are intruded near the Yuba River by the Devonian Bowman Lake Batholith (Girty, et al., 1984; Hanson, et al., 1988) and truncated by a pre-Upper Devonian unconformity (Fig. 6) (for a recent review cf. (Harwood, 1988)). The maximum age of the Shoo Fly is not well constrained, but the unit is known to contain Ordovician fossils (Girty and Wardlaw, 1985; Hannah and Moores, 1986), late Cambrian or early Ordovician detrital zircons (506 ± 22 Ma) (Girty and Wardlaw, 1984), and Proterozoic detrital zircons (Girty and Wardlaw, 1985).

Devonian - Mississippian volcanic and sedimentary rocks (Grizzly, Sierra Buttes, Taylor and lower Peale Fm) overlie the Shoo Fly Complex unconformably and constitute a regionally extensive volcanic arc (D'Allura, et al., 1977; Varga and Moores, 1981) . The arc is characterized by rhyolitic to dacitic compositions and abrupt variations of stratigraphic thicknesses and both volcanic and sedimentary facies (Brooks, et al., 1982; Hannah, 1980; Hanson, 1983). Volcanic activity extended into Mississipian and was followed by deposition of Carboniferous ribbon chert (Upper Member of the Peale).

Volcanic activity was renewed during the Permian (Arlington, Goodhue and Reeve Formations) with the deposition of basalt, andesite, and volcaniclastic rocks unconformably on the older Devonian-Mississippian volcanic arc. The Permian volcanic sequence, in turn, is overlain unconformably by Upper Triassic limestone and Jurassic volcaniclastic rocks near the N. Fork of the American River (Fig. 6) (Harwood, 1983).

Jurassic volcanic and volcaniclastic sedimentary rocks extend the entire length of the Eastern Belt from the Mt. Jura area in the north to the North Fork of the American River (Fig. 6). The volcanic rocks are no older than Middle Jurassic (Imlay, 1961) and are dominantly andesitic and dacitic flows, tuffs, breccias, and volcaniclastic sedimentary rocks. In the south, the sequence is thin, overlies the Upper Paleozoic rocks on a marked pre-Upper Triassic unconformity and is intruded by abundant Jurassic and Cretaceous granitoid plutons of the Sierra Nevada batholith (Harwood, 1983). In the north, the Jurassic rocks are overthrust by the Paleozoic section along the Taylorsville fault, but the basement on which they were deposited is not exposed (Diller, 1892; Diller, 1908).

Age of Deformation

The geologic relations in the Eastern Belt provide evidence for pre-late Devonian, pre-late Triassic and middle Jurassic or younger deformations that may correspond to the Antler, Sonoma, and Nevadan orogenies, respectively (Dickinson, 1981). The pre - late Devonian and pre -l ate Triassic unconformities are profound, but high grade metamorphism is not associated with either event. Middle Jurassic or younger deformation is indicated by the thrust faults that deform the Jurassic rocks in the vicinity of Mt. Jura; Other faults, such as the Grizzly fault, which repeats the Paleozoic section, may also reflect Jurassic deformation.

The regional scale faults and penetrative fabrics of rocks in the Western, Central and Feather River Belts are primarily the result of Jurassic deformation. The earliest systematic surveys of California established that the steeply dipping "auriferous slates" contained Jurassic fossils and were overlain unconformably by nearly flat-lying, unmetamorphosed Cretaceous sedimentary rocks (Whitney, 1865). That Jurassic deformation is now known as the "Nevadan Orogeny" but the tectonic significance and duration of that deformation remain subjects of considerable interest.

Blackwelder (1914) used the term "Nevadian" to describe the Jurassic deformation that affected the Sierra Nevada and much of the western margin of North and South America and the term was later modified to "Nevadan" (Hinds, 1932,1935). Taliaferro (1942) provides a good historical overview and his definition of Nevadan is still in use today:

"...an...orogeny...which deformed the [late Jurassic] Mariposa and older beds and resulted in tight folding, overturning, thrust faulting and formation of dynamically metamorphosed rocks over wide areas in the Sierra Nevada." (Taliaferro, 1942) (p. 92).

The tectonic significance and duration of the Nevadan orogeny are still debated. The principal structural features of the Nevadan orogeny are the Foothills Fault System of regional scale faults and associated folds and penetrative cleavages (Fig. 2, 3) (Clark, 1960; Clark, 1964). Strike-slip movements on these faults are implied by the reconstruction of plate movements (Saleeby, 1981), but only steep, reverse, dip-slip structures have been recognized (eg. (Day, et al., 1985; Miller and Paterson, 1991)). Many workers in the Central Sierra have proposed that the steep faults are steepened west-vergent thrust faults; In the northern Sierra, we have proposed that the steep faults may truncate or deform earlier east-vergent thrust faults (Day, et al., 1985; Edelman, et al., 1989; Moores and Day, 1984).

Because the youngest rocks deformed by these steep faults are Kimmeridgian, the Nevadan is considered by many workers to be a short lived, late Jurassic event (Knopf, 1929; Smith, 1909; Taliaferro, 1942), perhaps at about 155 ± 3 Ma (Schweickert, et al., 1984). However, a considerable body of evidence suggests that deformation commonly considered as Nevadan began during early or middle Jurassic (Day, et al., 1988; Edelman, et al., 1989) and continued into the Cretaceous in some areas (Tobisch, et al., 1989).

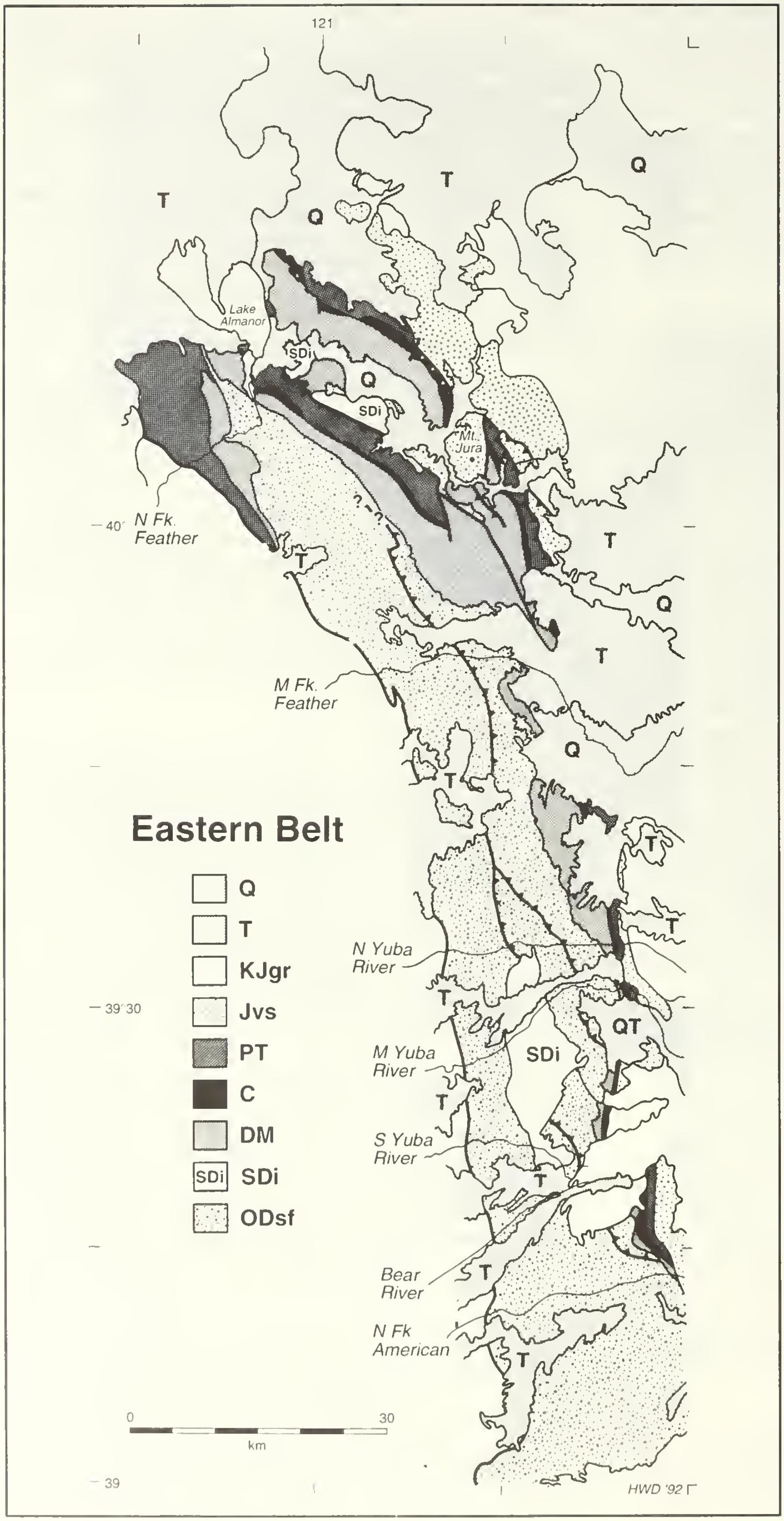

Fig. 6. Geological Sketch Map of the Eastern Belt. Abbreviations: Q & T: Quaternary and Tertiary sedimentary and volcanic cover; KJgr - Cretaceous and Jurassic granitoid intrusives; Jvs - Jurassic volcanic and sedimentary rocks; PT - Permo-Triassic volcanic rocks; C - Carboniferous Chert; DM - Devonian - Mississippian volcanic rocks; SDi - Silurian - Devonian intrusive rocks; ODsf -Ordovician (?) - Devonian(?) Shoo Fly Complex, primarily siliciclastic sedimentary rocks.

The presence of 174 Ma, or older, blueschists in the Feather River Belt implies early Mesozoic subduction (Schweickert, et al., 1980); The thrust fault between the ~205 Ma Slate Creek Complex and its underlying basement is cut by a ~165 Ma pluton (Edelman, et al., 1989) and by younger steep faults. Both observations imply first order convergent deformation during the early Jurassic and possibly earlier. The relationships of the Yuba Rivers Pluton (159 Ma , U-Pb, zircon (Edelman, et al., 1989)) (Fig. 5) to the adjacent rocks in the Western and Central Belts suggests that some steep faults must be older than about 160 Ma. The pluton intrudes and is deformed by the Wolf Creek fault (Day, et al., 1985) and its contact aureole overprints earlier fabrics (Clark, 1960). Furthermore, it cuts steep fault contacts among units in the Older Ophiolite unit and the Lake Combie Complex (Fig. 5), implying that at least some of the steep faults were active before intrusion. Finally, hornblende barometry of Jurassic plutons from both sides of the Wolf Creek - Big Bend fault zone (Fig. 4, 5) limits the amount of vertical offset on the fault since 160 Ma to no more than two or three kilometers (McLeod and Day, 1991). Farther south in the vicinity of the Cosumnes and Mokelumne rivers, Duffield and Sharp (1975) recognized a belt of melange that is summarized in Figure 3 as early Jurassic sedimentary rocks. They suggested that most faulting occurred before late Jurassic tilting to the present steep dips and that the melange was formed before the deposition of Callovian volcanic rocks (Logtown Ridge Formation). Edelman et al. (1989) suggested that "suspect terranes" in the Central and Feather River Belts must have been amalgamated prior to about 163 Ma and that many of the steep faults of the Foothills Fault System reactivated older, cryptic terrane - bounding faults during late Jurassic deformation.

These observations and interpretations suggest that large scale transport and convergent deformation of Mesozoic rocks began no later than early Jurassic (174 Ma?); that some (presently) steep faults and associated penetrative cleavages are older than ~160 Ma; and that fault movements, folding and cleavage formation continued into the late Jurassic, or possibly, early Cretaceous. The angular unconformity of Upper Cretaceous sedimentary rocks on steeply dipping, late Jurassic slates suggests that the major exhumation or orogenic phase of the deformation took place during the Cretaceous. In the absence of evidence that deformation subsided for a significant interval, it seems unjustified to restrict the notion of "Nevadan" to a brief interval during the late Jurassic. Rather, we adopt a broader connotation that may be useful to indicate the Jurassic and younger deformation that occurred prior to deposition of Upper Cretaceous sediments unconformably on the "auriferous slates."

Summary of Mesozoic Tectonic History

The Mesozoic rocks of the Western Metamorphic Belt have been the focus of renewed interest during the past twenty years, but no consensus about the tectonic significance of these rocks has been reached. Jurassic rocks in the Western and Eastern Belts have been attributed to either one or two magmatic arcs (Burchfiel and Davis, 1972; Moores, 1972; Schweickert and Cowan, 1975). The major faults of the Foothills Fault System have been viewed as west-vergent thrust faults that may or may not have been related to east-dipping subduction (Ernst, 1983; Schweickert, et al., 1988), east-vergent thrust faults (Day, et al., 1985; Moores and Day, 1984), west-vergent faults followed by east-vergent faulting (Edelman, et al., 1989), and as the result of strike-slip and transpressional tectonics (Saleeby, 1981). What is clear is that no simple tectonic model is likely to explain the diverse structural and stratigraphic relationships that have been observed along the entire length of the Western Metamorphic Belt.

The Western Belt contains extrusive, intrusive, and sedimentary products of a rifted volcanic arc. The basement of this arc is exposed only in the north and appears to be disrupted portions of a 200 Ma volcanic arc and associated sedimentary rocks in the Central Belt. The Central Belt itself is composed of fragments of late Paleozoic and Mesozoic oceanic, volcano-plutonic complexes and sedimentary sequences. The western half of the Central Belt contains one or more late Triassic - early Jurassic volcanic terranes that were juxtaposed at least in part by thrust faulting no later than middle Jurassic (~165 Ma). The eastern half, contains a Carboniferous or younger, chert-argillite sequence and volcanic rocks of unknown provenance and age. The Feather River Belt juxtaposes Paleozoic ultramafic and mafic rocks of uncertain origin with Mesozoic, blueschist facies metasedimentary and metavolcanic rock. Finally, the Eastern Belt displays an intact record of Paleozoic through Mesozoic sedimentary and volcanic activity that appears to have taken place at the margin of the North American continent.

Late Jurassic deformation is evident in the folding, faulting, and penetrative fabrics of late Jurassic rocks in the Western Metamorphic Belt. Some of this deformation may have continued into the early Cretaceous. The importance of active tectonic environments during middle and early Jurassic, however, is becoming increasingly apparent, especially in the Central and Feather River Belts. Some of the tectonism, and presumably coeval metamorphism, undoubtedly took place in an oceanic setting and should be distinguished from orogenic deformation

Most workers agree that the Jurassic history of the Sierra records the complex processes by which volcanic arcs and associated marine sedimentary assemblages are added to the continental margin. Progressively younger, marine volcanic and sedimentary rocks were added to the continental margin during late Paleozoic - Triassic and Jurassic time. Jurassic volcanic complexes were formed in a dynamic tectonic setting and were amalgamated no later than about 165 Ma (Edelman and Sharp, 1989). It is not clear, however, whether the added material was exotic or "near-continental." Continental influence is evident in the provenance of late Jurassic siliciclastic sedimentary rocks, xenocrystic, Precambrian zircon in mid - late Jurassic plutonic rocks (Bickford and Day, 1988), and the provenance of mid-Jurassic or older quartz conglomerates in the Central Belt , south of the Cosumnes River (Fig. 3) (Duffield and Sharp, 1975), but there is no direct evidence for the distance from a true continental margin. Evidence for polarity of one or more subduction zones is circumstantial. Both directions may have operated at different times during the Jurassic.

METAMORPHISM – AN OUTLINE

Although there has been a substantial amount of interest in contact aureoles and ore deposits associated with the intrusion of the Sierra Nevada batholith, there has been very little systematic work on the regional metamorphism and thermal history of the Sierra Nevada. Most of the available information comes from observations that were incidental to the main focus of structural or stratigraphic studies. Notable contributions include the early work of Best and Baird in the Central Sierra and of Heitanen in the northern Sierra (Baird, 1962; Best, 1962; Hietanen, 1951; Hietanen, 1973). No detailed regional metamorphic map of the area has ever been made, but Ernst presented a metamorphic map of California in which the northern Sierra was included(Ernst, 1983). Day et al. (1988) discussed the metamorphism of the northern Sierra based on a review of the literature and preliminary field and petrographic observations. Much of the following is summarized from that review.

Several different views of the regionalmetamorphism have emerged from these incomplete studies. The Sierra Nevada is widely regarded as a greenschist facies metamorphic belt punctuated by contact aureoles related to the Sierra Nevada batholith. The low grade regional metamorphism has been explained as: (a) an effect of Nevadan deformation (Taliaferro, 1942); (b) a Cretaceous, low P/T belt paired with the Franciscan high P/T blueschists (Miyashiro, 1961; Miyashiro, 1973); (c) a Jurassic subduction complex (Ernst, 1983); (d) a collage of tectonically juxtaposed metamorphic terranes (Day, et al., 1988); (e) the thermal consequence of the construction and burial of volcanic arcs (Day, et al., 1988). Recent work suggests that the metamorphic history may be as rich and complex as the tectonic history outlined above and that no simple model is likely to accomodate all the observations.

Figure 7 (modified after Day et al., 1988) summarizes our current understanding of the ages and conditions of metamorphism in the northern Sierra. Volcanic rocks in the Smartville Complex of the Western Belt are relatively undeformed and only weakly recrystallized, except in contact aureoles. Prehnite and pumpellyite are widespread, but actinolite is also abundant (Springer, et al., 1992). Contact aureoles of ca. 161 Ma plutons overprint the prehnite and pumpellyite assemblages in volcanic rocks of approximately the same age. Some of these contact aureoles contain granulite facies, two-pyroxene assemblages and evidence for partial melting (Beard, 1990). Greenschist facies assemblages, actinolite + albite + epidote + chlorite, are common in the hypabyssal dike complex and may be the result of autometamorphism or deuteric alteration (Day, et al., 1988). Epidosites probably are the result of hydrothermal processes associated with the intrusive activity. The regional metamorphism must be synchronous with or slightly older than the main intrusive episode, implying that the regional, contact, autometomorphic and hydrothermal metamorphic processes are all part of the construction and burial of the Smartville volcanic complex.

Much of the Central Belt (Fig. 7) contains greenschist facies assemblages and actinolite and biotite are much more widely reported than in the Smartville Complex. However, post-tectonic plutons are abundant in the northern part of the Central Belt and it is not yet clear whether the regional assemblages might be related to the plutonism. The Older Ophiolite unit contains assemblages of the greenschist and epidote amphibolite facies (actinolite + albite; bluish-green hornblende + albite; hornblende + actinolite + albite-oligoclase; actinolite + oligoclase). Pumpellyite has not yet been confirmed in the Slate Creek Complex, but the preservation of delicate quench textures in some volcanic rocks suggests that recrystallization is weak in some areas and that pumpellyite may have been overlooked. Alternatively, low grade assemblages may have been overprinted by greenschist facies assemblages in some places. Springer (unpublished) has identified pumpellyite in hypabyssal intrusives in the Lake Combie Complex, and prehnite has been reported from tuffaceous rocks in the chert-argillite unit (Edelman, et al., 1989).

The age(s) of metamorphic events in the Central Belt are poorly constrained, but must be early Jurassic or younger because the mafic rocks in the western part of the Central Belt are no

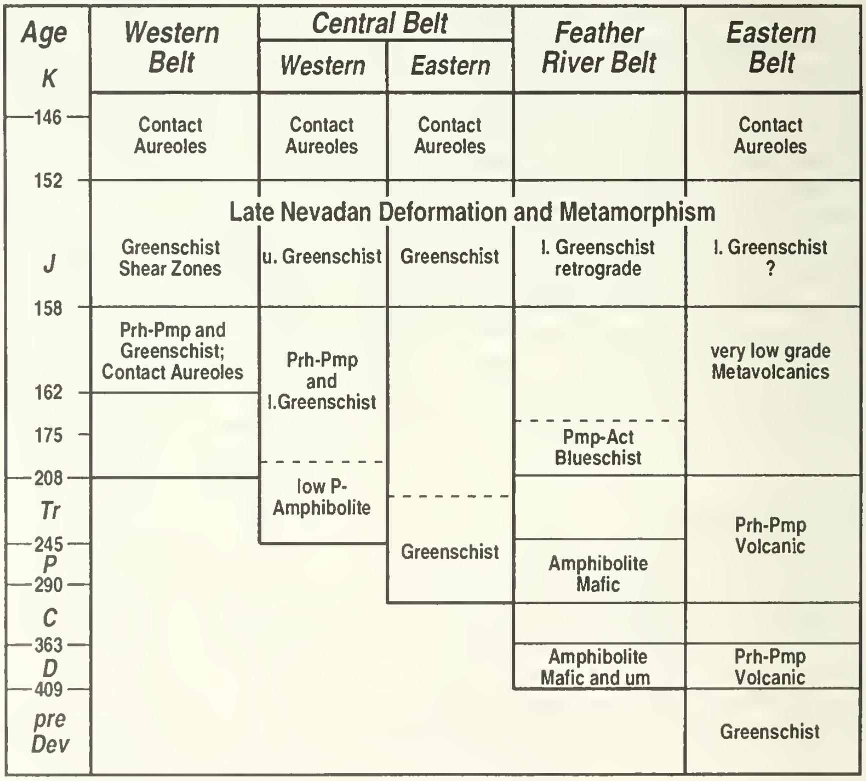

Age	Western Belt	Central Belt		Feather River Belt	Eastern Belt
		Western	Eastern		
K					
146	Contact Aureoles	Contact Aureoles	Contact Aureoles		Contact Aureoles
152	Late Nevadan Deformation and Metamorphism				
J	Greenschist Shear Zones	u. Greenschist	Greenschist	l. Greenschist retrograde	l. Greenschist ?
158	Prh-Pmp and Greenschist; Contact Aureoles	Prh-Pmp and l.Greenschist			very low grade Metavolcanics
162					
175				Pmp-Act Blueschist	
208 / Tr		low P-Amphibolite	Greenschist		Prh-Pmp Volcanic
245 / P / 290				Amphibolite Mafic	
C					
363 / D / 409				Amphibolite Mafic and um	Prh-Pmp Volcanic
pre Dev					Greenschist

Fig. 7. Metamorphism as a Function of Age and Lithotectonic Belt.

older than ~200 Ma. In the Older Ophiolite unit, the assemblage actinolite + oligoclase is found in the deformed outer margin of a flaser diorite that is interpreted to have formed during the late- or post - magmatic cooling of the pluton (Day, et al., 1988; Mazaheri, 1982) at about 204 Ma (Saleeby, et al., 1989). North of the N. Yuba River, greenschist and epidote-amphibolite assemblages are found in foliations and fault zones that are truncated by the ~159 Ma Yuba Rivers Pluton.

The Feather River Belt (Figure 7) contains the highest grade rocks exposed in the northern Sierra, outside of contact aureoles. Amphibolites yielding Permian and Devonian argon ages on hornblende contain typical lower amphibolite facies hornblende+ oligoclase (Bohlke and McKee, 1984; Hietanen, 1981) and metaperidotites contain anthophyllite (Ehrenberg, 1975). Peak metamorphic temperatures in amphibolites and intercalated metasediments were 600 ± 50 °C at 5 ± 3 kbar and they appear to have been overprinted by Jurassic(?) pumpellyite + actinolite assemblages (Hacker and Peacock, 1990). Greenschist facies actinolite + albite + epidote appear to be later than the amphibolite facies recrystallization, especially in shear zones. Metasedimentary and metavolcanic blueschists occur in fault contact with the high grade mafic and ultramafic rocks. Glaucophane - bearing amphibolites in the Feather River Belt were first described by Ferguson and Gannett (Ferguson and Gannett, 1932) in the Alleghany gold district near the Middle Yuba River and lawsonite + albite was later reported from the same area by Rosenbaum (unpublished). Glaucophane + lawsonite + epidote blueschists were described by Schweickert and others and Heitanen north of the North Yuba River(Hacker and Goodge, 1990; Hietanen, 1981; Schweickert, et al., 1980). The metamorphism of the blueschists was 174 Ma or older (Schweickert, et al., 1980), but the geological relationships among the occurrences north and south of the N. Yuba river are not clear. More detailed petrological work suggests that glaucophane + lawsonite and crossite + epidote were formed at 6 - 7 kbar, 300 ± 50 °C and that the blueschist assemblages are overprinted by pumpellyite + actinolite (Hacker and Goodge, 1990).

The Eastern Belt (Figure 7) contains widespread lower greenschist and sub-greenschist facies assemblages. The pre-Devonian Shoo Fly Complex contains the common assemblage quartz + chlorite + white mica. Biotite and stilpnomelane are reported as less common accessory minerals but detrital biotite has been reported (D'Allura, 1977) and it is not clear that all biotite is neoblastic. Recent studies of illite crystallinity in the Shoo Fly suggest that the Complex is in the "epizone," comparable to the lower greenschist facies (Robinson and Bevins, personal communication). The Devonian-Mississippian volcanic rocks of the northern Sierra contain widespread prehnite and pumpellyite (Hannah, 1980), (Brooks, unpublished; Schiffman, unpublished) that appear to be overprinted by greenschist assemblages near Cretaceous granitoid plutons. Permo-Triassic volcanic rocks also contain pumpellyite and prehnite (Bevins and Robinson, personal communication). Jurassic volcanic and sedimentary rocks near Mt. Jura show only evidence of very low grade metamorphism. Prehnite and pumpellyite have not been reported and recrystallization of the rocks is minimal except in narrow deformation zones or in obvious contact aureoles near Cretaceous intrusions.

It is especially noteable in the Eastern Belt of the northern Sierra that there is no regional increase of metamorphic grade toward the Sierra Nevada batholith on the east. In particular, the lowest grade rocks appear to be the Jurassic metavolcanic and metasedimentary rocks immediately adjacent to the large Cretaceous granitoid intrusions in the vicinity of Mt. Jura (Fig. 6). The highest (biotite) grade rocks are most abundant in the Shoo Fly Complex on the western margin of the Eastern Belt. The highest grades of regional metamorphism in the northern Sierra, in fact, occur in the Feather River Belt to the west.

The time(s) of low - grade metamorphism in the Eastern Belt are unclear. Some of the metamorphism is clearly pre-Upper Devonian because foliated metasedimentary clasts of Shoo Fly lithologies occur in the lower part of the overlying Devonian units (Varga and Moores, 1981). Harwood attributed most of the metamorphic alteration to a late Jurassic metamorphic overprint (Harwood, 1988). Day et al. (1988) suggested that prehnite + pumpellyite assemblages might be the result of alteration during the construction and burial of Paleozoic volcanic arcs, in much the same way as documented in the Jurassic Smartville Complex to the west. No definitive evidence has yet been offered to resolve the issue.

Late Nevadan shear zones in the northern Sierra are everywhere associated with greenschist facies metamorphism. In late Nevadan shear zones truncating or bounding the Smartville Complex, actinolite + albite + epidote + chlorite is a common assemblage. Upper greenschist or epidote amphibolite assemblages are common in the northern parts of the Central Belt, where metamorphic foliations and contact aureoles are nearly ubiquitous. Retrograde greenschist assemblages are commonly associated with faults and cleavages in the Feather River Belt. Likewise, fault zones in the Eastern Belt also contain greenschist facies assemblages.

Contact metamorphism occurred in aureoles surrounding Paleozoic and younger gabbroid and granitoid plutons in all except the Feather River Belt of the northern Sierra. All known metamorphic assemblages suggest low pressures of intrusion and contact metamorphism. Andalusite, andalusite + cordierite, and andalusite + staurolite assemblages are known from several contact aureoles and suggest pressures of metamorphism of about 3 kbar (Bobbitt, 1982; Day, et al., 1988; Hietanen, 1973; Hietanen, 1976; McMath, 1958; Swanson, 1970). This estimate is supported by hornblende barometry on plutons in the Central and Western Belts (Lang and Manduca, 1991; McLeod and Day, 1991).

DISCUSSION

The northern Sierra Nevada is primarily a low grade metamorphic terrane composed of both sedimentary and volcanic protoliths. The thermal history of low-grade terranes such as this are notoriously difficult to determine because of the poor sensitivity of the major lithologies to metamorphic recrystallization at low temperatures and because of the complex and incompletely understood tectonic history. Despite the near absence of systematic and detailed studies of the metamorphism, some broad features of the thermal and tectonic history are beginning to emerge.

Conditions of Metamorphism

The pressures and temperatures of metamorphism in the Sierra Nevada metamorphic belt are only broadly constrained, in part because we are only beginning to recognize multiple events and, in part because data are sparse. Figure 8 (modified after (Day, et al., 1988; Liou, et al., 1985) illustrates estimates of the conditions of metamorphism based on the limited petrological information available and estimated equilibrium conditions for iron-free phases. The presence of prehnite and pumpellyite in the Smartville Complex, Western Belt, suggests temperatures of about 275 -300°C and pressures of about 2.5 - 3.0 kbar (Day et al., 1988; Springer et al., 1992). Recent hornblende barometry of syn - and post - metamorphic plutons in the Western and Central Belts, likewise, suggests that pressures were in the range of 2.5 - 3.5 kbar (Lang and Manduca, 1991; McLeod and Day, 1991). Actinolite is abundant in late "Nevadan" shear zones everywhere in the northern Sierra and probably formed at 350 °C - 400 °C at about the same pressure. Both actinolite + oligoclase and hornblende + albite are found in the Older Ophiolite unit of the Central Belt suggesting lower pressures, perhaps as low as 1.5 - 2 kbar (Fig. 8). The pressures at which amphibolite facies assemblages in the Feather River Belt formed are not constrained in a significant way, but the coexistence of epidote + glaucophane in the Feather River blueschists appears to require significantly higher than "normal" pressures. Based on the iron-free system (Fig. 8), pressures may have been above 8 kbar, whereas estimates based on analyses of the natural phases are about 6 kbar (Hacker and Goodge, 1990).

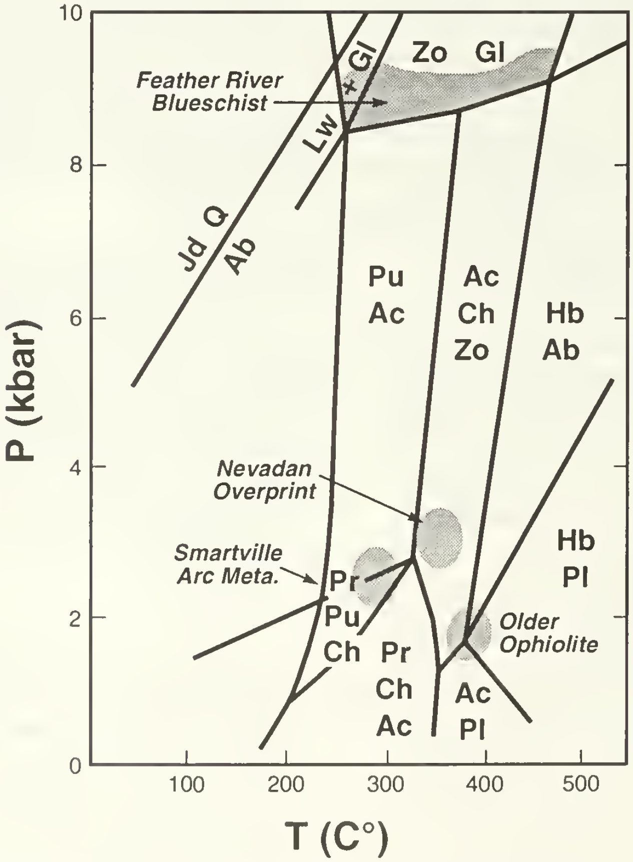

Fig. 8. P-T Conditions of Metamorphism in the Western Metamorphic Belt. Equilibria are shown for iron-free minerals (modified after Liou et al., 1985; Springer et al., 1992).

Times of Metamorphism

Most of the metamorphism in the northern Sierra Nevada occurred before the main phase of Cretaceous intrusions in the Sierra. Indeed, there is little unambiguous regional metamorphism associated with the emplacement of the Sierra Nevada batholith in the northern Sierra. In general, narrow contact aureoles of Cretaceous plutons overprint regional metamorphic fabrics and, outside the aureoles, regional metamorphic grade seems to increase from east to west across the Eastern Belt, away from the main exposures of the batholith.

Although late Jurassic metamorphism is clearly evident in the greenschist facies assemblages of late Nevadan shear zones, the sparse data available suggest also that there have been several earlier episodes of Paleozoic and Mesozoic low grade metamorphism. In the Western Belt, contact aureoles of 161 ± 2 Ma plutons overprint Prh + Pmp assemblages in late middle Jurassic volcanic rocks, implying middle Jurassic low grade metamorphism (Day, et al., 1988). Pumpellyite in intrusives of the Lake Combie Complex, Central Belt, similar to occurrences in the Western Belt (Springer, et al., 1992), suggest that low grade metamorphism is related to the igneous activity by which the arc was constructed, but the age is uncertain. In the Older Ophiolite unit of the Central Belt, early and middle Jurassic metamorphism is suggested by upper greenschist facies metamorphism, which appears to be associated with intrusions emplaced in an oceanic fracture zone at about 204 Ma, and greenschist assemblages in the fault zones, which must be older than the 159 ± 2 Ma Yuba Rivers Pluton. In the Feather River Belt, rocks of widely differing metamorphic grade and age are tectonically juxtaposed by faults in the Foothills Fault System that, elsewhere, deform fossiliferous late Jurassic rocks. Ar ages of amphibole in amphibolites require minimum ages of metamorphism that are Permian and Devonian. Blueschist metamorphism is unrelated to the amphibolite facies metamorphism, but must be early Jurassic or older. The age of metamorphism in the Eastern Belt is not directly constrained. It is very likely that some of the low greenschist facies metamorphism of the Shoo Fly Complex is pre-Upper Devonian. We have proposed that the prehnite + pumpellyite facies assemblages of the Paleozoic volcanic rocks may be related to the construction and burial of the volcanic complexes in much the same way that we observe in the Smartville Complex (Day, et al., 1988) (Beiersdorfer and Day, this volume).

Tectonic Implications

The Western, Central and parts of the Feather River Belts (Fig. 2) contain late Paleozoic and Mesozoic volcanic arc, ophiolitic and marine sedimentary assemblages that were amalgamated with the Eastern Belt during the Jurassic Nevadan deformation. The major regional faults of the Foothills Fault System juxtapose rocks of significantly different age and metamorphic grade and the amalgamation of the lithotectonic belts separated by these faults may have occurred largely before ~165 Ma (Edelman, et al., 1989; Edelman and Sharp, 1989). The deformation of late Jurassic rocks along these faults may represent, therefore, reactivation of earlier, cryptic faults (Edelman, et al., 1989). The evidence for early, middle and late Jurassic, as well as early Cretaceous, deformation suggests that the Nevadan was not an event of short duration. Rather, a broader view of Jurassic deformation may be more appropriate, as suggested previously for the Klamath Mountains (Wright and Fahan, 1988).

There have been several episodes of Paleozoic and Mesozoic low grade metamorphism and much of the low grade metamorphic character of Sierran rocks may have been acquired in volcanic arc or other oceanic settings prior to, and modified during, the latest Nevadan deformation. Overprinting of low grade regional assemblages by contact aureoles of Jurassic and Cretaceous plutons gives only broad constraints on the age(s) of regional metamorphism. The tectonic juxtaposition of rocks with significantly different metamorphic grade during late Jurassic deformation, especially in the Feather River Belt, testifies to the pre-late Jurassic age of some of the metamorphism. Late Jurassic metamorphism occurred primarily in relatively narrow deformation zones, but implies that rocks were buried at conditions appropriate to the greenschist facies at that time. There is no documented regional metamorphism associated with the Cretaceous intrusion of the Sierra Nevada batholith. In fact, Cretaceous must have been a time of major exhumation, because the late Jurassic and early Cretaceous contact aureoles formed at approximately 3 kbar and are overlain by Eocene and younger sedimentary and volcanic rocks.

The picture that is emerging, therefore, is that metamorphism in the Sierra occurred in a variety of oceanic, volcanic arc, and subduction environments prior to the latest Jurassic phases of the Nevadan orogeny. Greenschist facies metamorphism overprinted the earlier assemblages and fabrics during the latest phases of the Nevadan deformation, followed by contact aureoles of post-tectonic plutons. Consequently, metamorphism is perhaps best viewed as a collage of various, pre-orogenic tectonic settings overprinted by the greenschist facies thermal effects of the final amalgamation and exhumation.

ACKNOWLEDGEMENTS

Over the past 15 years, I have benefitted immensely from the hard work and stimulating discussion of my colleagues and students. Eldridge Moores introduced me to the geology and tectonics of the Sierra and much of my early work was done jointly with him. Our former students J. S. Beard, S. H. Edelman, J. L. Hannah, A Tuminas have been major influences on my thinking and our progress owes much to their efforts and insights. I am most grateful to P. Schiffman, D. Robinson, and R. Bevins for permission to cite unpublished data. Critical reviews of the manuscript by J.S. Beard, T. Fagan, D. Robinson, and X. Zhai were greatly appreciated. This review has been supported by NSF grants EAR-9119390 and EAR-9017844.

REFERENCES

Baird, A. K., 1962, Superposed deformation in the central Sierra Nevada Foothills east of the Mother Lode: California University Publications of Geological Sciences, v. 42, p. 1-70.

Bateman, P. C., Harris, A. G., Kistler, R. W. and Krauskopf, K. B., 1985, Calaveras reversed: Westward younging is indicated: Geology, v. 13, p. 338-341.

Beard, J. S., 1990, Partial melting of metabasites in the contact aureoles of gabbroic rocks in the Smartville Complex, Sierra Nevada, California, in Anderson, J. L., ed., The nature and origin of Cordilleran magmatism: Boulder, Colorado, The Geological Society of America, p. 303 -313.

Beard, J. S. and Day, H. W., 1987, The Smartville intrusive complex, Sierra Nevada, California: The core of a rifted arc: Geological Society of America Bulletin, v. 99, p. 779-791.

Beard, J. S. and Day, H. W., 1988, Petrology of reversely zoned gabbro-diorite plutons, Smartville complex, northern Sierra Nevada, California: Journal of Petrology, v. 29, p. 965-995.

Beiersdorfer, R. E., Beard, J. S., Day, H. W. and Moores, E. M., 1991, Igneous and metamorphic features of the Smartville Complex, northern California, in Walawender, M. J. and Hanan, B. B., ed., Geologic Excursions in Southern California and Mexico: Geological Society of America Guidebook for the 1991 Annual Meeting: Boulder, Colorado, Geological Society of America, p. 68-92.

Best, M. G., 1962, Petrology and structural analysis of metamorphic rocks in the southwestern Sierra nevada foothills, California: California University Publications of Geological Sciences, v. 42, p. 111 - 158.

Bickford, M. E. and Day, H. W., 1988, Jurassic ages of arc-ophiolite complexes, northern Sierra Nevada: Implications for duration ofthe Nevadan "Orogeny".: Geological Society of America Abstracts with Programs, v. 20, p. 274.

Bobbitt, J. B., 1982, Petrology, structure and contact relations of part of the Yuba Rivers Pluton, northwestern Sierra Nevada foothills, California [M.Sc. thesis]: Davis, California, University of California, 160 p.

Bohlke, J. K. and McKee, E. H., 1984, K-Ar ages relating to metamorphism, plutonism, and gold-quartz vein mineralization near Allegheny, Sierra County, California: Isochron/West, v. 39, p. 3-7.

Bond, G. C. and DeVay, J. C., 1980, Pre-upper Devonian quartzose sandstones in the Shoo Fly Formation, northern California - Petrology, provenance, and implications for regional tectonics: Geology, v. 88, p. 285-308.

Brooks, E. R., Wood, M. M. and Garbutt, P. L., 1982, Origin and metamorphism of peperite and associated rocks in the Devonian Elwell Formation, northern Sierra Nevada, California: Geological Society of America Bulletin, v. 93, p. 1208-1231.

Burchfiel, B. C. and Davis, G. A., 1972, Structural framework and evolution of the southern part of the Cordilleran orogen, Western United States: American Journal of Science, v. 272, p. 97-118.

Burchfiel, B. C. and Davis, G. A., 1981, Triassic and Jurassic tectonic evolution of the Klamath Mountains-Sierra Nevada geologic terrane, in Ernst, W. G., ed., The Geotectonic Development of California: Englewood Cliffs, N.J., Prentice-Hall, p. 50-70.

Clark, L. D., 1960, Foothills fault system, western Sierra Nevada, California: Geological Society of America Bulletin, v. 71, p. 483-496.

Clark, L. D., 1964, Stratigraphy and structure of part of the western Sierra Nevada metamorphic belt, California: U.S. Geological Survey Professional Paper, v. 410, p. 70.

Creely, R. S., 1965, Geology of the Oroville quadrangle, California: California Division of Mines and Geology Bulletin, v. 184, p. 1-86.

D'Allura, J. A., 1977, Stratigraphy, structure, petrology and regional correlations of metamorphosed Upper Paleozoic volcanic rocks in portions of Plumas, Sierra, and Nevada Counties, California [Ph.D dissertation]: Davis, California, University of California, 338 p.

D'Allura, J. A., Moores, E. M. and Robinson, L., 1977, Paleozoic rocks of the northern Sierra Nevada, their structural and paleogeographic implications, in Stewart, J. H., Stevens, C. H. and Fritche, A. E., ed., Paleozoic Paleogeography of the Western United States: Pacific Coast Paleogeography Symposium 1: Pacific Section, Society of Economic Paleontologists Mineralogists, p. 395-408.

Day, H. W., Moores, E. M. and Tuminas, A. C., 1985, Structure and tectonics of the northern Sierra Nevada: Geological Society of America Bulletin, v. 96, p. 436-450.

Day, H. W., Schiffman, P. and Moores, E. M., 1988, Metamorphism and tectonics of the northern Sierra Nevada, in Ernst, W. G., ed., Metamorphism and Crustal Evolution of the Western United States: Engelwoods Cliffs, N.J., Prentice Hall, Inc, p. 737-763.

Dickinson, W. R., 1981, Plate tectonics and the continental margin of California, in Ernst, W. G., ed., The Geotectonic Development of California: Engelwood Cliffs, N.J., Prentice Hall, Inc, p. 1-28.

Dilek, Y. and Moores, E. M., 1986, A possible allochthonous oceanic transform fault zone in the northwestern Sierra Nevada, California: Geological Society of America Abstracts with Programs, v. 18, p. 101.

Dilek, Y., Thy, P., Moores, E. M. and Grundvig, S., 1990, Late Paleozoic - early Mesozoic oceanic basement of a Jurassic arc terrane in the northwestern Sierra Nevada, California, in Harwood, D. S. and Miller, M. M., ed., Paleozoic and early Mesozoic paleogeographic relations; Sierra Nevada, Klamath Mountains, and related terranes: Boulder, Colorado, Geological Society of America, p. 351 - 370.

Diller, J. S., 1892, Geology of the Taylorsville region of California: Geological Society of America Bulletin, v. 3, p. 369-394.

Diller, J. S., 1908, Geology of the Taylorsville region, California: U.S. Geological Survey Bulletin, v. 353, p. 1-128.

Duffield, W. A. and Sharp, R. V., 1975, Geology of the Sierra foothills melange and adjacent areas, Amador County, California: U. S. Geological Survey Professional Paper, v. p.

Edelman, S. H., 1986, Structure across the northern Sierra Nevada Foothills suture zone, California: Geological Society of America Abstracts with Programs, v. 18, p. 103.

Edelman, S. H., Day, H. W. and Bickford, M. E., 1989, Implications of U-Pb zircon ages for the tectonic settings of the Smartville and Slate Creek Complexes, northern Sierra Nevada, California: Geology, v. 17, p. 1032-1035.

Edelman, S. H., Day, H. W., Moores, E. M., Zigan, S. M., Murphy, T. P. and Hacker, B. R., 1989, Structure across a Mesozoic ocean-continent suture zone in the northern Sierra Nevada, California: Geological Society of America Special Paper, v. 224, p. 1-56.

Edelman, S. H. and Sharp, W. D., 1989, Terranes, early faults, and pre-Late Jurassic amalgamation of the western Sierra Nevada metamorphic belt: Geological Society of America Bulletin, v. 101, p. 1420-1433.

Ehrenberg, S. M., 1975, Feather River ultramafic body, northern Sierra Nevada, California: Geological Society of America Bulletin, v. 86, p. 1235-1243.

Ernst, W. G., 1983, Phanerozoic continental accretion and metamorphic evolution of northern and central California: Tectonophysics, v. 100, p. 287-320.

Ferguson, H. G. and Gannett, R. W., 1932, Gold quartz veins of the Alleghany district, California: U.S. Geological Survey Professional Paper, v. 172, p. 1-139.

Gefell, M. J., 1989, Shear sense for the bounding faults of the Feather River peridotite, northern Sierra Nevada, California [M.S. thesis]: Davis, California, University of California, 51 p.

Girty, G. H. and Wardlaw, M. S., 1984, Was the Alexander terrane a source of feldspathic sandstones in the Shoo Fly Complex, Sierra Nevada, California?: Geology, v. 12, p. 339-342.

Girty, G. H. and Wardlaw, M. S., 1985, Petrology and provenance of pre-Late Devonian sandstones, Shoo Fly Complex, northern Sierra Nevada, California: Geological Society of America Bulletin, v. 96, p. 516-521.

Girty, G. H., Wardlaw, M. S., Schweickert, R. A., Hanson, R. and S., B., 1984, Timing of pre-Antler deformation in the Shoo Fly Complex, Sierra Nevada, California: Geology, v. 12, p. 673-676.

Hacker, B. R. and Goodge, J. W., 1990, Comparison of early Mesozoic high-pressure rocks in the Klamath Mountains and Sierra Nevada, in Harwood, D. S. and Miller, M. M., ed., Paleozoic and early Mesozoic paleogeographic relations; Sierra Nevada, Klamath Mountains, and related terranes: Boulder, Colorado, Geological Society of America, p. 277 - 295.

Hacker, B. R. and Peacock, S. M., 1990, Comparison of of the Central Metamorphic Belt and Trinity terrane of the Klamath Mountains with the Feather River terrane of the Sierra Nevada, in Harwood, D. S. and Miller, M. M., ed., Paleozoic and early Mesozoic paleogeographic relations; Sierra Nevada, Klamath Mountains, and related terranes: Boulder, Colorado, Geological Society of America, p. 75 - 92.

Hannah, J. L., 1980, Stratigraphy, petrology, paleomagnetism, and tectonics of Paleozoic arc complexes, Northern Sierra Nevada, California [Ph.D. dissertation]: Davis, California, University of California, 323 p.

Hannah, J. L. and Moores, E. M., 1986, Age relations and depositional environment of Paleozoic strata, northern Sierra Nevada, California: Geological Society of America Bulletin, v. 97, p. 787-797.

Hanson, R. E., 1983, Volcanism, plutonism and sedimentation in a Late Devonian submarine island-arc setting, northern Sierra Nevada, California [Ph.D. dissertation]: New York, N.Y., Columbia University, 345 p.

Hanson, R. E., Saleeby, J. A. and A., S. R., 1988, Composite Devonian island-arc batholith in the northern Sierra Nevada, California: Geological Society of America Bulletin, v. 100, p. 446-457.

Harland, W. B., Armstrong, R. L., Cox, A. V., Craig, L. E., Smith, A. G. and Smith, D. G., 1990, A geologic time scale 1989: Cambridge, U. K., Cambridge University Press, 263 p.

Harwood, D. S., 1983, Stratigraphy of Upper Paleozoic rocks and regional unconformities in part of the northern Sierra terrane, California: Geologic Society of America Bulletin, v. 94, p. 413-422.

Harwood, D. S., 1988, Tectonism and metamorphism in the Northern Sierra Terrane, northern California, in Ernst, W. G., ed., Metamorphism and Crustal Evolution of the Western United States: Engelwood Cliffs, N.J., Prentice Hall, Inc, p. 764-788.

Hietanen, A., 1951, Metamorphic and igneous rocks of the Merrimac area. Plumas National Forest, California: Geologic Society of America Bulletin, v. 67, p. 565-607.

Hietanen, A., 1973, Geology of the Pulga and Bucks Lake quadrangles, Butte and Plumas counties, California: U.S. Geological Survey Professional Paper, v. 731, p. 1-66.

Hietanen, A., 1976, Metmorphism and plutonism around the middle and south forks of the Feather River, California: U.S. Geological Survey Professional Paper, v. 920, p. 1-30.

Hietanen, A., 1977, Paleozoic-Mesozoic boundary in the Berry Creek quadrangle, northwestern Sierra Nevada, California: U.S. Geological Survey Professional Paper, v. 1027, p. 1-22.

Hietanen, A., 1981, Geology west of the Melones Fault between the Feather and North Yuba Rivers, California: U. S. Geological Survey Professional Paper, v. 1226-A, p. 1-35.

Hietanen, A., 1981, Petrologic and structural studies in the northwestern Sierra Nevada, California: U.S. Geological Survey Professional Paper, v. 1226, p. 1-59.

Imlay, R. W., 1961, Late Jurassic ammonites from the western Sierra Nevada, California: U.S. Geological Survey Professional Paper, v. 374-D, p. 1-30.

Irwin, W. P., Jones, D. L. and Kaplan, T. A., 1978, Radiolarians from pre-Nevadan rocks of the Klamath Mountains, California and Oregon, in Howell, D. G. and McDougall, K. A., ed., Mesozoic Paleogeography of the Western United States: Pacific Coast Paleogeography Symposium 2: Pacific Section, Society of Economic Paleontologists Mineralogists, p. 303-310.

Kistler, R. W. and Peterman, Z. E., 1973, Variations in Sr, Rb, K, Na, and initial 87Sr/86Sr in Mesozoic granitic rocks and intruded wall rocks in central California: Geological Society of America Bulletin, v. 84, p. 3489-3512.

Knopf, A., 1929, The Mother Lode system of California: U.S. Geological Survey Professional Paper, v. 157, p. 1-88.

Lang, R. A. and Manduca, C. A., 1991, Application of the aluminum-in - hornblende igneous geobarometer to the Oliver Lake pluton, Feather River area, northern Sierra Nevada: Geological Society of America, Abstracts with Programs, v. 23, p. 44.

Liou, J. G., Maruyama, S. and Cho, M., 1985, Phase equilibria and mineral parageneses of metabasites in low grade metamorphism: Mineral. Mag., v. 49, p. 321-334.

Marlette, J. W., Akers, R. J., Cole, K. A. and McJunkin, R. D., 1979, Geologic Investigations, in the August 1, 1975 Oroville Earthquake Investigations: Department of Water Resources Bulletin, v. 203-78, p. 15-11.

Mazaheri, S. A., 1982, The petrology and metamorphism of ultramafic and mafic rocks near Pulga, Butte County, California [M.Sc. thesis]: Davis, California, University of California, 139 p.

McLeod, M. and Day, H., 1991, Hornblende barometry of calc-alkaline plutons and movement history of the Big Bend fault zone northernSierra Nevada, CA.: Geological Society of America Abstracts with Programs, v. 23, p. 78.

McMath, V. E., 1958, The geology of the Taylorsville area, Plumas County, California [Ph.D. disseration]: Los Angeles, California, University of California, 199 p.

Miller, R. B. and Paterson, S. R., 1991, Geology and tectonic evolution of the Bear Mountains fault zone, Foothills Terrane, Central Sierra Nevada, California: Tectonics, v. 10, p. 995-1006.

Miyashiro, A., 1961, Evolution of Metamorphic Belts: Journal of Petrology, v. 2, p. 277-311.

Miyashiro, A., 1973, Metamorphism and Metamorphic Belts: New York, John Wiley & Sons, 492 p.

Moores, E. M., 1972, Model for Jurassic island arc, continental margin collision in California: Geological Society of America Abstracts with Programs, v. 4, p. 202.

Moores, E. M. and Day, H. W., 1984, An overthrust model for the Sierra Nevada: Geology, v. 12, p. 416-419.

Saleeby, J. B., 1981, Ocean floor accretion and volcano plutonic arc evolution in the Mesozoic Sierra Nevada, in Ernst, W. G., ed., The Geotectonic Development of California: Englewood Cliffs, N.J., Prentice-Hall, p. 132-181.

Saleeby, J. B., 1981, Ocean floor accretion and volcano-plutonic arc evolution of the Mesozoic Sierra Nevada, California, in Ernst, W. G., ed., The Geotectonic Development of California: Englewood Cliffs, N. J., Prentice-Hall, p. 132-181.

Saleeby, J. B. and Moores, E. M., 1979, Zircon ages on northern Sierra Nevadan ophiolite remnants and some possible regional correlations: Geological Society of American Abstracts with Programs, v. 11, p. 125.

Saleeby, J. B., Shaw, H. F., Niemeyer, S., Moores, E. M. and Edelman, S. H., 1989, U/Pb, Sm/Nd and Rb/Sr geochronological and isotopic study of Northern Sierra Nevada ophiolitic assemblages, California: Contributions to Mineralogy and Petrology, v. 102, p. 205-220.

Schweickert, R. A., 1981, Tectonic Evolution of the Sierra Nevada Range, in Ernst, W. G., ed., The Geotectonic Development of California: Englewood Cliffs, N. J., Prentice-Hall, p. 87-131.

Schweickert, R. A., Armstrong, R. L. and Harakal, J. E., 1980, Lawsonite blueschist in the northern Sierra Nevada, California: Geology, v. 8, p. 27-31.

Schweickert, R. A., Bogen, N. I., Girty, G. H., E., H. R. and Merguerian, C., 1984, Timing and structural expression of the Nevadan orogeny, Sierra Nevada, California: Geological Society America Bulletin, v. 95, p. 967-979.

Schweickert, R. A. and Cowan, D. S., 1975, Early Mesozoic tectonic evolution of the western Sierra Nevada, California: Geological Society of America Bulletin, v. 86, p. 1329-1336.

Schweickert, R. A., Harwood, D. S., Girty, G. H. and Hanson, R. E., 1984, Tectonic development of the Northern Sierra terrane — An accreted Late Paleozoic island arc and its basement, in Lintz, J., Jr., ed., Western Geological Excursions, Vol. 4: Geological Society of America Guidebook, p. 1-65.

Schweickert, R. A., Merguerian, C. and Bogen, N. L., 1988, Deformational and metamorphic history of Paleozoic and Mesozoic basement terranes in the western Sierra Nevada metamorphic belt, in Ernst, W. G., ed., Metamorphism and Crustal Evolution of the Western United States: Engelwood Cliffs, N.J., Prentice Hall, Inc, p. 789 - 822.

Schweickert, R. A. and Snyder, W. S., 1981, Paleozoic plate tectonics of the Sierra Nevada and adjacent regions, in Ernst, W. G., ed., The Geotectonic Development of California: Englewood Cliffs, N. J., Prentice-Hall, p. 182-201.

Sharp, W. D., 1988, Pre-Cretaceous crustal evolution in the Sierra Nevada region, California, in Ernst, W. G., ed., Metamorphism and Crustal Evolution of the Western United States: Engelwood Cliffs, N.J., Prentice Hall, Inc, p.

Smith, J. P., 1909, Salient events in the geologic history of California: Science, v. 30, p. 346-351.

Souter, B. and Day, H. W., 1991, Arc basement of the Smartville Complex, northern Sierra Nevada, California: Geological Society of America Abstracts with Programs, v. 23, p. 99.

Springer, R. K., Day, H. W. and Beiersdorfer, R. E., 1992, Prehnite-pumpellyite to greenschist facies transition, Smartville Complex, near Auburn, California: Journal of Metamorphic Geology, v. 10, p. 147 - 170.

Standlee, L. A., 1978, Geology of the northern Sierra Nevada basement rocks, Quincy-Downieville area, California [Ph.D. dissertation]: Houston, Texas, Rice University, 176 p.

Standlee, L. A., 1978, Middle Paleozoic ophiolite in the Melones fault zone, northern Sierra Nevada, California: Geological Society of America Abstracts with Programs, v. 10, p. 148.

Standlee, L. A. and Nestell, M. K., 1985, Age and tectonic significance of terranes adjacent to the Melones fault zone, N. Sierra Nevada, California: Geologic Society of America Abstracts with Programs, v. 17, p. 410.

Swanson, S. E., 1970, Mineralogy and petrology of the Rocklin pluton, Placer and Sacramento Counties, California [M.Sc. thesis]: Davis, California, University of California, 85 p.

Taliaferro, N. L., 1942, Geologic history and correlation of the Jurassic of southwestern Oregon and California: Geological Society of America Bulletin, v. 53, p. 71-112.

Tobisch, O. T., Paterson, S. R., Saleeby, J. B. and Geary, E. E., 1989, Nature and timing of deformation in the Foothills terrane, central Sierra Nevada, California: Its bearing on orogenesis: Geological Society of America Bulletin, v. 101, p. 401-413.

Tuminas, A. C., 1983, Structural and stratigraphic relations in the Grass Valley-Colfax area of the northern Sierra Nevada foothills, California [Ph.D. dissertation]: Davis, California, University of California, 415 p.

Turner, H. W., 1897, Downieville Folio, California: Geologic Atla of the United States, v. Folio 37, p.

Vaitl, J., 1980, Geology of the Cherokee area, northern Sierra Nevada, California [M.Sc. thesis]: Davis, California, University of California, 93 p.

Varga, R. J. and Moores, E. M., 1981, Age, origin and significance of an unconformity that predates island-arc volcanism in the northern Sierra Nevada, California: Geology, v. 9, p. 512-518.

Weisenberg, C. W., 1979, Structural development of the Red Hill portion of the Feather River ultramafic complex, Plumas County, California [Ph.D. dissertation]: Houston, Texas, University of California, 166 p.

Weisenberg, C. W. and Ave Lallemant, H., 1977, Permo-Triassic emplacement of the Feather River ultramafic body, northern Sierra Nevada mountains, California: Geological Society of America Abstracts with Programs, v. 9, p. 525.

Whitney, J. D., 1865, Geology of California: Sacramento, Geological Survey of California, 498 p.

Wright, J. E. and Fahan, M. R., 1988, An expanded view of Jurassic orogenesis in the western United States Cordillera; Middle Jurassic (pre-Nevadan) regional metamorphism and thrust faulting within an active arc environment, Klamath Mountains, California.: Geological Society of America Bulletin, v. 100, p.

Xenophontos, C., 1984, Geology, petrology, and geochemistry of part of the Smartville Complex, northern Sierra Nevada, California [Ph.D. dissertation]: Davis, California, University of California, 446 p.

Zigan, S. M., 1981, Structure and stratigraphy of the LaPorte ophiolite sequence, northern Sierra Nevada, California [M.S.]: Davis, California, University of California, 100 p.

METAMORPHIC FEATURES OF THE SMARTVILLE COMPLEX, NORTHERN SIERRA NEVADA, CALIFORNIA

RAYMOND E. BEIERSDORFER
and
HOWARD W. DAY
Department of Geology
University of California, Davis
Davis, CA 95616

INTRODUCTION

Regional Setting

The Smartville Complex is a suite of Jurassic metaigneous and metasedimentary rocks that are interpreted to represent a rifted volcanic arc, portions of its igneous basement, and fragments of its post-volcanic sedimentary cover. It occupies the westernmost of four fault-bounded lithotectonic belts in the northern Sierra Nevada that represent the transition from a continental margin assemblage in the east to accreted oceanic rocks on the west (see Day, Chapter 2).

The Smartville Complex (Fig. 1) is unconformably overlain on the west by Upper Cretaceous and younger rocks of the Great Valley. The Big Bend-Wolf Creek fault zone separates the complex from sedimentary rocks of the Central Belt to the north and east. Along much of the eastern boundary, the Yuba Rivers Pluton intrudes both the Smartville Complex and the Central Belt and is itself deformed by the fault (Day et al.,1985) . The Smartville Complex south of the Bear River (Springer et al., 1992; unpublished data) can be correlated with the Gopher Ridge and Copper Hill volcanics and similar rocks that are known to extend at least as far south as the Merced River (Clark, 1964).

The metaigneous rocks of the Smartville Complex are overlain, in the northwest, by fossiliferous, quartz-lithic metasandstones of the Monte de Oro Formation and the Penz Sandstone (Creely, 1965) that we include in the Smartville Complex. Elsewhere, the Smartville Complex is overlain by Tertiary volcanic rocks and auriferous gravels that were hydraulically mined during the nineteenth century and are being actively reworked today. Half-windows through the Smartville Complex expose metasedimentary rocks of the Central Belt in the northwest and in the southeast.

Age

Fossil and radiometric data suggest that most of the Smartville Complex is Upper Jurassic. Fossils are known from several localities in the upper volcanic unit and its sedimentary cover (Penz Sandstone, Monte de Oro Fm). In each case, the fossils indicate that the rocks formed near the Oxfordian-Kimmeridgian boundary (Creely, 1965;

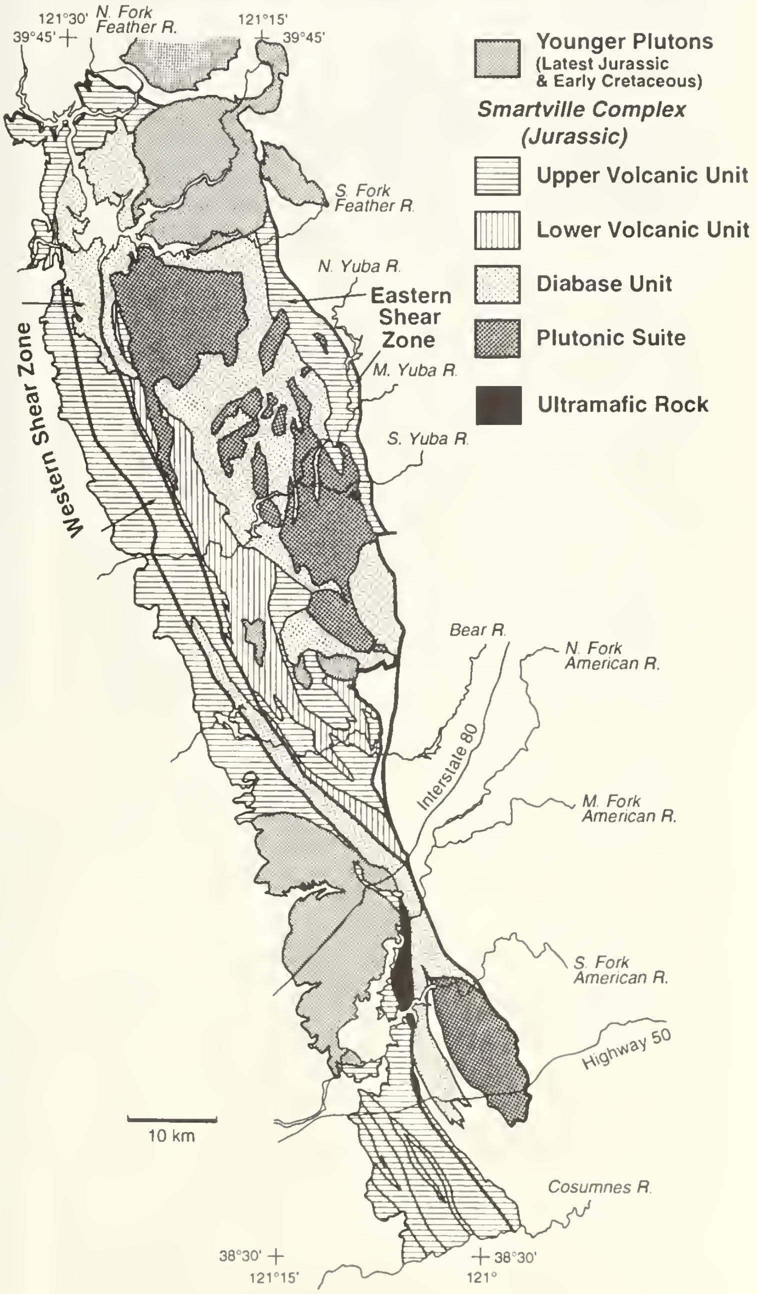

Figure 1. Geologic map of the Smartville Complex, California.

Marlette et al., 1979; Xenophontos , 1984). Radiometric ages from the Smartville Complex range from 159±2 to 164±2 Ma, which is consistent with the fossil data (U-Pb, zircon; Saleeby et al., 1989; Edelman et al., 1989; Bickford and Day, 1988, in prep.). Recent radiometric data suggest that the circa 160 Ma volcanic-plutonic suite was constructed on a basement that contained elements of an older circa 200 Ma magmatic arc (Bickford and Day, 1988; Day and Bickford, 1989; Edelman et al., 1989).

GEOLOGIC UNITS

From west to east , the Smartville Complex consists of upper and lower volcanic units, a diabase unit and plutonic suite (Fig. 1).

Upper Volcanic Unit (Stops 3,6,7).

The upper volcanic unit is exposed along the western, eastern, and southern flanks of the Smartville Complex (Fig. 1). A wide variety of volcanogenic rocks are present in the unit, including massive and pillowed flows of basaltic to andesitic composition, mafic to silicic pyroclastic rocks, well-bedded epiclastic rocks, and silicic domes and flows. In general, hetero- and homo-lithic volcaniclastic conglomerates, well-bedded sand to cobble-sized volcaniclastics and pyroxene-andesite breccias (Photo 1) predominate (Xenophontos, 1984). An accurate determination of the thickness of the unit is difficult due to poor exposures and structural complications (mostly shearing and faulting). Buer (1979) determined the upper volcanic unit, north of the Yuba River to be 3.2 km thick. Xenophontos (1984) estimated the upper volcanic unit to be from 1.5 km to 4.5 km thick in the vicinity of the Bear River.

Igneous and sedimentary textures are well-preserved despite pervasive low-grade metamorphism. Rocks in the upper volcanic unit typically are porphyritic. Albitized plagioclase is a common phenocryst phase, comprising 20% of some samples. Clinopyroxene is common and is the most conspicuous phenocryst phase in the upper volcanic unit (Photos 2 & 3). The clinopyroxene is low-Al augite or diopsidic augite with formula Ti usually < 0.015 per 6 oxygen. Upper volcanic unit rocks average 60% SiO2 , andesites are common and most rocks are calc-alkaline by standard whole-rock discriminants (Xenophontos, 1984). Diabase intrusives occur locally as dikes (Photo 3), sills and irregular masses.

The contact between the upper and lower volcanic units is exposed along the north bank of the Yuba River, downstream from Stop 1. The contact is marked by approximately 4 m of thinly-bedded sandstone to silty mudstone lying conformably on close-packed pillows. South of the Bear River, the contact between the upper and lower volcanic units is characterized by 50 to 100 m of thinly-laminated tuffaceous chert, traceable along strike for 10 km (Springer et al., 1992).

Lower Volcanic Unit (Stop 1).

The lower volcanic unit crops out in a north-northwest trending belt approximately 60 kilometers long (Fig 1). The unit consists largely of massive and pillowed flows and pillow breccias of basaltic composition. Igneous textures, on scales ranging from outcrop to thin section, are commonly well preserved. Pillow structures are especially well developed and exposed along the Yuba River at Parks Bar (Stop 1) (Photo 4). Red and green interpillow chert and hyaloclastite material occur locally. Pillow rinds preserve skeletal crystal forms in a matrix of devitrified glass. Crystals in the pillow cores tend to be somewhat larger, suggesting continued crystallization after eruption (Xenophontos and Bond, 1978). Vesicles are sparse and commonly filled with metamorphic quartz, chlorite, epidote, prehnite and pumpellyite.

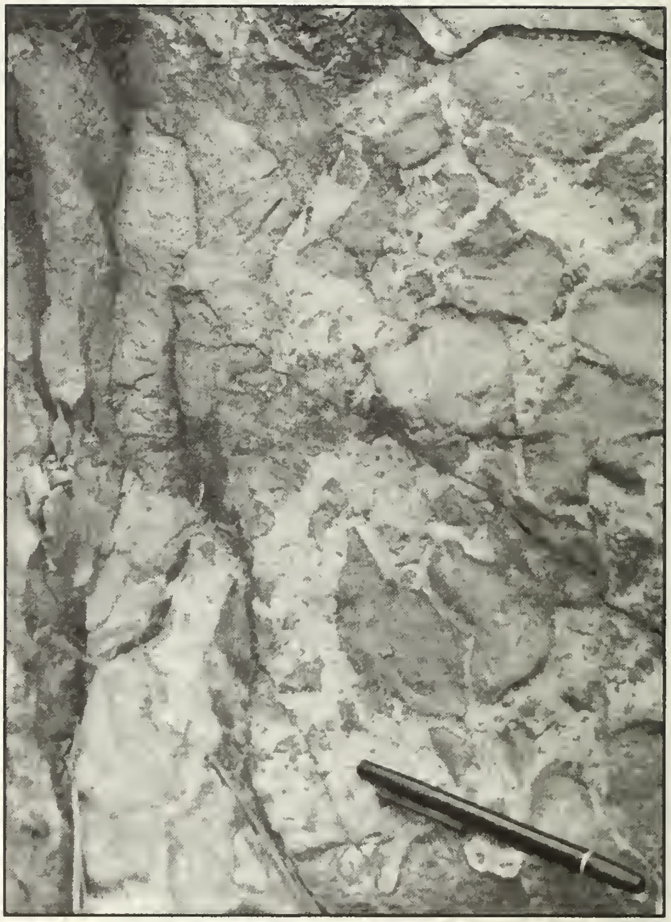

Photo 1. Field photograph of volcanic breccia in the upper volcanic unit at Stop 6. The light color of the matrix reflects an abundance of epidote.

Rocks in the lower volcanic unit are aphyric to porphyritic. Augite and plagioclase are the most common phenocryst phases (Photo 5). Plagioclase is typically altered to albite, but a few unaltered grains are An60-66 (Xenophontos, 1984). Clinopyroxene chemistry spans the range of island-arc and ocean-floor basalt (Day et al., 1982; Beiersdorfer et al, 1991). Detailed stratigraphic (Xenophontos and Bond, 1978) and geochemical studies (Moores and Hoeck, in prep.) suggest that there is substantial intercalation of tholeiitic and calc-alkaline rocks within the lower volcanic unit. There appears to be a tendency for the rocks to become increasingly calc-alkaline up section, consistent with the interpretation, first put forth by Xenophontos and Bond (1978), that the contact between the lower and upper volcanic units is gradational.

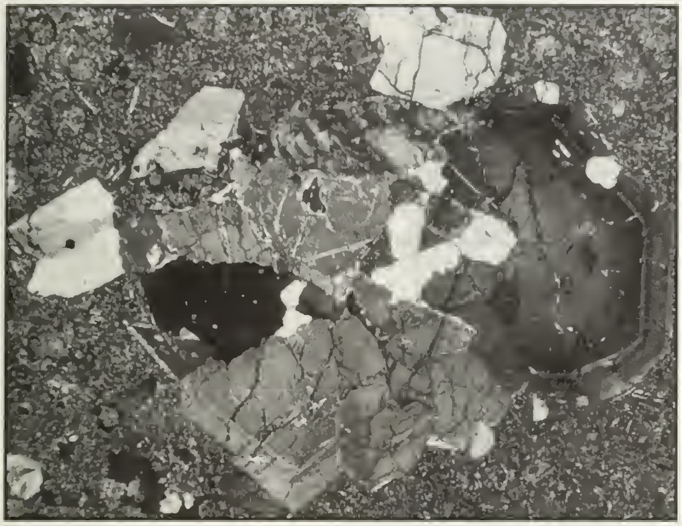

Photo 2. Photomicrograph of clinopyroxene phenocryst in meta-andesite of the upper volcanic unit at Stop 3.

Photo 3. Field photograph of clinopyroxene rich volcaniclastic (left) intruded by a dike with epidote veins and a well-developed chilled margin, at Stop 3. Diameter of coin is 18 mm.

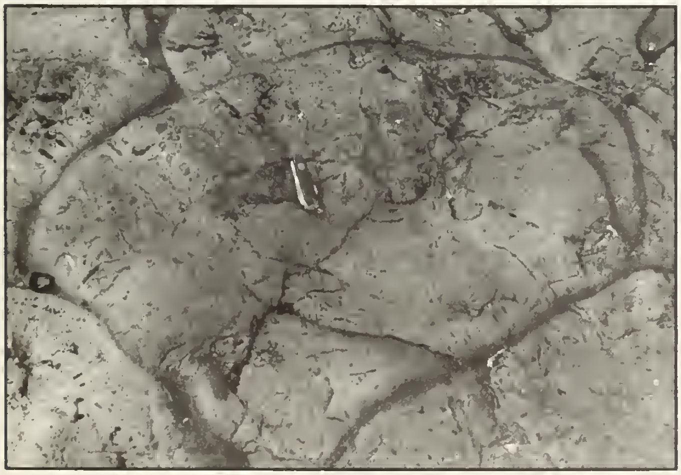

Photo 4. Field photograph of pillow basalt in the lower volcanic unit at Stop 1.

Diabase Unit

The area mapped as the Diabase Unit on Figure 1 consists of massive diabase and dike complex. Massive diabase refers to metadiabases, metadiorites and metagabbros that have been intruded by all other intrusive rocks in the Smartville Complex (Beard and Day, 1987). Metagabbro and metadiorite occur as bodies ranging in size from small pods about 1 meter in maximum dimension to kilometer scale, coarse-grained, foliated, irregular shaped plutons. The massive diabase is everywhere metamorphosed, generally to greenschist facies. Pyroxene hornfels are found in contact aureoles. Relict igneous phases include zoned plagioclase, rare clinopyroxene and late magmatic hornblende.

The massive diabase unit is older than all other intrusive rocks with which it is in contact (Beard and Day, 1987) and occurs in close spatial relationship with 198 Ma deformed tonalite (Edelman et al., 1989; Souter and Day, 1991). These observations are consistent with the hypothesis that the massive diabase may be part of the basement of the Smartville Complex. Testing of this hypothesis by determination of the age of the massive diabase unit awaits further work.

The dike complex consists of hypabyssal rocks of 100% dikes or 100% dikes with well-developed sheeted structure. The dike complex has been mapped and described by Day (1977), Buer (1979), Xenophontos (1984), and Beard (1985). The dike complex intrudes both the lower and upper volcanic units. The contacts between the dike complex and the lower and upper volcanic units are gradational. Over a distance of approximately 1 km, the proportion of dikes in the volcanic units increases until outcrops consist of 100% dikes. Rare screens of volcanic rocks can be found in the dike unit near the contact. The dike unit also passes gradually into tonalite plutons with decreasing density of dikes. Screens and dikes of sodic tonalite (plagiogranite) are found in the dike complex near the contact and mafic dikes are mutually intrusive with the tonalite plutons. Gabbro-diorite plutons intrude the dike complex.

Sheeted dikes are best exposed on Stanfield Hill (Stop 4). This locality was studied in detail by S. D. Day (1977). At this outcrop chilled dike margins are abundant and dike-within-dike (sheeted) structure is well developed (Photo 6). Cross-cutting dikes are common but most dikes are subparallel, strike N15°-40°W and dip about 60°NE. Basaltic, intermediate, and silicic dikes all appear to belong to the main intrusive phase of the dike complex. Most dikes contain plagioclase and/or clinopyroxene phenocrysts, but aphyric basaltic dikes are common. These aphyric basaltic dikes are, for the most part, later than the main phase.

Most of the dikes contain plagioclase, clinopyroxene, quartz, opaques, apatite and zircon. Igneous textures are well-preserved, but most dikes are altered and contain metamorphic minerals such as actinolite, chlorite, epidote or clinozoisite, sphene, calcite, and sericite. Amygdules are common and are filled by calcite, epidote, chlorite and quartz. Epidote, quartz, calcite, and pyrite in veins are common. Normally zoned plagioclase in one sample of a basalt dike shows a core to rim variation

Photo 5. Photomicrograph of albitized plagioclase phenocryst containing pumpellyite, in metabasalt from the lower volcanic unit at Stop 1.

of An58 - An31 (Day, 1977, p. 27), but homogeneous albite phenocrysts are common in more silicic lithologies. Clinopyroxene compositions cluster near Wo40 En50Fs10.

Smartville Plutonic Suite.

The plutonic rocks in the Smartville Complex can be divided into gabbroic and silicic intrusions (Beard, 1985; Beard and Day, 1988). Gabbroic intrusions include 1) small, unzoned bodies that consist largely of olivine gabbro and olivine clinopyroxenite, a kilometer or less in diameter; 2) intermediate, 5-8 km wide, reversely zoned, pyroxene gabbro plutons cored by olivine gabbro; and 3) large, 25 km, reversely zoned plutons ranging in composition from quartz diorite to olivine gabbro. Silicic intrusive rocks occur as 1) elongate biotite-hornblende tonalite plutons; 2) elongate hornblende tonalite ("plagiogranites") plutons; and 3) granodiorite plutons. In addition, areas of intrusive breccia having tonalite or granodiorite matrix are common (Beard , 1985; Beard and Day 1987).

Younger Plutons

Latest Jurassic/Early Cretaceous plutons are intrusive into the Smartville Complex (Fig. 1). In the north the Bald Rock Batholith (Compton, 1955) is made up of leucotrondhjemite, trondhjemite, granodiorite and tonalite. The contacts between these units are gradational (Compton, 1955). In the south, the Smartville Complex is intruded by the composite Penryn/Rocklin pluton. The southerly Rocklin pluton is a Lower Cretaceous (128 Ma) silicic quartz diorite (30% average modal quartz) that is intrusive into intermediate quartz diorite (16% average modal quartz) of the Upper Jurassic (136 Ma) Penryn pluton (Olmstead, 1971; Swanson, 1978).

Photo 6. Field photograph of a dike intruding into other dikes of the dike complex of diabase unit, at Stanfield Hill, Stop 4.

DEFORMATION

The Smartville Complex is structurally uncomplicated. The major structural features present are northwest trending folds and two major shear zones, the western and eastern shear zones. In general, the folds are upright open folds (wave lengths approximately 1 - 6 km), that are determined by changes in younging direction within the upper and lower volcanic units (Xenophontos, 1984; Beard and Day, 1987). Beard and Day (1987) have determined that the folding of the upper and lower volcanic units pre-dates the intrusion of the dike complex.

The western shear zone occurs within the upper volcanic and diabase units. It is characterized by a near vertical foliation that results in a tombstone appearance of outcrops. In detail, the foliation is defined by subparallel alignment of chlorite, amphibole and epidote (Photo 7). The western shear zone ranges in width from approximately 1 to 6 kilometers. Based on overturned bedding and the orientation of rare kink folds, Xenophontos (1984) has determined that reverse (east-side up) dip-slip movement was dominant.

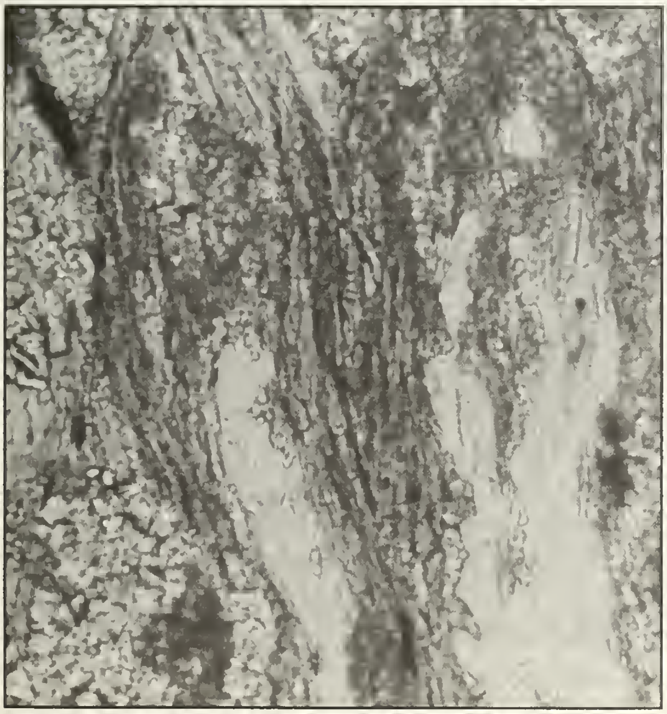

Photo 7. Photomicrograph of foliated greenschist in upper volcanic unit within western shear zone, north of Stop 3.

The western shear zone was originally thought to be the northern continuation of the Bear Mountains Fault Zone (Cady, 1975) and to represent a major suture between the Smartville ophiolite to the east and island arc complex to the west (Schweickert and Cowan, 1975). Xenophontos and Bond (1978) and Buer (1979) have shown that foliated metavolcanic rocks within the zone are equivalent to undeformed rocks to the east and west; therefore, the shear zone does not represent a major suture and displacement along it was minor (Xenophontos and Bond 1978).

The eastern shear zone occurs along the faulted margin separating the Smartville Complex from the Central Belt (see Day, Chapter 2). This shear zone is part of the Wolf Creek Fault Zone of Tuminas (1983) and continues to the north as the Big Bend Fault (Hietanen, 1973). In the southern part of the complex, the Bear Mountain Fault Zone (Cady, 1975) separates the Smartville Complex from the Central Belt (see Day, Chapter 2). The eastern shear zone occurs within the upper volcanic unit and is characterized by a steeply dipping foliation, defined by subparallel alignment of amphibole, epidote and biotite. Near the eastern margin of the shear zone, the foliation is so well developed that the determination of the original rock type is very difficult . This is illustrated by comparison of field trip stops six and seven, located less than a kilometer apart. Stop six consists of a homolithic volcaniclastic breccia whose volcaniclastic origin is readily discernible (Photo 1). Stop seven consists of a penetratively foliated rock containing epidote boudins and lozenges of various sizes and shapes (see road log).

METAMORPHISM

Previous Work

Initial work in the Smartville Complex suggested that Nevadan regional greenschist facies metamorphism produced the observed assemblages (2e. g. Hietanen, 1951, 1973, 1976; Compton, 1955; Clark, 1960, 1964). Xenophontos and Bond (1978) reported pumpellyite-bearing assemblages in the complex but considered the bulk of the metamorphic rocks to belong to the greenschist facies. Beiersdorfer (1982), Beiersdorfer and Day (1983) and Xenophontos (1984) reported the common occurrence of sub-greenschist prehnite- and/or pumpellyite-bearing assemblages.

Occurrence of Metamorphic Minerals

The metamorphic minerals identified in the Smartville Complex are pumpellyite, prehnite, epidote, quartz, albite and feldspar, chlorite, muscovite, biotite, amphibole, pyroxene, garnet, calcite, sphene, magnetite and pyrite (Figure 2).

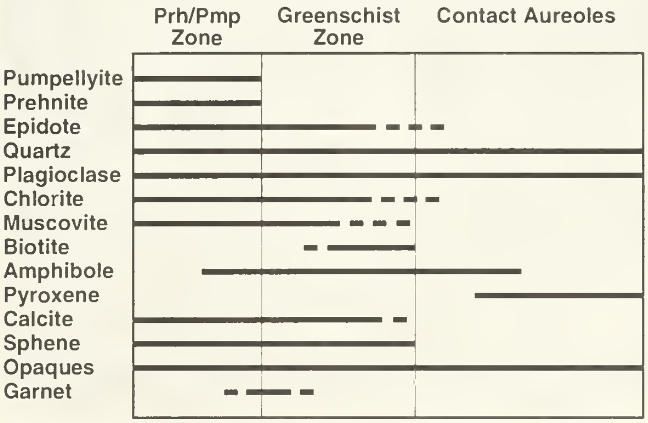

Figure 2. Occurrence of metamorphic minerals in the metamorphic zones of the Smartville Complex, California.

Pumpellyite: Pumpellyite occurs sporadically in rocks of the upper and lower volcanic unit. It occurs in amygdules, in veins, in the groundmass and as alteration of relict plagioclase phenocrysts (Photo 5). Radial aggregates of acicular crystals filling amygdules are common (Photo 8). Pumpellyite commonly exhibits colorless to green pleiochroism, although non-pleochroic brown and golden pumpellyite also occur but are less common.

Prehnite: Prehnite occurs sporadically in rocks of the upper and lower volcanic unit. It occurs as radial aggregates of acicular crystals in amygdules (Photo 9), as acicular and prismatic crystals in veins, as alteration of relict plagioclase phenocrysts and as irregular fine grained masses in the groundmass.

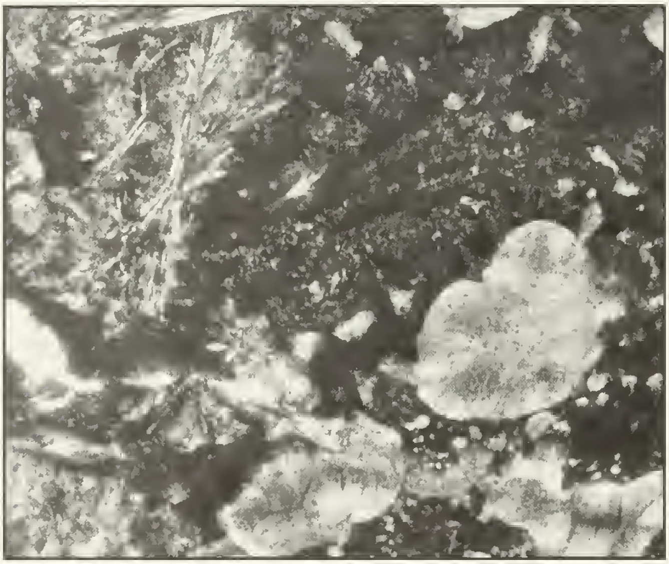

Photo 8. Photomicrograph of pumpellyite-filled amygdules in pillow basalt containing swallow tailed plagioclase feldspar, lower volcanic unit, Stop 1.

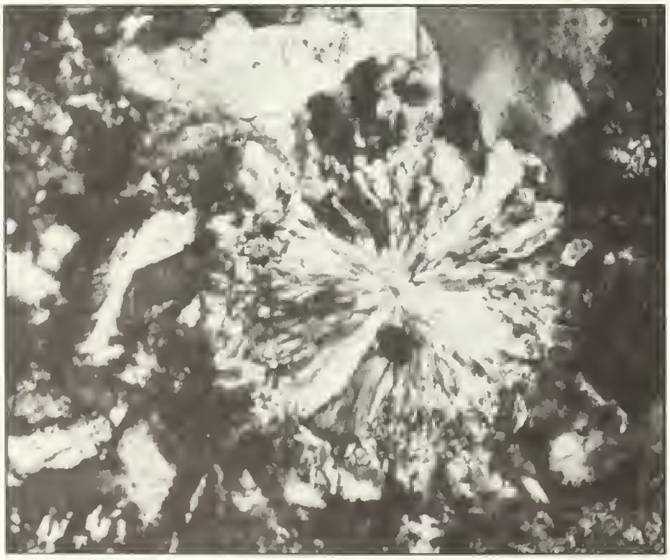

Photo 9. Photomicrograph of radial prehnite in an amygdule from an amygdaloidal basalt of the lower volcanic unit.

Epidote: Epidote is the most common calc-silicate mineral in the Smartville Complex. It occurs in rocks of all the units of the complex. Common occurrences of epidote include preferential alteration of the matrix (Photo 1) and diffuse epidotization of clasts and matrix (Photo 10) in volcaniclastic rocks. In outcrops containing dikes, epidote commonly is concentrated along dike margins (Photo 11). In thin section it occurs as polycrystalline masses in amygdules and veins (Photo 12) and as xenoblastic and acicular inclusions in relict plagioclase phenocrysts. Within the groundmass, epidote occurrence ranges from individual crystals to granular aggregates to regions consisting almost entirely of epidote with minor amounts of quartz (Photo 13). These epidote-quartz rocks are called epidosites and are thought to form due to hydrothermal replacement during sub-seafloor metamorphism (Schiffman et al., 1990). Color ranges from colorless to yellow to light yellow-green.

Photo 10. Field photograph of diffuse epidote alteration in volcaniclastic of the upper volcanic unit, Stop 3.

Quartz: Quartz is ubiquitous in the Smartville complex, occurring in veins and in the groundmass of all rock types and in amygdules in the upper and lower volcanic units. Quartz commonly occurs as xenoblastic crystals within the groundmass and as microcrystalline aggregates in amygdules and veins.

Plagioclase Feldspar: Plagioclase feldspar occurs in rocks of all units of the Smartville Complex. Alteration of primary plagioclase compositions to albite is ubiquitous, though variable, throughout the non-plutonic units of the Smartville Complex (Xenophontos, 1984, Beard and Day, 1987). Relict phenocrysts of plagioclase feldspar typically are altered to various combinations of quartz, epidote, prehnite and pumpellyite (Photo 5). Textures characteristic of quenching (Bryan, 1972), such as "swallow tail" (Photos 5 & 8) and "belt buckle" plagioclase are common in samples from the lower volcanic unit.

Chlorite: Chlorite is the most common phyllosilicate mineral in the Smartville Complex, occurring in amygdules, veins or groundmass of most rocks of the non-plutonic units. However its modal abundance is significantly less in the diabase unit compared to the upper and lower volcanic units. It commonly occurs as fine-grained microcrystalline mats in amygdules (Photo 12), in veins, in the groundmass and as pseudomorphs after clinopyroxene phenocrysts (Photo 14). It varies in color from colorless to light green. Birefringence colors are anomalous varying from blue to violet to brown.

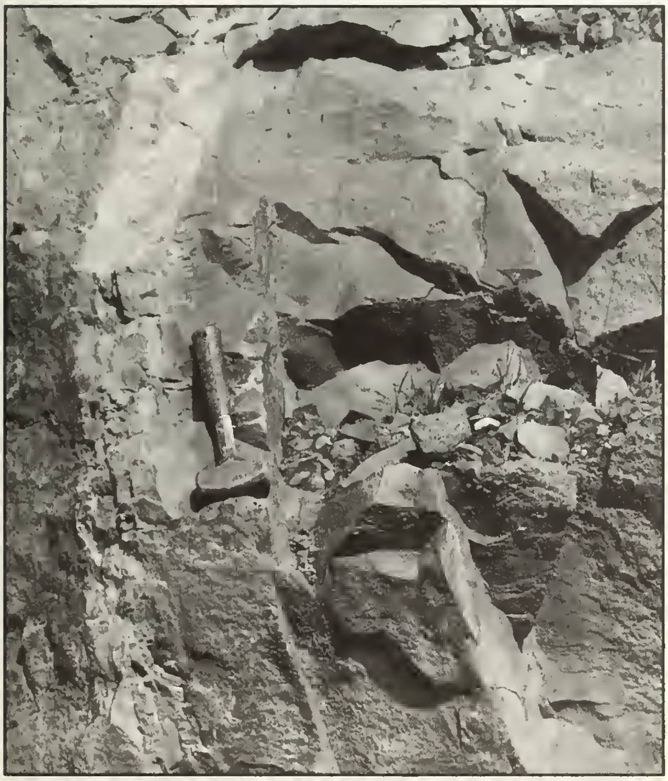

Photo 11. Field photograph of dike intrusive into volcaniclastic, epidote alteration is concentrated along dike margin, upper volcanic unit, Stop 3.

Muscovite: Muscovite occurs rarely in rocks of the upper and lower volcanic units. It commonly occurs, in minor amounts, as aggregates of fine-grained platy crystals in amygdules or within the groundmass.

Biotite: Metamorphic biotite occurs in rocks of upper volcanic, lower volcanic and diabase units of the Smartville Complex, but is rare. It occurs primarily within the groundmass as aggregates of platy crystals, as individual xenoblastic crystals or as intergrowths with amphibole. It is pleochroic from light green to olive-green.

Amphibole: Metamorphic amphibole occurs in rocks of all units of the Smartville Complex. It occurs as acicular or prismatic crystals within the groundmass and as acicular crystals in amygdules and veins. Acicular inclusions within plagioclase, epidote and polycrystalline chlorite (Photo 14) are common. Amphibole also occurs as uralitic alteration of clinopyroxene and in hornblende hornfels occurring within the contact aureoles of some plutons (Photo 15). Rare intergrowths with platy biotite also occur. Color ranges from light green to bluish-green to olive green.

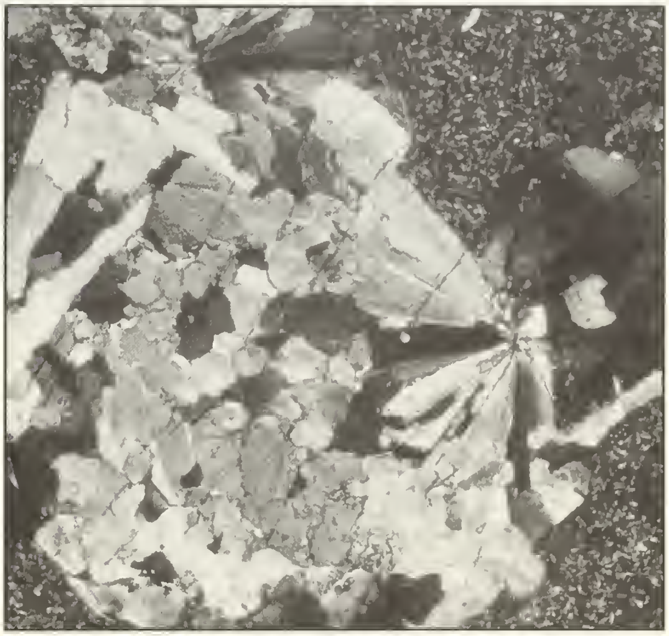

Photo 12. Photomicrograph of epidote- and chlorite-filled amygdules, upper volcanic unit, Stop 3.

Photo 13. Photomicrograph of epidosite, lower volcanic unit, near Smartville, California.

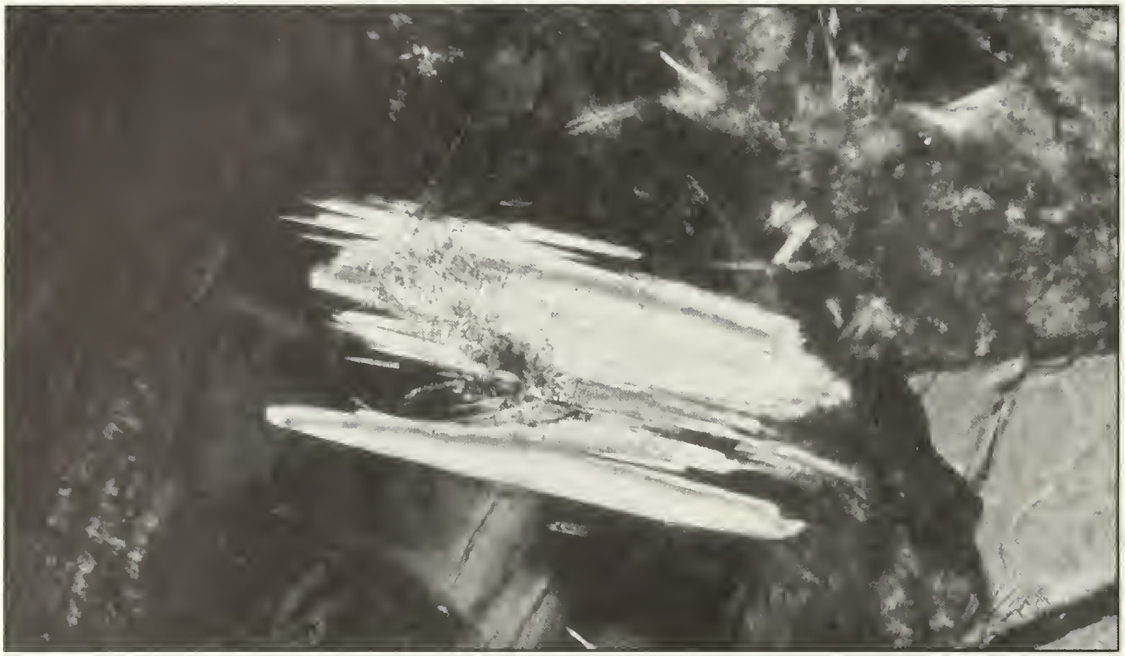

Photo 14. Photomicrograph of acicular actinolite in chlorite, upper volcanic unit, Stop 3.

Pyroxene: The occurrence of metamorphic pyroxene is restricted to rocks displaying well developed hornfelsic texture (Photo 16), that crop out in the contact aureoles of gabbroic plutons. Pyroxene hornfels contain abundant clinopyroxene and subordinate orthopyroxene.

Garnet: Garnet has been reported in single samples from three studies (Xenophontos, 1984; Springer et al., 1992; this study). It occurs as idioblastic to hypidioblastic crystals within amygdules in rocks of the prehnite-pumpellyite zone (Springer et al., 1992) and greenschist zone (this study).

Calcite: Calcite occurs in rocks of all units of the Smartville Complex. It commonly occurs as microcrystalline aggregates in amygdules, veins or the groundmass. Calcite inclusions in relict plagioclase phenocrysts, xenoblastic crystals in the groundmass and radial aggregates of bladed crystals in amygdules are also common.

Sphene: Sphene is ubiquitous in the Smartville Complex, occurring in almost all samples from all rock units. It occurs in the groundmass as dusty cryptocrystalline aggregates commonly associated with fine grained magnetite. Liou and others (1977) have attributed this textural and mineralogical association to the exsolution of titanomagnetite to magnetite and ilmenite and the alteration of ilmenite to sphene during subsequent low grade metamorphism.

Opaque Minerals: Magnetite and pyrite, occurring in the Smartville complex, have been identified by reflective light microscopy and by qualitative electron probe microanalysis. Magnetite commonly occurs associated with sphene as discussed above. Pyrite occurs as small well developed crystals. Rare hematite is also present as psuedomorphs after pyrite.

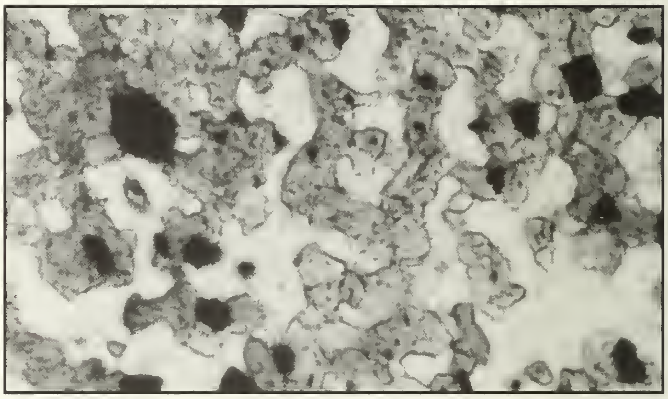

Photo 15. Photomicrograph of hornblende hornfels, diabase unit, Stop 5.

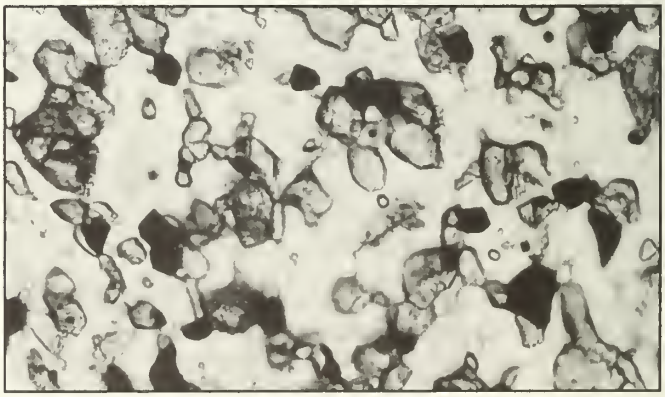

Photo 16. Photomicrograph of pyroxene hornfels, diabase unit, north of Dobbins, California.

Metamorphic Zones

Based on the distribution of these metamorphic minerals, the Smartville Complex can be divided into zones of 1) sub-greenschist prehnite- and/or pumpellyite-bearing assemblages; 2) greenschist assemblages and 3) hornblende and pyroxene hornfels assemblages in the contact aureoles of gabbroic plutons. Metamorphic minerals that occur in each zone are shown in Figure 2. Rocks in the prehnite-pumpellyite and greenschist zones both contain the assemblage: chlorite + albite + quartz + sphene ± actinolite ± epidote ± calcite + magnetite ± white mica. The difference between the two zones is that the prehnite-pumpellyite zone contains prehnite and pumpellyite, whereas prehnite and pumpellyite bearing rocks are absent in the greenschist zone. Rocks in the contact aureoles of gabbroic plutons have hornfelsic textures and contain metamorphic hornblende, clinopyroxene and/or orthopyroxene.

The mapped metamorphic zones are shown in Figure 3. Three prehnite-pumpellyite zones have been mapped (Beiersdorfer et al., 1991; Springer et al., 1992; Beiersdorfer, in prep; Springer, in prep.) and will be referred to as the northern, central, and southern prehnite-pumpellyite zones.

The Northern Prehnite-pumpellyite Zone: The northern prehnite-pumpellyite zone occurs in the northwestern part of the Smartville Complex and is in contact with greenschist assemblages to the east and south (Figure 3). In the northern part of the zone, the transition from prehnite-pumpellyite to greenschist may be related to lithology. Prehnite and/or pumpellyite are restricted to rocks of the upper and lower volcanic unit. These rocks are in contact with sheeted and unsheeted dikes of the diabase unit that contain greenschist facies assemblages. As the trace of the metamorphic boundary is followed to the south, the geologic nature of the boundary changes to a deformational boundary within the upper volcanic unit. South of the southernmost exposures of lower volcanic unit and diabase unit, the prehnite/pumpellyite zone to greenschist zone boundary occurs within the upper volcanic unit. This boundary coincides with the western margin of the western shear zone. Undeformed upper volcanic unit rocks contain metamorphic assemblages characteristic of the prehnite-pumpellyite zone and deformed rocks contain metamorphic assemblages characteristic of the greenschist zone. Chlorite-epidote-actinolite define the foliation in rocks from the western shear zone. The southern boundary of the northern prehnite-pumpellyite zone occurs within the upper volcanic unit and coincides with the Yuba River. Prehnite-pumpellyite zone assemblages occur north of the river and greenschist zone assemblages occur to the south. The geologic significance of this transition is currently under investigation.

The Central Prehnite-pumpellyite Zone: The central prehnite-pumpellyite zone consists of a northwest trending belt of prehnite and/or pumpellyite bearing rocks that is bordered on the east, west and south by greenschist assemblages (Figure 3). On the east , the transition from the prehnite-pumpellyite zone to the greenschist zone occurs within the lower volcanic unit and is subparallel to the stratigraphy of the volcanic units. On the west, the transition occurs within the upper volcanic unit and coincides with the eastern boundary of the western shear zone. The trace of western transition continues to the south where its northwest trend changes to east-west, cuts across stratigraphic contacts, and is sub-parallel to the northern margin of the Cretaceous Rocklin pluton. This east-west trending transition occurs in the vicinity of the town of Auburn, CA and has been discussed in detail by Springer and others (1992). The prehnite-pumpellyite to greenschist transition occurs with pumpellyite disappearing before prehnite. The pumpellyite-out and prehnite-out isograds are sub-parallel and are spaced approximately one kilometer apart (Springer et al., 1992).

The Southern Prehnite-pumpellyite Zone: The southern prehnite-pumpellyite zone occurs in upper volcanic unit rocks exposed in the southernmost part of the Smartville Complex

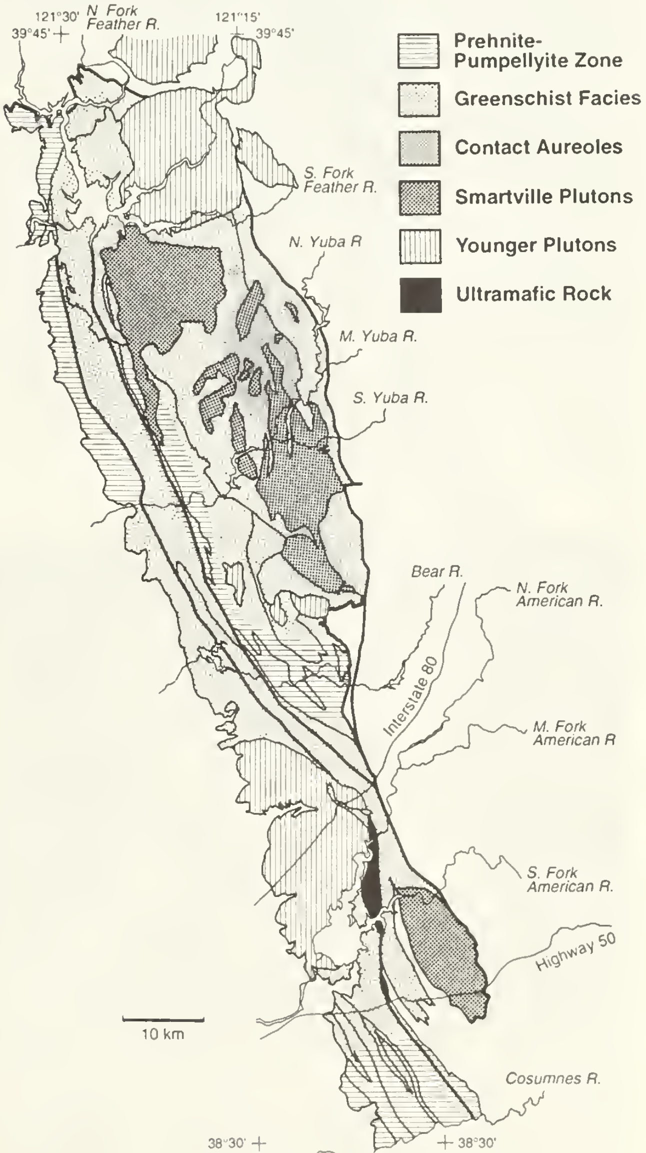

Figure 3. Metamorphic map of the Smartville Complex, California; based on Beard and Day (1988) Beiersdorfer et al. (1991) and Beiersdorfer (in prep), north of the Bear River, and Springer et al (1992) and Springer (in prep), south of the Bear River.

(Figure 3). These rocks are known as the Copper Hill and Gopher Ridge volcanics (Wagner et al., 1981) but are lithologically equivalent to the upper volcanic unit of the Smartville Complex (Springer, in prep). The northern border of the southern prehnite-pumpellyite zone trends east-west and cuts across stratigraphic contacts. It is sub-parallel to the southern margin of the Cretaceous Rocklin pluton.

Greenschist Zone

Greenschist zone rocks are characterized by having the assemblage: chlorite + albite + quartz + sphene ± actinolite ± epidote ± calcite ± magnetite ± white mica and by the absence of prehnite and pumpellyite (Photo 17). Greenschist zone rocks occur in the upper and lower volcanic units and the diabase unit. The diabase unit is, everywhere, restricted to the greenschist zone. The transitions from the greenschist zone to the prehnite-pumpellyite zone are discussed above.

Contact Aureoles: The geographic distribution of metamorphic rocks containing hornfelsic textures are shown as contact aureoles in Figure 3. The extent and nature of these contact metamorphic zones varies with the type of gabbroic plutons forming the contact aureole (Beard, 1990). The large, complexly zoned plutons are surrounded by a relatively narrow, hornblende hornfels facies contact aureole. The smaller, more mafic plutons are surrounded by wider, pyroxene hornfels aureoles. In the northern part of the intrusive complex, where small, mafic plutons are common, there are extensive areas of contact metamorphosed rocks, including high-grade pyroxene hornfelses and rocks that are apparently migmatitic (Photo 18) (Beard and Day, 1988; Beard, 1990).

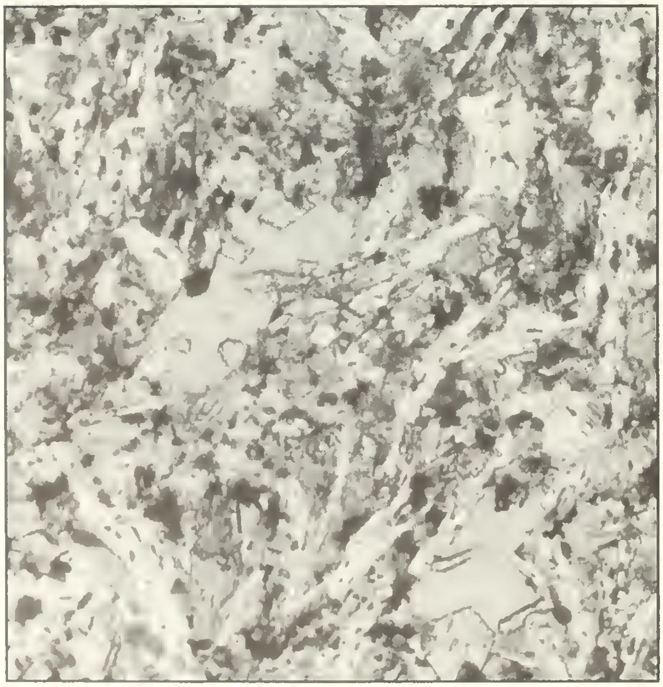

Photo 17. Photomicrograph of chlorite, epidote, amphibole, albite, quartz, sphene and opaques in greenschist zone pillow lava, lower volcanic unit, west of Stop 4.

Areas of hydrothermal alteration

The Smartville Complex makes up part of the Foothills Volcanogenic Massive Sulfide Belt (Martin, 1988). This belt of copper and zinc sulfide mineralization occurs in late Jurassic metavolcanic and metavolcaniclastic rocks and extends for approximately 300 km (Heyl, 1948). Localities within the Smartville Complex showing the effects of hydrothermal alteration, such as massive sulfide mineralization and epidosites, are shown in Figure 4.

Massive sulfide was first discovered in the Smartville Complex at Spenceville (Stop 2) in 1862 (Aubury, 1908). In addition, mining has also occurred at the Big Bend, Dairy Farm and

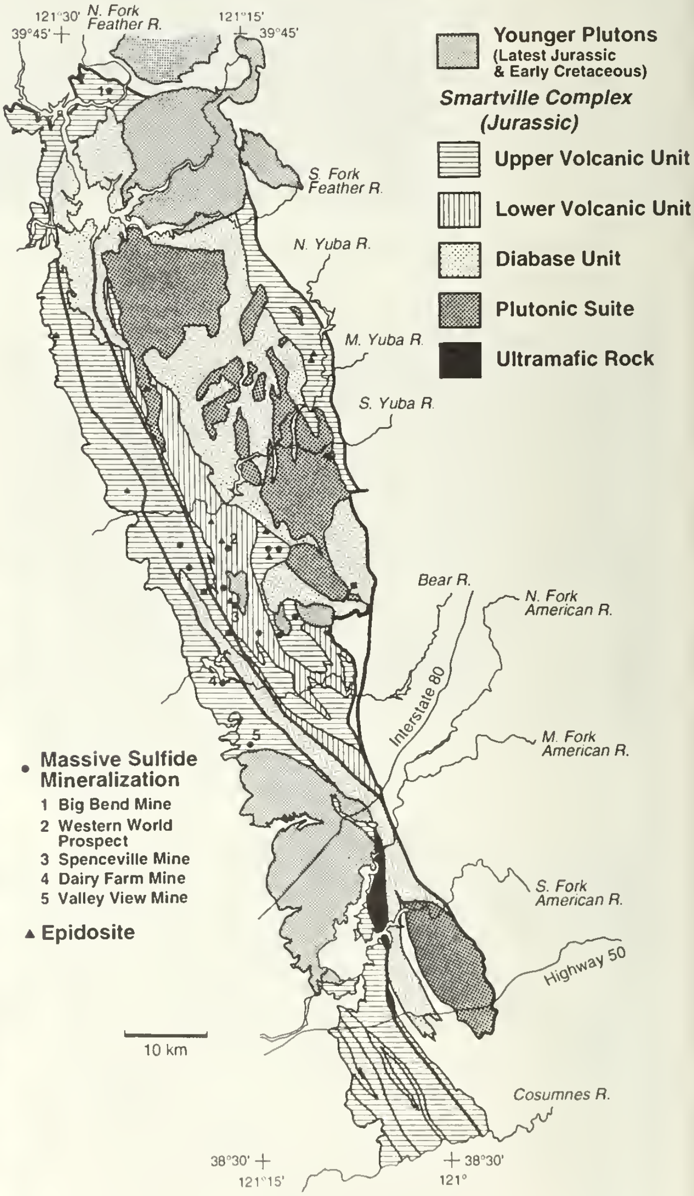

Figure 4. Geologic map of the Smartville Complex, California showing the distribution of massive sulfide deposits and epidosites.

Valley View mines (Fig. 4). The authorization procedures to begin mining at Western World (Kilbreath, 1984; Taylor, 1990) are currently underway. The region between the Yuba and Bear Rivers was explored by Nevcam Inc. for volcanogenic massive sulfide deposits during the early 1980's. Several areas of subeconomic mineralization were discovered and are shown in Figure 4. The ore body at the Big Bend mine consists of pyrite, sphalerite and chalcopyrite with minor galena and bornite. The average grade of the ore body is 13% zinc and 2% copper (Eric, 1948). The ores at Western World, Spenceville, Dairy Farm and Valley View are copper (chalcopyrite) dominated with substantial zinc (sphalerite) and minor gold and silver (Martin, 1988). The lack of recognized massive sulfide deposits north of the Yuba River may be due to a lack of detailed exploration or may reflect the observation by Kemp (1982) that the ore bodies occur in clusters spaced approximately 40 km apart along the massive sulfide belt.. The next cluster, to the south, occurs near the Copper Hill mine, just south of the Cosumnes River (Martin, 1988).

Localities of epidosite mineralization are shown in Figure 4. Epidosites in the Smartville Complex are one-half meter to meter sized bodies consisting of epidote and minor quartz and chlorite. These epidosites are comparable in size and shape to those described in the Josephine Ophiolite of the Klamath Mountains in northern California by Harper and others (1988) and Harper (1991) but are quite different from the kilometer sized epidosites described from the Troodos Ophiolite, Cyprus (Schiffman et al., 1990).

DISCUSSION

Styles of Metamorphism

Based on a comparison of metamorphic assemblage with rock type, stratigraphic position, presence or absence of foliation or relict quench textures, and proximity to plutons, several different styles of metamorphism in the Smartville Complex can be discerned. They are burial metamorphism within the volcanic pile, contact metamorphism by Smartville and younger plutons, hydrothermal metamorphism, autometamorphism and dynamothermal metamorphism. Evidence for each of these interpretations is described below. Localities where each style is thought to occur are highlighted in Figure 5.

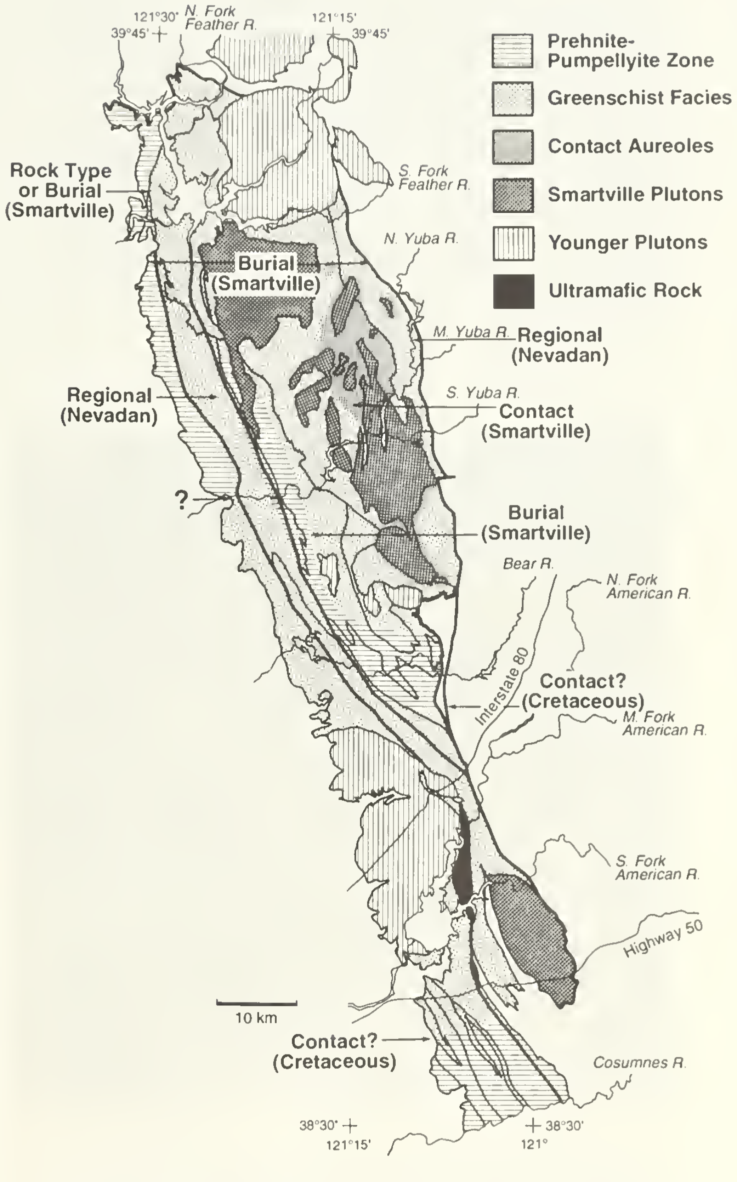

Figure 5. Interpreted metamorphic map of the Smartville Complex, California.

Burial Metamorphism of the Volcanic Rocks. Several lines of evidence support the interpretation that the Smartville Complex has suffered burial metamorphism as defined by Coombs and others (1959). In the central prehnite-pumpellyite zone, the eastern transition from prehnite-pumpellyite zone to greenschist zone occurs within the lower volcanic unit. The transition is subparallel to the stratigraphy of the volcanic units and higher grade rocks occur on the stratigraphically lower side of the transition (Fig. 5). In addition, volcanic rocks and massive diabase exposed in the deepest part of the complex (eastern side) contain upper greenschist (amphibole, biotite, no chlorite) facies assemblages. On the other hand, pyroclastic and volcaniclastic rocks exposed in the upper part of the complex (western side) contain prehnite-pumpellyite and lower greenschist (chlorite, amphibole, no biotite) facies assemblages. The absence of widespread penetrative deformation and the presence of relict quench textures (Photos 5 & 8) in many prehnite-pumpellyite zone samples suggests that metamorphism has occurred in a static environment and is consistent with a burial metamorphism interpretation.

An alternative interpretation is that, since the deepest parts of the Smartville Complex correspond to its plutonic axis, the metamorphic transitions observed may reflect the outermost thermal effects of the plutons. This interpretation requires that these thermal effects are occurring up to ten kilometers away from relatively small plutons that have hornfels zones restricted to within 500 meters of the pluton margin (Fig 5).

Contact Metamorphism: The occurrence of hornblende (Photo 15) and pyroxene (Photo 16) hornfels in the margins of Smartville plutons supports the hypothesis that contact metamorphism was occurring during the 160 Ma. Smartville plutonism. The hornfels that occur in the contact aureoles of small olivine gabbro intrusions typically are mixed rocks of pyroxene hornfels and diorite (Beard and Day, 1988; Beard, 1990) (Photo 18). Based on inferred chemical equilibrium between hornfels and diorite, the high calculated temperatures of formation and the estimated major element chemistry of the hornfelses, Beard (1990) has concluded that, although these rocks resemble intrusive breccias, they are migmatitic and are a result of the partial melting of Smartville metabasite.

Photo 18. Field photograph of mixed rock of pyroxene hornfels (see Photo 16) and diorite that is interpreted by Beard & Day,(1988) and Beard (1990) to be an intrusive breccia, diabase unit, north of Dobbins, California. Diameter of coin is 18 mm.

Hornfelses also occur around the margins of the Late Jurassic/Early Cretaceus Rocklin/Penryn and Bald Rock Plutons indicating Cretaceous contact metamorphism. In addition, the southern border of the central prehnite-pumpellyite zone and the northern border of the southern prehnite-pumpellyite zone cut across stratigraphy and are subparallel to the margins of the Rocklin/Penryn pluton (Fig. 5) and may represent the thermal effects of this large composite magmatic body.

Hydrothermal Metamorphism and Epidosites: The strongest evidence for hydrothermal activity in the Smartville Complex is the numerous occurrences of volcanogenic massive sulfide mineralization (Fig. 4). In addition, epidote veins and small pods of epidosite are widespread throughout the Smartville Complex. Based on a study of the mineralogy and geochemistry of epidosite from the Troodos Ophiolite, Cyprus, Schiffman and others (1990) concluded that the epidosites formed by recrystallization within the high temperature upflow portions of a submarine hydrothermal cell. Although the Smartville epidosites occur on a much smaller scale than those observed at Troodos, they probably represent the high temperature interaction of sea water with Smartville metabasite.

Autometamorphism: The main evidence for autometamorphism is the occurrence of greenschist assemblage-bearing dikes intrusive into rocks of the prehnite-pumpellyite zone. Autometamorphism of the dikes results in the dikes having a higher grade assemblage than the surrounding country rock (Beiersdorfer, 1982; Beiersdorfer and Day, 1983). At the time of intrusion, the molten dikes are at a much higher temperature than their surroundings, which results in the rapid crystallization of the dikes. Shortly after, or perhaps during the last stages of crystallization, glass and clinopyroxene within the dikes react with a fluid phase to form chlorite and amphibole. In effect, the dikes are providing their own source of heat and, possibly, hydrothermal fluid, hence the term autometamorphism. The hydrothermal alteration of plutons may also be examples of autometamorphism.

Dynamothermal Metamorphism: Evidence for dynamothermal metamorphism in the Smartville Complex can be found in the western and eastern shear zones where the foliation is defined by subparallel alignment of chlorite, amphibole

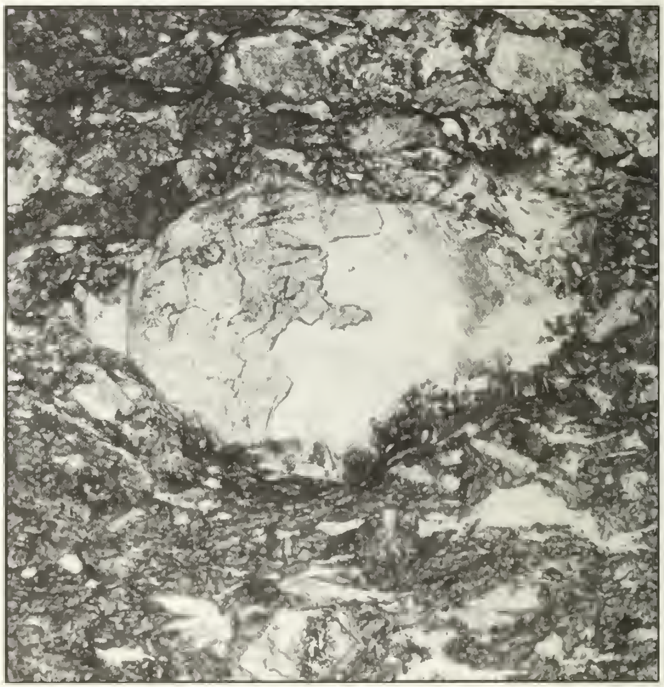

Photo 19. Photomicrograph of pre-tectonic amygdule containing quartz and epidote in foliated volcaniclastic from the upper volcanic unit, within western shear zone, located near Yuba River, west of Stop 1.

and epidote (Photo 7). At some localities, the foliation is seen wrapping around epidote-filled amygdules (Photo 19). This texture is interpreted to indicate that epidote formed prior to the foliation and that the shear zones are regions that have suffered two phases of metamorphism. Although the amount of displacement along these shear zones is controversial (see above) most workers agree that they formed during the late Jurassic Nevadan Orogeny. The eastern shear zone deforms the 160 Ma. Yuba Rivers Pluton (Day et al., 1985).

Physical Conditions of Metamorphism

Using the petrogenetic grid of Liou and others (1987), which is based on mineral equilibria in a model basaltic system (NCMASH), Springer and others (1992) concluded that the burial metamorphic mineral assemblages in the Smartville Complex indicate temperatures of 250 to 350°C, and pressures near 2.5 kbar. The assemblage Ep + Chl + Qtz is virtually ubiquitous in the Smartville Complex, laumontite has not been found and zeolites are notably absent. These observations suggest that temperatures exceeded about 250°C. The common occurrence of Pmp +Chl + Qtz suggests that temperatures have not exceeded about 350°C. The temperatures attained in the contact aureoles of gabbroic plutons were much higher. Beard (1990) has calculated temperatures between 705 and 765°C, based on the two-pyroxene geothermometer of Lindsley (1983), and between 740 and 792°C , based on the Fe-Ti oxide geothermometer (Buddington and Lindsley, 1964; Lindsley,1976).

Metamorphic pressures were probably less than 3 kbar. The widespread occurrence of Pmp+Chl+Amp+Prh in the Smartville Complex suggests that metamorphism occurred at pressures near 2.5 kbar (Springer et al., 1992). Beard and Day (1986) and McLeod and Day (1991) reported pressures of 2.5 to 3 kbar for tonalite and monzodiorite plutons that intruded the Smartville Complex during the interval 160 Ma-140 Ma. The pressure estimates were based on the aluminum content of hornblende (Hammarstrom & Zen, 1986; Johnson & Rutherford, 1989). The estimated temperature and pressure conditions suggest an apparent geothermal gradient near 30°C/km, and are consistent with those of other terranes subjected to burial metamorphism.

The prevalence of prehnite, sphene, and the relative absence of calcite in mineral assemblages of the prehnite-pumpellyite metamorphic zone indicates that XCO2 of the fluid phase was <0.1 (Liou et al., 1987), and that variations in XCO2 were not an important control on mineral assemblages in the study area. The presence of magnetite as the only iron oxide mineral in the mineral assemblages of the study area indicates that the oxygen fugacity of the fluid phase was between that of the hematite-magnetite and the quartz-fayalite-magnetite buffers.

Tectonic Environment of Metamorphism

At least four tectonic models have been proposed to explain the metamorphism observed in the northern Sierra Nevada. The metamorphic rocks of the northern Sierra Nevada have been considered as greenschist facies rocks metamorphosed during the Jurassic Nevadan Orogeny (e.g. Taliaferro, 1942; Hietanen, 1951; Compton, 1955; Clark, 1960). Alternatively, regional metamorphism might have accompanied the emplacement of the Cretaceous Sierra Nevada Batholith and formed a low P/T terrane paired with the high P/T Franciscan Formation (Ernst, 1974). Ernst (1983) further speculated that the tectonic belts of the northern Sierra, now bounded by steeply east-dipping faults, define an east-dipping subduction complex of Late Jurassic age because the age of rocks and grade of metamorphism appeared to decrease towards the west. Day et al. (1988) summarized the sparse data about metamorphism in the northern Sierra. They emphasized: (1) that sub-greenschist facies assemblages are widespread; (2) that much of the metamorphism was pre-Nevadan; and (3) that there is virtually no clear evidence for post-Nevadan regional metamorphism in that region. Such observations are difficult to reconcile with any of the three models proposed above. Instead, Day et al. (1988) suggested that much of the regional metamorphism in the northern Sierra may have occurred in the volcanic and magmatic arcs where many of the rocks formed and that these arcs may have been juxtaposed by later tectonic events.

The metamorphism of the Smartville Complex can be subdivided into pre-Nevadan and Nevadan stages. The pre-Nevadan metamorphism consists of: (1) Burial metamorphism in the volcanic pile; (2) Contact metamorphism by coeval plutons; (3) Hydrothermal metamorphism that produced epidosites and massive sulfide deposits; and (4) Autometamorphism of dikes intrusive into the volcanic pile. The burial metamorphism may have occurred in response to loading of volcaniclastic and epiclastic material or in response to enhanced thermal gradients and emplacement of plutons during extension of the volcanic arc. Contact metamorphosed volcanic and hypabyssal rocks occur around arc-related plutons. The effects of hydrothermal alteration and/ or autometamorphism are interesting because they are clearly products of processes occurring during the construction of the volcanic arc.

These observations suggest that metamorphism of the Smartville Complex occurred during the active constructional phase of the magmatic arc. Hydrothermal metamorphism, autometamorphism and contact metamorphism probably were more or less contemporaneous with burial metamorphism within the volcanic pile because the ages of the volcanic, hypabyssal and plutonic rocks are restricted to such a short interval. In the Smartville Complex, Nevadan metamorphism appears to be restricted to recrystallization in shear zones and post-Nevadan metamorphism is presently recognized only in contact aureoles.

CONCLUSIONS

The pre-orogenic metamorphism of the Smartville Complex may be characteristic of the metamorphism that occurs during the construction and rifting of a volcanic arc. Volcanic arcs are found in every major mountain belt in the world and their metamorphism can be used to determine the mountain belt's thermal history. However, it is important to be able to distinguish metamorphism that occurred within the volcanic arc environment prior to mountain belt formation from the metamorphism that occurred during the plate collision by which the mountain belt formed.

ROAD LOG

The locations of stops 1 - 8 are illustrated on a geologic map (Fig. 6) and on a road map (Fig. 7).

Directions to Stop 1

From Sacramento. From Sacramento take Highway 99 north to Yuba City. At Yuba City turn east onto Highway 20. Follow Highway 20 for 19 miles to the Yuba River at Park's Bar. Cross the bridge and make an immediate left turn onto the river road. Park and walk down to river level. Watch out for poison oak.

From Nevada City. From Nevada City drive 5 miles south on Highway 49/20 to Grass Valley. Take Highway 20 towards Marysville. Drive 16 miles west to the Yuba River at Park's Bar. Just before Highway 20 crosses the bridge, make an immediate right turn onto the river road. Park and walk down to river level. Watch out for poison oak.

(Note: At the time of publication, the construction of a new bridge at Park's Bar had begun. Future visitors to this geologic site may have to alter their route to get to Stop No. 1 or visit an alternate pillow lava site in the immediate vicinity. The best exposure of pillow lavas at Park's Bar is near the southern abutment of the old bridge.)

Stop 1 - Parks Bar Bridge

Pillow Basalts of the Lower Volcanic Unit

Beneath the bridge at the southern abutment is a well exposed section of pillowed flows of the lower volcanic unit. The pillowed basalts trend north-northwest and dip approximately 70 degrees west. Pillow morphology indicates stratigraphic younging is to the west. Most pillows are concentrically zoned from an aphanitic, black to green, former glassy rind several centimeters thick to a vesicle-rich zone and a massive vesicle-poor core. Relict igneous mineralogy consists of plagioclase and pyroxene. Plagioclase and pyroxene occur as microlites in the fine grained groundmass and as euhedral phenocrysts. Oscillatory and sector zoning of the clinopyroxenes are common (Day et al., 1982). Interpillow material consists of chloritized and epidotized glass shards, plagioclase crystals, and rare recrystallized radiolaria in a matrix of microcrystalline quartz. Metamorphic minerals present at this outcrop include pumpellyite, chlorite, quartz, calcite, albite, white mica, prehnite, sphene and an opaque phase. This outcrop is mapped within the prehnite-pumpellyite zone.

Directions to Stop 2

Drive east on Highway 20 for 3.0 miles to Smartville Road. (Note: there will be a sign at Smartville Road for "Beale Air Force Base") Turn southwest (right) onto Smartville Road. At 0.9 miles the road will fork, continue on Smartville Road to the southwest (left). At 4.3 miles from the junction of Smartville Road with Highway 20 you will reach the junction with Waldo Road. (Note: Waldo Road is a gravel road). Turn south (left) onto Waldo Road and drive 1.7 miles to the junction with Spenceville Road. (Note: just before the junction, you will cross a bridge over Dry Creek) Turn east (left) onto Spenceville Road. Drive east on Spenceville Road 2.25 miles to the Spenceville Mine Site (Stop 2). (Note: at 0.4 miles from the Waldo Road - Spenceville Road junction you will reach a fork in the road, continue east [keep to the left]). Park vehicle on south side of Dry Creek. Walk across bridge to the Spenceville Mine Site.

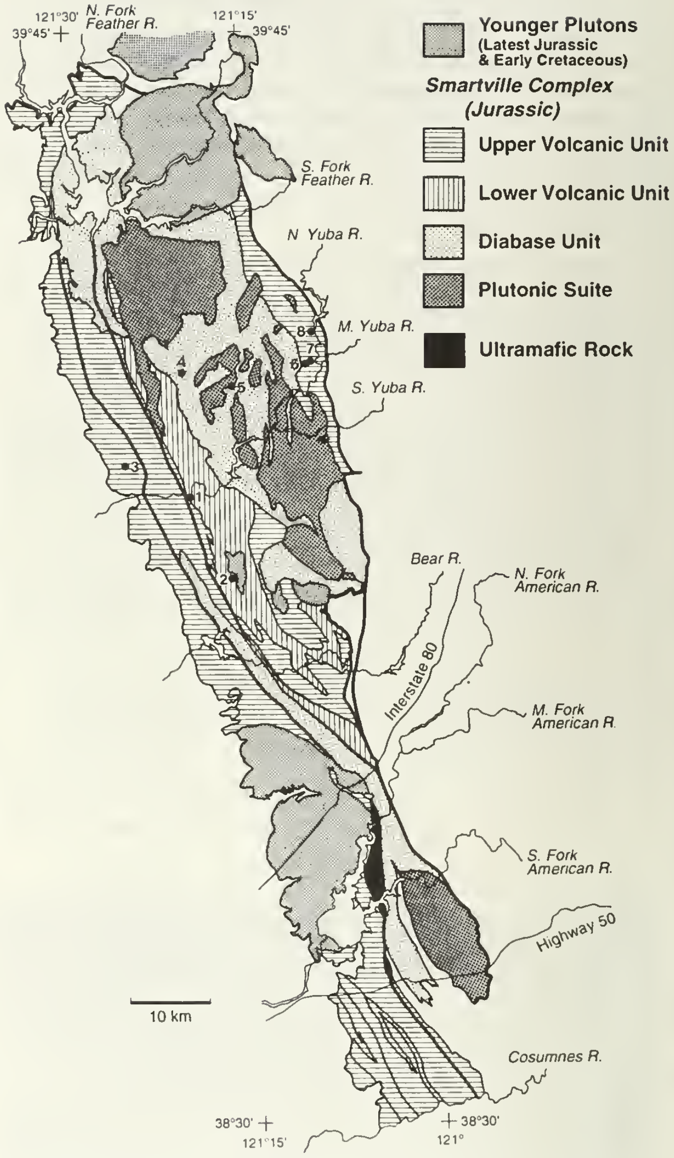

Figure 6. Field trip stops located on a geologic map of the Smartville Complex, California.

Stop 2 - Spenceville Mine Site

Hydrothermal Mineralization

The Spenceville Mine Site (Photo 20) is one of several massive sulfide deposits occurring within the Smartville Complex (see Figure 4). Copper ore was first discovered at Spenceville in 1862 and mining began in 1875. From 1875 to 1888 approximately 150,000 tons of ore, averaging 5% copper with trace

Photo 20. Field photograph of Spenceville Mine Site, Stop 2.

gold and silver, was removed. Mining was originally underground with shafts and drifts to 150 feet. In 1880 the underground workings caved in due to insufficient timbering. Mining resumed as an open cut which became 300 feet long, 70 feet wide and 75 feet deep. (The open cut is located at the fenced off pond area.) The ore body consists predominantly of pyrite and chalcopyrite. The copper was extracted by the method of roasting and leaching. The gold and silver was not recovered. From 1892 to 1897 the roasted ore was utilized in the manufacture of high quality red metallic paint (Aubury, 1908; Lardner and Brock, 1924).

The ore body at Spenceville occurs within pillow lavas of the lower volcanic unit in proximity to an undated granodiorite pluton exposed to the east (Fig. 4). The most obvious features at the mine site are the large tailings piles. The cream to yellow piles of tailings are waste from the mining operation. The red to dark red colored tailings are waste from the roasting procedure. Pillow lavas immediately adjacent to the ore body are exposed in the hill above the tailings pile. The pillow lavas contain abundant epidote occurring in amygdules and veins. The entire metamorphic assemblage consists of amphibole, chlorite, albite, epidote, quartz, sphene, opaque and calcite. This outcrop is mapped within the greenschist zone.

Directions to Stop 3

Retrace your path to the Highway 20 - Smartville Road junction. Turn west (left) on Highway 20 and drive for 10.0 miles to Joines Road.(Note: at 3.0 miles you will pass Stop No. 1 and cross the Yuba River). Turn north (right) on Joines Road and drive 3.2 miles to the entrance to the Carl J. Woods Co. Quarry (the entrance has a large white gate; this is private property so please obtain permission prior to entering this quarry). (Note: at 0.8 miles from the intersection of Highway 20 and Joines Road, Joines Road will merge with Spring Valley Road.)

Stop 3- Rock Quarry on Spring Valley Road

Upper Volcanic Unit

Stop three is located within the upper volcanic unit and contains lithologies representative of the unit. The quarry trends east-west. The south face of the quarry consists of predominantly coarse-grained clinopyroxene-rich volcaniclastic rocks. The north face contains volcanic-rich sandstones in addition to coarse-grained volcaniclastic rocks. Some of the sandstone beds exhibit graded bedding which strikes N55W and dips 40° northeast.

A striking feature of the quarry is the numerous (feeder?) dikes intrusive into the volcaniclastic rocks. These dikes typically have concentrations of epidote near their chilled margins (Photo 11). The abundance of dikes and the large clast size of much of the volcaniclastic rocks are consistent with proximity to a submarine volcanic center. The volcanic sandstones may represent deposition of sediments from a distal source region during periods of volcanic quiescence.

This outcrop is mapped within the prehnite-pumpellyite zone. However in a detailed petrographic study of 37 samples from this outcrop, pumpellyite has not been observed. The common metamorphic assemblage consists of chlorite, epidote, actinolite, albite, quartz, sphene and an opaque phase. Prehnite, occurring in amygdules or veins, was observed in three samples. Relict clinopyroxene phenocrysts are abundant.

Directions to Stop 4

Continue north-east on Spring Valley Road for 2.3 miles to Marysville Road (Road E21). Turn north (left) onto Marysville Road. The prominent buff colored peak directly ahead of you is Payne's Peak which is composed of massive microcrystalline quartz (Buer, 1979). Drive 6.0 miles north to the large road cut on the east side of the road. (Note: the road cut is just south of (before) the intersection of Marysville Road and the entrance to the Collins Lake Recreation Area.

Stop 4- Stanfield Hill

Sheeted Dikes

The road cut at Stanfield Hill is one of the best exposures of sheeted dikes in North America. The outcrop is composed of dikes and minor plutonic screens. A majority of the dikes are subparallel and strike approximately N10W with dips ranging from 65 to 80 degrees northwest (Day, 1977). The average dike thickness is between one and two meters. Numerous chilled margins, including one-way chilled margins, are present. This outcrop was studied in detail by S. D. Day (1977). By use of cross-cutting relationships he documented a sequence of five intrusive events. From oldest to youngest they are: 1) medium grained quartz albitite, diabase and altered screens of porphyritic basalt with phenocrysts of plagioclase; 2) dikes of diabase, basaltic andesite, and dacite; 3) complete diabase dikes showing less alteration and epidotization than earlier intrusive phases; 4) thin non-porphyritic basalt dikes; 5) a 3.5 meter thick dike of rhyolite porphyry with plagioclase phenocrysts. The metamorphic phases calcite, chlorite, actinolite, epidote, quartz and pyrite occur in amygdules and veins. This outcrop is mapped within the greenschist zone.

Directions to Stop 5

Continue north 1.6 miles on Marysville Road (Road E21) toward Oregon House. Turn east (right) on Marysville Road (Road E20) and continue 7.4 miles to Lake Francis Road. Turn south (right) on Lake Francis Road and continue 4.0 miles to the end of the road at the Colgate Powerhouse. Park in the large flat area on the right side of the road.

Stop No. 5 - Colgate Powerhouse

Hornfels Xenoliths in Biotite-hornblende Tonalite

The outcrop occurs within a mapped elongate pluton of biotite-hornblende tonalite and contains plagioclase (52%), quartz (30%), orthoclase (2%), biotite, hornblende, magnetite and ilmenite (16% total mafics). Zircons separated from the tonalite at this outcrop yield a U/Pb age of 161 ± 2 Ma (Bickford, in prep.). Mutually intrusive relationships between tonalite and mafic dikes are

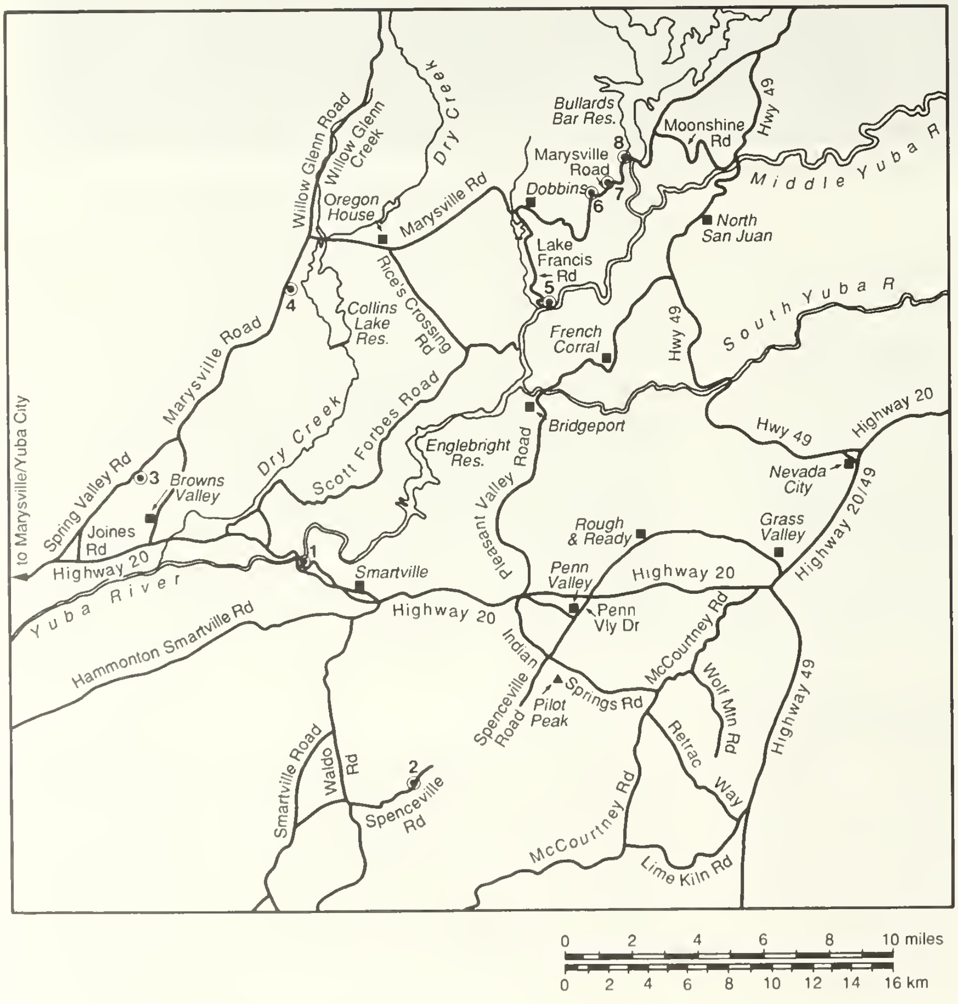

Field trip stops illustrated on a road map.

illustrated by 5 to 100 cm. thick dikes that are intrusive into the tonalite but are also intruded by tonalite. The outcrop contains numerous mafic xenoliths particularly in the vicinity of the penstock and powerhouse. The xenoliths consist of blocks of intrusive breccia, hornblende hornfels, pyroxene hornfels and migmatite. The xenoliths and tonalite are crosscut by 1 to 10 cm. thick veins of epidote, quartz and chlorite. The epidote veins are particularly abundant near the penstock.

Directions to Stop 6

Return on Lake Francis Road to Marysville Road. Turn east (right) onto Marysville Road and drive 3.9 miles and park at the turn out on the right (south) side of the road in front of a yellow road side reading "Caution Slide Area Next 2 Miles". Stop 6 is the road cut on the opposite side of the road. Watch out for vehicles.

Stop 6 - Marysville Road

Metavolcanics on the East Side of the Smartville Complex

The road cut exposed at Stop 6 consists of volcaniclastic breccia (Photo 1) from the upper volcanic unit exposed on the east side of the Smartville Complex (Fig. 6). The breccia is homolithic but does exhibit slight differences in the percentage of amygdules. The clasts are variable in angularity, ranging from angular to spherical. Clast size ranges from less than 1 cm to greater than 15 cm. The breccia also varies from clast-supported to matrix-supported in correlation with clast size. The smaller clasts (< 3 c.m.) tend to be matrix-supported whereas the rest of the clasts are clast-supported. Clasts are light to medium gray green in color with slightly darker colored margins. The matrix is a light yellow green color reflecting an abundance of epidote. Metamorphic minerals present at this outcrop include amphibole, chlorite, albite, epidote, quartz, sphene and opaque. This outcrop is mapped within the greenschist zone.

Directions to Stop 7

Continue east on Marysville road 0.9 miles to the entrance to a large rock quarry on the north (left) side of the road. Stop 7 is the road cut exposure outside of the quarry gate.

Stop 7 -Ye Olde Epidote Blob Rock

Stop 7 (Photo 21) occurs within a shear zone related to the Big Bend-Wolf Creek fault zone along the eastern margin of the Smartville Complex. We interpret the rocks at Stop 7 to be penetratively-deformed volcaniclastic rocks of the upper volcanic unit. These strongly foliated rocks were, prior to deformation, most likely similar in appearance to the rocks exposed at Stop 6. Like the rocks at Stop 6, the matrix of the volcaniclastic rocks at Stop 7 was preferentially altered to epidote, prior to deformation. During the deformation, the epidote-rich zones formed into boudins and lozenges of various sizes and shapes. The more competent epidote lozenges have quartz- and chlorite-filled tension gashes. The schistosity in the region strikes at N15W and dips 75° to the east. Metamorphic minerals present at this outcrop include amphibole, chlorite, albite, epidote, biotite, quartz, sphene and opaque. This outcrop is mapped within the greenschist zone.

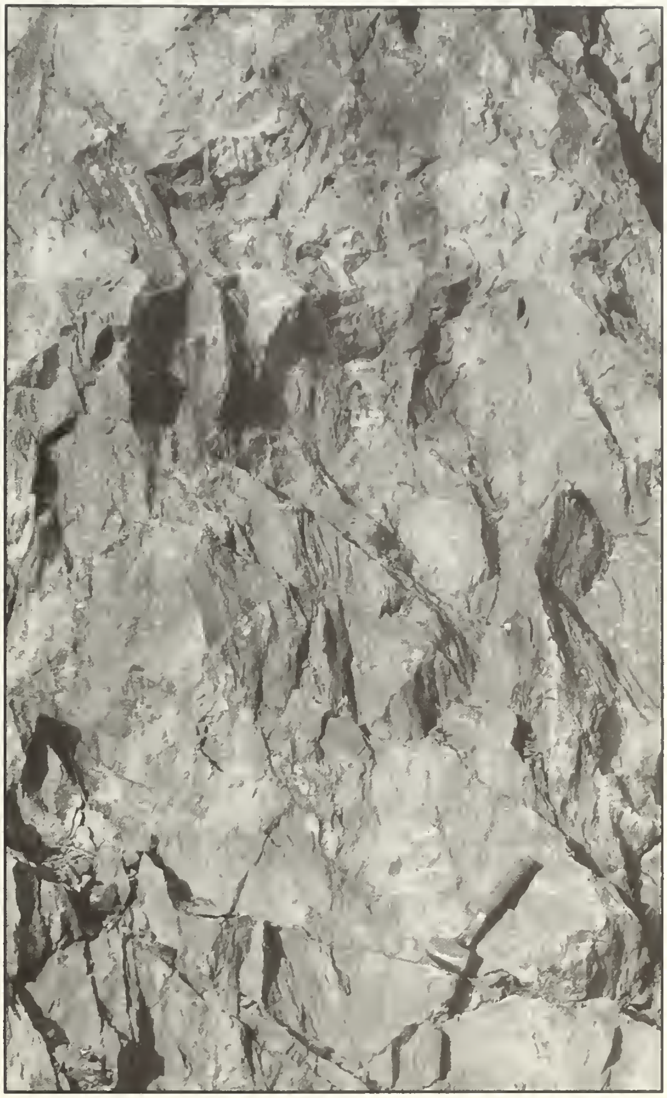

Photo 21. Field photograph of epidote-rich boudins and lozenges of various sizes and shapes, upper volcanic unit, within eastern shear zone, at Stop 7.

Directions to Stop 8

Continue east on Marysville road 3.8 miles to the Bullards Bar dam. Park on the south (right) side of the road just before the dam. Stop 8 is across the road.

Stop 8 - Bullards Bar Dam

Deformed Metavolcanics on the East Side of the Smartville Complex

Stop 8 occurs within a shear zone related to the Big Bend-Wolf Creek fault zone along the eastern margin of the Smartville Complex. Exposed here are penetratively deformed volcaniclastic rocks of the upper volcanic unit. The schistosity strikes at N15W and dips 75° to the east. Like Stop 7, Stop 8 contains epidote-rich boudins and lozenges of various sizes and shapes. Metamorphic minerals present at this outcrop include chlorite, epidote, amphibole, biotite, quartz, plagioclase and sphene. This outcrop is mapped within the greenschist zone.

Directions to Sacramento

There are two options for the return drive to Sacramento.

Option one is to turn around and drive west on Marysville Road (Road E20) 16.0 miles to Marysville Road (Road E21). Turn south (left) on Marysville Road (Road E21) and continue 11.2 miles to Highway 20. Turn west (right) on Highway 20 and continue approximately 15 miles to Yuba City. At Yuba City, drive south on Highway 99 to Sacramento.

Option two is to follow the directions to Nevada City, listed below, and to continue south on Highway 49 to Auburn. At Auburn, drive west on Interstate 80 to Sacramento.

Directions to Nevada City

Drive east over the Bullards Bar Dam and continue on Marysville Road approximately 2.0 miles to Moonshine Road. Turn east (right) on Moonshine Road and drive 5 miles to Highway 49. Turn south (right) on Highway 49 and cross over the Middle Yuba River. Drive 17 miles south through North San Juan to Nevada City. At the bridge crossing the South Yuba River, you may wish to stop for a look at the Yuba Rivers Pluton.

ACKNOWLEDGEMENTS

Our work has been supported by the National Science Foundation (grant EAR9017844), the Geological Society of America, the Northern California Geological Society, Sigma Xi and the Durrell Fund of the University of California at Davis. We thank J.S. Beard, R.C. Loyd, E. M. Moores, P. Schiffman and R. K. Springer for many stimulating discussions about the geology of the northern Sierra Nevada. We thank R.E. Bevins and R. K. Springer for their helpful reviews. We thank N. Winter for his invaluable assistance in all aspects of sample preparation. Also, our special thanks to J. Fong for preparation of the figures and to M. Graziose for developing and printing all the photographs.

REFERENCES

Aubury, L. E., 1908, The Copper Resources of California: California State Mining Bureau Bulletin 50, 366 p.

Beard, J. S., 1985, The Geology and petrology of the Smartville Intrusive Complex, northern Sierra Nevada foothills, California. [Ph.D. thesis] : Davis, University of California, 356 p.

Beard, J.S., 1990, Partial melting of metabasites in the contact aureoles of gabbroic plutons in the Smartville Complex, Sierra Nevada, California: Geological Society of America Memoir 174, p. 303-314.

Beard, J.S. and Day, H.W., 1986, Origin of gabbro pegmatite in the Smartville intrusive complex, northern Sierra Nevada, California: American Mineralogist, v. 71, p. 1085-1099.

Beard, J.S. and Day, H.W., 1987, The Smartville intrusive complex, northern Sierra Nevada: The core of a rifted volcanic arc: Geological Society of America Bulletin, v. 99, p. 779-791.

Beard, J.S. and Day, H.W., 1988, Petrology and emplacement of reversely zoned gabbro-diorite plutons in the Smartville Complex, northern California: Journal of Petrology, v. 29, p. 965-995.

Beiersdorfer, R.E., 1982, Metamorphic petrology of the Smartville Complex, northern Sierra Nevada foothills, California [M.Sc. thesis] : Davis, University of California, 152 p.

Beiersdorfer, R.E. and Day, H.W., 1983, Pumpellyite-actinolite facies metamorphism in the Smartville Complex, northern Sierra Nevada [abs.] : Geological Society of America Abstracts with Programs, v. 15, p. 436.

Beiersdorfer, R. E., Beard, J.S., Day, H.W. and Moores, E.M., 1991, Igneous and metamorphic features of the Smartville Complex, northern California, in Walawender, M.J. and Hanan, B.B., ed., Geological Excursions in southern California and Mexico: Geological Society of America, Guidebook for the 1991 Annual Meeting, San Diego, CA, p.68-92.

Bickford, M.E. and Day, H.W., 1988, Jurassic ages of Arc-ophiolite complexes, northern Sierra Nevada: implications for the duration of the"Nevadan" orogeny [abs.] : Geological Society of America Abstracts with Programs, v. 20, p. 274.

Bryan, W.B., 1972, Morphology of quench crystals in submarine basalts: Journal of Geophysical Research, v. 77, p. 5812-5819.

Buddington, A.F. and Lindsley, D.H., 1964, Iron-titanium oxide minerals and synthetic equivalents: Journal of Petrology, v. 5, p. 310 - 357.

Buer, K.Y., 1979, Stratigraphy, structure and petrology of a portion of the Smartville ophiolite, Yuba County, California [M.Sc. thesis] : Davis, University of California, 120 p.

Cady, J.W., 1975, Magnetic and gravity anomalies in the Great Valley and western Sierra Nevada metamorphic belt, California: Geological Society of America Special Paper 168, 56 p.

Clark, L.D., 1960, Foothills fault system, western Sierra Nevada, California: Geological Society of America Bulletin, v. 71, p. 483-496.

Clark, L.D., 1964, Stratigraphy and structure of part of the western Sierra Nevada metamorphic belt: U.S. Geological Survey Professional Paper 410, 70 p.

Compton, R., 1955, Trondhjemite batholith near Bidwell Bar, California: Geological Society of America Bulletin, v. 66, p. 9-44.

Coombs, D. S., Ellis, A.J., Fyfe, W.S. and Taylor, A.M., 1959, The zeolite facies, with comments on the interpretation of hydrothermal syntheses: Geochimica et Cosmochimica Acta, v. 17, p. 53-107.

Creely, R.S., 1965, Geology of the Oroville quadrangle, California: California Division of Mines and Geology Bulletin 184, 86 p.

Day, H. W. and Bickford, M. E., 1989, The Nevadan "Orogeny" in the northern Sierra Nevada: new constraints from U-Pb zircon ages [abs.] : EOS (American Geophysical Union Transactions), v. 70-15, p. 490.

Day, H.W., Beiersdorfer, R.E. and Fenn, P.M., 1982, Chemistry of volcanic clinopyroxene from the Smartville Complex, northern Sierra Nevada foothills [abs.] : Geological Society of America Abstracts with Programs, v. 14, p. 168.

Day, H. W., Moores, E.M. and Tuminas, A.C., 1985, Structure and tectonics of the northern Sierra Nevada: Geological Society of America Bulletin, v. 96, p. 436-450.

Day, H. W., Schiffman, P. and Moores, E.M., 1988, Metamorphism and tectonics of the northern Sierra Nevada, in Ernst, W. G., ed., Metamorphism and Crustal Evolution of the Western United States, Rubey Volume VII: Englewood Cliffs, N. J., Prentice Hall, p.737 - 763.

Day, S. D., 1977, The petrology of a mafic dike complex near Smartville, Yuba Co., CA [M.Sc. thesis] : Davis, University of California, 113 p.

Edelman, S.H., Day, H.W. and Bickford, M.E., 1989, Implications of U-Pb zircon ages for the tectonic settings of the Smartville and Slate Creek complexes, northern Sierra Nevada, California: Geology, v. 17, p. 1032-1035.

Eric, J.H., 1948, Zinc-copper deposits of the big bend mine, Butte County, California, in Jenkins, O.P., ed., Copper in California, California Division of Mines and Geology Bulletin 144: p.31-42.

Ernst, W.G., 1974, Metamorphism and ancient convergent continental margins, in Burk, C. A. and Drake, C. L., ed., The Geology of Continental Margins: New York., Springer Inc., p. 907 - 919.

Ernst, W.G., 1983, Phanerozoic continental accretion and the metamorphic evolution of northern and central California.: Tectonophysics, v. 100, p. 287-320.

Hammarstrom, J.M. and Zen, E-An, 1986, Aluminum in hornblende: an empirical igneous geobarometer: American Mineralogist, v. 71, p. 1297 - 1313.

Harper, G.D., 1991, Metasomatism and permeability controls during formation of epidosites in the Josephine ophiolite [abs.] : EOS (American Geophysical Union Transactions), v. 72-44, p. 553.

Harper, G.D., Bowman, J.R. and Kuhns, R., 1988, A field, chemical, and stable isotope study of subseafloor metamorphism of the Josephine Ophiolite, California - Oregon: Journal of Geophysical Research, v. 93, p. 4625 - 4656.

Heyl, G.R., 1948, Foothill copper-zinc belt of the Sierra Nevada, California, in Jenkins, O.P., ed., Copper in California, California Division of Mines and Geology Bulletin 144: p.11-31.

Hietanen, A., 1951, Metamorphic and igneous rocks of the Merrimac area, Plumas National Forest, California: Geological Society of America Bulletin, v. 67, p. 567-607.

Hietanen, A., 1973, Geology of the Pulga and Bucks Lake quadrangles, Butte and Plumas counties, California: U.S. Geological Survey Professional Paper 731, 66 p.

Hietanen, A., 1976, Metamorphism and plutonism around the middle and south forks of the Feather River, California: U.S. Geological Survey Professional Paper 920, 30 p.

Johnson, M. C. and M. J. Rutherford, 1989, Experimental calibration of the aluminum-in-hornblende geobarometer with application to Long Valley caldera (California) volcanic rocks: Geology, v. 17, p. 837-841.

Kemp, W. R., 1982, Petrochemical affiliations of volcanogenic massive sulfide deposits of the foothill copper - zinc belt, Sierra Nevada, California [Ph.D. thesis] : Reno, University of Nevada, 458 p.

Kilbreath, S.P., 1984, The western world massive sulfide deposit, Yuba County, California, in Johnson, J.L., ed., Exploration for ore deposits of the North American cordillera, The Association of Exploration Geochemists Regional Symposium: p.FT6.1-4.

Lardner, W.B., and Brock, M.J., 1924, History of Placer and Nevada Counties, California: Los Angeles, Historic Record Company, p. 434-435.

Lindsley, D. H., 1976, Experimental studies of oxide minerals, in Rumble, D., ed., Mineralogical Society of America Reviews in Mineralogy: p.61 - 88.

Lindsley, D. H., 1983, Pyroxene thermometry: American Mineralogist, v. 68, p. 477 - 493.

Liou , C.G., Lan, C.Y., Suppe, J. and Ernst, W.G., 1977, The east Taiwan ophiolite: its occurrence, petrology, metamorphism and tectonic setting: Taiwan Mining Research Service Organization Special Report 1, 212 p.

Liou, J. G., Maruyama, S. and Cho, M., 1987, Very low-grade metamorphism of volcanic and volcaniclastic rocks: mineral assemblages and mineral facies, in Frey, M., ed., Low Temperature Metamorphism: Glasgow, Blackie, p. 59 - 113.

Marlette, J. W., Akers, R. J. , Cole, K. A. and McJunkin, R. D., 1979, The Aug. 1, 1975 Oroville Earthquake Investigations: California Department of Water Resources Bulletin 203-78, p. 15-101.

Martin, R.C., 1988, Volcanogenic massive sulfide belt of the western Sierra Nevada foothills: California Geology, v. 41, p. 195-204.

McLeod, M. and Day, H. W., 1991, Hornblende barometry of calc-alkaline plutons and movement history of the Big Bend fault zone, northern Sierra Nevada, CA [abs.] : Geological Society of America Abstracts with Programs, v. 23 -2, p. 78.

Olmstead, F.H., 1971, Pre-Cenozoic geology of the southern half of the Auburn 15-minute quadrangle, California: U.S. Geological Survey Bulletin 1341, 30 p.

Saleeby, J., Shaw, H. F. , Moores, E.M. and Edelman, S.H., 1989, U/Pb, Sm/Nd and Rb/Sr geochronological and isotopic study of northern Sierra Nevada ophiolitic assemblages, California: Contributions to Mineralogy and Petrology, v. 102, p. 205-220.

Schiffman P., Bettison, L. A. and Smith, B. M., 1990, Mineralogy and geochemistry of epidosites from the Solea graben, Troodos ophiolite, Cyprus, in Malpas, J. , Moores, E. M. , Panayiotou, A. and Xenophontos, C., ed., Ophiolite, Oceanic Crustal Analogues: Geological Survey of Cypress, p.673 - 683.

Schweickert, R.A. and Cowan, D.S., 1975, Early Mesozoic tectonic evolution of the western Sierra Nevada, California: Geological Society of America Bulletin, v. 86, p. 1329-1336.

Souter B.J. and Day, H. W., 1991, Arc basement of the Smartville Complex, northern Sierra Nevada, CA [abs.] : Geological Society of America Abstracts with Programs, v. 23 -2, p. 99.

Springer, R. K., Day, H. W. and Beiersdorfer, R. E., 1992, Prehnite-Pumpellyite to Greenschist Facies Transition, Smartville Complex, near Auburn, California: Journal of Metamorphic Geology, v. 10, p. 147-170.

Swanson, S. E., 1978, Petrology of the Rocklin pluton and associated rocks, western Sierra Nevada, California: Geological Society of America Bulletin, v. 89, p. 679-686.

Taliaferro, N.L., 1942, Geologic history and correlation of the Jurassic of southwestern Oregon and California: Geological Society of America Bulletin, v. 53, p. 71-112.

Taylor, G.C., 1990, Mineral land classification of the Western World Mining Company copper-zinc deposit near Smartville, Yuba County, California: California Division of Mines and Geology Open File Report 90-1, 22 p.

Tuminas, A.C., 1983, Geology of the Grass Valley-Colfax Area, Northern Sierra Nevada, California [Ph.D. thesis] : Davis, University of California, 415 p.

Wagner, D.L., Jennings, C.W. , Bedrossian, T.L and Bortugno, E.J., compilers, 1981, Geologic map of the Sacramento quadrangle, California: California Division of Mines and Geology Regional Geologic Map Series, scale 1:250,000.

Xenophontos, C., 1984, Geology, petrology and geochemistry of part of the Smartville Complex, northern Sierra Nevada foothills [Ph.D. thesis] : Davis, University of California, 446 p.

Xenophontos, C. and Bond, G. C., 1978, Petrology, sedimentation and paleogeography of the Smartville terrane (Jurassic): bearing on the genesis of the Smartville ophiolite, in Howell, D.G. and MacDougall, K. A., ed., Mesozoic Paleogeography of the Western United States: Society of Economic Paleontologists and Mineralogists, p.291-302.

A GLIMPSE OF THE CENTRAL AND FEATHER RIVER BELTS, NORTHERN SIERRA NEVADA

HOWARD W. DAY
Department of Geology
University of California
Davis, California 95616

INTRODUCTION

The Central and Feather River Belts of the northern Sierra Nevada are a structurally complex group of rocks that lie between the relatively little deformed Jurassic Smartville volcanic arc in the Western Belt and the stratigraphically intact, Paleozoic and Mesozoic sequences of the Eastern Belt (Fig. 1). The geology and metamorphism of these belts has been outlined earlier (Day, 1992). In the Yuba river region, the Central Belt is separated from the Smartville Complex on the west by the Wolf-Creek fault, and , from the Feather River Belt to the east by the Goodyear's Creek fault. Near the North Yuba river, the Feather River Belt is very narrow and is bounded on the east by the Downieville fault.

The Central Belt is structurally complex and contains rocks that have been described as melanges (Schweickert and Cowan, 1975). Recent work, however, has shown that large areas of the Central Belt are underlain by relatively intact, stratigraphic sedimentary sequences or pseudostratigraphic sequences of ultramafic, plutonic and volcanic rocks (Day, et al., 1985; Day, et al., 1988; Edelman, et al., 1989b; Tuminas, 1983). The ages and relationships among these units continue to be studied, but it is becoming clear that the Central Belt is dominantly Mesozoic and that Late Triassic and Early Jurassic sedimentary and volcanic rocks are abundant.

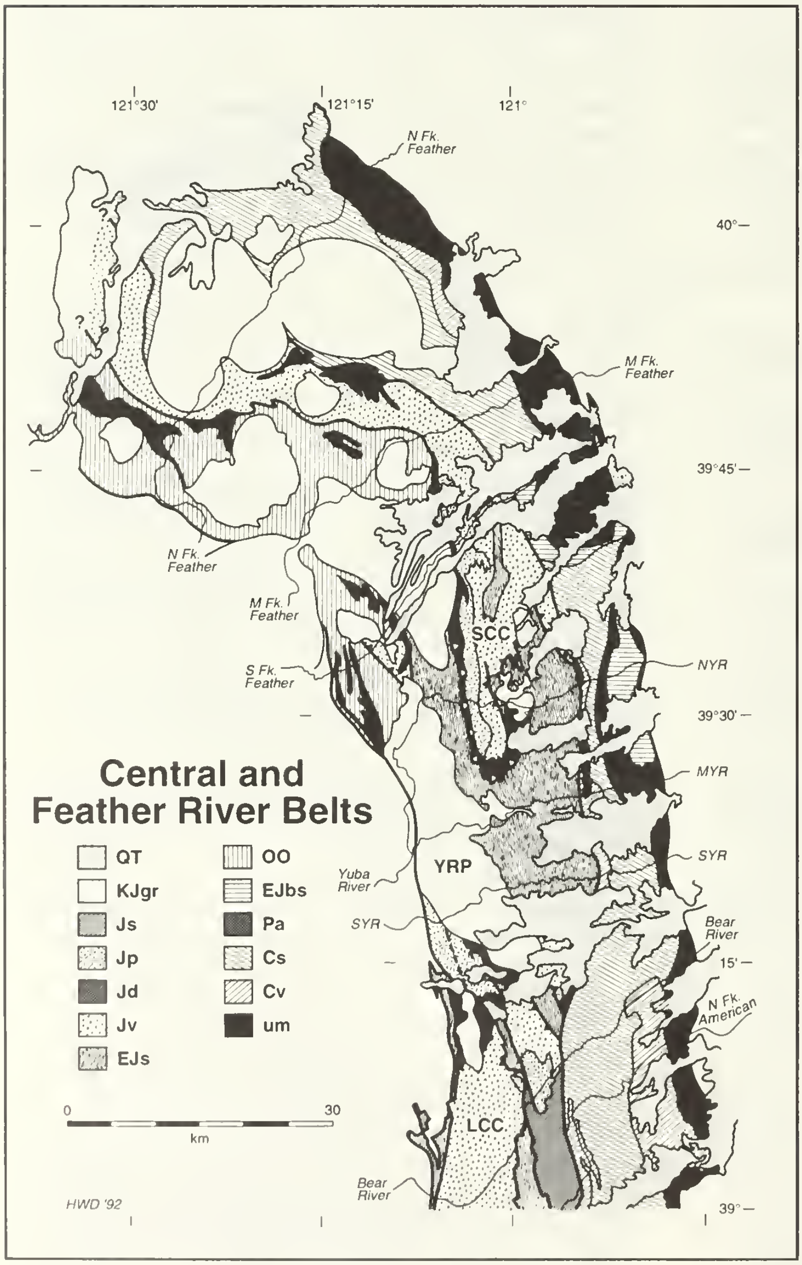

Fig. 1. Geologic sketch map of the Central and Feather River Belts. Abbreviations: QT - Quaternary and Tertiary sedimentary cover; KJgr - Cretaceous and Jurassic granitoid plutons. Js - Late Jurassic sedimentary cover; Jp - Jurassic gabbro and diorite; Jd - diabase dikes and massive diabase; Jv - Jurassic volcanic rocks. EJs - Early Jurassic or older chert argillite, siliciclastic sedimentary rocks.and fine-grained volcanic rocks; OO - melange of ultramafic, volcanic, and plutonic rocks; includes some EJs sedimentary rocks; EJbs - Early Jurassic or older blueschists in the Feather River Belt; Pa - Devonian and Permian amphibolite in the Feather River Belt; Cs - Carboniferous (?) or Triassic (?) chert argillite and phyllite; Cv - metavolcanic rocks associated with Cs; um - Feather River peridotite and serpentinite; undifferentiated ultramafics in the Central Belt.

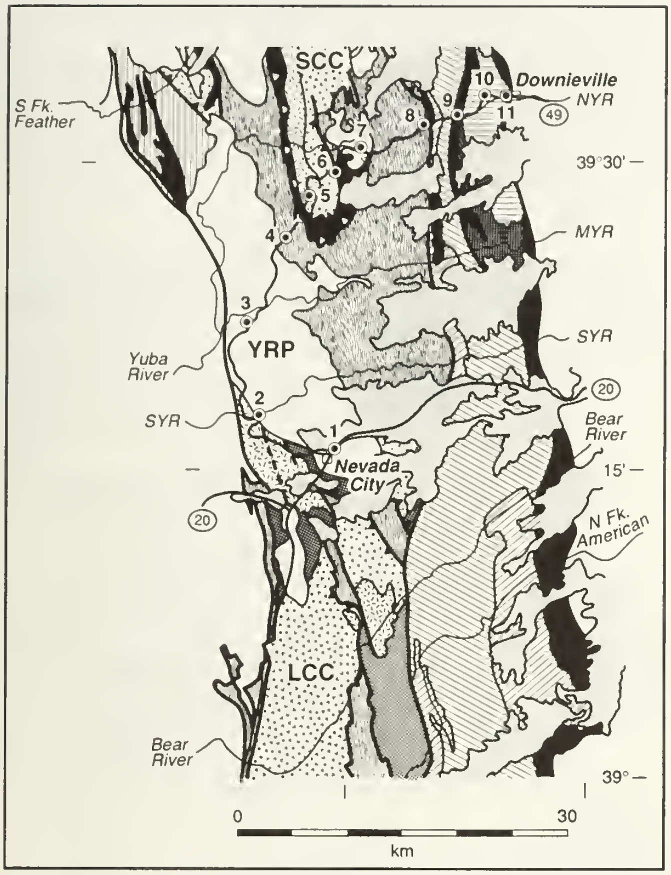

Figure 2. Enlarged view of a portion of Figure 1. See Figure 1 for legend. Highways 20 and 49 are indicated by the circled numbers. Filled circles and numbers indicate the field trip stops along Hwy 49 between Nevada City and Downieville.

The Feather River Belt is highly disrupted by steep faults and contains serpentinized peridotite and sepentinite that are intruded by mid-Paleozoic plutonic rocks, mid- and late-Paleozoic amphibolite, and Mesozoic, glaucophane-bearing metasediments and metavolcanics (Day, 1992).

The route of this field trip, from Nevada City to Downieville along State Highway 49, traverses elements of most of the major lithotectonic units of the Central and Feather River Belts. Exposure is excellent in the major river valleys, but limited elsewhere along the major highways.

CENTRAL BELT

The Central Belt, west of the Dogwood Peak - Gillis Hill fault, includes rocks assigned to the Lake Combie and Slate Creek Complexes as well as Older Ophiolite, Early Jurassic sedimentary and volcanic rocks, and Mid- to Late Jurassic sedimentary rocks (Fig. 1) have been considered together as the Fiddle Creek Complex (Edelman, et al., 1989b). The Lake Combie Complex (LCC. Fig. 1, 2) is an assemblage of igneous and sedimentary rocks that is interpreted as a volcanic arc (Tuminas, 1983). No reliable radiometric or fossil data are available, but the Complex is probably Jurassic in age. Ultramafic, plutonic, hypabyssal, and volcanic rocks form an arc-ophiolite pseudostratigraphy similar to that in the Smartville Complex to the West and the Slate Creek Complex to the north (Fig. 3a). Although detailed geochemical studies have not been made, the compositions of volcanic and plutonic rocks are probably intermediate andesites or basaltic andesites. The Lake Combie Complex differs from the Smartville by the lack of significant pillow lavas and sheeted dikes and, from the Slate Creek Complex by the absence of a continuously exposed ultramafic unit (Tuminas, 1983).

The Slate Creek Complex (Fig. 1, 2) is an Early Jurassic assemblage of ultramafic, plutonic, volcanic and volcaniclastic sedimentary rocks with a pronounced pseudostratigraphy (Fig. 3b). This Complex also is interpreted as a fragment of ~200 Ma volcanic arc crust based on 206Pb/238U ages of zircon from the plutonic unit (Edelman, et al., 1989a; Saleeby, et al., 1989), but the complex differs from the ~160 Ma Smartville Complex also by its notable lack of extensive hyabyssal rocks and pillow lavas. The plutonic and volcanic rocks are dominantly tonalitic and andesitic, but detailed geochemical studies have not been made.

The Slate Creek and Lake Combie Complexes are in tectonic contact over Early Jurassic volcanic and sedimentary rocks, and, indirectly, over Mid-Late Jurassic sedimentary rocks and Older Ophiolite that were included in the Fiddle Creek Complex by Edelman et al. (1989b). The tectonic contacts have been interpreted as thrust faults, truncated or otherwise deformed by later steep faults and folds (Day, et al., 1985; Edelman, et al., 1989b; Moores and Day, 1984).

The inferred stratigraphic relationships among the units included in the Fiddle Creek Complex are illustrated in Figure 3c. The Mid-Late Jurassic siliciclastic sediments, included in the Fiddle Creek Complex as Colfax Sequence (?), occur only as areas too small to be shown in Figure 1 and 2 and cannot be correlated directly with the extensive outcrops in the southeast (Fig. 1 and 2). The Early Jurassic volcanic and sedimentary unit (Clipper Gap Formation) has been studied very little and may eventually yield to further subdivision. Chert in this unit contain Triassic - Early Jurassic radiolaria (Hietanen, 1981) and limestone blocks, interpreted as olistoliths (Day, et al., 1985), contain Early Carboniferous crinoid and brachiopod fragments (Lindgren, 1900). The age of volcanic and ophiolitic rocks in the Older Ophiolite unit have not been determined in the area of Figure 2, but similar rocks in the N. Fk. Feather River, about 50 km to the northwest, have been found to be ~200 Ma or older (Saleeby, et al., 1989).

The Yuba Rivers and Indian Valley Plutons (Fig. 2) intrude the Fiddle Creek Complex and provide important constraints on the times of deformation. The Indian Valley Pluton is a biotite - hornblende granodiorite that intrudes the contact between the ultramafic rocks of the Slate Creek Complex and the volcanic and sedimentary rocks of the Fiddle Creek Complex along the N. Yuba River (Fig. 2). Zircons from this body yield 206Pb/238U ages of 152 ± 2 Ma (Bickford, Day & Orrell, in preparation). The age of emplacement of the Slate Creek Complex is

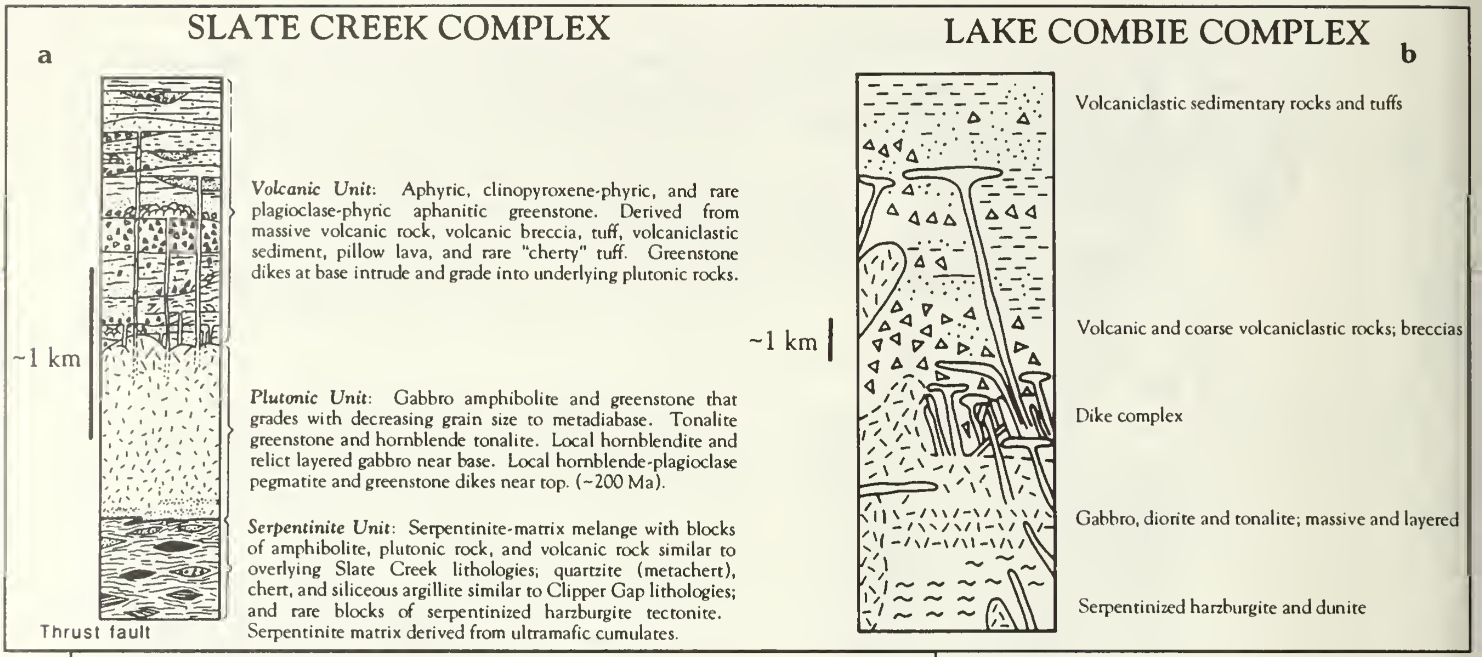

Volcanic Unit: Aphyric, clinopyroxene-phyric, and rare plagioclase-phyric aphanitic greenstone. Derived from massive volcanic rock, volcanic breccia, tuff, volcaniclastic sediment, pillow lava, and rare "cherty" tuff. Greenstone dikes at base intrude and grade into underlying plutonic rocks.

Plutonic Unit: Gabbro amphibolite and greenstone that grades with decreasing grain size to metadiabase. Tonalite greenstone and hornblende tonalite. Local hornblendite and relict layered gabbro near base. Local hornblende-plagioclase pegmatite and greenstone dikes near top. (~200 Ma).

Serpentinite Unit: Serpentinite-matrix melange with blocks of amphibolite, plutonic rock, and volcanic rock similar to overlying Slate Creek lithologies; quartzite (metachert), chert, and siliceous argillite similar to Clipper Gap lithologies; and rare blocks of serpentinized harzburgite tectonite. Serpentinite matrix derived from ultramafic cumulates.

Volcaniclastic sedimentary rocks and tuffs

Volcanic and coarse volcaniclastic rocks; breccias

Dike complex

Gabbro, diorite and tonalite; massive and layered

Serpentinized harzburgite and dunite

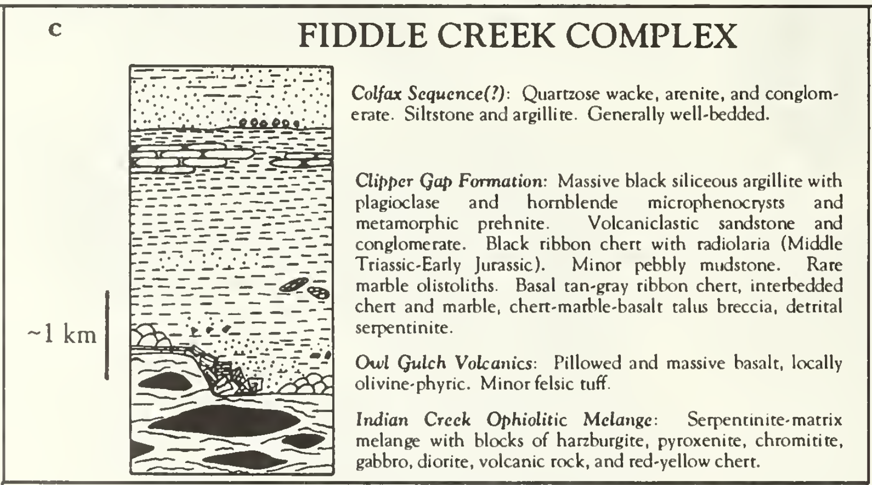

Colfax Sequence(?): Quartzose wacke, arenite, and conglomerate. Siltstone and argillite. Generally well-bedded.

Clipper Gap Formation: Massive black siliceous argillite with plagioclase and hornblende microphenocrysts and metamorphic prehnite. Volcaniclastic sandstone and conglomerate. Black ribbon chert with radiolaria (Middle Triassic-Early Jurassic). Minor pebbly mudstone. Rare marble olistoliths. Basal tan-gray ribbon chert, interbedded chert and marble, chert-marble-basalt talus breccia, detrital serpentinite.

Owl Gulch Volcanics: Pillowed and massive basalt, locally olivine-phyric. Minor felsic tuff.

Indian Creek Ophiolitic Melange: Serpentinite-matrix melange with blocks of harzburgite, pyroxenite, chromitite, gabbro, diorite, volcanic rock, and red-yellow chert.

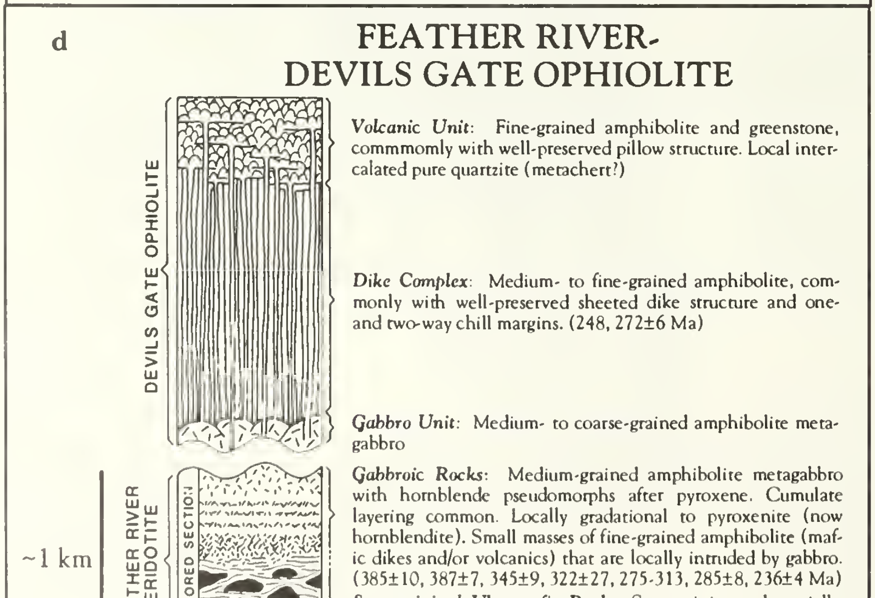

Volcanic Unit: Fine-grained amphibolite and greenstone, commmomly with well-preserved pillow structure. Local intercalated pure quartzite (metachert?)

Dike Complex: Medium- to fine-grained amphibolite, commonly with well-preserved sheeted dike structure and one- and two-way chill margins. (248, 272±6 Ma)

Gabbro Unit: Medium- to coarse-grained amphibolite metagabbro

Gabbroic Rocks: Medium-grained amphibolite metagabbro with hornblende pseudomorphs after pyroxene. Cumulate layering common. Locally gradational to pyroxenite (now hornblendite). Small masses of fine-grained amphibolite (mafic dikes and/or volcanics) that are locally intruded by gabbro. (385±10, 387±7, 345±9, 322±27, 275-313, 285±8, 236±4 Ma)

Serpentinized Ultramafic Rocks: Serpentinite and partially serpentinized peridotite tectonic and massive dunite

Figure 3. Schematic Geologic Columns. (a) Lake Combie Complex (After Tuminas, 1983); (b) Slate Creek Complex (after Edelman et al., 1989b); (c) Fiddle Creek Complex (after Edelman et al., 1989b); (d) Feather River-Devils Gate Ophiolite (after Edelman et al., 1989b).

further constrained by the 165±3 Ma age of the Scales Pluton (Fig. 1) , which cuts the contact between the volcanic unit of the Slate Creek Complex and the Fiddle Creek Complex (Edelman, et al., 1989a; Saleeby, et al., 1989). The Yuba Rivers Pluton is a dominantly tonalitic body that intrudes and metamorphoses the Fiddle Creek Complex at its eastern contact, cuts steep faults and cleavages at both its northern and southern borders, intrudes the Smartville Complex to the west and, yet, is deformed in the Wolf Creek fault zone that separates the Smartville Complex and Central Belt. Numerous zircon 206Pb/238U ages demonstrate that the Yuba Rivers is 160 ± 2 Ma, indistinguishable from the age of tonalite and gabbro in the Smartville Complex (Edelman, et al., 1989a; Saleeby, et al., 1989). A small body of garnet - muscovite - sillimanite granodiorite(~154 Ma, Bickford, Day & Orrell, in preparation) intrudes the Yuba Rivers Pluton near the Middle Yuba River.

Phyllite, chert and minor volcanic rocks east of the Dogwood Peak - Gillis Hill fault zone in the Central Belt are assigned to the Calaveras Complex (Edelman, et al., 1989b). These rocks are believed to be Late Paleozoic or Early Mesozoic in age based on regional correlations and fossils found farther north (Hietanen, 1981; Standlee and Nestell, 1985). Only a very narrow belt of these rocks is exposed along the route of the field trip in an area that is very highly deformed between two major faults.

FEATHER RIVER BELT

The Feather River Belt is named after the large body of metaperidotite exposed in the drainages of the various forks of the Feather River (Fig. 1). In the region of this field trip the metaperidotite is reduced to narrow serpentinite bodies and structurally interleaved with amphibolite and both metasedimentary and metavolcanic blueschists. The structural and genetic relationship of these units is very poorly understood.

Amphibolites north of the N. Yuba river (Fig. 1) contain sheeted dikes and pillowed flows and have been named Devils Gate ophiolite by Edelman et al. (1989b). The Feather River peridotite and associated gabbro and the Devils Gate amphibolite were considered a disrupted, "polygenetic" ophiolite (Fig. 3d) by Edelman et al. (1989b). However, the amphibolites yield Permian ages (K-Ar and 40Ar/39Ar on hornblende) and the intrusives in the peridotite appear to be Devonian (see Edelman et al., 1989b for review). Amphibolite south of the N. Yuba River (Fig. 1, 2) yields Devonian argon ages on hornblende (Bohlke and McKee, 1984).

Edelman et al. (1989b) applied the name Red Ant Schist to metasedimentary and metavolcanic rocks between the Goodyear's Creek and Downieville faults. Blueschist assemblages occur sporadically in disharmonically folded quartz mica phyllites and schists and in structurally interleaved greenstones. Crossite, glaucophane, pumpellyite, stilpnomelane, lawsonite, albite, white mica, chlorite and quartz have been described (Hacker and Goodge, 1990; Hacker and Peacock, 1990; Hietanen, 1981; Schweickert, et al., 1980). K-Ar data indicate that blueschist metamorphism is 175 Ma or older, but the ages of the protoliths are unknown (Schweickert, et al., 1980).

METAMORPHISM

The metamorphism of the Central and Feather River belts has not been studied systematically. Aside from a broad overview (Day, et al., 1988), the only detailed studies have emphasized the Feather River Belt (Hacker and Goodge, 1990; Hacker and Peacock, 1990). A brief overview of the essential results is given in Chapter 1 of this volume (Day, 1992). Volcanic rocks of the Lake Combie Complex display primarily greenschist assemblages (actinolite, chlorite, epidote, albite ± quartz) but pumpelleyite has been reported (Springer, personal communication). Early Jurassic sedimentary and volcanic rocks of the Clipper Gap formation (Fig. 1, 2, and 3) are barely recrystallized near the Yuba rivers, but rare prehnite was reported by Edelman et al. (1989b). Mafic rocks associated with the Older Ophiolite and Indian Creek ophiolitic melange contain upper greenschist assemblages transitional to amphibolite facies (Day, et al., 1988). Volcanics in the Slate Creek Complex and Calaveras Complex are known to contain greenschist assemblages but their metamorphism has not been studied systematically.

The Feather River Belt contains the highest grade metamorphic rocks exposed in the Sierra as well as the only known blueschists. The metaperidotite contains anthophyllite (Ehrenberg, 1975) , which is diagnostic for the amphibolite facies, but near the N. Yuba river and farther south only serpentinite has been reported. Mafic rocks contain clinopyroxene + hornblende + andesine ± garnet (Hacker and Peacock, 1990). The amphibolite facies assemblages are probably Paleozoic, but a pumpelleyite-actinolite facies overprint of possible Jurassic age has been recognized by detailed back-scattered electron microscopy (Hacker and Peacock, 1990). Early Mesozoic high pressure rocks are also found within the Feather River Belt (Day, et al., 1988; Hacker and Goodge, 1990; Hietanen, 1981; Schweickert, et al., 1980). The protoliths of the so-called Red Ant schists were probably oceanic chert-argillite and volcanic rocks that now are represented by disharmoni- cally folded, laminated, quartz schists and greenstones. These rocks contain glaucophane + lawsonite and crossite + epidote suggesting metamorphic pressures of about 6 kbar or more (Day, et al., 1988; Hacker and Goodge, 1990). The blueschist assemblages have been overprinted by pumpelleyite + actinolite (Hacker and Goodge, 1990). The age of the metamorphism is not well-constrained but must be 174 Ma or older (Schweickert, et al., 1980).

ROAD LOG

The route of this field trip is entirely along California State Highway 49, north of Nevada City. The route passes across or along the canyons of the South, Middle, and North Yuba Rivers and is a narrow, winding road. Because traffic is heavy and large logging trucks are common, it is important to exercise extreme caution in parking or walking along the highway. Many areas are not suitable for stopping, especially with groups of people.

The route of the field trip (Fig. 2) passes through poorly exposed parts of the northern Lake Combie Complex and extensive exposures of the Yuba Rivers Pluton. On the east side of the Yuba Rivers pluton, the rocks of the Fiddle Creek Complex are widespread, especially along the North Yuba River. Although the route passes through the southern part of the Slate Creek Complex, outcrops are generally poor. The Feather River Belt is moderately well-exposed along the highway, but most outcrops are not suitable for large groups.

California State Highways 20 and 49 coincide as a single divided freeway between the towns of Grass Valley and Nevada City. From Nevada City, proceed north on the combined Hwy 49 & 20 to the Jct where Hwy 49 leaves Hwy 20. Turn left (west) on Hwy 49 and park on the shoulder.

Stop 1. 0.0 miles.

Yuba Rivers Pluton. The outcrop is about 100 m north of the Jct of Hwy 49 and 20 on the west side of Hwy 20. This outcrop is typical of the main mass of the batholith. The tonalite commonly contains both hornblende and biotite with macroscopic sphene as a common accessory mineral. Zircon from a sample at this outcrop yielded a 206Pb/238U age of 158±2 Ma (Bickford, Day & Orrell, in prep.). Continue west on Hwy 49.

Stop 2. 7.0 miles.

Yuba Rivers Pluton. S. abutment of bridge over S. Yuba River. (A new bridge is under construction at the time of this writing, May, 1992). These outcrops are along the southwestern contact of the Yuba Rivers Pluton with tonalite and diorite of the Lake Combie Complex. The contact, about 500 m downstream, is sharp, but no intrusive features, contact metamorphism, or deformation are obvious. At the bridge, it is possible to see large boulders and outcrops of tonalite containing large angular mafic inclusions as well as schlieren and on the north side of the canyon, late, fine-grained felsic dikes are common.

9.5 miles. Good outcrops of Yuba Rivers Pluton near the southwestern contact with slightly more mafic tonalite and diorite of the Lake Combie Complex.

10.9 miles Road to Malakoff Diggings State Park.

12.0 miles Hamlet of Sweetland Good outcrops of foliated Yuba Rivers Pluton can be seen in the bed of Sweetland Creek about 0.5 - 1 km west of Hwy 49. This deformation is associated with the Wolf Creek fault that separates the Smartville Complex and the Central Belt.

14.4 miles. Village of North San Juan

Stop 3. 15.8 miles

Garnet - muscovite - sillimanite granodiorite intrusive into the Yuba Rivers Pluton. Parking is available 0.1 miles north of the outcrop. Peraluminous granitic rocks are very rare in the Sierra Nevada. This body is an equi-dimensional plug about 1 km in diameter that is best exposed in the Middle Yuba River to the west. The body is normally zoned with a granodiorite core and a tonalite rim (Lombardi and Day, 1989). Garnet and white mica are common; coarse grained sillimanite is rare and is overgrown by white mica. Zircon from a sample at this outcrop yielded a 206Pb/238U age of 154 ± 2 Ma (Bickford et al., in prep.).

17.2 miles. M. Yuba River. Parking and picnic area on the north side of the river.

20.6 miles. Contact of Yuba Rivers Pluton with country rock of the Fiddle Creek Complex.

20.9 miles. Marysville - Dobbins road and U.S. Forest Service Headquarters.

Stop 4. 21.6 miles.

Contact aureole of the Yuba Rivers Pluton. Very fine-grained to fine grained hornfels with variable metamorphic foliation and cleavage. The rocks contain actinolite + plagioclase + sphene + opaque ± quartz ± epidote ± carbonate ± garnet ± clinopyroxene. These protoliths of these rocks are interpreted as tuffs and volcaniclastic sandstones of the Fiddle Creek Complex.

23.8 miles. Serpentinites on the right are mapped as part of the ultramafic unit of the Slate Creek Complex

24.1 miles. Strongly deformed, mylonitic tonalites mapped as part of the plutonic unit of the Slate Creek Complex.

Stop 5. 24.8 Miles.

Slate Creek Complex, plutonic unit. Sleighville Creek Road. Tonalite has been mapped continuously for a distance of about 30 km south of the S. Fk. Feather River (Fig. 1) and defines a plutonic unit in the Slate Creek Complex. The plutonic rocks intrude serpentinized ultramafic rocks on the west and the volcanic unit on the east. On a regional scale, the plutonic rocks tend to be more mafic on the west and more silicic on the east side. The textures and composition of the tonalite show remarkable meter-scale heterogeneity in some outcrops. The plutonic unit is poorly exposed south of the N. Yuba River and this dusty outcrop is typical. Zircon from a sample at this outcrop yielded a 206Pb/238U age of 204 ± 2 Ma (Bickford et al., in prep.).

27.2 miles. Cenozoic sands and gravels.

Stop 6. 28.4 miles.

Slate Creek and Fiddle Creek Complexes. The outcrops along the highway in both directions from this stop are a testament to the difficulties of unraveling complex structures in rocks that are a challenge to identify and interpret in the field. A steep fault exposes fault slices of Early Jurassic(?) volcanic and sedimentary rocks of the Fiddle Creek Complex, fine grained volcanic and volcaniclastic rocks of the Slate Creek Complex and serpentinized and contact metamorphosed ultramafic rocks. Pebbly mudstones with chert and carbonate clasts, slates, and massive metasandstones are abundant east of this stop. Serpentinized ultramafic rocks can be studied along the side road to the east and along the main highway to the north. They are locally metamorphosed (tremolite + olivine) by the Indian Valley Pluton. Fine grained volcanic rocks and volcaniclastic metasediments are interpreted as the southern part of volcanic unit of the Slate Creek Complex.

30.5 miles. N. Yuba River

30.9 miles. Outcrops of Indian Valley Pluton

31.4 miles. Fiddle Creek

Stop 7. 32.0 miles.

Indian Valley pluton. The Indian Valley pluton is a biotite, hornblende granodiorite with distinctive books of euhedral biotite. The pluton intrudes the contact between the ultramafic unit of the Slate Creek Complex and sedimentary rocks of the Fiddle Creek Complex. Dikes of this pluton intrude pavement outcrops of the Fiddle Creek in the bed of the N. Yuba River to the east. Zircon from a sample at this outcrop yielded a 206Pb/238U age of 152 ± 2 Ma (Bickford et al., in prep.).

32.9 miles. Indian Valley Pluton intrusive into Fiddle Creek Complex.

33.6 miles. Dikes of Indian Valley Pluton in Fiddle Creek Complex. No Parking.

Stop 8. 36.9 miles.

Fiddle Creek Complex. This outcrop of chert and black, siliceous argillite is typical of the large parts of the Fiddle Creek Complex. Near the eastern end of the outcrop Hietanen (1981) reported that the chert contains fossils of Middle Triassic to Early Jurassic radiolaria Other parts of the Fiddle Creek containing similar appearing siliceous argillite are clearly silicified tuffs with broken microphenecrysts of plagioclase and hornblende. Volcaniclastic rocks, pebbly mudstone and carbonate detritus are also common.

37.4 miles. Road to Rams Horn Campground.

38.5 miles. Deformed slates and metavolcanic rocks assigned to the Calaveras Complex.

Stop 9. 39.2 miles.

Serpentinites at Goodyear's Bar. These serpentinites are thought to be remnants of the Feather River Peridotite farther north and represent the first outcrops of the Feather River Belt, bounded on the west by the Goodyear's Creek Fault. Chrysotile fibers are abundant on the slickensided surfaces, but massive serpentinite probably contains antigorite. Edelman etal. (1989b) suggested that a large body of quartztite in this outcrop is similar to rocks in the Paleozoic Shoo Fly formation, the nearest exposures of which are east of Downieville.

Stop 10. 41.5 miles. Rossassco Ravine. Blueschist facies metavolcanic and metasedimentary rocks of the Feather River Belt (Red Ant Schist of Edelman et al. 1989b). Parking for access to these outcrops is on the north side of the highway at a major bend. Please use extreme care in leaving and re-entering the highway.

Disharmonically folded, laminated quartz schists and phyllites are typical of the Red Ant schist in the Feather River Belt. Such structures and quartz banding are not found in any other unit of the northern Sierra. Metavolcanic greenstones associated with the metasedimentary rocks contain sporadic glaucophane + lawsonite or crossite + epidote. Metasedimentary rocks contain lawsonite + albite + quartz + chlorite ± stilpnomelane ± pumpellyite.

Stop 11. 42.8 miles.

Overlook of Downieville. Lawsonite + albite + quartz + chlorite can be found in disharmonically folded, graphitic metasedimentary rocks.

43. 4 miles. Bridge over the north Yuba River, Downieville.

REFERENCES

Bohlke, J. K. and McKee, E. H., 1984, K-Ar ages relating to metamorphism, plutonism, and gold-quartz vein mineralization near Alleghеny, Sierra County, California: Isochron/West, v. 39, p. 3-7.

Day, H. W., 1992, Tectonics and Metamorphism of the Northern Sierra Nevada, in Schiffman, P. and Wagner, D., ed., California Division of Mines and Geology, p.

Day, H. W., Moores, E. M. and Tuminas, A. C., 1985, Structure and tectonics of the northern Sierra Nevada: Geological Society of America Bulletin, v. 96, p. 436-450.

Day, H. W., Schiffman, P. and Moores, E. M., 1988, Metamorphism and tectonics of the northern Sierra Nevada, in Ernst, W. G., ed., Metamorphism and Crustal Evolution of the Western United States: Engelwoods Cliffs, N.J., Prentice Hall, Inc, p. 737-763.

Edelman, S. H., Day, H. W. and Bickford, M. E., 1989a, Implications of U-Pb zircon ages for the tectonic settings of the Smartville and Slate Creek Complexes, northern Sierra Nevada, California: Geology, v. 17, p. 1032-1035.

Edelman, S. H., Day, H. W., Moores, E. M., Zigan, S. M., Murphy, T. P. and Hacker, B. R., 1989b, Structure across a Mesozoic ocean-continent suture zone in the northern Sierra Nevada, California: Geological Society of America Special Paper, v. 224, p. 1-56.

Ehrenberg, S. M., 1975, Feather River ultramafic body, northern Sierra Nevada, California: Geological Society of America Bulletin, v. 86, p. 1235-1243.

Hacker, B. R. and Goodge, J. W., 1990, Comparison of early Mesozoic high-pressure rocks in the Klamath Mountains and Sierra Nevada, in Harwood, D. S. and Miller, M. M., ed., Paleozoic and early Mesozoic paleogeographic relations; Sierra Nevada, Klamath Mountains, and related terranes: Boulder, Colorado, Geological Society of America, p. 277 - 295.

Hacker, B. R. and Peacock, S. M., 1990, Comparison of of the Central Metamorphic Belt and Trinity terrane of the Klamath Mountains with the Feather River terrane of the Sierra Nevada, in Harwood, D. S. and Miller, M. M., ed., Paleozoic and early Mesozoic paleogeographic relations; Sierra Nevada, Klamath Mountains, and related terranes: Boulder, Colorado, Geological Society of America, p. 75 - 92.

Hietanen, A., 1981, Petrologic and structural studies in the northwestern Sierra Nevada, California: U.S. Geological Survey Professional Paper, v. 1226, p. 1-59.

Lindgren, W., 1900, Colfax Folio, California; Geologic Atlas of the United States, Historical Geology sheet: U.S. Geological Survey Folio, v. 66, p.

Lombardi, M. R. and Day, H. W., 1989, Peraluminous granitoid intrusives, Yuba Rivers pluton, northwestern Sierra Nevada foothills, California.: Geological Society of America Abstracts with Programs, v. 21, p. 108.

Moores, E. M. and Day, H. W., 1984, An overthrust model for the Sierra Nevada: Geology, v. 12, p. 416-419.

Saleeby, J. B., Shaw, H. F., Niemeyer, S., Moores, E. M. and Edelman, S. H., 1989, U/Pb, Sm/Nd and Rb/Sr geochronological and isotopic study of Northern Sierra Nevada ophiolitic assemblages, California: Contributions to Mineralogy and Petrology, v. 102, p. 205-220.

Schweickert, R. A., Armstrong, R. L. and Harakal, J. E., 1980, Lawsonite blueschist in the northern Sierra Nevada, California: Geology, v. 8, p. 27-31.

Schweickert, R. A. and Cowan, D. S., 1975, Early Mesozoic tectonic evolution of the western Sierra Nevada, California: Geological Society of America Bulletin, v. 86, p. 1329-1336.

Standlee, L. A. and Nestell, M. K., 1985, Age and tectonic significance of terranes adjacent to the Melones fault zone, N. Sierra Nevada, California: Geologic Society of America Abstracts with Programs, v. 17, p. 410.

Tuminas, A. C., 1983, Structural and stratigraphic relations in the Grass Valley-Colfax area of the northern Sierra Nevada foothills, California [Ph.D. dissertation]: Davis, California, University of California, 415 p.

GEOLOGY OF THE EASTERN BELT OF THE NORTHERN SIERRA NEVADA

ELWOOD R. BROOKS
Department of Geosciences
Hayward State University
Hayward, CA 94542-3088

The Eastern Belt of the northern Sierra Nevada (Day and others, 1985)— also known as the Northern Sierra terrane (Coney and others, 1980) —lies east of the Feather River Peridotite Belt (Melones fault zone). It consists largely of the early Paleozoic Shoo Fly Complex, to the west, and unconformably overlying late Paleozoic and Jurassic volcanic-arc sequences (Fig. 1).

Shoo Fly Complex

The angular unconformity at the base of the Upper Devonian Grizzly and Sierra Buttes Formations (the former not shown separately in Fig. 1) is a profound one, truncating faults that subdivide the Shoo Fly Complex into four imbricate thrust blocks. In ascending structural order, these thrust-bounded units are the Lang sequence ("'Lang-Halsted' unit" in Fig. 1), the Duncan Peak chert, the Culbertson Lake allochthon, and the Sierra City melange (Girty and others, 1990).

The 375+/-10 Ma Bowman Lake batholith (Hanson and others, 1988) stitches the three structurally lowest units of the Shoo Fly Complex (Fig. 1, where "Bowman Lake trondhjemite" = the Bowman Lake batholith). The 378+/-5 Ma Wolf Creek granitic stock actually intrudes the unconformity between the Shoo Fly Complex and the Sierra Buttes Fm. near Greenville, north of Figure 1 (Saleeby and others, 1987). These plutons are considered sources of Upper Devonian volcanic rocks in the Sierra Buttes Fm.

The time of deposition of the Shoo Fly Complex is difficult to determine, because nearly all radiometric ages and fossils have come from blocks (or suspected blocks) in melange. U/Pb zircon ages range from 423+/-8 Ma (Silurian; Saleeby and others, 1987) to approximately 600 Ma (latest Proterozoic, probably SFC basement; Saleeby and others, 1989), and brachiopods and conodonts are Middle to Late Ordovician (Potter and others, 1990; Harwood and Murchey, 1990). Radiolarian cherts in the Culbertson Lake allochthon probably are post-Cambrian (Girty and others, 1990).

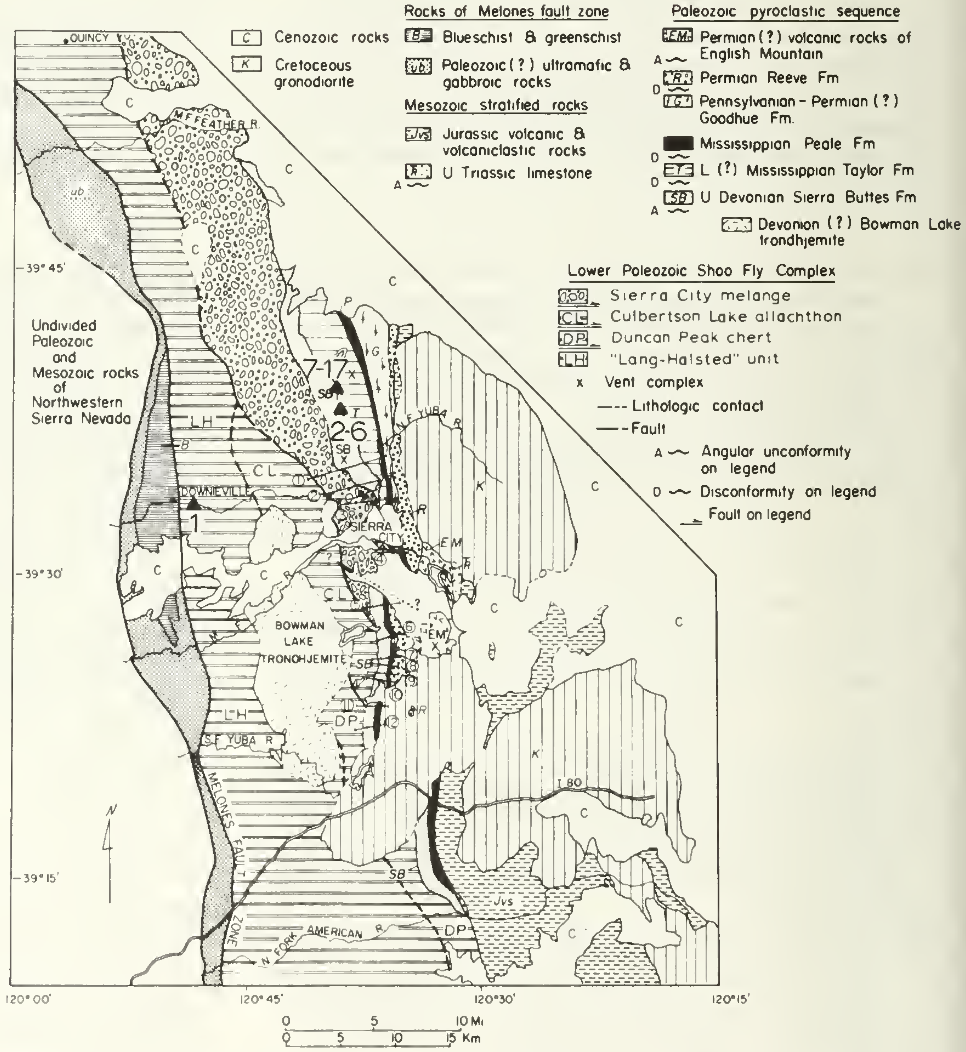
C Cenozoic rocks
K Cretaceous granodiorite
Rocks of Melones fault zone
B Blueschist & greenschist
ub Paleozoic (?) ultramafic & gabbroic rocks
Mesozoic stratified rocks
Jvs Jurassic volcanic & volcaniclastic rocks
Ŧ U Triassic limestone
Paleozoic pyroclastic sequence
EM Permian (?) volcanic rocks of English Mountain
RR Permian Reeve Fm
G Pennsylvanian - Permian (?) Goodhue Fm.
Mississippian Peale Fm
T L (?) Mississippian Taylor Fm
SB U Devonian Sierra Buttes Fm
Devonion (?) Bowman Lake trondhjemite
Lower Paleozoic Shoo Fly Complex
Sierra City melange
CL Culbertson Lake allochthon
DP Duncan Peak chert
LH "Lang-Halsted" unit
x Vent complex
Lithologic contact
Fault
A Angular unconformity on legend
D Disconformity on legend
Fault on legend
QUINCY
M F FEATHER R
N F YUBA R
DOWNIEVILLE
SIERRA CITY
BOWMAN LAKE TRONDHJEMITE
S F YUBA R
MELONES FAULT ZONE
N FORK AMERICAN R
I 80
Undivided Paleozoic and Mesozoic rocks of Northwestern Sierra Nevada
7-17
2-6
1
N
39° 45'
39° 30'
39° 15'
120° 00'
120° 45'
120° 30'
120° 15'
0 5 10 Mi
0 5 10 15 Km

FIGURE 1. Generalized geologic map of the Sierra Buttes-Bowman Lake region (Fig. 2 in Brooks and Schweickert, 1982). Locations of field trip stops 1-17 are shown by the filled triangles. Mapping by R.A. Schweickert, R.E. Hanson, G.H. Girty, and G.C. Bond, 1973-82; area south of I-80 from Harwood (1983). Readers are urged to consult Plate 1 in Harwood (1992) for a more detailed and up-to-date geologic map of the region.

Edelman and others (1989, p. 8) remind us that "the abundance of monocrystalline and coarsely polycrystalline framework quartz grains...suggests a continental provenance, generally assumed to be North America". Also, current workers evidently still agree generally with R.A. Schweickert and R.E. Hanson (Brooks and Schweickert, 1982, p. 3) that the Shoo Fly Complex along the North Yuba River "...can be interpreted as...part of a...subduction complex (Sierra City melange) which has incorporated large slabs of sediment from continentally-derived deep-sea fans (Culbertson Lake allochthon) and which ultimately scraped up and incorporated part of a continental slope and rise assemblage as the subduction complex approached a continental margin". We will look at the Shoo Fly Complex only once on this field trip, in the Lang sequence (STOP 1).

Taylorsville Sequence

The submarine volcanic and volcaniclastic rocks, radiolarian cherts, and locally prominent epiclastic deposits which unconformably overlie the Shoo Fly Complex— referred to as the Taylorsville sequence by Harwood (1988) —range in age from Late Devonian (Frasnian) to late Early Permian (Wordian) (Harwood, 1988). The Taylorsville sequence ("Paleozoic pyroclastic sequence" in Fig. 1) consists of two distinct volcanic assemblages separated by radiolarian chert (chert member of the Peale Fm.) that signals a long period of volcanic quiescence and pelagic deposition (from Middle Mississippian to at least Middle Pennsylvanian). Furthermore, the Taylorsville sequence is subdivided by a major erosional unconformity that spans the Late Pennsylvanian and Early Permian (Fig. 2); the unconformity is thought to reflect uplift associated with crustal heating and extension prior to late Early Permian basaltic volcanism (Goodhue Fm.; Harwood, 1988). The Taylorsville sequence was succeeded, in the Early and Middle Jurassic, by yet a third volcanic assemblage, and, during the Late Jurassic Nevadan orogeny, all rocks were folded into the Nevadan synclinorium. Rocks of the Taylorsville sequence along the North Yuba River occupy the homoclinal western limb of the synclinorium, so that all of them face easterly (and most dip easterly).

Estimates of relative abundance of volcanic rocks made by Harwood (1988) indicate that volcanism began with voluminous eruption of magmas of the Sierra Buttes Fm. in the latest Devonian (mid-Famennian; Hanson and Schweickert, 1986), continued at a high rate during accumulation of the Taylor Fm., but waned dramatically in the Early Mississippian, with eruption of the lower, volcanic member of the Peale Fm. Permian volcanism produced only about half the amount of material recorded in either the Sierra Buttes or Taylor Fms. (Harwood, 1988).

We will concern ourselves on this field trip only with the first-formed, Upper Devonian-Lower Mississippian volcanic assemblage, and will view rock units belonging to three of its formations, the dacitic to andesitic Sierra Buttes Fm., the andesitic Elwell Fm., and the andesitic basaltic to basaltic Taylor Fm. (we will not see the Grizzly or Peale Fms.). The Elwell Fm. is sandwiched between the other two formations north of the North Yuba River, but is considered the uppermost member of the Sierra Buttes Fm. in that area by Hanson and Schweickert (1986). I follow Durrell and D'Allura (1977) in mapping it separately.

Concentrations of immobile trace elements in the basaltic rocks show that they originated in an island arc and belong to the tholeiitic rock association (Brooks and Coles, 1980). Also of interest is that the Upper Devonian-Lower Mississippian island arc is compositionally inverted, volcanism commencing with dacites (Sierra Buttes Fm.) and progressing to basaltic andesites and basalts (Taylor Fm.). The earliest silicic lava flows in the Sierra Buttes Fm. have epsilon Nd from -15 to -20, suggesting derivation wholly or in part from Early Proterozoic or Archean continental crust, consistent with the notion that the island-arc rocks and their basement of Shoo Fly Complex originated along the western margin of North

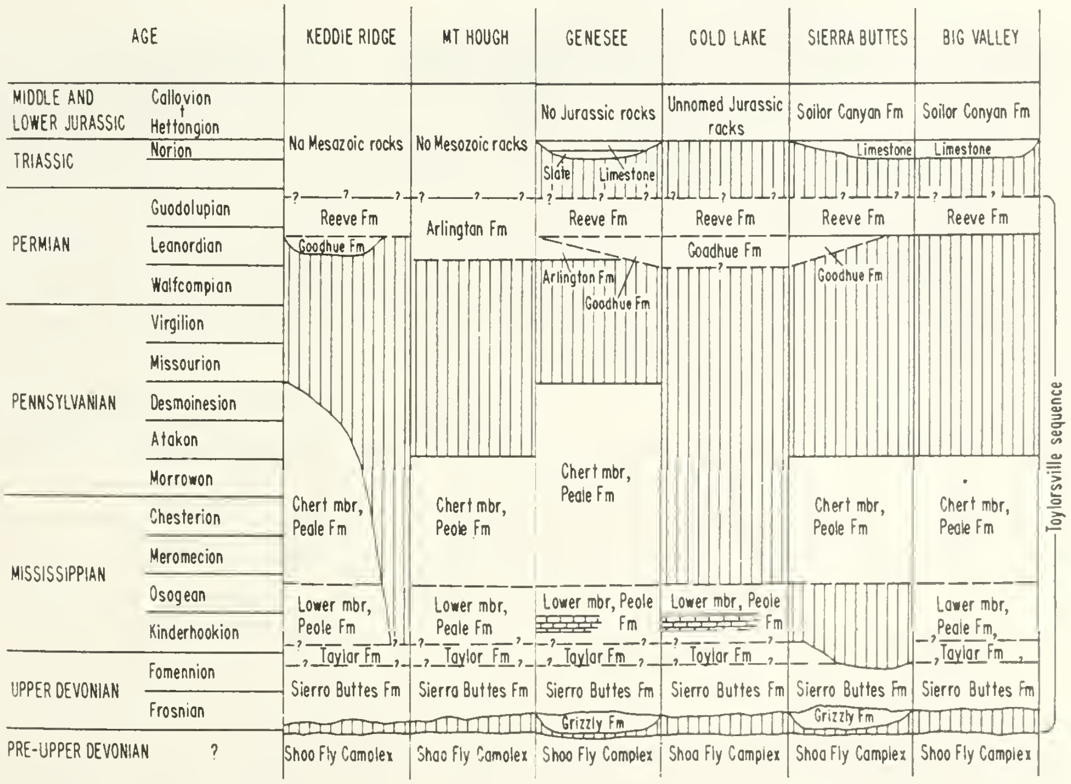

FIGURE 2. Stratigraphic columns in the Eastern Belt, from NW (Keddie Ridge) to SE (Big Valley) along the strike; field trip is in the Gold Lake-Sierra Buttes area (Fig. 28-3 in Harwood, 1988).

America (Silva and others, 1991). Harwood and Murchey (1990) review stratigraphic and tectonic evidence suggesting that the Upper Devonian-Lower Mississippian arc formed along the active North American margin.

Sierra Buttes Formation

R.E. Hanson has written extensively about the Sierra Buttes Fm. (Hanson and Schweickert, 1986; Hanson, 1991). Figure 3 shows the distribution and internal stratigraphy of the Sierra Buttes Fm. for a strike length of about 30 km (Hanson and Schweickert, 1986); the Sierra Buttes Fm. is about 1.75 km thick at the type section in the Sierra Buttes. According to Hanson (1991, p. 807), the Sierra Buttes Fm. "...consists of submarine andesitic to rhyolitic pyroclastic and volcaniclastic deposits penetrated by numerous related hypabyssal intrusions". In the Sierra Buttes Lookout area, "massively bedded lapilli tuffs and tuff-breccias are randomly intercalated with finer grained tuff turbidites, horizontally laminated ash-fall tuffs, and numerous horizons of radiolarian chert", and "penecontemporaneous hypabyssal intrusions range from basaltic andesite to rhyolite in composition..." (Hanson, 1991, p. 807).

Elwell Formation

I studied the problematic Elwell Fm. – established by Durrell and D'Allura (1977) – along strike between Mt. Elwell and Dugan Pond, and found it to be characterized in that 11-km interval by black phosphatic chert interbedded with turbidites and debris-flow deposits rich in silicic detritus, penecontemporaneous andesitic sills and minor peperite, and, locally, andesitic pillow lava (Brooks and others, 1982). South of Dugan Pond, Hanson and Schweickert (1986, p. 993) found that the Elwell Fm. (Member C of their Sierra Buttes Fm.) consists of "...coarse-grained subaqueous volcaniclastic mass-flow deposits interbedded with finer -grained tuffaceous rocks and chert", and that "...pumice is...abundant..." Evidently, a pyroclastic component entered the Elwell Fm. south of Dugan Pond, and Judith Hannah reports that the Elwell Fm. "is almost wholly pyroclastic on Keddie Ridge" to the north (personal communication, 1992). Member C of the Sierra Buttes Fm. is 360 m thick at the type section in the Sierra Buttes (Hanson and Schweickert, 1986).

Taylor Formation

According to Hanson and Schweickert (1986, p. 996), the Taylor Fm. south of Dugan Pond "consists predominantly of fragmental andesitic debris in the form of grossly tabular units of massively bedded, very poorly sorted lapilli tuff and tuff-breccia intercalated with finer-grained andesitic tuffs". North of Dugan Pond, I find that the Taylor Fm. consists of pillow lava of basalt and basaltic andesite intercalated with varied, typically block-rich volcaniclastic rocks, as if a vent were being more closely approached in this direction. Correspondingly, the Taylor Fm., only 200 m thick south of Interstate Highway 80 (Harwood and others, 1991), is 2.3 km thick east of Dugan Pond and about 3.1 km thick north of Gold Lake. The reader will note a difference of opinion regarding the composition of rocks in the Taylor Fm. Although most authors refer to andesite, my chemical analyses indicate that these clinopyroxene- and plagioclase-phyric rocks are basalt and basaltic andesite (17 of 19 analysed samples have SiO2 between 50.5 and 56.2 wt. %).

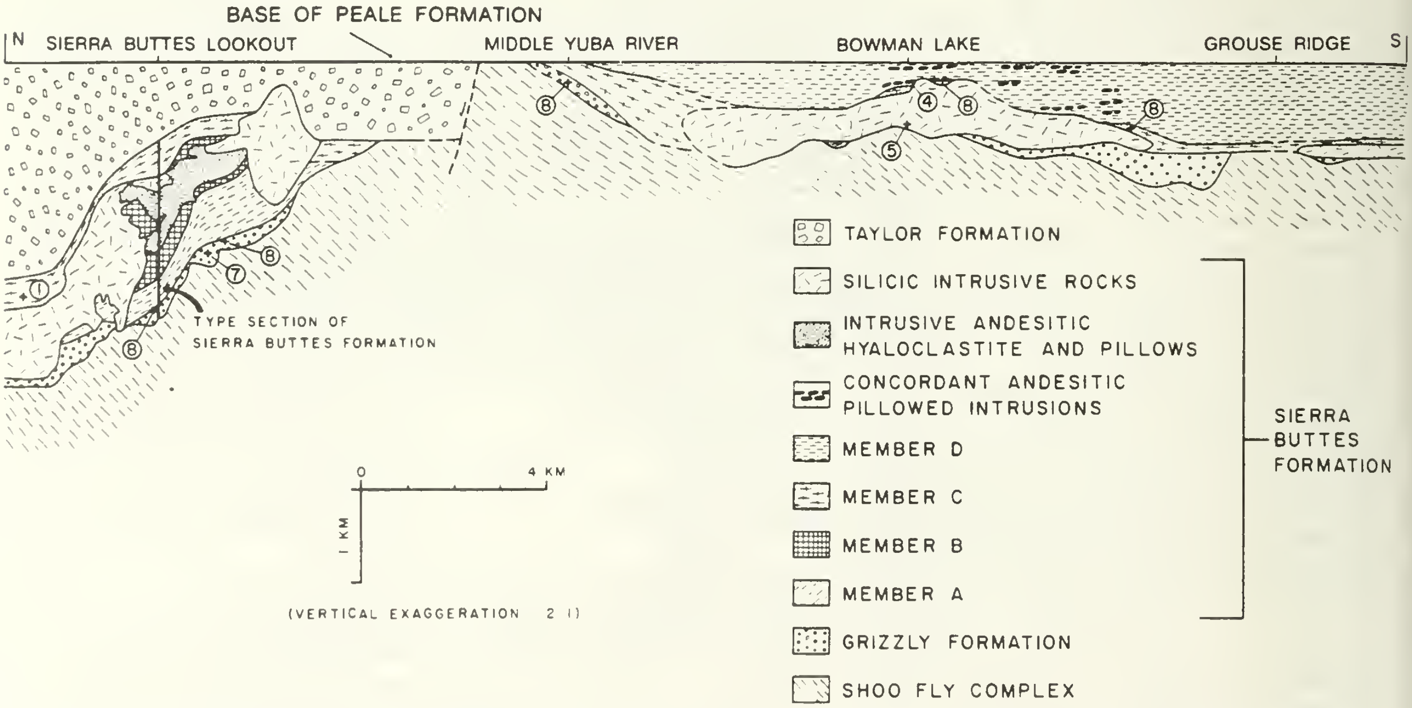

FIGURE 3. Longitudinal section of Grizzly, Sierra Buttes, and Taylor Fms. between Dugan Pond (circled locality 1) and Grouse Ridge; base of chert member of Peale Fm. used as datum (Fig. 2 in Hanson and Schweickert, 1986). In area of Sierra Buttes Lookout, Member C of Sierra Buttes Fm.=Elwell Fm., and, according to Harwood and others (1991), Member D of Sierra Buttes Fm.=Taylor Fm. south of Middle Yuba River.

FIELD TRIP LOG

The balance of this chapter consists of descriptions of 17 field trip stops in the Eastern Belt. Figure 1 shows that the 17 stops are divided among three areas separated by considerable distances. STOP 1 is located beside California Highway 49 just east of Downieville, while STOPS 2-6 and 7-17 are reached from trailheads west of the Gold Lake Road, which connects California Highways 49 and 89 across the crest of the Sierra Nevada. The locations of STOPS 2-6 and 7-17 are indicated on topographic map bases in Figures 4 and 11, respectively. Most field trip stops include detailed petrographic descriptions that are identified by finer typeface.

Directions to STOP 1

Take California Highway 49 north from Nevada City to Downieville. At the T-intersection in the middle of Downieville, turn right (south), following Highway 49 across the Downie River. For several hundred feet, we drive approximately along the fault— the Downieville fault of Edelman and others (1989) — that marks the eastern edge of the Melones fault zone (Fig. 1). STOP 1 is 1.4 miles from the T-intersection in Downieville, along a south-trending stretch of the highway. Limited parking is present on the left side of the highway. Ahead is a blind curve, so LISTEN and WATCH for traffic before crossing the highway and descending the path to the North Yuba River.

STOP 1 (FIGURE 1) - North side of North Yuba River east of Downieville (Downieville 7 1/2 ` quadrangle)

Lang sequence, Shoo Fly Complex

This stop is a good place to view mesoscopic structures in the westernmost, structurally lowest part of the Shoo Fly Complex, the Lang sequence of Harwood (1988). The Lang sequence is the most extensive of the four thrust-bounded units making up the Shoo Fly Complex and the only one that we will look at on this trip ("'Lang-Halsted' unit" in Fig. 1). According to R.A. Schweickert and R.E. Hanson, the Lang sequence consists of "...phyllite and quartzose sandstone with chert and rare marble", in which "...locally preserved sedimentary features and the overall lithic succession suggest the original depositional environment may have been continental rise and/or slope" (Brooks and Schweickert, 1982, p. 2).

The stream-polished outcrops adjoining the North Yuba River reveal tight, approximately similar (Class 2), mesoscopic folds that deform thinly interlayered black pyritic phyllite and gray metachert(?). Some folds are nearly isoclinal, and some have kink-like hinges. The cleavage in the phyllite, which is axial planar to the folds, has the attitude N5°W, 85°E. One can see it refracted across metachert(?) layers in places. Lineation parallel to the fold hinges plunges 65° N5°W. Small folds in the east limb of a relatively large fold exhibit s-asymmetry. According to R.A. Schweickert, "...the lithologic layering is really a structural surface which has formed as a result of transposition of bedding into parallelism with axial surfaces of early isoclines" (Brooks and Schweickert, 1982, p. 1-6). Can you find the early isoclinal fold hinges? Early isoclines would be interpreted as pre-Late Devonian, and the prominent, approximately similar folds as Late Jurassic and related to the Nevadan orogeny.

You may notice the coarsely phyric boulders in flood deposits adjacent to the Shoo Fly outcrops. The plagioclase-phyric boulders were derived from the Reeve Fm. (Permian) far upstream, while the quartz-phyric boulders are from the nearer Bowman Lake batholith (Devonian).

Thin-section petrography

The black phyllite consists almost entirely of quartz, pyrite, and carbonaceous material. Some of the carbonaceous material occupies roundish specks about 0.006 mm in diameter; the rest is present as finer "dust" strung out along the cleavage. Pyrite euhedra occur prominently as "pupils" centered in lenses of granular quartz flattened in the cleavage; pyrite crystals often are tabular parallel to the cleavage.

The gray metachert(?) exhibits several interesting features in thin section. Rhombic single crystals of calcite averaging about 0.3 mm in length form tiny porphyroblasts (revealed on the weathered surfaces by pinhole-size solution pits). Rock cleavage bends around the porphyroblasts, and films of carbonaceous material coat certain parts of the calcite crystal faces. Pyrite euhedra and elliptical bodies of relatively coarsely recrystallized quartz are nearly as large as the calcite porphyroblasts. The elliptical bodies of granoblastic quartz suggest completely recrystallized radiolarians; the quartz occupies polygonal crystals with straight boundaries that frequently intersect to form triple points. The matrix of the metachert(?) is much finer-grained and consists largely of quartz, calcite, carbonaceous material, iron oxide, and aligned flakes of white mica.

A thin section of the kinked hinge of one of the approximately similar folds discloses sub-millimeter-scale lithologic layering and strong axial-plane cleavage; carbonaceous material is both concentrated in some of the thin layers and present as films along the cleavage. The well-developed cleavage is largely attributable to the presence of extremely fine-grained, but voluminous white mica. The elliptical bodies of relatively coarsely recrystallized quartz are very numerous and generally much smaller than those described above (a large one is 0.2 mm long). They are strongly flattened into biconvex lenses that lie in the cleavage, and resemble poorly preserved radiolarians in cleaved carbonaceous chert in the Devonian Elwell Fm. (Brooks and others, 1982). The protolith probably was radiolarian "siliceous argillite".

Directions to STOPS 2-6

Continue eastward on California Highway 49 to Sierra City. About 5 miles beyond Sierra City, the Gold Lake Road joins Highway 49 at the way station of Bassetts. Turn left (north) on the Gold Lake Road and drive 1.3 miles to its junction with the Sardine Lake-Packer Lake Road.

Turn left (west) on the Sardine Lake-Packer Lake Road, go 0.3 mile, and turn right on the Packer Lake Road. Drive 2.4 miles and park at the Packsaddle Campground on your left. The Deer Lake trailhead is 200' to the northeast, back down the Packer Lake Road. We will hike for about 25 minutes (a bit over a mile) northwestward along the Deer Lake Trail to STOP 2, in "Prehnite Valley" about 450' above the trailhead.

Initially, the trail is on ground moraine associated with the latest glacial advance in this region, termed "later post-Sangamon" by Mathieson (1981). The conspicuous quartz-phyric boulders of dacite were excavated from the Sierra Buttes Fm. not far southwest of us by the "Packer Lake Canyon Glacier" (Mathieson, 1981). Beyond the second stream crossing, the trail climbs in a single switchback to the crest of the northern lateral moraine associated with this later post-Sangamon glacial advance.

STOPS 2-6 are linked by a counterclockwise circuit about midway between Deer and Packer Lakes, in the Gold Lake 7 1/2' quadrangle (Fig. 4). STOPS 2 and 6 are in the Sierra Buttes Fm., STOPS 3-5 in the Elwell Fm. (Fig. 4).

Almost every sample you pick up this afternoon will have prehnite, pumpellyite, or both prehnite and pumpellyite in it; some will contain prehnite + actinolite. PLEASE COLLECT SAMPLES FROM THE ABUNDANT TALUS, NOT FROM THE OUTCROPS.

STOP 2 (FIGURES 1 and 4) - View stop, with orientation to the stratigraphy

The Sierra Buttes south-southeast of us (Fig. 5) were mapped by R.E. Hanson, but their name was given to the Sierra Buttes Fm. much earlier by V.E. McMath (1966). According to Hanson (1991), the high peaks consist mostly of andesitic and silicic hypabyssal intrusions and hydroclastic breccias formed during emplacement of magma into wet sediments beneath the sea floor. The Taylor Fm. underlies the small peak S30°E of us; the tree line approximately marks its contact with the underlying Elwell Fm. (Fig. 5).

We are standing on a heavily iron oxide-stained lapilli tuff called the "cannonball tuff" because of its spheroidal weathering. This bright red, exceptionally pyritic unit extends N40°W to the hill on the skyline south of Deer Lake (Fig. 4). It is rich in microvesicular pumice and is thought to be a subaqueous pyroclastic-flow deposit, like the Tamarack tuff occurring beneath it to the southwest. To the west-southwest, joint-controlled surfaces inclined toward us approximately parallel rare bedding in the Tamarack tuff (Legler and others, 1991). (All beds in this area dip and face easterly.) The upper contact of the Tamarack tuff is near the west edge of the silted pond below us, and its lower contact mostly runs just behind the high ridge forming the western skyline. The Tamarack tuff rests depositionally upon dacite (an unroofed hypabyssal intrusion ?) like that seen as boulders in the later post-Sangamon ground moraine.

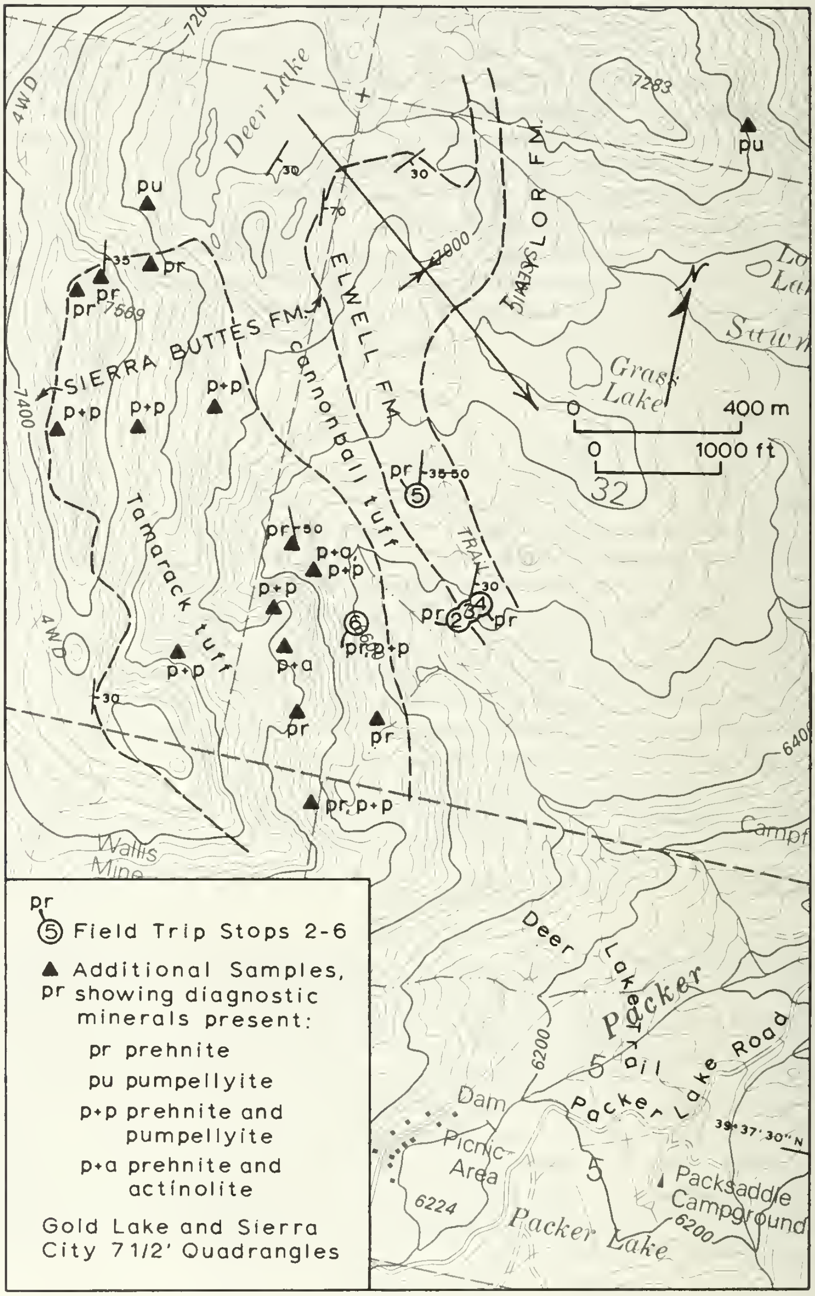

FIGURE 4. Field trip stops 2-6 in "Prehnite Valley" north of Packer Lake. Prehnite-pumpellyite and prehnite-actinolite assemblages in the Elwell and Sierra Buttes Fms.

The ridge just northeast of us is held up by a relatively thick, coarse-grained sill of tholeiitic andesite (Brooks and others, 1982). Note the rough columnar jointing, better seen to the north-northwest. The top of the next lower sill is in contact with black phosphatic chert just across the old trail from us, at STOP 3. The andesitic sills and black phosphatic chert belong to the Elwell Fm. The contact between Elwell and Sierra Buttes Fms. is placed in the valley along the old trail, the subaqueous pyroclastic-flow deposits being assigned to the Sierra Buttes Fm.

STOP 3 (FIGURE 4) - Chert and andesite in the Elwell Fm.

Here is a knife-sharp, largely concordant contact between black phosphatic chert and the top of one of the numerous andesitic sills that cut the Elwell Fm. Some sills encountered still-

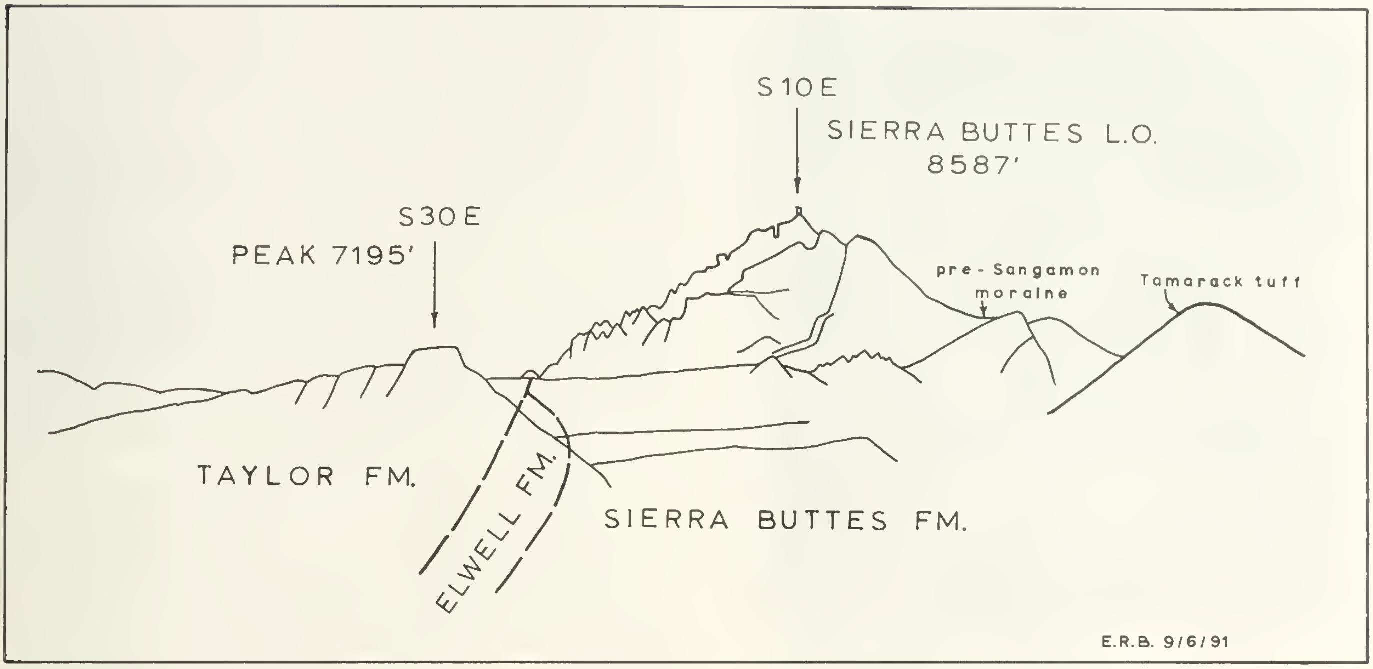

FIGURE 5. View to the SSE from stop 2, showing the Sierra Buttes, Elwell, and Taylor Fms. in the Sierra Buttes Lookout area.

moist, incompletely lithified chert during emplacement, resulting in generation of peperite (Brooks and others, 1982), but this undisrupted contact is the kind most frequently found. Distinctive, closely spaced (here 1-2 cm) sheets of tiny vesicles adjoin both margins of the sills; the vesicles probably formed along slip planes separating rapidly congealing andesite laminae. Note that the contact, the vesicle sheets, and white to gray phosphatic lenses and laminae, which mark bedding in the chert, are all parallel.

Examine the loose blocks of black phosphatic chert to discover the curious primary geometry of the phosphatic masses, thought to be the result of direct inorganic precipitation of fluorapatite from pore water (Brooks and others, 1982). The white-weathering phosphatic nodules, lenses, and laminae consist largely of quartz and collophane, the black chert largely of quartz and carbonaceous material, probably graphite (Brooks and others, 1982). The chert is rich in radiolarians, and such black phosphatic radiolarian cherts, widespread in Paleozoic rocks of the western U.S., are thought to have accumulated in a few thousand meters, or less, of water, adjacent to the North American continent (Coles and Varga, 1988).

Thin-section petrography

The undeformed, relatively weakly recrystallized samples of black phosphatic chert available at this locality exhibit poorly- to reasonably well-preserved radiolarians belonging to the family Entactiniidae, Paleozoic spumellarians with single or multiple, spherical or ellipsoidal lattice shells (Brooks and others, 1982). Poorly preserved radiolaria are represented simply by granoblastic aggregates of quartz free of the carbonaceous material that encloses and draws attention to them; these are commonly circular or elliptical and a little over 0.1 mm long. Even more-poorly preserved radiolaria appear as ill-defined, lens-shaped quartz aggregates lying in the bedding. Lenticular masses of carbonaceous material also parallel the bedding, but most of the voluminous carbonaceous material occurs as finely divided "dust". Not all of the carbonaceous material was expunged from radiolarians in other samples, and lattice shells (Fig. 6) and spines, occasionally still attached to shells, are preserved.

In the phosphatic lenses and laminae, microgranular quartz is charged with tiny formless masses of brown isotropic collophane; in places, collophane occupies 0.02-mm spherules with uncertain internal structure. (The most-recrystallized chert elsewhere contains colloform fluorapatite masses whose edges bristle with stout prisms 0.005 to 0.015 mm long.)

A sample of aphanitic andesite collected 10 cm from the contact with black phosphatic chert shows that the vesicle sheets are only one vesicle thick, and that the vesicles, widely spaced and still largely open, are flattened in the plane of the vesicle sheets. The original andesite was charged with tiny prismatic plagioclase microlites; quenched hopper microlites appear near the vesicle sheets. The microlites now consist of simply twinned albite. Small (e.g., 0.35-mm), irregularly shaped quartz poikiloblasts have replaced much of the original, presumably glassy matrix between the plagioclase microlites and thereby incorporated them. Quartz poikiloblasts occupy most of the rock along the vesicle sheets, and some individual poikiloblasts grew into the vesicles, where they formed euhedral, inclusion-free crystals. Abundant chlorite also replaced original glassy matrix. The andesite also is rich in finely granular sphene, and apatite needles may be found in the quartz poikiloblasts.

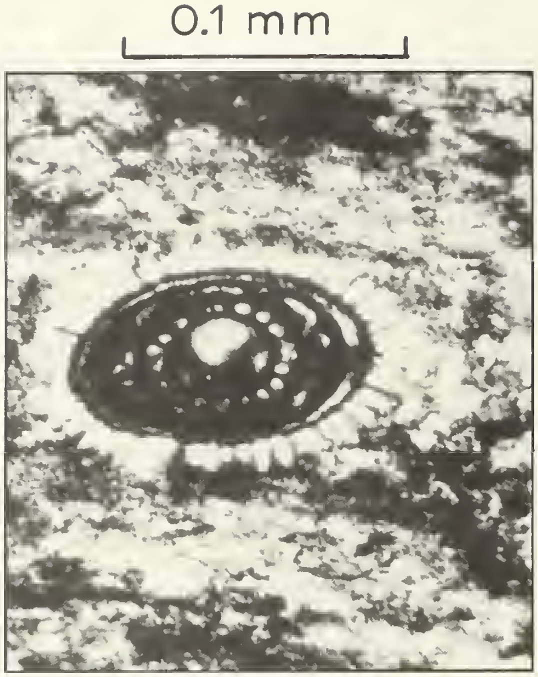

FIGURE 6. Radiolarian in black chert, the lattice shell preserved by carbonaceous material. Collected at stop 3 in the Elwell Fm.

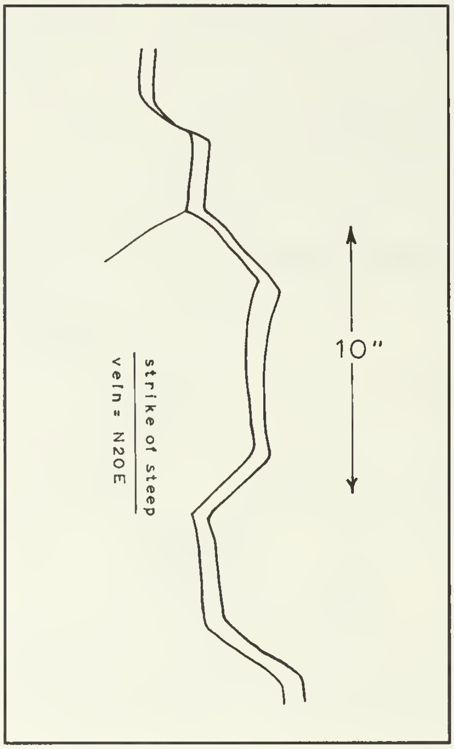

FIGURE 7. Black chert vein occupying columnar joints in andesite sill; direction of view approximately normal to plane of sill. Stop 4 in the Elwell Fm.

STOP 4 (FIGURE 4) - Chert veins in andesite sill in the Elwell Fm.

We are standing on the uppermost exposed part of the next higher, relatively thick andesite sill (about 12 m are exposed). Crude columnar jointing is apparent near the base of the sill. The andesite here is finely granular because it is more coarsely recrystallized than that at STOP 3; the larger, 0.5-mm grains prove to be quartz poikiloblasts. If you look closely, you will find scattered, gray, bipyramidal quartz megacrysts in the andesite. These are quite large— up to nearly 1 cm across —and though often embayed, straight sides are common.

The sill is traversed by persistent, long (a few meters), roughly planar veins of black chert. These dip steeply and strike N20°E, and are up to 4 cm thick and widely spaced (up to about 2 m). One of them clearly follows columnar joints in the andesite (Fig. 7), and others abruptly branch and pass into small patches of peperite. Evidently, fluid chert injected these shrinkage joints as they opened.

The average major-element oxide analysis of five samples of andesite collected from sills between this locality and Mt. Elwell appears in Table 1 below (Brooks and others, 1982, Table 1; H_2O, P_2O_5, and CO_2 were not determined).

Except for substantially higher FeO* and lower CaO, the average analysis is similar to that of classical Fijian tholeiitic andesites. More convincing evidence of the tectonic setting of volcanism are the rare-earth abundance patterns of the five sills (samples 5, 15, 20, 35, and 43A in Fig. 8; Brooks and others, 1982, Fig. 13). Except for relative enrichment of LREE in sample 15, the samples possess parallel, nearly flat patterns with slight relative depletion of LREE. Such patterns characterize the tholeiitic rock association in island arcs.

Thin-section petrography

Again, the original andesite contained abundant unoriented, prismatic plagioclase microlites, averaging perhaps 0.1 mm long, which now consist of simply or polysynthetically twinned albite. These are poikiloblastically enclosed in large (e.g., 0.55 mm) quartz porphyroblasts that tend to be idioblastic. The central parts of the porphyroblasts contain delicate radial sprays of albite fibers, perhaps originating by devitrification of glass during

TABLE 1. Composition of andesite sills in Elwell Fm.

		recalculated to 100 wt. %
SiO_2	56.80	60.40
TiO_2	0.99	1.05
Al_2O_3	13.81	14.67
FeO*	10.97	11.65
MgO	3.34	3.55
CaO	4.54	4.82
Na_2O	3.37	3.58
K_2O	0.11	0.12
MnO	0.17	0.18
Sum	94.14	100.00

*all Fe calculated as FeO

sea-floor alteration. Inclusion-free edges of the quartz porphyroblasts are in contact either with large interstitial patches of chlorite that also enclose relict plagioclase microlites or with spherulite-like, radiating clusters of prehnite fibers. Rhombic to square sphene grains replace relict euhedral magnetite microlites. Epidote is intergrown with the prehnite, and acicular apatite again appears in the quartz.

STOP 5 (FIGURE 4) - Peperite in the Elwell Fm.

A relatively well-exposed section about 17 m thick discloses at least four andesite sills intercalated with black phosphatic chert and peperite. A sill about 0.3 m thick was almost completely transformed to peperite in situ ; vesicle sheets at its base remain undisturbed in places. Closely spaced (2-5 mm) vesicle sheets occur prominently at the top or bottom of each of the sills.

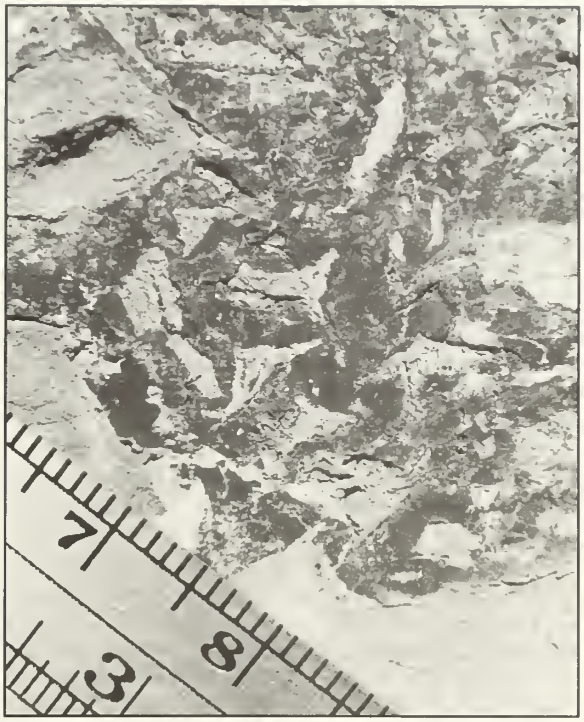

FIGURE 9. Poorly sorted "non-dispersed" peperite in the Elwell Fm. at stop 5. Note sharply pointed corners and simple shapes of the fine lapilli-size andesite fragments, each bounded by just 3 or 4 conchoidal fractures. Distance between numbers 7 and 8 on the scale is 1 cm.

The most dramatic examples of peperite are found at the base of the uppermost, thick sill (about 9 m are exposed), at the southeast end of the outcrop near the double pine tree. Here, the vertical outcrop surfaces, and blocks in the talus littering the slope below, exhibit hairline, black chert-filled, relict shrinkage fractures, some of which narrow upward, away from the bottom of the sill. Andesite fragments are bounded by straight to sharply curved shrinkage fractures whose intersection frequently resulted in sharply pointed, fragile corners (Fig. 9). Curved bounding fractures are both convex- and concave-outward, and, indeed, individual fractures may change rapidly from one configuration to the other when traced laterally. Three- or four-cornered, equant to platy fragments are common (Fig. 9). The base of the thick sill, here fragmented and converted to peperite, is intact to the northwest, where it exhibits vesicle sheets parallel to a knife-sharp, concordant contact with underlying black phosphatic chert: peperite occurs only sparingly along the edges of the sills, evidently only where the chert was sufficiently fluid to inject shrinkage fractures opening in the freezing sill margins. The peperite at this locality is "poorly sorted" (ash- to coarse block-size andesite fragments), and many fragments ("puzzle fragments") can be imagined easily fitted back together by removing the thin films of chert separating them; this sort of peperite, reflecting non-explosive, cooling-contraction granulation of quenched glassy lava, may be referred to as "non-dispersed".

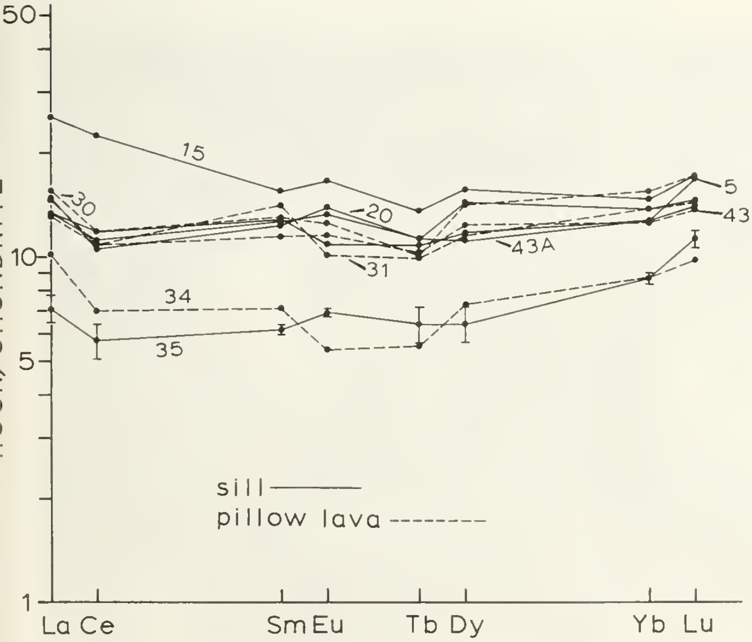

FIGURE 8. Chondrite-normalized rare-earth abundance patterns for 9 samples collected from andesitic sills and pillow lavas in the Elwell Fm. (Fig. 13 in Brooks and others, 1982).

Thin-section petrography

Black phosphatic chert at this locality contains relatively coarse (e.g., 0.4 mm long) prehnite. Crystals are tabular parallel to {001}, display distinct {001} cleavage, and have a large 2VZ (r>v, weak); birefringence is about 0.027. Also, relatively large, highly irregular prehnite grains occur in the black chert matrix of some peperite samples. Harper (1991) reports prehnite in chert in the Josephine ophiolite where the chert adjoins broken pillows;

formation of this prehnite is attributed to hot-spring activity at a spreading center.

Narrow (e.g., 0.03 and 0.5 mm) black chert veins variously terminate abruptly, gradually pinch out, contain ash-size andesite fragments, and have carbonaceous material variably concentrated in strips parallel to vein walls, doubtless the result of laminar flow of chert injecting shrinkage fractures.

Originally glassy andesite fragments in the peperite contained numerous plagioclase microlites, but no vesicles. Glass in the interior of one fragment having a high proportion of glass to microlites (hyalopilitic texture) was completely replaced by chlorite. The relict plagioclase microlites have prominent brown jackets of extremely fine-grained sphene; most microlites are lath-shaped, averaging perhaps 0.09 mm in length. Tiny square sections of microlites indicate that many were square prisms, but occasional large rhombic sections show that some were rhombic tablets. Microlites were replaced by twinned albite, the composition plane(s) of which parallel their long axes. Calcite joins chlorite in the edge of this andesite fragment, where it replaced both glass and plagioclase microlites, and the sphene here occupies 0.01-mm spherules that nucleated both on plagioclase microlites and within glass. Other, more richly microlitic andesite fragments in the same sample are replaced by finely granular mixtures of chlorite, calcite, sphene, quartz, etc. In another sample, glass in the edge of a fragment was replaced by chlorite whereas that in the central part of the fragment now is represented almost entirely by calcite. In general, the nature of glass replacement is complex. Sphene may be concentrated in bands just inside and parallel to fragment boundaries, perhaps another relic of sea-floor alteration.

The smallest andesite fragments (ash- and fine lapilli-size) tend to be bounded by two long fractures, resulting in sharply pointed slivers; fragments as small as 0.075 mm long are recognizable. Relict plagioclase microlites may project beyond fractured fragment margins into adjacent chert, and microlites freed from broken fragments are enclosed in chert.

STOP 6 (FIGURE 4) - Tamarack tuff in the Sierra Buttes Fm.

The Tamarack tuff (Brooks and Legler, 1989; Legler and others, 1991) crops out discontinuously for at least 11 km along strike; a conservative estimate of the preserved thickness in the Packer Lake-Deer Lake area is 145 m. It consists almost entirely of juvenile tephra (about 1/6 pumice blocks and coarse lapilli, about 5/6 generally less richly vesicular, fine lapilli and ash); lithic clasts of quartz-phyric dacite and, rarely, trondhjemite and black phosphatic chert constitute but a tiny fraction of the Tamarack tuff. The Tamarack tuff was emplaced subaqueously by a mass flow that locally underwent laminar flow, as indicated by dimensional preferred orientation of spindle-shaped blocks, and by alternately block-free and block-rich layers (this locality). Pumice blocks are large, the very largest exceeding 2 m in length. The average maximum dimension of the five largest blocks at 20 survey stations varied from 15 to 49.5 cm. The coarsest blocks (>30 cm) were found among the southernmost outcrops, near Young America and Tamarack Lakes, which are thought to be most proximal by June Legler (Legler and others, 1991). Though many pumice blocks are equant (this locality), many others were drawn out into distinctive spindles lineated parallel to their long axis (Fig. 10; aspect ratio ranges up to 16:1). Spindles were broken off at either end, and ends often are rounded, presumably by abrasion during transport in the mass flow (Fig. 10). Spindles commonly are distorted, even isoclinally folded; such ductile behavior most likely occurred during toothpaste-like extrusion of viscous pumice blocks (Fig. 10). Hanson (1991) thinks that the pumice blocks are pillows in isolated-pillow breccia.

Pumice blocks have been selectively silicified and phosphatized. Vesicles largely are filled with quartz and blocks weather white. Twelve of 27 pumice blocks analysed contain over 1 wt. % P2O5 (1.18-5.17); (PO4)-rich sea water evidently entered vesicles at the time of deposition of the mass flow. Assuming constant Al, the average pumice block (N=27) gained P, Si, Na, and Ca, and lost K, Ti, Fe, Mn, and Mg, with respect to the average matrix sample (N=19). The composition of the average matrix sample, recorded in Table 2 below, is thought to approximate, except for high FeO* and low CaO, that of the low-K, high-SiO2 andesite erupted originally. The composition of the average matrix sample— recalculated to 100 wt. %, volatile- and P2O5-free —is compared in Table 2 to the average composition of nine samples of andesitic sills and pillow lavas in the Elwell Fm. (Brooks and others, 1982, Table 1). I believe that

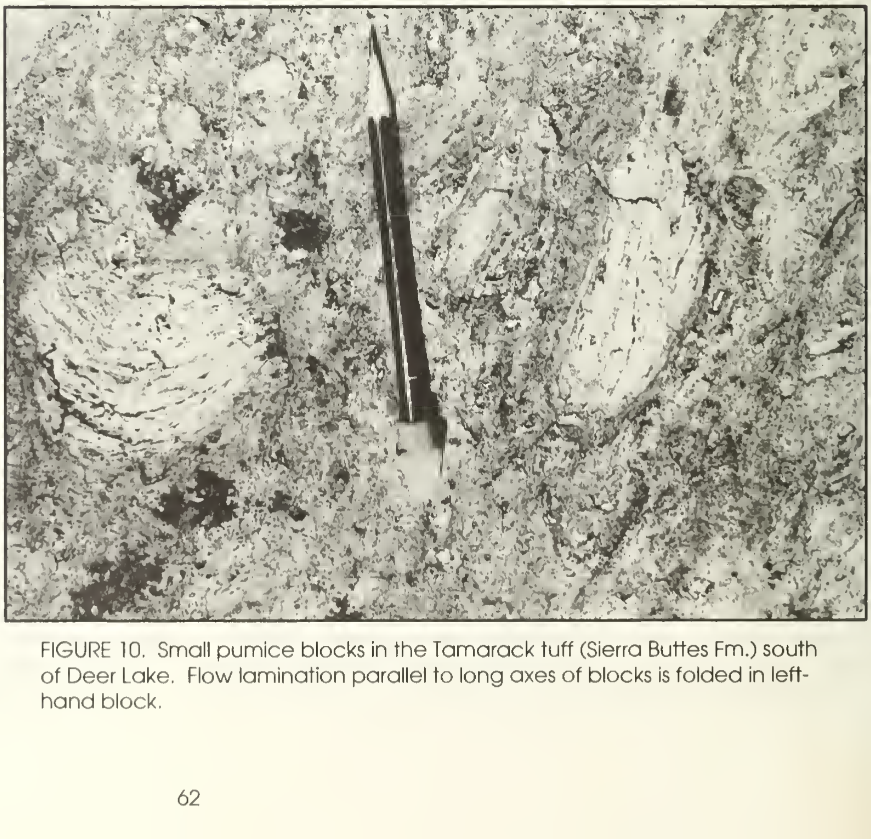

FIGURE 10. Small pumice blocks in the Tamarack tuff (Sierra Buttes Fm.) south of Deer Lake. Flow lamination parallel to long axes of blocks is folded in left-hand block.

the Tamarack tuff represents the explosively erupted, volatile-rich upper portion of an andesitic magma body that somewhat later was the source of the Elwell sills and lava flows.

TABLE 2. Composition of andesitic matrix of Tamarack tuff (Sierra Buttes Fm.) compared to that of andesitic sills and pillow lavas in the Elwell Fm.

	average of 19 Tamarack tuff matrix samples	average of 9 Elwell Fm samples
SiO_2	60.5	61.2
TiO_2	0.72	1.06
Al_2O_3	16.59	14.43
FeO^*	9.88	11.54
MgO	4.54	3.19
CaO	4.51	4.26
Na_2O	2.48	3.60
K_2O	0.62	0.62
MnO	0.17	0.15

The obviously out-of-place block that constitutes STOP 6 is quite unrepresentative of the Tamarack tuff, in that it exhibits size sorting of tephra into several distinct beds. Most Tamarack tuff is structureless and poorly sorted, presumably the result of deposition by a turbulent mass flow. The white-weathering, originally pumiceous blocks and lapilli are supported by a darker, chloritic matrix of originally microvesicular ash and fine lapilli. Pumice blocks and lapilli, the largest of which are 35-45 cm long, are square or rectangular to rounded, and usually equant. They seldom are deformed at this locality, and lineated spindles also are rare. Your hand lens will reveal tiny round quartz amygdules in both pumice blocks and matrix, and both also contain sparse small quartz phenocrysts, some euhedral.

Thin-section petrography

A block has finely granular epidote concentrated in patches and streaks that parallel original flow lamination, the latter marked by aligned, tiny , relict plagioclase microlites and relatively large (e.g., 2-mm long), elongated amygdules. Most pumice blocks in the Tamarack tuff exhibit close-packed, spheroidal, relict microvesicles averaging about 0.07 mm across (51-68% vesicles in eight point-counted blocks), and this block has abundant, round to elliptical microamygdules averaging about 0.05 mm long. All amygdules in this block consist of relatively coarsely granular quartz, sometimes accompanied by prehnite, sometimes by pumpellyite (pleochroic, pale yellow-brown to bright green (=Y); anomalous blue and red-brown interference colors). Rare plagioclase microphenocrysts were replaced by mixtures of albite and highly irregular quartz. A solitary plagioclase phenocryst 1.5 mm long now consists mostly of quartz and prehnite. Two relict quartz phenocrysts are present, the larger one 1.85 mm across. Tiny pyrite euhedra, some replaced by iron oxide, pervade the sample, and sphene occupies crude spherules only about 0.008 mm in diameter.

Lapilli-size, originally microvesicular and microlitic fragments are easily recognized in the Tamarack tuff matrix at STOP 6, but recrystallization has obliterated details of ash-size fragments. The vesicles, now occupied and overgrown by chlorite, quartz, prehnite, and epidote, typically are elongated in a direction parallel to aligned relict plagioclase microlites, tiny fibers averaging 0.035 mm long. Lapilli also contain scattered relict quartz and plagioclase phenocrysts 0.3 to 1.75 mm in maximum dimension. The larger of the embayed quartz phenocrysts have been shattered in situ into many fragments. The matrix sample is rich both in prehnite and epidote, both of which may be idioblastic. Prehnite (2VZ large, r>v weak; distinct {001} cleavage; tabular parallel to {001}) occupies grains as large as 0.55 mm, and often comprises aggregates with epidote. Finely granular sphene also is abundant. Small unoriented prehnite tablets occur with quartz in veins. Elsewhere, matrix samples are seen to consist of well-sorted coarse ash and fine lapilli that are equant or elongated and often blocky or three-cornered; subaqueous eruption of tephra is indicated.

Directions to STOPS 7-17

Drive southeastward on California Highway 70 to its junction with California Highway 89. Turn right (south) on Highway 89 and drive 2.7 miles through Graeagle to the intersection with the Gold Lake Highway (U.S.F.S. Highway 24). Turn right (west) on the Gold Lake Highway and drive 11.6 miles to the junction with the Salmon Lake Road. Turn right (west) on the Salmon Lake Road and go 1 mile to its end at Upper Salmon Lake, crossing several recessional moraines associated with the later post-Sangamon advance of the "Salmon Creek Canyon Glacier" (Mathieson, 1981). Park at Upper Salmon Lake. There will be a 15-minute hike to STOP 7.

STOPS 7-17 are linked by a clockwise circuit south, southwest, and west of Upper Salmon Lake, in the Gold Lake 7 1/2' quadrangle (Fig. 11). STOPS 7-10 and 14 are in the Taylor Fm., STOPS 11, 13, 15, and 17 in the Elwell Fm., and STOPS 12 and 16 along the contact between the two formations (Fig. 11). We will be mostly in lower-greenschist rocks in this area, though some rocks containing prehnite + actinolite also occur.

Scramble south on a narrow, rough fisherman's path along the east side of Upper Salmon Lake. Note the glacial striae trending S50°E at the lake outlet at the dam. The striae are developed on plagioclase-phyric, pumice-rich lapilli tuff in the Taylor Fm. Continue southwestward around the south end of Upper Salmon Lake. Where the path becomes tangent to the overhead power line, note that the Taylor lapilli tuff underfoot contains widely scattered blocks, some amygdaloidal (quartz and chlorite amygdules). Similar lapilli tuff and tuff-breccia underlie the knob you have just passed on your left (to the south). At least 95 m of such rocks are exposed there, without obvious depositional break. How did these materials originate, and how did they accumulate in such great thicknesses?

STOP 7 (FIGURES 1 and 11) - Debris-flow deposit and ash turbidites in the Taylor Fm.

The origin of some of the coarser debris in these thick-bedded volcaniclastic rocks is obvious here: broken pillows (Fig. 12).

This nice broken-pillow breccia (Brooks and Garbutt, 1972) is interpreted as the basal part of a normally graded debris-flow deposit produced by slumping of the oversteepened flank of a pile of pillows onto contemporaneously erupted tephra (represented by the lapilli tuff supporting the pillow fragments). We are standing on a bedding surface. The pillow fragments are distinctively plagioclase-glomerophyric and also exhibit sparse, small clinopyroxene phenocrysts and quartz amygdules, some elongated perpendicular to pillow margins. They have prominent, pale (epidote-rich) outermost rims followed abruptly inward by dark brick-red (actinolite-rich) selvages which grade into the pillow interior (Fig. 12). The pale outermost rim represents part of the original glassy pillow rind. Note that the broken edges of pillows are irregular; these pillows were not prismatically jointed (Fig. 12). The derivation of the large, rimless, clinopyroxene- and plagioclase-phyric blocks containing abundant, large quartz amygdules is unknown, but they might be disrupted sills. The broken-pillow breccia displays normal grading of blocks and lapilli, and comprises the lowest exposed 1.2 m of the debris-flow deposit (the bottom of the deposit was cut away by the prominently layered sill). The overlying 1.2 m consist of structureless lapilli tuff just like that forming the matrix of the broken-pillow breccia, and this passes upward into the final 0.6 m of vaguely stratified tuff and lapilli tuff.

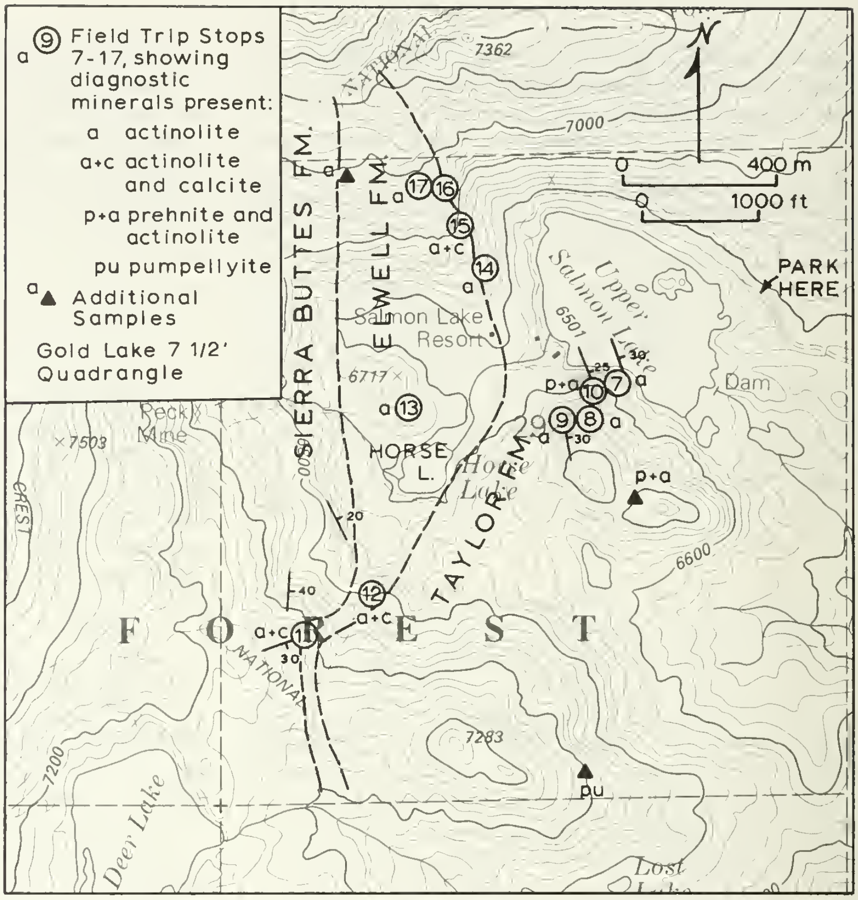

FIGURE 11. Field trip stops 7-17 in the Upper Salmon Lake area. Greenschist and prehnite-actinolite assemblages in the Taylor and Elwell Fms.

The strikingly bedded rocks which overlie the debris-flow deposit are upward-fining ash turbidites. The finest ash always weathers white. Evidence of scour (and resulting cross-stratification) is present, and possible Tabc Bouma sequences can be found (Ta(=S3)=basal, massive lapilli tuff or coarse tuff; Tb=finer, plane-parallel-laminated tuff; Tc=uppermost, fine, rippled tuff). Most interesting is the curious bedding feature I call "sled structure", which here involves lots of indistinctly stratified, coarse and fine tuff, and occurs in groups at the same horizon (representing the edge of a laterally migrating channel ?). I have seen similar features in turbidites in the Ordovician Bedded Pyroclastic Fm. on Snowdon, Wales, where they are termed "birds-foot laminae" by Peter Kokelaar, and occur in catastrophic incursions of volcanogenic sediment; deposition was from high-density turbidity currents, and S2/S3 and Tb divisions are characteristic (Orton and others, 1990). Figure 13 is a sled structure photographed some distance south of us; since the incorporated pillow fragment is standing on end, deposition from a high-density turbidity current, or even more-cohesive flow, is indicated.

Thin-section petrography

The interior of a pillow fragment, just within the 1-cm thick epidote-rich rim, exhibits prominent, sharply euhedral, relict phenocrysts and glomerocrysts of plagioclase and clinopyroxene. Individual crystals of plagioclase reached 1.65 mm in maximum dimension, those of clinopyroxene 1.15 mm. Plagioclase also formed euhedral microphenocrysts and sparse, unoriented microlites, and relict clinopyroxene microlites can be found as well. Plagioclase now consists mostly of albite (An0-10, chessboard structure) flecked by white mica and epidote, clinopyroxene of various mixtures of relatively coarse quartz and epidote, and extremely fine-grained chlorite and actinolite. Not much can be told about the original pillow-interior matrix, which now consists of albite with undulatory extinction, variously oriented sheaves of parallel to radiating actinolite fibers, sphene granules, and some epidote and chlorite. As the epidote-rich rim is approached closely, sinuous films of hematite appear and the abundant actinolite coarsens to bundles of parallel, more-birefringent fibers, and individual prisms as long as 0.1 mm that are sometimes simply twinned. This coarsening is accompanied by loss of dark "dust" and sphene granules.

The matrix in the epidote-rich rim certainly consisted originally of glass, for curved, relict perlitic and/or thermal-contraction cracks are apparent where highlighted by hematite. Relict plagioclase microphenocrysts and microlites are jacketed by gray "dust" present in the original glass, as are occasional small (e.g., 0.4 mm), round to elliptical amygdules occupied largely by radiating sprays of actinolite bristling from the original vesicle walls. The glassy matrix was largely replaced by xenoblastic to idioblastic epidote of widely variable grain size; some chlorite, at least, also is present.

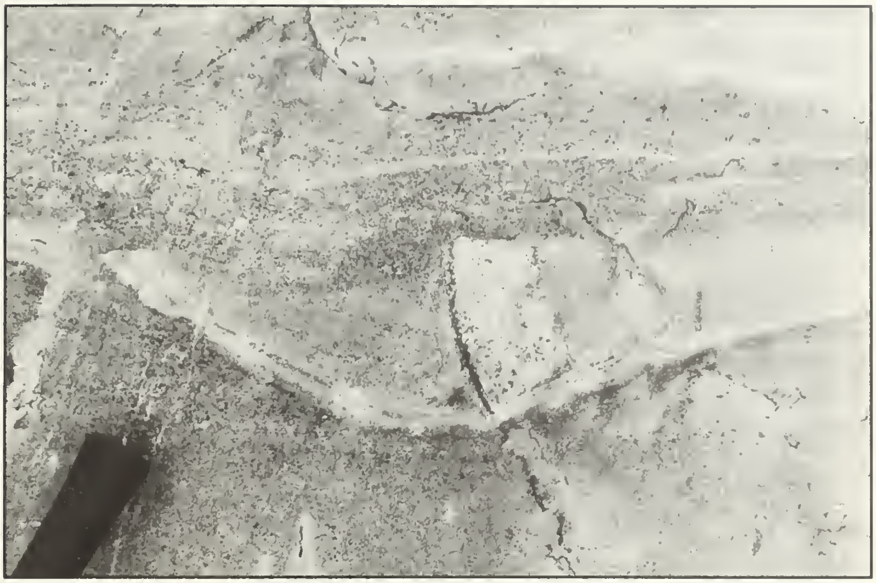

FIGURE 13. "Sled structure" in high-density turbidites in the Taylor Fm. Note the pillow fragment standing on end.

The pillow fragments are supported by massive lithic-crystal lapilli tuff of similar composition (basalt to basaltic andesite). Lapilli tuff adjoining the epidote-rich, originally glassy pillow rims contains no obvious pillow-rim spall; instead, the richly phyric (but not prominently glomerophyric) ash and lapilli generally were more vesicular than the pillow rims (amygdules consist mostly of chlorite and actinolite). Plagioclase phenocrysts again were replaced by albite riddled by white-mica inclusions, clinopyroxene mostly by coarse actinolite (minor chlorite, epidote, and quartz); a little clinopyroxene, rimmed by actinolite, survived. The matrix of ash and lapilli now consists of actinolite (variably oriented needles and bundles of parallel needles or fibers) and very dark, "cloudy" sphene, and lacks the albite with undulatory extinction present in pillow fragments (calcite-rich samples appear to lack the actinolite, as well). Some lapilli are so charged with amygdules as to have been scoriaceous. Round to elliptical vesicles at least as small as 0.05 mm were filled with chlorite (the smallest ones) or with chlorite, calcite, epidote, and quartz in various proportions (the larger ones, which average perhaps 0.3 mm in diameter). The largest amygdules (e.g., 2.75 mm long) are quite irregularly shaped. Many ash-size fragments consist simply of broken plagioclase phenocrysts.

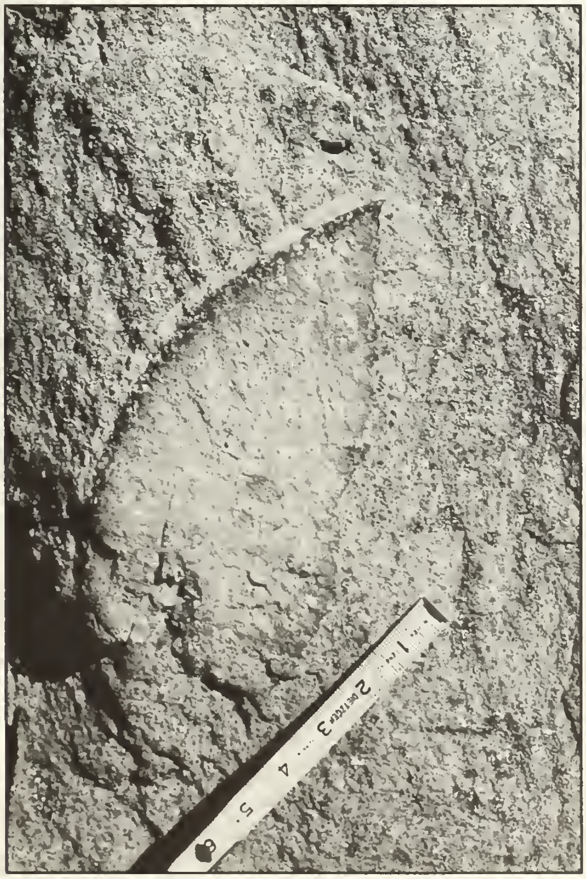

FIGURE 12. Broken pillow in Taylor Fm. debris-flow deposit at stop 7. The pale outermost rim represents part of the original glassy rind of the pillow. Scale is in inches.

STOP 8 (FIGURE 11) - Pillow lava in the Taylor Fm.

Walk southwestward uphill from STOP 7 to a plagioclase- and clinopyroxene-phyric, basaltic dike that trends N80°W. Walk westward along the dike until it intersects pillow lava present near the base of the Taylor Fm.

These discrete, unconnected, ellipsoidal pillows are embedded in a relatively voluminous, locally subtly stratified, tuffaceous matrix; this is as close-packed as they get (Fig. 14). The pillows reach approximately 3 m in maximum dimension. A few are broken. The small plagioclase glomerocrysts are characteristic of Taylor pillow lavas; small clinopyroxene phenocrysts are rare. When present, large (to nearly 4 cm) quartz amygdules usually occur near pillow margins and may be elongated perpendicular thereto (Fig. 14). The complex mineralogic zoning of pillow margins is interesting. The gradual reddening toward a pillow margin is due in part to outward increase in the amount of metamorphic actinolite (or actinolite and chlorite), and the pale outer rim is epidote-rich, as already mentioned. In places, an outermost, brick-red, chlorite-rich rim is preserved; together with the epidote-rich rim, it represents the original glassy pillow rind (Fig. 14). It often was granulated by thermal contraction, the fragmented glass preserved in situ or partially or wholly stripped away.

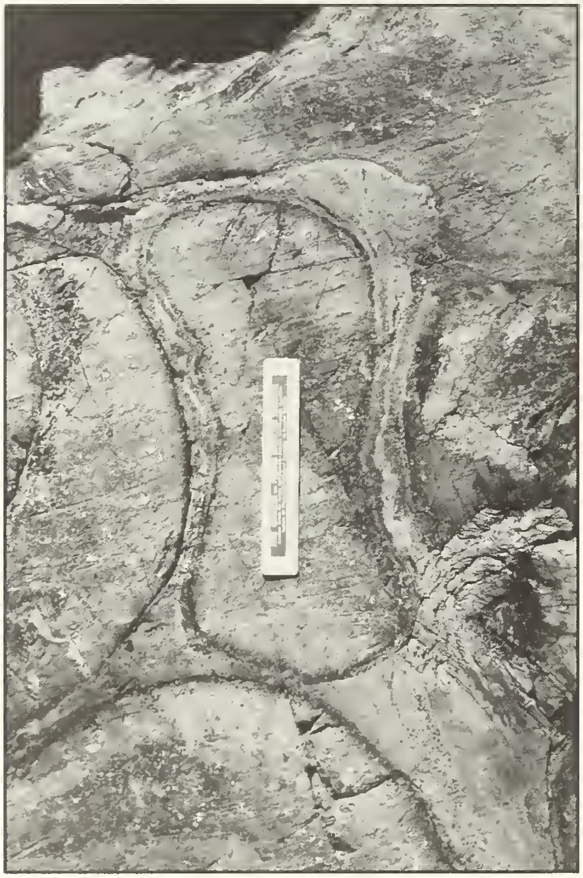

FIGURE 14. Close-packed pillows with ,complexly mineralogically zoned rims. Stop 8 in the Taylor Fm. Scale is 16.5 cm long.

The chemical anaylsis of the aluminous core of a basaltic andesite pillow collected just south of us appears in Table 3 below (sample C36), together with the average analysis of 19 Taylor lavas collected between Sierra City and Long Lake (second column). The standard deviation divided by the mean is over 25 wt. % for all oxides save SiO2, TiO2, and FeO*, partly reflecting element mobility during metamorphism.

TABLE 3. Composition of basalt and basaltic andesite lavas in Taylor Fm.

	C36	**average**
SiO2	55.0	53.8
TiO2	0.41	0.47
Al2 O3	20.31	15.98
FeO*	9.12	9.07
MgO	4.08	5.96
CaO	3.91	7.50**
Na2O	4.15	3.17
K2O	nd	0.35***
MnO	0.15	0.18
Sum	97.13	96.48

**average of 18 analyses; CaO was not detected by INAA in one sample.

***average of 12 analyses; K2O was not detected (nd) by INAA in 7 samples. The detection limit was about 0.1 wt. % K2O.

Thin-section petrography

A thin section cut near the core of a pillow shows that pillow interiors are less recrystallized than pillow rims: actinolite is almost nonexistent, and abundant clinopyroxene microlites are unreplaced, even where adjacent to clinopyroxene phenocrysts that have been wholly recrystallized to chlorite, quartz, and epidote. The clinopyroxene microlites occur as stout prisms often 0.1-0.2 mm long, and display weak hourglass color-zoning (brown to nearly colorless) and some simple {100} twins. The pillow core also is relatively rich in relict plagioclase microlites. These are of widely variable size, from tiny slivers to laths 0.25 mm and more long, and, together with the clinopyroxene microlites, exhibit haphazard arrangement. Abundant relict plagioclase glomerocrysts, each consisting of many unoriented euhedra, range up to about 4 mm across; one individual crystal is 3.9 mm long. These sometimes incorporated clinopyroxene crystals, and clinopyroxene also formed a few glomerocrysts unaccompanied by plagioclase. Plagioclase glomerocrysts mostly are replaced by albite single-crystal pseudomorphs riddled by inclusions of epidote. Some clinopyroxene glomerocrysts are pristine, some completely replaced as described above. Scattered, relatively large (often 0.75 mm), round amygdules largely consist of quartz, which bears apatite prisms near original vesicle walls; very narrow linings of chlorite and a little actinolite may intervene between the quartz fillings and vesicle walls. A few of these amygdules are filled with radiating epidote prisms.

Relatively large epidote crystals occur frequently in the matrix of this pillow-core material, as do rounded to irregular patches of chlorite at least as small as 0.03 mm that represent tiny amygdules. The remainder of the matrix consists of sphene granules and delicate radiating sprays of fibers which now, at least, consist of albite with undulatory extinction. The latter are most apparent adjacent to relict vesicles, and must have originated by crystallization of glass (during sea-floor alteration ?). The gradual reddening of the edges of pillows just inside the pale, epidote-rich rims may be partly the result of loss of this albite.

A thin section cut across the outer 17 mm of another pillow intersected all three of the selvages that sometimes are present:

the innermost, dark brick-red selvage; the medial, pale selvage, here <1 mm wide; and the outermost, brick-red rim, up to 7 mm wide in this sample. Not until one is within a few millimeters of the pale, <l-mm selvage does actinolite first appear abundantly in the pillow-lava matrix and as pseudomorphs of clinopyroxene microlites. Also, red iron oxide gradually increases in amount over this interval, eventually becoming concentrated, with very dark brown leucoxene, in sinuous, anastomosing films coinciding with the <1-mm selvage. The films, together with increased amounts of chlorite, comprise a foliation parallel to the edge of the pillow. The <1-mm selvage consists of granoblastic epidote with red-brown pigment that encloses delicate sliver- to lath-like plagioclase microlites originally enclosed in glass; most microlites display the characteristic jackets of dark "dust". Outboard of this selvage is the final rim, undisrupted in this sample, which originally was particularly glass-rich, enclosing many fewer microlites. The glass now consists largely of almost isotropic chlorite (anomalous blue and purple interference colors) charged with birefringent sphene granules and dark brown, cloudy patches of leucoxene, at least some of which originally enclosed tiny microlites. Relatively coarse, idioblastic actinolite and epidote (the angle between Z and a is at least 29°) are scattered through this material, and chlorite amygdules outlined by necklaces of granular sphene also appear. The latter often are shaped like biconvex lenses and parallel to the pillow margin. A sample in which the glass was affected by cooling-contraction granulation has angular relict glass fragments to 8 mm long bounded by flat to sharply curved conchoidal fractures.

The matrix between pillows consists of tuff largely replaced by fine-grained, granoblastic epidote (hence the pale color of the matrix material). Coarse-ash grains bear actinolite, as well.

STOP 9 (FIGURE 11) - Pillow lava, ash turbidites, and debris-flow deposits in the Taylor Fm. Walk west to STOP 9.

Taylor pillow lava here is overlain by well-bedded (N10°W, 30°E) crystal-lithic-vitric tuffs, which in turn are surmounted by lithic-vitric lapilli tuff containing pillow fragments and china-white lumps of pumice (look for tiny round quartz amygdules with the hand lens). (Remember that the facing direction is easterly.) Detailed mapping discloses that the Taylor pillowed flows have flat bases, steep flanks, and highly irregular upper surfaces (Brooks and Garbutt, 1972). The tuffs were erupted contemporaneously with the pillows, and thereby comprise their matrix. When pillows were not being formed, tuffs with tabular stratification continued to be deposited from turbidity currents (evidence for this depositional mechanism is discussed at STOPS 7 and 10). The interbedded lapilli tuffs and tuff-breccias containing pillow fragments and pumice lumps (broken-pillow breccias) are debris-flow deposits; debris flows evidently were initiated by slumping of the oversteepened flanks of the pillowed flows.

Noteworthy in this outcrop are: 1) the apparent differential compaction of tuff where it drapes large pillows; 2) pillows broken in situ and veined by tuffaceous matrix; 3) the pinching out of the bedded tuff sequence against the underlying pillow lava (buttress unconformity); 4) trace fossils in the bedded tuff; and 5) pillow fragments in the lithic-vitric lapilli tuff, some with quartz amygdules elongated perpendicular to pillow margins, some with pale, epidote-rich rims.

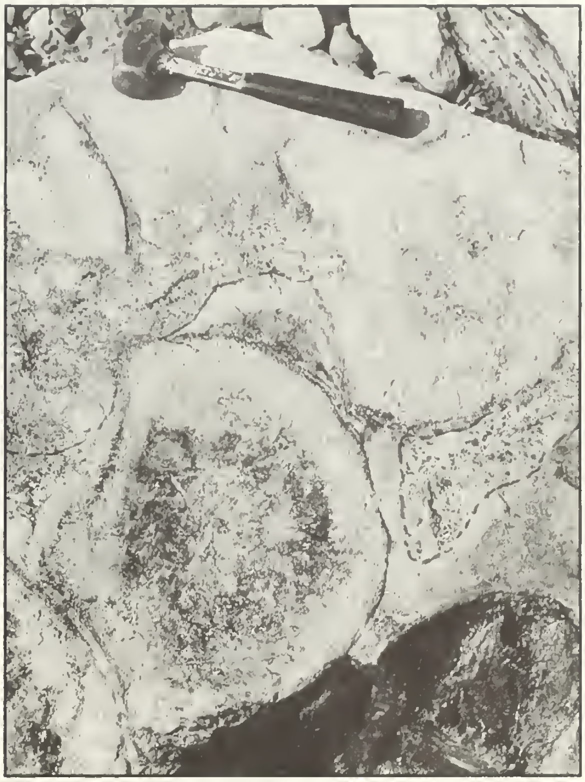

FIGURE 15. Debris-flow deposit (beneath sledge) in sharp, irregular contact (marked with pen) with close-packed, in situ pillows. Stop 9 in the Taylor Fm.

A large slab fortuitously lying on the ground nearby shows a fossil debris flow directly in contact with pillow lava (Fig. 15). One can imagine that the debris flow, derived farther up the paleoslope, lodged against the steep, slumped flank of a pile of pillows, several of which are seen still molded to one another along one edge of the slab. A line can be drawn on the slab which separates the finer, better-sorted tuffaceous matrix of the pillows from that of the debris flow, which contains white-weathering pumice lapilli (Fig. 15). The former tuffaceous matrix is locally faintly stratified, and the stratification is truncated by the debris-flow deposit (Fig. 15). The debris-flow deposit contains both broken and whole pillows.

Finally, note the draping of pillows one over another in the adjacent outcrop. The upper pillow apparently sagged downward between the two underlying, already-solid pillows, which themselves were draped over subjacent, solid pillows. Quartz amygdules in the upper pillow coarsen upward; some are elongated perpendicular to the upper margin of the pillow, suggesting continuing growth of vesicles on a crystallization front as it moved toward the pillow center.

Thin-section petrography

The lithic-vitric lapilli tuff contains two kinds of lapilli, both originally plagioclase-phyric: one was pumiceous, lacking, or nearly lacking, plagioclase microlites; the other was microlite-rich and generally poorly vesicular. Though relict plagioclase microlites consist of albite, plagioclase phenocrysts may consist largely of aggregates of quartz, some quite fine-grained, and these evidently masquerade as quartz phenocrysts under the hand lens; millimeter-scale silica metasomatism clearly took place. The matrix of the microlite-rich lapilli always contains abundant actinolite as tiny sheaves of fibers or as relatively coarse, acicular crystals having rhombic cross sections. The few vesicles present are filled, in various combinations, by apatite-bearing quartz, chlorite, epidote, and subspherulitic, pleochroic brown stilpnomelane. In contrast, the matrix of the originally pumiceous lapilli often is chlorite-rich. Chlorite both replaced glass and filled vesicles, so that the latter would not be apparent were it not for their dark brown necklaces of sphene/leucoxene. The close-packed, round to elliptical vesicles, from 0.05 to 0.35 mm across, often were distorted (elongated) next to plagioclase phenocrysts. The chlorite-rich matrix contains unoriented, acicular actinolite crystals and xenoblastic to idioblastic epidote. Some pumiceous lapilli have the matrix largely replaced by acicular actinolite, with chlorite apparently confined to amygdules, and, in still other such lapilli, relatively very large crystals of epidote (e.g., 0.65 mm) and quartz (e.g., 1.3 mm) have replaced glass, individual crystals of each growing across many vesicles in the process. Where quartz replaced glass, it contains acicular actinolite, but chlorite again is relegated to amygdules. One pumice fragment was replaced by granoblastic epidote containing a little actinolite and the usual brown sphene/leucoxene marking relict vesicles. The china-white pumice lumps so conspicuous in outcrop probably were replaced mostly by quartz and epidote, but their pale color actually may be due largely to a dearth of dark brown, sphene/leucoxene pigment.

In less recrystallized samples, preserved edges of lapilli are seen to be scalloped where vesicles were broken across, and a few ash grains largely bounded by concave-outward vesicle walls have the form of sharply pointed shards. Lapilli range up to about 9 mm long in thin section.

A sample of the well-bedded tuff contains several of the white-weathering laminae representing the originally finest ash. These are 2- to 5-mm thick and consist almost wholly of cloudy (brown pigment), finely granoblastic epidote (xenoblastic grains). Actinolite needles and quartz also may be present. None of the original fabric is discernible in these laminae, but no relict plagioclase crystals are present and the ash may have been vitric. Relict ash and lapilli up to 2.8 mm long can be recognized in the coarser interbeds, however. Many of these are nonvesicular, possess relict plagioclase microlites, and are actinolite-rich. Many others comprise relict plagioclase phenocrysts freed from their nonvesicular, microlitic matrix. A few sparsely vesicular fragments have a matrix rich in albite fibers and laths, the latter clearly relict plagioclase microlites. Large, xenoblastic to subidioblastic epidote crystals replaced much of this coarser tuff, and may poikiloblastically enclose relict plagioclase microlites; also present are quartz, sphene, and considerable chlorite.

Other samples of tuff contain no relict plagioclase crystals of any sort, contain many richly vesicular ash grains, and doubtless represent vitric tuff. Ash grains are roughly equant to elongated.

STOP 10 (FIGURE 11) - Ash turbidites and debris-flow deposits in the Taylor Fm.

Walk northeastward downhill to STOP 10.

Thinly stratified tuffs here are characterized by repeated, fining- upward packages thought to represent Tabc Bouma sequences, and accordingly they are considered to be ash turbidites deposited from low-density turbidity currents. The coarsest, structureless Ta (=S3 of Lowe, 1982) division of a turbidite is followed upward by the plane-parallel-laminated Tb division, which in turn is succeeded by the finest (white-weathering), rippled Tc division (Fig. 16). Crests of Tc ripples commonly are truncated at the base of the next higher turbidite (Fig. 16). A colleague asserts that the finest tuffs represent Te instead of Tc divisions. What do you think? Ta divisions may be normally graded, with respect to lithic tephra, or reversely graded, with respect to pumice.

Trace fossils again appear, in the finest, rippled Tc (Te?) divisions of turbidites. According to W.C. Miller III (personal communication, 1989), the branching forms are Chondrites, the meandering ones Helminthopsis, and the entire assemblage is characteristic of upper bathyal to supratidal depths. The joint-controlled outcrop surface intersects bedding at a very small angle, so that the amplitudes of ripples are greatly accentuated. Actual amplitudes and wavelengths average about 1-1.5 cm and 10 cm, respectively. We have never seen storm-wave ripples.

Interbedded (N20°W, 25°NE) with the ash turbidites are relatively thin (e.g., about 90 cm) beds of lapilli tuff containing pillow fragments. A fallen slab shows two such debris-flow deposits, separated by a little stratified tuff. Pillow fragments project from the top of the lower debris-flow deposit, which is reversely graded with respect to the pillow fragments, and load casts occur at the base of the upper one.

STOP 11 (FIGURES 11 and 17) - Andesite and basalt sills and volcanogenic sandstone in the Elwell Fm.

Walk westward to join the trail to Horse Lake. Beyond Horse Lake, leave the trail above several switchbacks and walk westward uphill to STOP 11.

The ridge forming the skyline to the north again displays the stratigraphic section nicely: the forested saddle is underlain by the Elwell Fm.; the bare, gray and red outcrops to the left (west) belong to the Sierra Buttes Fm.; and the darker outcrops to the right make up the lower part of the Taylor Fm.

A thick sill of Elwell andesite intruded the Sierra Buttes Fm. a few hundred meters north of us, then became dike-like and climbed stratigraphically until it turned on its side to become sill-like again at this location, the stratigraphic horizon occupied by the Elwell Fm. (Fig. 17). The orientation of the sill here is revealed by the steeply plunging columnar structure (75° N30°W). The sill overlies up to 12 cm of epiclastic volcanic sandstone interstratified with black phosphatic chert (note the white phosphate nodules). Some sandstone beds, rich in gray quartz and white plagioclase derived from dacite in the Sierra Buttes Fm.,

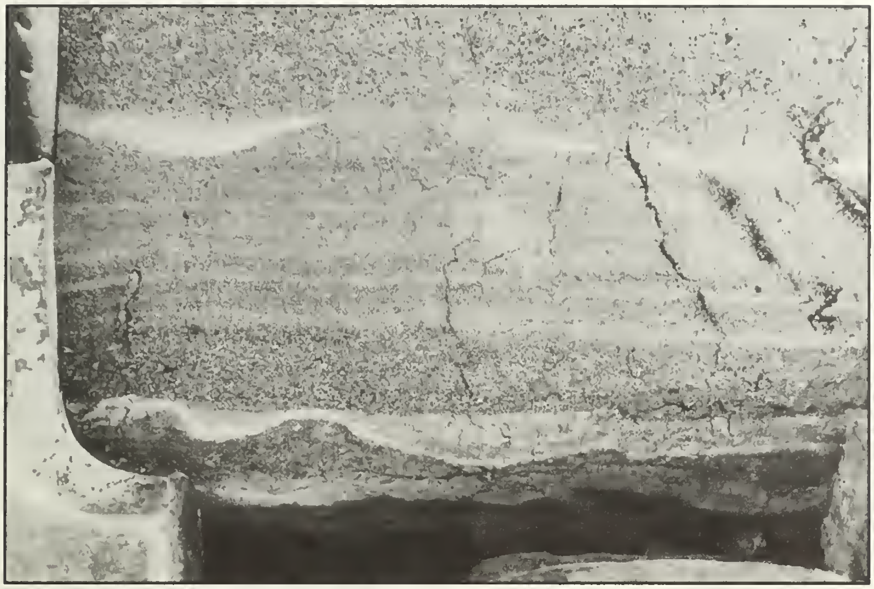

FIGURE 16. Tabc Bouma sequence in an ash turbidite (central third of figure) whose planar base partially truncated ripples in the underlying Tc division. Stop 10 in the Taylor Fm.

are quite coarse (sand grains up to 1.5 mm in diameter). Appearing beneath the Elwell sedimentary rocks is the top of another sill of quite a different kind. This one is choked with large (to 1 cm long), unaltered, light green clinopyroxene phenocrysts. Sills of this type occur voluminously at and near the stratigraphic horizon of the EF, and are thought to represent cumulates complementary to the aphyric andesite sills. They are basaltic, and reach thicknesses of at least 34.5 m. This sill is about 2 m thick nearby, where its base is exposed, and most of the top one meter is exposed here. The 10-cm thick, clinopyroxene-rich edge of the sill gives way downward to a 15-cm thick, clinopyroxene-free but originally relatively vesicular zone (amygdules of quartz and chlorite to 5 mm); this zone passes back to 60 cm or so of generally clinopyroxene-rich basalt. Such interlayering presumably is the result of elutriation during sill emplacement. No chemical analysis is available for this sill, but the average analysis of three other of these richly clinopyroxene-phyric intrusions follows.

The modes of the three analysed samples contain from 12 to 35% clinopyroxene phenocrysts and from 0 to 16.5% plagioclase phenocrysts. All three samples are classed as subalkaline, tholeiitic, and basaltic by all major-element and norm criteria recommended by Irvine and Baragar (1971). All three are hy-normative, and one is ol-normative (ol=11.41), the other two weakly Q-normative (Q=1.97, 2.70). Abundances of the immobile elements Ti, Zr, Y, Cr, and Ta show that these basalts belong to the tholeiitic rock association of island arcs (Brooks and Coles, 1980). An island-arc tholeiite origin also is indicated by the concentrations of heavy to intermediate rare earths (Sm-Lu), which range from 3.5 to 6 times chondritic abundances. Zr values are low, probably because of dilution by accumulation of clinopyroxene phenocrysts, and Cr values are high for the same reason.

TABLE 4. Composition of clinopyroxene-phyric basalt intrusions.

oxide wt. %		immobile trace element ppm	
SiO_2	49.6	Zr	15.9
TiO_2	0.44	Nb	3.9
Al_2O_3	13.74	Cr	358.0
Fe_2O_3	1.73	V	333.0
FeO	8.60	Y	6.6
MgO	9.34	Sm	0.905
CaO	9.90	Eu	0.309
Na_2O	1.58	Yb	0.973
K_2O	0.87	Lu	0.168
MnO	0.20		
P_2O_5	0.05		
H_2O+	2.96		
H_2O-	0.17		
CO_2	0.09		
Sum	99.25		

Thin-section petrography

The aphyric, andesitic sill rock was greatly affected by millimeter-scale metasomatism, so that the original fabric is nearly obliterated. However, it is certain that the andesite contained numerous, unoriented, lath-shaped plagioclase microlites, averaging perhaps 0.1 mm long, and abundant, tiny (e.g., 0.025 mm), octahedral magnetite microlites, as well as ellipsoidal and spheroidal vesicles ranging from 0.1 to 2.25 mm in length. Most of the latter are filled with chlorite, quartz, epidote, and stilpnomelane (flakes intimately intergrown with the chlorite and strongly pleochroic to deep red-brown), but a single large vesicle was completely filled by calcite. Most of the sill rock now consists of finely granular, xenoblastic epidote charged with brown cloudy leucoxene in which ghostly, relict plagioclase microlites are outlined by the brown pigment. This granoblastic epidote is mottled by large (e.g., 0.7 mm), roughly equant, irregularly bounded quartz grains in which the relict plagioclase microlites are more apparent, even though completely replaced by the quartz. Also conspicuous in the quartz are square to rhombic sphene grains which replaced the magnetite microlites. The andesitic sill rock also contains calcite, abundant chlorite, highly irregular patches of black iron oxide, and elusive bundles of parallel fibers and larger, simply twinned crystals of actinolite.

The thicker laminae of volcanic sandstone, though apparently fining upward, are quite well-sorted, sand grains averaging nearly 1 mm across. These consist of quartz, weakly twinned albite, and very finely granular quartzofeldspathic material. The

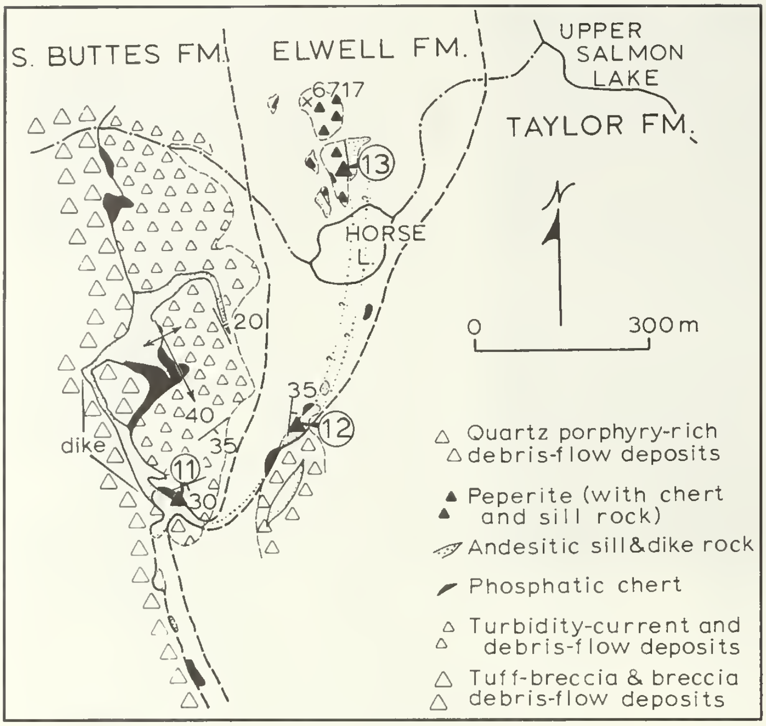
S. BUTTES FM.
ELWELL FM.
UPPER SALMON LAKE
TAYLOR FM.
x6717
13
HORSE L.
N
0
300 m
20
40
35
dike
11
30
35
12
Quartz porphyry-rich debris-flow deposits
Peperite (with chert and sill rock)
Andesitic sill & dike rock
Phosphatic chert
Turbidity-current and debris-flow deposits
Tuff-breccia & breccia debris-flow deposits

FIGURE 17. Outcrop map of the Horse Lake area, showing locations of stops 11-13 (filled triangles). After mapping by M.M. Wood, 1980.

quartz and albite grains were derived from phenocrysts of quartz and plagioclase, the finely granular grains from the matrix— now recrystallized —in which these phenocrysts originally were embedded. Indeed, some finely granular grains bear relict quartz phenocrysts rounded by magmatic corrosion; some euhedral, relict plagioclase phenocrysts; and a few, lath-shaped, relict plagioclase microlites. Some quartz grains are highly angular. All of these materials evidently were eroded from dacite in the underlying Sierra Buttes Fm. Films of nearly isotropic chlorite separate the sand grains, and sphene and epidote also are concentrated there.

The black chert laminae consist of granular quartz and epidote, and black, dust-like carbonaceous material, as well as scattered detrital grains; radiolarians are not apparent.

Although almost nothing can be told about the original condition of the matrix of the richly clinopyroxene-phyric sill rock, the clinopyroxene phenocrysts themselves are nearly pristine. They comprise stout prisms considerably rounded by magmatic corrosion (colorless, {100} polysynthetic twinning, birefringence about 0.027, the angle between Z and c =41°). Optically continuous, irregular actinolite grains fleck interiors of the clinopyroxene phenocrysts, and actinolite may form serrated fringes along their margins. Though much actinolite is colorless, some individual crystals are color-zoned, with Z colorless to rather deep brown, or brown to blue-green. The matrix of the basaltic sill rock is rich in actinolite (bundles of parallel fibers and coarser prisms), granular sphene, and xenoblastic epidote. Many relatively large (e.g., 0.4 mm), equant to elongated, round or elliptical to irregular, single crystals or crystal aggregates of quartz are present; some of these probably represent amygdules, but others appear to contain relict plagioclase microlites, as in the andesitic sill rock. Relict magnetite microlites also occur. The matrix in addition exhibits irregular patches of black iron oxide and lenticular bodies— probably deformed amygdules —of chlorite+/-calcite+/-quartz.

STOP 12 (FIGURE 17) - Elwell andesite sill and overlying debris-flow deposit

Walk downhill to the southeast, approximately along the contact between the aphyric and clinopyroxene-rich Elwell sills, rejoining the trail; aphyric sill rock along the way contains exceptionally abundant, large, chlorite- and quartz-filled amygdules. Walk northeastward toward Horse Lake.

This sill is the same, aphyric one examined at STOP 11, here with magnificently displayed columnar structure in its lower part (Fig. 18). Look for the poorly exposed black phosphatic chert that concordantly underlies the sill. The sill rock here is unusual in that it exhibits scattered small glomerocrysts of plagioclase and clinopyroxene. It also contains unusually abundant gray quartz megacrysts that greatly resemble large quartz phenocrysts which choke some dacitic rock units in the Sierra Buttes Fm. Are these crystals xenocrysts or phenocrysts ? The hand lens shows that they commonly are deeply embayed and highly irregularly shaped.

The top of the sill is missing, having been eroded, together with overlying rocks, and replaced by an epiclastic debris flow charged with large clasts of phyric Sierra Buttes dacite, Elwell sill rock, black phosphatic chert, etc. Many sand grains in the matrix of the debris-flow deposit consist of smoky quartz derived from phyric Sierra Buttes dacite. Such debris-flow deposits make up the basal member of the Taylor Fm., as I define it. The contact between the decapitated sill and fossil debris flow is very sharp and highly irregular; it intersects vesicles flattened in the plane of the sill during its emplacement. Look for steeply dipping, tabular, black chert veins in the sill below the contact; still-fluid chert injected columnar joints as they opened during shrinkage of the solidifying sill. The tabular chert veins have to be distinguished from nodular xenoliths of chert picked up by the sill during its emplacement, which also are present.

Thin-section petrography

Relict euhedral plagioclase phenocrysts in the sill range up to 1.35 mm long and commonly form clusters of 2 or 3 individuals. They have been completely repalced by an array of minerals— epidote, calcite, albite, quartz, actinolite, chlorite, and white mica —in various combinations and proportions. Subhedral to euhedral, prismatic, clinopyroxene microphenocrysts and phenocrysts up to 1.5 mm long (colorless, simply twinned, birefringence about 0.025, 2VZ moderate (r>v), the angle between Z and c =40°), again commonly clustered, have been partially replaced by chlorite, actinolite, epidote, quartz, calcite, and sphene, in a seemingly endless variety of combinations. Relict clinopyroxene, plagioclase, and magnetite microlites occur in the sill-rock matrix. The former comprise poorly terminated prisms simply twinned on {100} which may display a second composition plane oriented normal to c, resulting in interesting fourlings. Many clinopyroxene microlites have been replaced along their edges, or throughout, by parallel fibers of actinolite. The quartz megacrysts were extensively corroded, with rounded edges and smooth, straight to gently curved "faces", both convex- and concave-outward. They display narrow, optically continuous quartz overgrowths, which in places poikiloblastically enclose albite and sphene pseudomorphs of plagioclase and magnetite microlites originally present in adjacent glassy matrix.

STOP 13 (FIGURES 17 and 19) - "Dispersed" peperite in the Elwell Fm.

Rejoin the trail and walk northeastward toward Horse Lake. Leave the trail south of Horse Lake, skirt the west side of the lake, and climb Hill 6717 north of the lake.

Much of the top of this hill consists of aphyric sill rock and peperite in the Elwell Fm. (Fig. 19 has the details). Here, invading andesitic magma encountered relatively wet black phosphatic chert and was quenched drastically, producing "dispersed" peperite: relatively well-sorted, fine-grained peperite, the voluminous chert matrix of which contains phosphatic nodules, both whole and broken, and chert fragments (Brooks and others, 1982). The phosphatic nodules must have formed diagenetically prior to lithification of the chert, and been shattered, together with locally lithified chert, by steam explosions. The drastic quenching of magma is indicated by relict quench microlites of plagioclase in andesite fragments (Fig. 20). One may search with the hand lens among the finer andesite fragments for those bounded by the characteristic conchoidal fractures representing thermal-contraction cracks developed in rapidly freezing, glassy lava. Spectacular examples of "dispersed" peperite may be collected from talus as we descend the southeast flank of Hill 6717 on our return to the trail.

Also notable at this locality are: 1) large deformed chert xenoliths enclosed in sill rock without intervening peperite, representing chert that was lithified when intruded; 2) peperite containing small pillows that were deformed ductilely during dispersal of the peperite by steam explosions (some lapilli-size andesite fragments at this locality also initially exhibited ductile behavior); and 3) the rarely observed passage of sill rock into peperite, where they adjoin once-wet chert.

Thin-section petrography

Ash- and lapilli-size, aphyric andesite fragments in the "dispersed" peperite are charged with strongly flow-aligned, prismatic, relict plagioclase microlites; flow lines may be folded. Straight to smoothly curved fragment boundaries, the result of thermal-contraction cracking of glassy andesite, frequently truncate flow lines. Fragments may have correspondingly simple shapes, produced by the intersection of these shrinkage cracks, or may exhibit complex outlines suggestive of fluidal behavior. Some fragments contain scattered, tiny (e.g., 0.15 mm long), elliptical amygdules.

The relict plagioclase microlites are embedded in green chlorite studded by sphene spherules, commonly 0.01 mm in diameter. Coarse epidote idioblasts also occur, each poikiloblastically enclosing several of the aligned plagioclase microlites. Calcite and relatively coarse quartz occur infrequently. Near fragment margins, plagioclase microlites served as nuclei for fringing overgrowths of additional albite.

Andesite fragments are rimmed (e.g., 0.2 mm wide) by extremely fine, axiolitic intergrowths of chalcedony and chlorite(?); these nucleated on plagioclase microlites, as well as on the bounding shrinkage fractures. Axiolitic rims may be followed inward by narrow bands of dark gray, cloudy leucoxene or red-brown, granular sphene. Cloudy leucoxene also may appear between plagioclase microlites and encrusting axiolitic intergrowths. The axiolitic intergrowths probably originated during sea-floor metamorphism, when fibrous quartz replaced fibropalagonite formed earlier at the edges of glassy fragments (Dimroth and Lichtblau, 1979). Such alteration would have been facilitated by the relatively copious quantities of heated pore water that apparently were present at this location following peperite formation.

The chert matrix of the peperite contains poorly preserved radiolarians, and consists, besides microgranular quartz and carbonaceous material, of chlorite and epidote. Andesite fragments at least as small as 0.35 mm long are recognized in the chert.

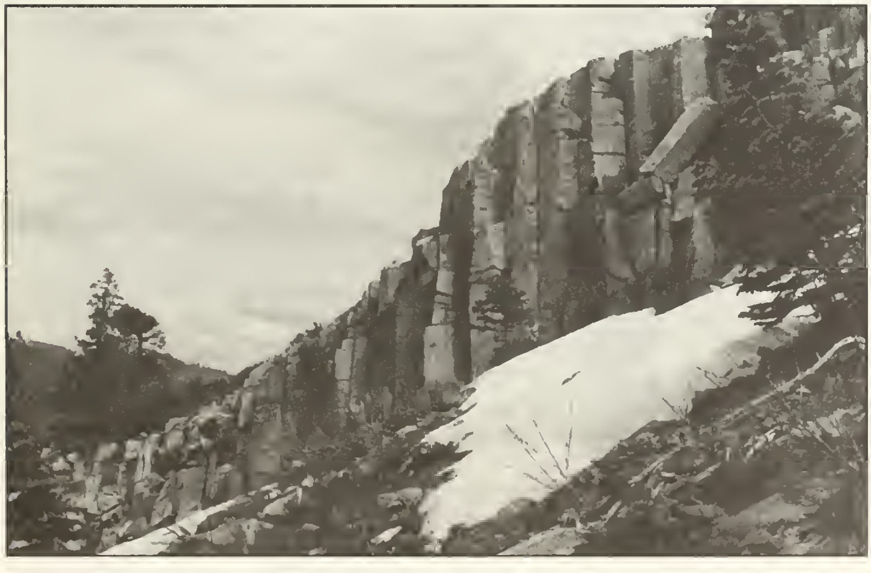

FIGURE 18. Columnar structure in lower part of Elwell andesite sill at stop 12. Columns to right are about 4 m long; note cross joints. Same as Fig. 8 in Brooks and others (1982) and Fig. 20 in Turner (1896).

FIGURE 19. Outcrop map of Hill 6717, north of Horse Lake, showing distribution of andesite, chert, and peperite in the Elwell Fm. (stop 13). After mapping by Christine Naschak, 1980.

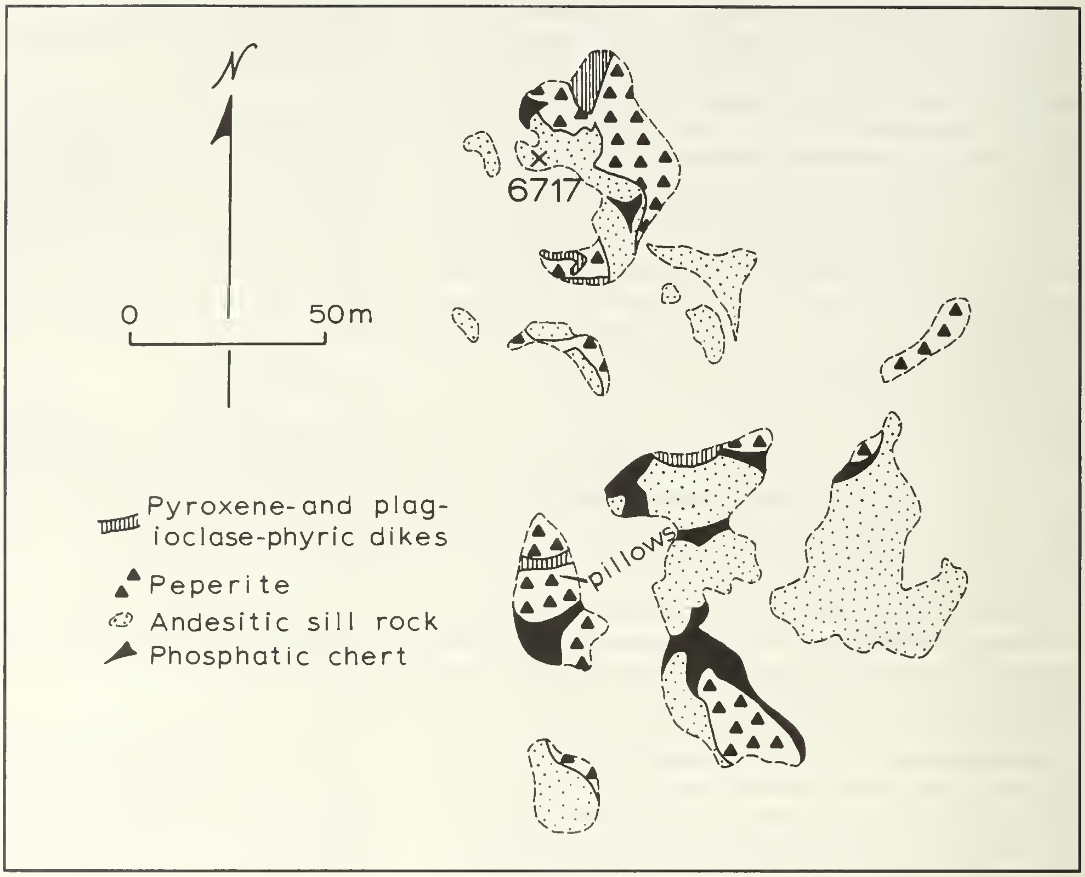

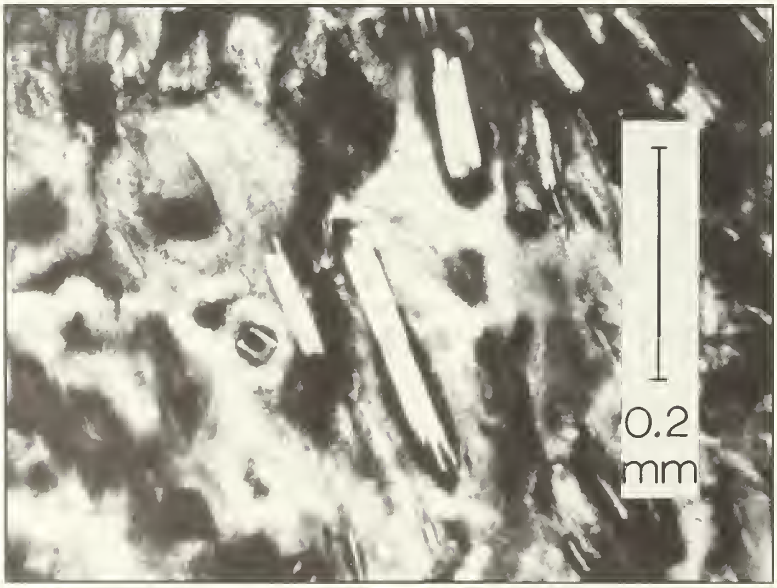

FIGURE 20. Relict quench microlites of plagioclase in andesite fragment in peperite on Hill 6717 (stop 13 in the Elwell Fm.). Note forked and notched ends of albite laths, square cross section of a hollow prism, and minute, splinter-like forms. Same as Fig. 22 in Brooks and others (1982).

STOP 14 (FIGURE 11) - Pillow lava in the basal Taylor Fm.

Rejoin the trail just after crossing the outlet of Horse Lake and follow it northward to the wooden bridge that recrosses the outlet near Salmon Lake Lodge. Leave the trail soon and continue northward up the ridge to STOP 14 near the water-storage tank.

Here is the lowest pillowed lava flow in the Taylor Fm. at this latitude (Fig. 21). The spheroidal pillows are closely packed, with only minor tuffaceous matrix evident at pillow junctions. They are characterized by elongated quartz-epidote amygdules that tend to occur all the way around a pillow, like the spokes in a wagon wheel (Fig. 21). Pillows frequently exhibit minor in situ fragmentation. Pistachio-green epidote is much in evidence, especially in the pillow rims.

The pillows are richly clinopyroxene-phyric and possibly contained some olivine phenocrysts as well. Cleavage flashes that extend completely across phenocrysts reveal igneous clinopyroxene. A chemical analysis of the central part of a large pillow, recalculated to 100 wt. %, volatile-free, follows.

TABLE 5. Analysis of the central part of a mafic Taylor Fm pillow.

SiO_2	56.10
TiO_2	0.24
Al_2O_3	9.82
FeO^*	10.46
MgO	8.92
CaO	11.76
Na_2O	2.19
K_2O	0.15
MnO	0.32

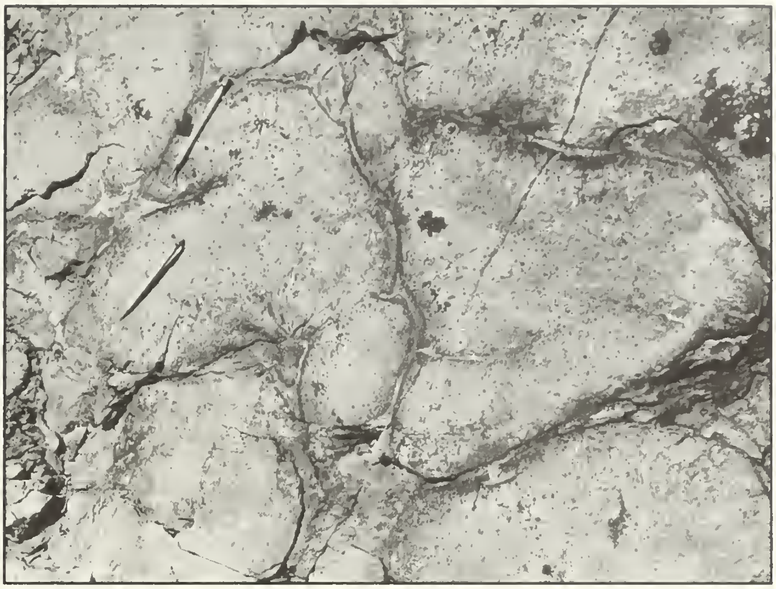

FIGURE 21. Close-packed pillows in basal Taylor Fm. at stop 14. Note elongated quartz amygdules round the outer parts of pillows. One of the pencils points out a portion of a pillow pressed back against itself.

Although in the basaltic andesite range in terms of silica content, this sample is otherwise very mafic, containing 842 ppm Cr but only 4 ppm Zr. Ti also is unusually low, and the values of all three elements doubtless were affected by accumulation of the mafic phenocrysts. Also, the rare-earth abundance pattern is the most primitive of all 19 of the Taylor lavas analysed, the concentrations of Sm and Eu being only 2 times their chondritic abundances. The pattern shows substantial relative depletion of LREE; La and Ce were not even measurable by INAA. A modal analysis recalculated to exclude amygdules resulted in 14.3% clinopyroxene phenocrysts, 2.9% relict olivine and/or plagioclase phenocrysts, and 82.8% matrix.

Thin-section petrography

Euhedral clinopyroxene phenocrysts and microphenocrysts are rimmed and veined by chlorite and uniformly oriented, finely prismatic actinolite. Chlorite tends to be in direct contact with ragged remnants of clinopyroxene, actinolite occupying central parts of veins and outermost parts of rims. The clinopyroxene has properties like that in the richly clinopyroxene-phyric sill at STOP 11; viz., stout, 8-sided prisms; polysynthetic twinning; colorless; 2VZ about 65° (r>v, weak); the angle between Z and c at least 41°.

Clusters of relatively coarse, mostly xenoblastic epidote crystals in some cases clearly have filled vesicles, in others just as clearly have completely replaced phenocrysts. Chlorite commonly accompanies the epidote, which is then idioblastic against it. Epidote amygdules are elliptical (e.g., 0.6 mm long) and exhibit haloes of dark gray, cloudy leucoxene. Epidote pseudomorphs display straight to curved, relict crystal faces, some concave outward, and rounded corners. These relict phenocrysts reach a maximum dimension exceeding 3.5 mm, and have shapes sometimes suggesting plagioclase, sometimes olivine. The epidote is weakly pleochroic (X=colorless, Y=Z=pale yellow), displays simple {100} twins, and has 2VX large (r>v, strong), birefringence about 0.03, and the angle between Z and a about 28°.

The matrix consists largely of unoriented bundles of parallel actinolite fibers, granular sphene, and relatively coarse, highly irregular epidote grains darkened by leucoxene; length-fast albite laths representing relict plagioclase microlites get lost in the actinolite but are not uncommon.

STOP 15 (FIGURE 11) - Pillowed sill at top of Elwell Fm.

Continue up the ridge to STOP 15.A thick sill of aphyric Elwell andesite, columnar-jointed at the bottom and layered in its central portion, has a pillowed top. It overlies black chert, and peperite can be found in its base. The prominent columnar structure involves 5- and 6-sided columns that are curved in places, plunging less steeply as the dip steepens northeasterly (Fig. 22). Cross fractures are present perpendicular to the long axis of the columns, which are, for example, 20 cm in diameter (Fig. 22). The columnar structure dies out upward in layered (flow-layered ?) andesite, which is sparsely amygdaloidal near the top (chlorite amygdules). Metamorphic cleavage, dipping more steeply northeastward than the layering, is apparent in the finer, thinner (2.5-5 cm), red-brown-weathered layers which separate the 20-30-cm-thick, pale gray-green layers. The darker, red-brown layers appear to represent a transition to the darker, purplish-weathered pillow lava above, into which the layered andesite passes through a thin zone of relatively small, deformed pillows broken in situ . The overlying, larger, close-packed pillows exhibit distinctive curved fractures concentric to the pillow margins. These developed parallel to closely spaced, very thin shells of microvesicles which appear to be equivalent to the vesicle sheets present at the edges of aphyric andesite sills (STOPS 3 and 5). Additionally, some pillows are divided by irregular, crudely prismatic shrinkage fractures. Neither the concentric nor the radially oriented fractures are found in Taylor pillows. It is worth emphasizing that the pillowed sill, together with nearby Elwell pillow lava (STOP 17), occur in the same area as peperite containing small pillows and ductilely deformed fragments (STOP 13); sill emplacement was essentially at the sediment-water interface, where sea-floor sediments were water-saturated.

Refer again to the rare-earth abundance patterns in Figure 8. Sample 43 was collected from a pillow about 0.75 m long in the pillowed top of this sill, sample 43A from the prominent curved column beneath the sledge just left of the center of Figure 22. The rare-earth patterns for these two samples essentially coincide, in accord with my inability to ever find a physical break between the pillowed and unpillowed parts of this rock mass. The chemical analyses of the two samples, recalculated to 100 wt. %, volatile-free, appear below.

TABLE 6. Comparison of compositions of pillowed top and columnar-jointed bottom of andesitic Elwell sill.

	43 (pillow)	**43A (column)**
SiO2	63.50	62.50
TiO2	1.22	1.15
Al2O3	12.42	12.18
FeO*	11.58	10.82
MgO	2.69	3.72
CaO	1.98	4.78
Na2O	5.91	4.44
K2O	0.62	0.18
MnO	0.06	0.18

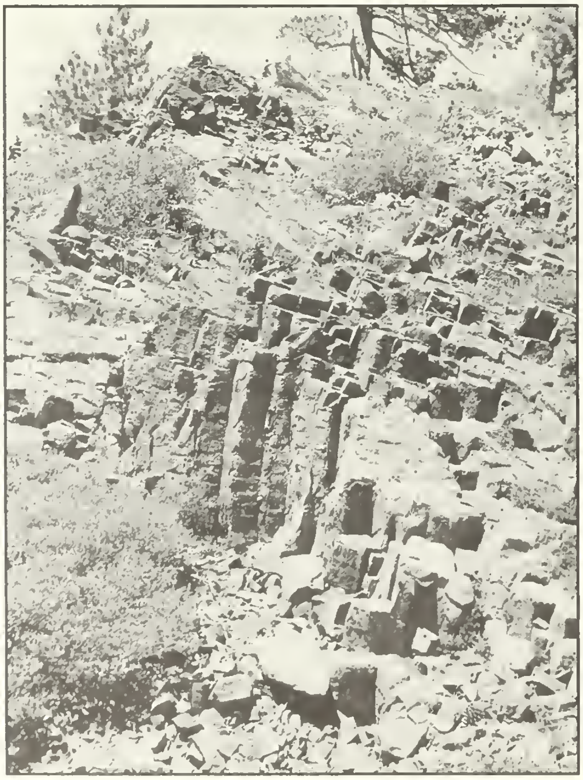

FIGURE 22. Columnar structure in basal part of a pillowed andesite sill present at the top of the Elwell Fm. (stop 15). Direction of view is NW.

The large differences in MgO, CaO, Na2O, and K2O doubtless reflect the mobility of these oxides during metamorphism.

Thin-section petrography

Thin sections cut from basal, columnar-jointed and central, layered parts of the pillowed sill show that the aphyric andesite originally possessed intersertal texture, being charged with plagioclase microlites. Although these at first appear to be arranged randomly, a closer look reveals that they actually display a limited number of definite orientations, perhaps determined by the structure of the congealing melt. The lamellar-twinned albite laths and fibers average 0.1 mm or less in length, and may be clustered in bundles of parallel laths.

The interstices between albite laths are occupied by relatively dark green chlorite, granular sphene, epidote, and quartz. Some samples contain calcite as well. The epidote is pleochroic, colorless to pale yellow, and has a birefringence greater than 0.035, indicating a fairly iron-rich epidote. A particularly strongly recrystallized sample has the original plagioclase microlites completely replaced by epidote single crystals or crystal aggregates, their ghostly outlines marked by parallel rows of red-brown, dust-like inclusions. This sample also contains coarse actinolite (Z=light blue-green).

Irregular strings of widely spaced amygdules probably represent vesicle sheets. In one sample, elongated (probably flattened) microamygdules (e.g., 0.2 x 0.7 mm) consist of epidote and have gray haloes of sphene/leucoxene. Rare chlorite amygdules in the same sample (e.g., 2.4 mm long) display necklaces of epidote only one grain (i.e., 0.1 mm) wide, and seem to be independent of the sheets of microamygdules. In another sample, amygdules consist largely of xenoblastic calcite.

STOP 16 (FIGURE 11) - Pillowed top of Elwell sill overlain by Taylor debris-flow deposit

Continue northwestward along the ridge to STOP 16, crossing a light-gray dike of deuterically altered hornblende andesite along the way. This unmetamorphosed andesite dike is Early Cretaceous (122 Ma) and originated from a tonalite pluton exposed at the northeast end of Gold Lake (Lull and Brooks, 1983).

The pillowed top of the sill at STOP 15 here is overlain abruptly by pebbly sandstone rich in detritus derived from the Sierra Buttes Fm. Indeed, pillows were decapitated in places prior to deposition of this epiclastic sediment, perhaps by slumping of pillows (Fig. 23). The contact between pebbly sandstone and pillow lava is very sharp and irregular, with fragile projections— partly bounded by relict shrinkage fractures —extending from decapitated pillows into the base of the pebbly sandstone (Fig. 23). The pebbly sandstone contains fragments of the subjacent pillows, and displays reverse grading of the coarser, mostly dacitic clasts (Fig. 23). Smoky-gray quartz and white feldspar grains derived from quartz and plagioclase phenocrysts choke the sand-size fraction of this debris-flow deposit (Fig. 23). Among the coarser clasts are, besides Sierra Buttes dacite and Elwell pillow fragments, probable quartz-phyric pumice, likely derived from the immediately underlying Sierra Buttes Fm., which is pumiceous in this area. Again, as at STOP 12, a debris-flow deposit rich in Sierra Buttes detritus marks the base of the Taylor Fm.

The large Elwell pillows, up to at least 2 m in diameter, are very closely packed. Large, pistachio-green, epidote-rich patches commonly dominate the interior parts of pillows. Crudely radially oriented, relict shrinkage fractures in the Elwell pillows are filled by dark reddish gray, porous material rich in magnetite and hematite, and, locally, by red jasper (hematite-rich chert). Also, masses of jasper at least 8 cm long appear in the pillow lava, and these may be separated from the lava by 5-10 mm of magnetic, dark gray, porous, magnetite-rich chert. Hematite in pillow lava in the Josephine ophiolite may have been formed by hot-spring activity on the sea floor (Harper, 1991), but Elwell pillow lavas were formed in an anoxic (black phosphatic chert) environment, and formation of the jasper has to be attributed to a subsequent hydrothermal event.

Thin-section petrography

The fine to coarse sand and fine pebbles in the Taylor pebbly sandstone consist of 1) former phenocrysts of embayed, bipyramidal quartz and euhedral plagioclase seemingly little affected by sedimentation processes (although fine quartz sand grains frequently exhibit sharply angular corners resulting from breakage); and 2) two kinds of relict groundmass in which the quartz and plagioclase phenocrysts were embedded, one now feldspathic, the other chloritic. Also, leucoxene grains representing former magnetite microphenocrysts are present.

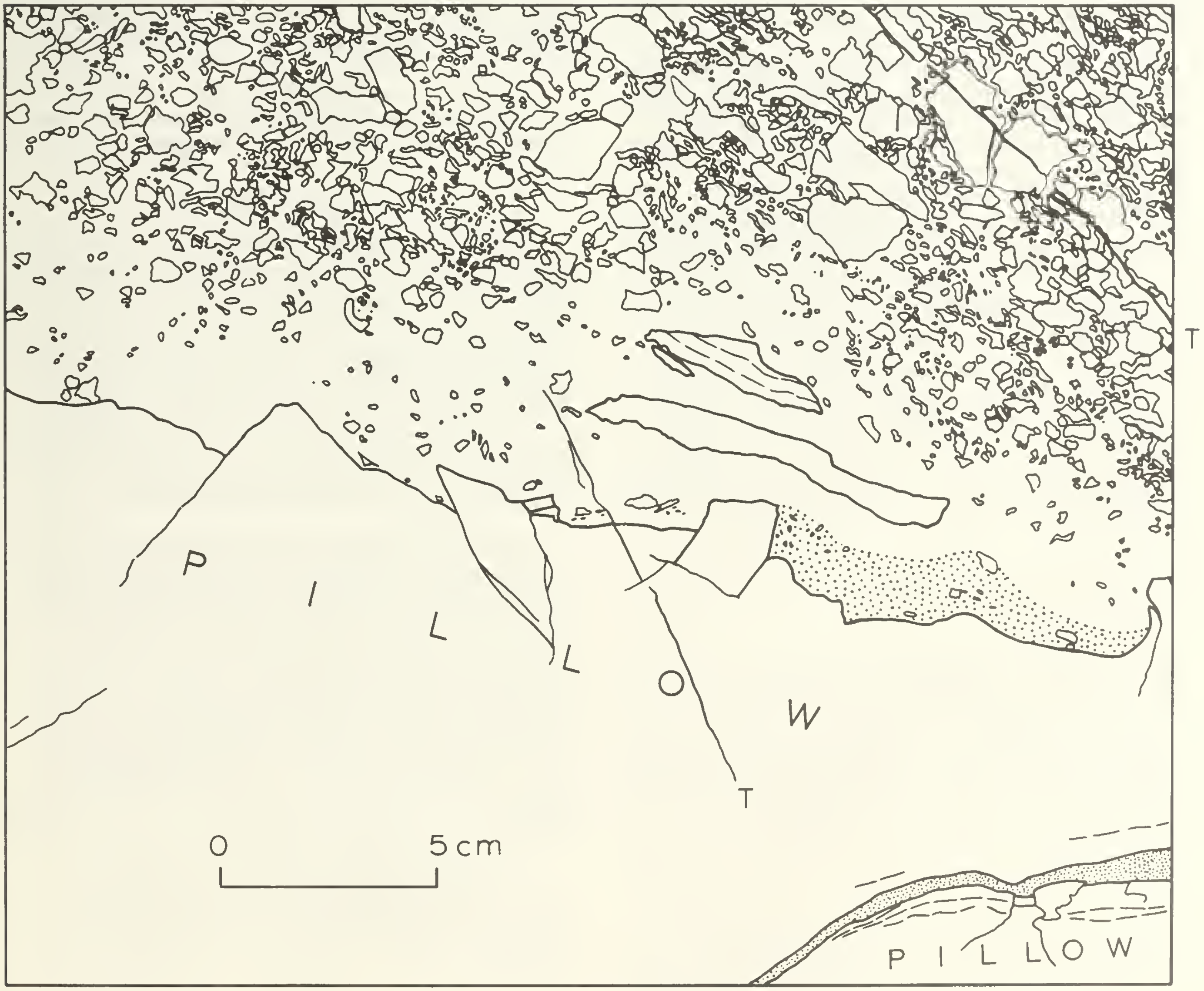

FIGURE 23. Close-packed, decapitated Elwell pillows overlain by debris-flow deposit rich in Sierra Buttes detritus at stop 16. Fine stipple is interpillow matrix, coarse stipple is quartz sandstone, and long dashes indicate color banding at edges of pillows. Grains smaller than about 0.5 mm are not shown. All fractures except the two labelled "T" (for tectonic) probably are relict shrinkage fractures. Same as Fig. 7 in Brooks and others (1982).

The very finely granular, feldspathic (quartzofeldspathic ?) type of relict groundmass contains some relict plagioclase microlites and spherulites up to 0.3 mm in diameter, both of which now consist of albite. The chloritic groundmass type, presumably also derived from the Sierra Buttes Fm., contains only relict quartz and plagioclase phenocrysts. Sand-size grains of this material consist of chlorite abundantly pockmarked by tiny (0.02 mm) feldspar(?) spherules, and pebbles of it comprise chlorite locally diversified by the feldspar(?) spherules, finely granular feldspar, idioblastic epidote and stilpnomelane (X=light yellow, Y=Z=deep olive green), white mica, etc. Sphene spherules generally a bit larger than the feldspar(?) spherules are scattered throughout the chlorite, which doubtless originally was glass.

Where one can be sure that the matrix of this poorly sorted pebbly sandstone is being examined— between the angular grains of fine quartz sand —it is too finely granular to work with, but consists largely of quartz and/or feldspar.

The magnetite-rich chert that separates jasper from adjacent Elwell pillow lava displays parallel, discontinuous streaks of virtually solid magnetite. The magnetite comprises sharply euhedral cubes and octahedrons from <0.01 to 0.1 mm across. There are also a few streaks and bands rich in epidote and/or stilpnomelane, and a little white mica is present. The jasper originally contained much less magnetite than the magnetite-rich chert, present as uniformly distributed, small patches and strings now largely replaced by hematite. Only irregular islands of magnetite remain, and the original form of most of it is not clear. Considerable fine-grained leucoxene accompanies the altered magnetite, so that it must have been titaniferous. Very finely divided hematite is concentrated in much larger, cloud-like masses separate from the small patches of altered magnetite, and it is this material that accounts for most of the red pigment in the jasper. The quartz comprising the bulk of the jasper exhibits a relatively coarse (grains to 0.04 mm across), granoblastic fabric suggestive of strong recrystallization; many straight grain boundaries— hence polygonal quartz grains —occur.

STOP 17 (FIGURE 11) - Pillow lava in the Elwell Fm.

Walk westward down-section to STOP 17.

The spheroidal geometry of Elwell pillows here is revealed in three dimensions. A brief search discloses that these discrete, 1-2-m, tightly molded pillows are separated by thin films of black chert. The roughly radially oriented fractures within pillows here are filled with black chert— weathered gray to white —indicating that they originated as prismatic shrinkage fractures that were injected by fluid chert as they opened. Some chert veins even were flow-laminated during this process (see below).

Thin-section petrography

Fluid chert injecting shrinkage fractures opening in the pillows resulted in irregular black chert veins that may pinch and swell, changing thickness rapidly. One vein, so rich in black carbonaceous material that no quartz is apparent, has a maximum thickness of only 0.25 mm; others are even thinner. A vein up to 4 mm thick displays flow laminae adjacent to both walls; these are made conspicuous by varying amounts of finely divided carbonaceous material and are surprisingly planar, considering the very irregular vein walls. Most of the chert is very fine, quartz grains averaging only about 0.01 mm across.

The pillows originally were rich in the usual plagioclase microlites, and contained a few plagioclase microphenocrysts. The former now consist mostly of albite, the latter of aggregates of epidote and chlorite. Vein walls quenched by fluid chert contain fewer relict plagioclase microlites. Small (e.g., 3.5 mm) volumes of the andesite were completely replaced by relatively coarse, xenoblastic quartz containing sphene and actinolite, and smaller (e.g., 0.5 mm), spheroidal volumes were similarly entirely replaced by reddish brown epidote aggregates. Tiny (e.g., 0.25 mm), formless patches of chlorite+/-epidote may represent microamygdules; others consist of epidote or quartz.

We will retrace our steps down the ridge to the trail and follow it around the north side of Upper Salmon Lake, thereby returning to the parking area. I hope you enjoyed the trip!

ACKNOWLEDGEMENTS

Some of the chemical data appearing here have never been published, so I must acknowledge those institutions instrumental in their acquisition. Most data were obtained while I held an Associated Western Universities-Department of Energy faculty participation appointment at the Lawrence Livermore National Laboratory; analytical costs were borne by the Earth Sciences Division, Lawrence Livermore National Laboratory. Silica analyses were paid by a grant from the Committee on Research, California State University, Hayward, and FeO, P2O5, H2O, and CO2 analyses (Table 4) were provided by the Branch of Analytical Chemistry, U.S. Geological Survey, Menlo Park.

I wish to pay tribute to the more than 400 students who have completed the California State University, Hayward, summer field geology course since it was instituted in 1970. They, together with the many teaching assistants and, especially, my colleagues Mike Wood and Phil Garbutt, have influenced in many ways my ideas about these often enigmatic rocks. For the same reason, I am greatly indebted to June Legler, John Lull, and Steve Silva, California State University, Hayward, students whose M.S. theses I supervised in the Eastern Belt. Christine Naschak, chiefly responsible for the outcrop map comprising Figure 19, was an undergraduate student in the 1980 field geology course.

I thank Peter Schiffman for getting me involved in these IGCP Project 294 field excursions, and Judy Hannah and Dave Harwood for extremely thorough and useful reviews of this chapter.

REFERENCES

Brooks, E.R., and Coles, D.G., 1980, Use of immobile trace elements to determine original tectonic setting of eruption of metabasalts, northern Sierra Nevada, California: Geological Society of America Bulletin, Part I, v. 91, p. 665-671.

Brooks, E.R., and Garbutt, P.L., 1972, Broken-pillow breccia in the northern Sierra Nevada, Sierra County, California: Geological Society of America Abstracts with Programs, v. 4, p. 131-132.

Brooks, E.R., and Legler, J.L., 1989, An unusual Devonian subaqueous pyroclastic-flow deposit in the northern Sierra Nevada, Sierra County, California: Geological Society of America Abstracts with Programs, v. 21, p. 59.

Brooks, E.R., and Schweickert, R.A., 1982, Geologic transect of the northern Sierra Nevada along the North Fork of the Yuba River: Peninsula Geological Society, 2nd Annual Sierra Nevada Field Trip, Guidebook, 34 p.

Brooks, E.R., Wood, M.M., and Garbutt, P.L., 1982, Origin and metamorphism of peperite and associated rocks in the Devonian Elwell Formation, northern Sierra Nevada, California: Geological Society of America Bulletin, v. 93, p. 1208-1231.

Coles, K.S., and Varga, R.J., 1988, Early to middle Paleozoic phosphogenic province in terranes of the southern Cordillera, western United States: American Journal of Science, v. 288, p. 891-924.

Coney, P.J., Jones, D.L., and Monger, J.W.H., 1980, Cordilleran suspect terranes: Nature, v. 288, no. 5789, p. 329-333.

Day, H.W., Moores, E.M., and Tuminas, A.C., 1985, Structure and tectonics of the northern Sierra Nevada: Geological Society of America Bulletin, v. 96, p. 436-450.

Dimroth, E., and Lichtblau, A.P., 1979, Metamorphic evolution of Archean hyaloclastites, Noranda area, Quebec, Canada: Part I: Comparison of Archean and Cenozoic sea-floor metamorphism: Canadian Journal of Earth Sciences, v. 16, p. 1315-1340.

Durrell, C., and D'Allura, J., 1977, Upper Paleozoic section in eastern Plumas and Sierra Counties, northern Sierra Nevada, California: Geological Society of America Bulletin, v. 88, p. 844-852.

Edelman, S.H., Day,H.W., Moores, E.M., Zigan, S.M., Murphy, T.P., and Hacker, B.R., 1989, Structure across a Mesozoic ocean-continent suture zone in the northern Sierra Nevada, California: Geological Society of America Special Paper 224, 56 p.

Girty, G.H., Gester, K.C., and Turner, J.B., 1990, Pre-Late Devonian geochemical, stratigraphic, sedimentologic, and structural patterns, Shoo Fly Complex, northern Sierra Nevada, California, in Harwood, D.S., and Miller, M.M., eds., Paleozoic and early Mesozoic paleogeographic relations; Sierra Nevada, Klamath Mountains, and related terranes: Geological Society of America Special Paper 255, p. 43-56.

Hanson, R.E., 1991, Quenching and hydroclastic disruption of andesitic to rhyolitic intrusions in a submarine island-arc sequence, northern Sierra Nevada, California: Geological Society of America Bulletin, v. 103, p. 804-816.

Hanson, R.E., and Schweickert, R.A., 1986, Stratigraphy of mid-Paleozoic island-arc rocks in part of the northern Sierra Nevada, Sierra and Nevada Counties, California: Geological Society of America Bulletin, v. 97, p. 986-998.

Hanson, R.E., Saleeby, J.B., and Schweickert, R.A., 1988, Composite Devonian island-arc batholith in the northern Sierra Nevada, California: Geological Society of America Bulletin, v. 100, p. 446-457.

Harper, G.D., 1991, Metasomatism and permeability controls during formation of epidosites in the Josephine ophiolite [abs.]: EOS (American Geophysical Union Transactions), v. 72, no. 44, p. 553.

Harwood, D.S., 1983, Stratigraphy of upper Paleozoic volcanic rocks and regional unconformities in part of the Northern Sierra terrane, California: Geological Society of America Bulletin, v. 94, p. 413-422.

Harwood, D.S., 1988, Tectonism and metamorphism in the Northern Sierra terrane, northern California, in Ernst, W.G., ed., Metamorphism and crustal evolution of the western United States, Rubey Volume 7: Englewood Cliffs, NJ, Prentice-Hall, p. 764-788.

Harwood, D.S., 1992, Stratigraphy of Paleozoic and lower Mesozoic rocks in the northern Sierra terrane, California: U.S. Geological Survey Bulletin 1957, 78 p.

Harwood, D.S., and Murchey, B.L., 1990, Biostratigraphic, tectonic, and paleogeographic ties between upper Paleozoic volcanic and basinal rocks in the northern Sierra terrane, California, and the Havallah sequence, Nevada, in Harwood, D.S., and Miller, M.M., eds., Paleozoic and early Mesozoic paleogeographic relations; Sierra Nevada, Klamath Mountains, and related terranes: Geological Society of America Special Paper 255, p. 157-173.

Harwood, D.S., Yount, J.C., and Seiders, V.M., 1991, Upper Devonian and Lower Mississippian island-arc and back-arc deposits in the northern Sierra Nevada, California, in Cooper, J.D., and Stevens, C.H., eds., Paleozoic paleogeography of the western United States-II: Pacific Section SEPM, v. 67, p. 717-733.

Irvine, T.N., and Baragar, W.R.A., 1971, A guide to the chemical classification of the common volcanic rocks: Canadian Journal of Earth Sciences, v. 8, p. 523-548.

Legler, J.L., Brooks, E.R., and Lull, J.S., 1991, Tamarack tuff: A Devonian submarine pyroclastic flow deposit in the northern Sierra Nevada, Plumas and Sierra Counties: California Geology, v. 44, p. 130-137.

Lowe, D.R., 1982, Sediment gravity flows: II. Depositional models with special reference to the deposits of high-density turbidity currents: Journal of Sedimentary Petrology, v. 52, p. 279-297.

Lull, J.S., and Brooks, E.R., 1983, Petrology and structure of an early Cretaceous dike swarm, northern Sierra Nevada, California: Geological Society of America Abstracts with Programs, v. 15, p. 411.

McMath, V.E., 1966, Geology of the Taylorsville area, northern Sierra Nevada, in Bailey, E.H., ed., Geology of northern California: California Division Mines and Geology Bulletin 190, p. 173-183.

Mathieson, S.A., 1981, Pre- and post-Sangamon glacial history of a portion of Sierra and Plumas Counties, California [M.S. thesis]: Hayward, California State University, 258 p.

Orton, G., Fritz, W., Kokelaar, P., and Howells, M., 1990, North Wales- An Ordovician marginal basin: IAVCEI/IAS, Field Wrokshop, Volcanogenic sedimentation in ancient terrains, Guidebook, 86 p.

Potter, A.W., Watkins, R., Boucot, A.J., Elias, R.J., Flory, R.A., and Rigby, J.K., 1990, Biogeography of the Upper Ordovician Montgomery Limestone, Shoo Fly Complex, northern Sierra Nevada, California, and comparisons of the Shoo Fly Complex with the Yreka terrane, in Harwood, D.S., and Miller, M.M., eds., Paleozoic and early Mesozoic paleogeographic relations; Sierra Nevada, Klamath Mountains, and related terranes: Geological Society of America Special Paper 255, p. 33-41.

Saleeby, J., Hannah, J.L., and Varga, R.J., 1987, Isotopic age constraints on middle Paleozoic deformation in the northern Sierra, California: Geology, v. 15, p. 757-760.

Saleeby, J.B., Shaw, H.F., Niemeyer, S., Moores, E.M., and Edelman, S.H., 1989, U/Pb, Sm/Nd and Rb/Sr geochronological and isotopic study of northern Sierra Nevada ophiolitic assemblages, California: Contributions to Mineralogy and Petrology, v. 102, p. 205-220.

Silva, S.R., Bullen, T.D., and Brooks, E.R., 1991, Isotopic evidence for a major contribution from Early Proterozoic to Archean crust in Devonian arc volcanic rocks, northern Sierra Nevada, California [abs.]: EOS (American Geophysical Union Transactions), v. 72, no. 44, p. 562.

Turner, H.W., 1896, Further contributions to the geology of the Sierra Nevada: U.S. Geological Survey Annual Report, 17th, Part I, p. 521-761.

THIS BOOK IS DUE ON THE LAST DATE
STAMPED BELOW

BOOKS REQUESTED BY ANOTHER BORROWER
ARE SUBJECT TO IMMEDIATE RECALL

APR 23'98
RECEIVED
APR 29 1998
PSL
RECEIVED
JUN 18 1999
Physical Sciences Library
JUN 30 2000
FEB 11 2005

LIBRARY, UNIVERSITY OF CALIFORNIA, DAVIS
http://www.lib.ucdavis.edu/access/circweb/patron.html
Automated Phone Renewal (24-hour): 752-1132
D4613 (5/97)M

THIS BOOK IS DUE ON THE LAST DATE
STAMPED BELOW

BOOKS REQUESTED BY ANOTHER BORROWER
ARE SUBJECT TO IMMEDIATE RECALL

RECEIVED
JUN 08 2001
Physical Sciences Library
JUN 30 2002
RECEIVED
JUN 28 2002
Physical Sciences Library
NOV 16 2002
RECEIVED
NOV 15 2002
PSL
APR 14 2003

RECEIVED
JUN 26 2003
PSL
FEB 1[illegible]
RECEIVED
FEB 09 2005
PSL
JUN 30 2006
FEB 08 2006
RECEIVED
FEB 09 2006
PSL

LIBRARY, UNIVERSITY OF CALIFORNIA, DAVIS
http://libnte.ucdavis.edu/PatronRenew.html
Automated Phone Renewal (24-hour): (530) 752-1132
D4613 (4/99)M